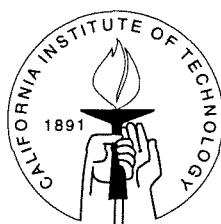


MULTIPLE STEADY STATES IN DISTILLATION

Thesis by
Nikolaos Bekiaris

In Partial Fulfillment of the Requirements
for the Degree of
Doctor of Philosophy



California Institute of Technology
Division of Chemistry & Chemical Engineering
Pasadena, California

1995
(Submitted May 10, 1995)

© 1995

Nikolaos Bekiaris

All Rights Reserved

Στούς γονείς μου Γιάννη και Μαρία

Dedicated to my parents Yanni and Maria

Acknowledgements

Foremost, I wish to thank my advisor, Manfred Morari, for his continuous support, encouragement and guidance during my graduate studies, for his trust in my judgement and for allowing me ample freedom in conducting this work. His insightful comments, suggestions and criticism are greatly appreciated in and out of the professional sphere.

I wish to thank all my teachers at Caltech and especially Prof. Wiggins for his teaching of nonlinear dynamical systems and bifurcations; these courses inspired me to work on the subject that is now the title of my thesis. I would like to thank Prof. Gavalas and Prof. Brady for their interest in my work and future plans. I thank all three professors for their roles in my thesis committee.

During these six years at Caltech, many people have helped me directly through discussion and criticism of my work and indirectly through companionship and friendship.

I wish to thank all the members of the Morari group¹ for their help and company along this “road” towards the completion of my Ph.D. Special thanks to my co-workers: Lionel Laroche, for his precious help and support at the early stages of my work at Caltech. Lionel was the perfect “senior group member;” without him, my “baptism of fire” into the world of graduate school research would not be so smooth and quick. George Meski, for his invaluable help with this project and the friendship, support and advice during the frustrating times of “job hunting.” Cris Radu, for his assistance with AUTO. Thomas Güttinger (ETH, Zürich), whose three-week intense-training visit revitalized me for my final “sprint.” Myung Wan Han, with whom,

¹the fellow graduate students, Lionel Laroche, Jay Lee, Frank Doyle, Tony Skjellum, Tyler Holcomb, Richard Braatz, Doug Raven, Simone Oliveira, Alex Zheng, Iftikhar Huq, Mayuresh Kothare, Cris Radu, Vassilis Hatzimanikatis, Matt Tyler, Carl Rhodes, Thomas Güttinger; the fellow researchers, Hector Budman, Arge Secchi, Petter Lundström, Elling Jacobsen, Morten Hovd, Yasushi Terao, Frank Allgöwer, Håkan Hjalmarsson, Serban Agachi, Frank Laganier, Thanos Tsirikis, Vicky Papageorgaki, Bruno Donno, Chris Swartz, George Meski, Knut Mathisen, Rosario Velardi, Kazuya Asano, Myung Han; Sergei Orlov; the secretaries, Stella Dunn, Patricia New, Adria McMillan, Kathy Lewis.

during the last months, I entered the realms of batch distillation. Working with all of you has been a true pleasure and a valuable experience.

I also want to thank the people (professors, staff and students) in the Chemical Engineering department at Caltech. Special thanks to Suresh Guptha for his immediate response to any computer-related problem and for his patience and help with all my questions and requests. I also thank Kathy Lewis and Adria McMillan for their help on various administrative matters.

I thank Prof. Gani (Danish Technical University, Lyngby) and Prof. Skogestad (Norwegian Technical University, Trondheim) for several enlightened discussions. I also thank Prof. Doherty and Jeffrey Knapp (University of Massachusetts, Amherst), Prof. Seider (University of Pennsylvania, Philadelphia) and Prof. Michelsen (Danish Technical University, Lyngby) for providing us thermodynamic data and subroutines.

I gratefully acknowledge the financial support of the I. S. Latsis Foundation which, for ten years now (since my first days at the National Technical University of Athens), has continuously supported me during my undergraduate and graduate studies. The financial support of the Donors of the Petroleum Research Fund administered by the American Chemical Society is greatly appreciated.

I wish to thank Mike Linden-Martin for the excellent “English in everyday life” courses (the only literally fun Caltech courses); my english would be much worse without the in depth, frame by frame, analysis of episodes of “Married with children” ☺. I also thank the people at the International Student Programs for their help with all the INS and IRS related issues.

Turning to the indirect, non-academic but equally important contributions, I want to thank my family - grandfather and grandmothers, aunts, uncles and cousins - and foremost my parents, Yanni and Maria, and my brothers, Apostoli and Vassili, for their love, care and continuous support and for everything they have done for me. I will never forget my parents’ moral support during some difficult times at Caltech (in the very beginning and at the end), the 2 a.m. “talk” sessions with my brothers and their commitment to updating me about family news via electronic mail, my grandfather’s calendars, Tzela’s and Dimitris’ letters and tapes, Froso’s and

Elpida's pine nuts ("I told you, I don't like them," ☺) ... It is because of you that I contributed (and I will continue to contribute) to the welfare of the long-distance telephone companies ☺.

I want to thank my friends and classmates from "Polytechnio" (NTUA) and especially Costas Bokis, Kostas Konstantopoulos and Christos Dalianis who also came to the U.S. to pursue a higher level of education, for the numerous discussions about common concerns and problems. I want to thank the friends I left in Greece, and particularly Yannis Koutsikos whose friendship will always be there, although we have not seen each other for six years.

Finally, I want to thank all the new friends I made at Caltech and in Los Angeles for the great time we had together - from the early lunch-breaks at the Athenaeum to the Hellenic Association meetings and parties of the 1991-1993 era and from the "clubbings" at Kontrol Faktory and Sin-a-matic to the latest Red Door Café coffee breaks (John Yamasaki, you are here ☺). Special thanks to Chrisa Economou, Vassilis Hatzimanikatis, Sophia Kyriazopoulou, Gautam Vasisht, Sarah Jones, Yorgos "Malik" Stylianos, Thanos Tsirukis, Vicky Papageorgaki, Polly Preventza, Dimitris Kallifatides, Panos Pantzicas, Petros Mouchtaris, Yannis and Erotokritos Katsavounides, Miltos Papalexandris, for contributing, one way or another, to my growth and my better understanding of what I want from life. Last but not least, I want to thank Andri Zapiti for her love and patience and for being a constant source of moral support during the last two years.

Abstract

We study multiple steady states in distillation. We first analyze the simplest case of ternary homogeneous azeotropic mixtures. We show that in the case of infinite reflux and an infinite number of trays (∞/∞ case) one can construct bifurcation diagrams on physical grounds with the distillate flow as the bifurcation parameter. Multiple steady states exist when the distillate flow varies non-monotonically along the continuation path of the bifurcation diagram. We derive a necessary and sufficient condition for the existence of these multiple steady states based on the geometry of the distillation region boundaries. We also locate in the composition triangle the feed compositions that lead to these multiple steady states.

We further note that most of these results are independent of the thermodynamic model used. We show that the prediction of the existence of multiple steady states in the ∞/∞ case has relevant implications for columns operating at finite reflux and with a finite number of trays. Using numerically constructed bifurcation diagrams for specific examples, we show that these multiplicities tend to vanish for small columns and/or for low reflux flows. Nevertheless, the ∞/∞ multiplicities do exist for columns at realistic operating conditions. We comment on the effect of multiplicities on column design and operation for some specific examples.

We then extend the homogeneous mixture results to ternary heterogeneous mixtures. We study the ∞/∞ case in much more depth and detail by demonstrating how the ∞/∞ analysis can be applied to different column designs. More specifically, we show how the feasible distillate and bottom product paths can be located for tray or packed columns, with or without decanter and with different types of condenser and reboiler. We derive the fully detailed, necessary and sufficient condition for the existence of these multiple steady states based on the geometry of the product paths. Simulation results for finite columns show that the predictions carry over to the finite case.

The complete list of the ∞/∞ case predictions is presented. The implications of these multiplicities for column design, synthesis and simulation are demonstrated. More specifically, we show how the ∞/∞ predictions can be useful for the selection of the entrainer, the equipment and the separation scheme. We show that, in some cases, the column operation at an unstable steady state may have some advantages. The important issue of the effect of the thermodynamic phase equilibrium on the existence of multiplicities is discussed. Using the ∞/∞ analysis, we identify entire mixture classes for which multiplicities are inherent and robust. Mixtures with ambiguous VLE data are studied; we show that in some cases a slight VLE difference between models and/or experimental data may affect the existence of multiplicities while other, major VLE discrepancies do not. Finally, we identify the key issues and the pitfalls one should be cautious about when designing or computing the composition profile of an azeotropic distillation column with a commercial simulator.

Contents

Acknowledgements	iv
Abstract	vii
1 Introduction	1
2 Multiple Steady States in Homogeneous Azeotropic Distillation	6
2.1 Introduction	6
2.2 Background	8
2.3 Infinite Reflux and Infinite Number of Trays	10
2.3.1 Existence of Multiple Steady States	15
2.3.2 Analysis	24
2.3.3 Curved Boundaries	32
2.3.4 A Degenerate Case	39
2.3.5 Summary	41
2.4 Finite Reflux and Finite Number of Trays	42
2.4.1 Varying the Distillate Flow	44
2.4.2 Varying the Entrainer and Reflux Flows	46
2.4.3 Effect of the number of trays	50
2.4.4 Curved Boundaries	52
2.5 Effect of the VLE model	57
2.6 Effect on Design and Operation	64
2.7 Conclusions	65
2.8 Literature Cited	69
2.9 Appendix	71
3 Multiple Steady States in Heterogeneous Azeotropic Distillation	74

3.1	Introduction	74
3.2	Preliminaries	77
3.2.1	Composition Profiles in the ∞/∞ Case	86
3.2.2	Existence of Multiple Steady States	91
3.3	Columns without decanter	94
3.3.1	Tray vs. packed columns	101
3.3.2	Summary	105
3.4	Columns with decanter	107
3.4.1	Geometrical Condition and Feed Region	116
3.5	Special Topics	121
3.6	Finite Reflux and Finite Number of Trays	137
3.7	Conclusions	145
3.8	Literature Cited	151
3.9	Appendix	153
4	∞/∞ Predictions and Implications for Design, Synthesis and Simulation.	156
4.1	Introduction	156
4.2	Tools and preliminaries	157
4.3	∞/∞ Analysis	160
4.3.1	Geometrical multiplicity condition	163
4.3.2	∞/∞ predictions	164
4.4	Implications for Design, Synthesis and Simulation	166
4.4.1	Entrainer selection	167
4.4.2	Column design and separation scheme selection	174
4.4.3	Critical VL(L)E data - Design of experiments	178
4.4.4	Operation	189
4.4.5	Simulation	194
4.5	Conclusions	205
4.6	Literature Cited	208

4.7 Appendix	209
5 Conclusion	211
6 Future Work	220

List of Figures

2.1	Acetone - heptane - benzene residue curve diagram.	11
2.2	The acetone - heptane - benzene separation sequence.	12
2.3	Acetone - heptane - benzene column composition profile. High conversion steady state.	13
2.4	Acetone - heptane - benzene column composition profile. Low conversion steady state.	14
2.5	Residue curve diagram of a 001 class ternary mixture.	16
2.6	a-d. Column profiles with infinite number of trays at infinite reflux. .	19
2.6	e-h. Column profiles with infinite number of trays at infinite reflux. .	21
2.7	Mole fraction of L in the distillate along the continuation path.	23
2.8	D increases monotonically for column profiles that contain only one saddle singular point.	26
2.9	Residue curve diagrams of a. a 000 class b. a 100 class ternary mixture. 28	
2.10	Geometry of the distillation region boundaries. a. D increases b. D decreases along the continuation path.	30
2.11	Residue curve diagram of a 231 class ternary mixture and the appropriate feed region.	31
2.12	The curvature of the boundary affects the appropriate feed region. . .	33
2.13	Residue curve diagram of a 021 class ternary mixture that contains a highly curved boundary.	35
2.14	Highly curved boundaries can induce multiplicities.	37
2.15	The appropriate feed region in the case of two curved boundaries. . .	38
2.16	Degenerate multiplicities for (a) a 000 class and (b) a 222-m class ternary mixture.	40
2.17	Acetone (L) - heptane (H) - benzene (I-E) azeotropic column.	43

2.18	Bifurcation diagrams for a column with $N=44$ trays, $E/F = 1$ and various R/F . The distillate flow is the bifurcation parameter.	45
2.19	Reflux - distillate multiplicity regions.	47
2.20	Entrainer - reflux multiplicity region and typical bifurcation diagrams with the entrainer and reflux flows as the bifurcation parameters. . .	48
2.21	Bifurcation diagram for a column with $N=44$ trays, $R = 500$ kmol/min and $D = 90.9$ kmol/min. The entrainer feed flow is the bifurcation parameter.	49
2.22	Bifurcation diagram for a column with $N=44$ trays, $E = 80$ kmol/min and $D = 90.9$ kmol/min. The reflux flow is the bifurcation parameter.	51
2.23	Vanishing multiplicity in small columns with $R = 1500$ kmol/min and $D = 90.9$ kmol/min.	53
2.24	Entrainer - reflux multiplicity region variation with the number of trays.	54
2.25	The acetone - methanol - chloroform residue curve diagram.	55
2.26	The four distillation regions and the appropriate feed region in the acetone - methanol - chloroform composition triangle.	56
2.27	First stable profile of a column with $N=30$ trays, $E/F = .5$ and $R/F = 100$.	58
2.28	Second stable profile of a column with $N=30$ trays, $E/F = .5$ and $R/F = 100$	59
2.29	Unstable profile of a column with $N=30$ trays, $E/F = .5$ and $R/F = 100$.	60
2.30	The three steady states of the acetone - methanol - chloroform column with $N=30$ trays, $E/F = .5$ and $R/F = 100$. in the composition triangle.	61
2.31	Bifurcation diagrams for the acetone - methanol - chloroform column with $N=30$ trays and various R/F . The distillate flow is the bifurcation parameter.	62
2.32	Reflux - distillate multiplicity and specifications regions.	66
2.33	Open-loop dynamical behavior under a feed composition disturbance.	67

3.1	Approximate distillation lines belonging to the same or different exact distillation lines may cross. The exact distillation lines do not cross. Points a and b belong to two different sequences of points calculated using equation (2).	80
3.2	The residue curve, the distillation line and the approximate distillation line that go through point \underline{x}	82
3.3	Residue curve diagram and VLLE of the mixture ethanol (L) - water (H) - benzene (I-E).	83
3.4	Distillation line diagram and VLLE of the mixture ethanol (L) - water (H) - benzene (I-E).	85
3.5	The actual, computed residue curve diagram and VLLE of the mixture ethanol - water - benzene.	87
3.6	The actual, computed distillation line diagram and VLLE of the mixture ethanol - water - benzene.	88
3.7	The three acceptable types of profiles in the ∞/∞ case.	90
3.8	The geometrical multiplicity condition is I. not satisfied (D increases along the continuation path) II. satisfied (D decreases along the continuation path).	93
3.9	For any D on the boundary segment ad , the appropriate feed region is the triangle $D1c$. For this mixture, the region of feed compositions that lead to multiplicities is the union of all these triangles, i.e., the shaded area $ad1c$	95
3.10	Packed columns without decanter: No multiplicities.	96
3.11	Tray columns without decanter: multiplicities for feeds in shaded region.	99
3.12	Tray columns without decanter: the continuation paths for D and B	100
3.13	Bifurcation diagram of the mole fraction of L in the bottoms vs. the distillate flow for tray columns without decanter.	102

3.14	The residue curve boundaries and the vapor line can be used for the qualitative predictions of multiplicities in tray columns without decanter. For the mixture shown, the different vapor line suggests that no multiplicities exist for tray columns without decanter.	106
3.15	Column with decanter	108
3.16	The feasible overhead vapor V, distillate D and bottom product B regions for a packed column with decanter and given feed F in the ∞/∞ case for type I profiles.	110
3.17	The feasible overhead vapor V, distillate D and bottom product B regions for a packed column with decanter and given feed F in the ∞/∞ case for type III profiles with V on TY.	111
3.18	The feasible overhead vapor V, distillate D and bottom product B regions for a packed column with decanter and given feed F in the ∞/∞ case for type III profiles with V on TX.	112
3.19	The feasible overhead vapor V, distillate D and bottom product B regions for a packed column with decanter and given feed F in the ∞/∞ case for type II profiles.	113
3.20	The feasible overhead vapor V, distillate D and bottom product B regions for a packed column with decanter and given feed F in the ∞/∞ case for all acceptable profiles.	114
3.21	The distillate and bottoms continuation paths for packed columns with decanter and $D_2=0$	115
3.22	Bifurcation diagram of the mole fraction of L in the bottoms vs. the distillate flow for packed columns with decanter and $D_2=0$	117
3.23	The three steady state profiles with the same distillate flowrate for packed columns with decanter and $D_2=0$	118
3.24	The information required to apply the geometrical condition and the feed composition region (shaded) that leads to multiplicities for packed columns with decanter and $D_2=0$	120

3.25	The effect of the use of a typical, partial reboiler on the bottom product composition for tray and packed columns.	122
3.26	The effect of the use of a typical, partial reboiler on type I profiles of packed columns.	123
3.27	The effect of the use of a typical, partial reboiler on the bottom product composition of type III profiles of packed columns.	124
3.28	The effect of the use of a partial condenser on the feasible distillate product composition of type III profiles of packed columns without decanter.	126
3.29	The region of feed compositions that lead to the degenerate type of multiplicity for tray columns without decanter.	129
3.30	Five different column profiles with identical B and D (degenerate multiplicity) for a tray column with decanter and $D_2=0$	131
3.31	The region of feed compositions that lead to the degenerate type of multiplicity for tray columns with decanter and $D_2=0$	132
3.32	The mole fraction of L in the bottoms vs. the distillate flow and the ratio D_1/D for packed columns with decanter. Numbers in italics: the number of heterogeneous steady states in the $D - D_1/D$ parameter space.	135
3.33	The column without decanter used in the numerical continuation calculations.	139
3.34	Bifurcation diagram with the distillate flow as the bifurcation parameter for the column without decanter.	141
3.35	The column with decanter used in the numerical continuation calculations.	143
3.36	Bifurcation diagram with the distillate flow as the bifurcation parameter for the column with decanter.	144
3.37	The general procedure for checking the existence of multiple steady states in the ∞/∞ case of any ternary mixture.	147

4.1	Illustration of the residue curve diagram of a ternary homogeneous mixture belonging to the 001 class, e.g., acetone (L) - heptane (H) - benzene (I-E).	159
4.2	The feasible distillate and bottoms lines for the mixture acetone (L) - heptane (H) - benzene (I) and some feed F.	161
4.3	Bifurcation diagram showing the light component mole fraction in the distillate x_{DL} as a function of the distillate flow.	162
4.4	Residue curve diagrams of four mixture classes with inherent multiplicities.	169
4.5	A heterogeneous VL(L)E diagram class without multiplicities.	170
4.6	The VL(L)E diagram of the heterogeneous mixture benzene (I) - heptane (H) - methanol (L). The shaded regions depict the feed regions for which multiple steady states exist for a column a. without decanter b. with decanter	172
4.7	The VL(L)E diagram of the heterogeneous mixture acetone (L) - chloroform (I) - water (H). The shaded regions depict the feed regions for which multiple steady states exist for a column a. without decanter b. with decanter.	173
4.8	The residue curve (a) and distillation line (b) diagrams of the heterogeneous mixture ethanol (L) - water (H) - benzene (I-E).	175
4.9	Two separation schemes for the separation of the ethanol (I) - water (H) azeotrope using ethyl ether (L-E) as the entrainer.	177
4.10	The two steady state profiles of the first column of scheme a.	179
4.11	Three residue curve (or distillation line) diagrams of mixtures belonging to the 222-m class (a,b,c) and a graphical illustration of the simplified multiplicity condition for 222-m class mixtures (d). a. Unique steady state b. and c. Multiple steady states for feed compositions in the shaded regions.	181
4.12	The residue curve diagram and the vapor line ZQ of the mixture ethanol (L) - water (H) - benzene (I-E).	183

4.13	The residue curve diagram and the vapor line ZQ of the mixture isopropanol (L) - water (H) - benzene (I-E).	184
4.14	The residue curve diagram of a 401 class mixture. The shaded region depicts the feed compositions for which multiple steady states exist. .	186
4.15	Two residue curve diagrams of mixtures belonging to the 021 class. a. Unique steady state b. Multiple steady states for feed compositions in the shaded region.	188
4.16	The location of the acetone (L) - heptane (H) and benzene (I) - heptane (H) azeotropes and the computed distillation line boundary using the Aspen Plus SYSOP7 physical properties set.	190
4.17	The feasible distillate and bottoms sets for a given feed F of the mixture acetone (L) - heptane (H) - benzene (I-E).	192
4.18	The location of the limit points along the distillate and bottoms continuation paths for the mixture ethanol (L) - water (H) - benzene (I-E). .	193
4.19	The stable and unstable steady state profiles satisfying the ethanol (L) - water (H) - benzene (I-E) column specification.	195
4.20	The three steady state profiles for the 001 class mixture acetone (L) - heptane (H) - benzene (I-E) and some given feed F.	197
4.21	The characteristics of the column simulated by Aspen Plus.	198
4.22	Two profiles, IP3-BF100 and IP1-BF10, used as initial estimates in simulations. Some indicative tray numbers are shown. BF: Benzene feed.	201
4.23	Solutions computed by Aspen Plus for $F_I=100$, $N_F=22$, $R=10000$ and $D=95$	204
4.24	Solutions computed by Aspen Plus for $F_I=10$, $N_F=32$, $R=1000$ and $D=93$	206
5.1	The general procedure for checking the existence of multiple steady states in the ∞/∞ case of any ternary mixture.	214

List of Tables

2.1	Acetone mole fraction in the distillate for various reflux flows.	15
2.2	Antoine coefficients for the components used in the simulations.	72
2.3	Van Laar coefficients for the acetone - heptane - benzene mixture.	72
2.4	Van Laar coefficients for the acetone - methanol - chloroform mixture.	73
3.1	Information along the continuation path for tray columns without de- canter.	101
3.2	Information along the continuation path for packed columns with de- canter and $D_2=0$	116
3.3	The distillate and bottoms routes for various types of equipment (con- denser/reboiler/decanter). a. tray columns b. packed columns.	148
3.4	Antoine coefficients for the components used in the chapter.	154
3.5	UNIQUAC pure component parameters used in this chapter.	154
3.6	UNIQUAC binary parameters a_{ij} in $^{\circ}\text{K}$ for the ethanol - benzene - water mixture.	154
4.1	Simulation results using Aspen Plus and different sets of benzene feed flowrate, F_I , feeds tray, N_F , reflux flowrate, R , distillate flow, D and with or without a user-supplied initial column profile. F_I , R and D in kmols/hr; CF: Convergence failure.	202
5.1	The distillate and bottoms routes for various types of equipment (con- denser/reboiler/decanter). a. tray columns b. packed columns.	216

Chapter 1 Introduction

Among the separation processes, distillation is undoubtedly the most widely practiced technique for separating mixtures in the chemical process industries. In the petroleum industry the separation of nonazeotropic mixtures is most common (standard or nonazeotropic distillation). In the chemical and specialty chemical industry, however, standard distillation is an exception and the separation of mixtures forming azeotropes is the rule (azeotropic distillation).

In this manuscript, the term “azeotropic distillation” covers the general notion of distillation of azeotrope forming mixtures. Therefore, this term includes the case where a solvent enhances separation (extractive distillation), as well as the case where the added component introduces a new azeotrope which is removed as either the distillate or the bottoms (classical definition of azeotropic distillation). But it also includes distillation-based separation schemes that are neither extractive nor azeotropic distillation in the conventional sense.

The use of the term “azeotropic distillation” with this broader meaning has been established during the last decade when a number of researchers have started looking at separation schemes other than the classical extractive and azeotropic distillation. These studies revealed the underlying common basis of all these processes and led to the development of tools and techniques applicable to any distillation process. Note that under this unifying methodology, standard distillation is just a special case.

Although the design and control of standard distillation have been extensively studied, this is not the case with azeotropic distillation. Some of the articles on azeotropic distillation provide strong evidence that the design and operation of azeotropic columns can present a serious challenge and can give rise to problems never encountered in standard distillation, e.g., steady state multiplicity, oscillations, counter-intuitive column design.

More specifically, Laroche et al. (1992) have shown that ternary homogeneous* azeotropic distillation columns can exhibit unusual features, not observed in standard distillation. For example, increasing the reflux does not always increase separation and infinite reflux does not imply maximum separation; meeting the same specifications with a larger number of trays sometimes requires higher internal flows; the direct and the indirect sequence of standard distillation are not feasible, while other separation schemes (in which the intermediate boiler is recovered as a pure distillate or bottom product) are. Laroche et al. (1992) show that the understanding of these features is critical for proper column design, control and simulation.

Among their surprising features, it has been discovered that azeotropic distillation columns can exhibit multiple steady states, i.e., two or more different steady states for the same set of operating parameters. The term “multiple steady states” is used in the literature to describe various, sometimes quite different situations. In this manuscript, by multiple steady states we mean what is generally referred to as *output multiplicities*, i.e., columns with the same inputs (the same feed, distillate, bottoms, reflux and boilup molar flows, the same feed composition, number of stages and feed location) but different outputs (product compositions) and hence different composition profiles. We are mainly investigating this type of multiplicities although we also discuss some aspects of *state multiplicities*, i.e., columns with the same inputs and outputs but with different composition profiles (states).

The implications of these multiplicities for distillation simulation, design and operation are numerous and can be critical for design decisions (see chapter 4 for more details). For example, the existence of multiple solutions may cause problems in simulations, such as, a higher convergence failure rate. Furthermore, the computation of only one solution may also result in misleading conclusions and decisions regarding the separation under consideration caused by disregarding some eligible, and possibly, attractive solutions.

Multiplicities may also cause problems in column operation and control. When

*The mixture under consideration is called homogeneous if only one liquid phase exists throughout the composition range and heterogeneous if two liquid phases exist for some compositions.

two or more steady states exist for the same inputs it is possible that under some disturbance, the column profile jumps from the desirable, in terms of product purity, steady state to another undesirable steady state, i.e., a steady state with low product purity. Evidence of the operational problems that multiple steady states can cause is given by Kovach and Seider (1987). Their conclusion is that the experimentally observed erratic behavior of the industrial tower they study is due to the existence of multiple steady states.

The study of multiplicities in distillation has a long history (see chapters 2 and 3 for more details). Rosenbrock (1962) proved that the steady state of distillation columns separating a binary homogeneous mixture is unique under the assumption of constant molar flows (i.e. neglecting the energy balances). Magnussen et al. (1979) first presented simulation results that show the existence of three steady states (two stable and one unstable) for the heterogeneous mixture of ethanol - water - benzene. The results of Magnussen et al. (1979) triggered great interest in multiple steady states in distillation. It was conjectured that multiplicities in distillation are caused by multiple phases but a rigorous explanation was lacking. The belief that heterogeneity is the cause for such multiple steady states directed the attention towards heterogeneous azeotropic distillation. Consequently, several articles were published where the results of Magnussen et al. (1979) were studied extensively and where multiplicities for other heterogeneous systems were reported.

Laroche (1991) first reported simulation results that show multiple steady states for a *homogeneous* ternary mixture (acetone - heptane - benzene) with nonideal vapor-liquid equilibrium (VLE) and under the assumption of constant molar flows. This discovery became the starting point for the study presented here. The aims of this work are: (1) to provide an explanation for the existence of multiple steady states in distillation, (2) to develop rules for the prediction of these multiplicities and (3) to demonstrate the implications of multiplicities for distillation column design, synthesis and simulation.

The work presented here is not a simulation-based case study. It is an analytical work based on physical grounds, and more specifically, on the analysis of the limiting

case of infinite reflux and infinite number of trays (the ∞/∞ case hereafter). Based on this analysis, we have been able to provide a physical explanation for the existence of multiple steady states in distillation and moreover we developed graphical rules for the prediction of these multiplicities. Using the ∞/∞ analysis, we can predict exactly when multiplicities occur in the ∞/∞ case. We show that the predictions carry over to columns operating at finite reflux and with a finite number of trays. The implications of these multiplicities for column design, synthesis and simulation are demonstrated. Numerical computations are used to illustrate the theoretical results.

The thesis overview has as follows:

In chapter 2 we first present a review of the literature on multiple steady states in distillation. The fact that the multiplicity reported by Laroche (1991) occurs in a column separating a homogeneous mixture at high reflux and with a large number of trays directs our study to the analysis of the ∞/∞ case. In chapter 2 we study the existence of multiple steady states in ternary *homogeneous* azeotropic distillation. The emphasis is on the basic development of the steps of the ∞/∞ analysis, the derivation of the multiplicity conditions and the implications of the ∞/∞ case multiplicities for columns at finite reflux and with a finite number of trays (finite case). In chapter 2 we show that the ∞/∞ multiplicities carry over to the finite case and moreover that they may exist at realistic operating conditions, that is, for small reflux and a small number of trays.

In chapter 3 we extend the homogeneous mixture results to ternary heterogeneous mixtures but more importantly we study the ∞/∞ case in much more depth and detail by demonstrating how the ∞/∞ analysis can be applied for different column designs. More specifically, we discuss the differences between packed and tray columns, columns with and without decanter, columns with partial and total condenser etc. In chapter 3 we present the fully detailed and general geometrical multiplicity condition. Simulation results for finite columns show that the predictions carry over to the finite case.

In chapter 4 the complete list of the ∞/∞ case predictions is presented. The

implications of these multiplicities for column design, synthesis and simulation are demonstrated. More specifically, we show how the ∞/∞ predictions can be useful for the selection of the entrainer, the equipment and the separation scheme. We show that, in some cases, the column operation at an unstable steady state may have some advantages. The important issue of the effect of the thermodynamic phase equilibrium on the existence of multiplicities is discussed. Using the ∞/∞ analysis, we identify entire mixture classes for which multiplicities are inherent and robust. Mixtures with ambiguous VLE data are studied; we show that in some cases a slight VLE difference between models and/or experimental data may affect the existence of multiplicities while other, major VLE discrepancies do not. Finally, we identify the key issues and the pitfalls one should be cautious about when designing or computing an azeotropic distillation column.

Finally, in chapter 5 we summarize the conclusions of the work presented here, and in chapter 6 we offer some future work perspectives.

References

- Kovach III**, J. W., and W. D. Seider, "Heterogeneous Azeotropic: Experimental and Simulation Results," *Comput. Chem. Eng.*, 1987, **11**(6), pp. 593-605.
- Laroche**, L., "Homogeneous Azeotropic Distillation: Entrainer Selection," Ph. D. Dissertation, California Institute of Technology, Pasadena, 1991.
- Laroche**, L., N. Bekiaris, H. W. Andersen, and M. Morari, "The Curious Behavior of Homogeneous Azeotropic Distillation - Implications for Entrainer Selection," *AIChE J.*, 1992, **38**(9), pp. 1309-1328.
- Magnussen**, T., M. L. Michelsen, and Aa. Fredenslund, "Azeotropic Distillation Using UNIFAC," *Inst. Chem. Eng. Symp. Ser.*, 1979, **56**, pp. 4.2/1-4.2/19.
- Rosenbrock**, H. H., "A Lyapunov Function with Applications to some Nonlinear Physical Systems," *Automatica*, 1962, **1**, pp. 31-53.

Chapter 2 Multiple Steady States in Homogeneous Azeotropic Distillation

2.1 Introduction

The study of multiplicities in distillation has a long history. Rosenbrock (1962) proved that the steady state of distillation columns separating a binary mixture is unique under the assumptions of (1) constant molar flows (i.e. neglecting the energy balances) and (2) that to every value of vapor composition y there corresponds a unique value of liquid composition x in equilibrium with y . This assumption does not exclude the cases of nonideal vapor-liquid equilibrium (including the cases where an azeotrope is formed between the two components).

Petlyuk and Avetyan (1971) first conjectured the possibility of multiple steady states in the distillation of ternary homogeneous systems under the assumptions of constant molar flows and nonideal vapor-liquid equilibrium (Wilson equation). They conjectured that multiple steady states exist when a distillation product region is a quadrangle. However, as we will show this condition is neither necessary nor sufficient for the existence of multiple steady states. Moreover, they do not identify any physical mixture that may lead to these multiple steady states.

Magnussen et al. (1979) present simulation results that show the existence of three steady states for the heterogeneous mixture of ethanol - water - benzene. In these calculations the phase splitter is removed; instead, a second feed at the top of the column is considered (this second feed is the same for all three steady states). Moreover, the liquid composition profiles of all three steady states lie entirely in the single liquid phase region. Therefore, although the mixture ethanol - water - benzene can exhibit liquid - liquid phase split, the multiplicities presented in that article cannot be explained by the heterogeneity of the mixture. Hence, the explanation for

the existence of the aforementioned multiplicities should be sought in the regime of *homogeneous* azeotropic distillation. Finally, it should be noted that the multiplicities were observed with the UNIQUAC and NRTL activity coefficient models but a unique steady state was found with the Wilson equation model.

Doherty and Perkins (1982) considered the case of nonideal vapor - liquid equilibrium and constant molar flows. They proved the stability of the unique steady state in binary distillations (uniqueness was already proven by Rosenbrock, 1962). They also prove that a unique steady state exists for single-staged columns of any multicomponent mixture. Using the above results, they conclude that the multiplicity reported by Magnussen et al. (1979) is a consequence of multiple components and multiple stages.

The results of Magnussen et al. (1979) triggered great interest in multiple steady states in distillation. The belief that heterogeneity is a possible cause for such multiple steady states directed the attention towards heterogeneous azeotropic distillation. Consequently, several articles were published where the results of Magnussen et al. (1979) were studied extensively and where multiplicities for other heterogeneous systems were reported (Prokopakis and Seider, 1983; Kovach and Seider, 1987; Widagdo et al., 1989; Rovaglio and Doherty, 1990; Bossen et al., 1993).

However, other types of systems have also been investigated. In a simulation study Chavez et al. (1986) and Lin et al. (1987) found multiple steady states in interlinked distillation columns. The multiplicity they report is due to the interlinking and is not found in single columns.

Sridhar and Lucia (1989) and Lucia and Li (1992) considered binary mixtures with nonideal VLE and included energy balances in the model. They showed that a unique steady state exists for binary homogeneous multistage separators for some sets of column specifications and identify specifications that can exhibit multiple steady states. Sridhar and Lucia (1990) show that a unique steady state exists for multicomponent homogeneous multistage separation processes with fixed temperature and pressure profiles.

Jacobsen and Skogestad (1991) present two different types of multiplicities in

binary distillation columns with ideal VLE:

- Multiplicity in Input Transformations.

Constant molar flows are assumed. Multiplicities occur when some flows are specified on a mass basis (instead of a molar basis) and are due to the nonlinear mass to molar flow transformation.

- Multiplicity when molar reflux and boilup are used as specifications (LV configuration).

Energy balances are included in the model. This type of multiplicity does not occur for the case of constant molar flows.

Kienle and Marquardt (1991) and Helfferich (1993) investigated multiplicities in single column sections. Helfferich (1993) argues that these types of multiplicities disappear in practice (finite length column sections with finite mass-transfer rates). The implications of those multiplicities for complete distillation columns are unclear. More recently, Kienle et al. (1992) reported multiple steady states in complete columns for the ternary homogeneous mixture of acetone, chloroform and methanol.

The starting point for the study presented here were the multiple steady states reported by Laroche et al. (1990, 1991, 1992) for a homogeneous ternary mixture (acetone - heptane - benzene) with nonideal VLE and under the assumption of constant molar flows.

2.2 Background

The term “homogeneous azeotropic distillation” covers the general notion of distillation of azeotrope forming mixtures where a single liquid phase exists in the region of interest. Usually, homogeneous azeotropic distillation units perform the separation of a binary azeotrope into two pure components through the addition of an entrainer which alters the relative volatility of the two azeotrope constituents without inducing liquid - liquid phase separation.

Unless stated otherwise, we use the following convention to refer to a given mixture: L (I, H respectively) corresponds to the component which has the lowest (intermediate, highest resp.) boiling point; we also denote the entrainer by E. We use the same notation in italics (L , I , H , E) to denote the corresponding flow rates of the components in the feed. The locations of the feed, distillate and bottoms in the composition triangle are denoted by F, D and B respectively. Again, the corresponding flowrates are denoted by the same letters in italics (F , D , B and R for the reflux flow).

In all simulations presented in this chapter, the column operates under atmospheric pressure, there is no pressure drop in the column and the condenser is total. Moreover, constant molar overflow and a tray efficiency of 1 are assumed. Vapor pressures are calculated using the Antoine equation and liquid activity coefficients are calculated using the Van Laar equation. The appendix contains more information on the thermodynamic model as well as the Antoine and Van Laar coefficients used in the examples. The tray counting starts from the reboiler (number 0) and ends at the top. Finally, in all composition profile figures the *liquid* mole fractions are depicted.

A widely used concept for the description of azeotropic distillation is that of the simple distillation residue curve (hereafter called residue curve). The *simple distillation process* involves charging a still with a liquid of composition \underline{x} and gradual heating. The vapor formed is in equilibrium with the liquid left in the still; the vapor is continuously removed from the still.

A residue curve is defined as the locus of the composition of the liquid remaining at any given time in the still of a simple distillation process. Residue curves are governed by the set of differential equations (Doherty and Perkins, 1978):

$$\frac{dx_i}{d\xi} = x_i - y_i, \quad i = 1, \dots, C - 1$$

where i is the component index, C is the number of pure components in the mixture, y_i (x_i) is the mole fraction of component i in the vapor (liquid) phase, and ξ is the

dimensionless warped time.

At infinite reflux, the differential equations which describe packed columns become identical to the residue curve equations. Thus residue curves coincide exactly with composition profiles of packed columns operated at total reflux, and they give a very good approximation of composition profiles of tray columns at infinite reflux.

In this manuscript, a *distillation region* is defined as a subset of the composition simplex in which all residue curves originate from the same locally lowest-boiling pure component or azeotrope and end at the same locally highest-boiling one. The curves which separate different distillation regions are called residue curve boundaries. In this manuscript, the term distillation region boundary (or just boundary) is used for both residue curve boundaries (interior boundaries) and the edges of the composition simplex.

2.3 Infinite Reflux and Infinite Number of Trays

In this section we present an extensive analysis of the case where the reflux and the number of trays are infinite (the ∞/∞ case hereafter). The idea for examining this situation came from the multiplicities reported by Laroche et al. (1990, 1991, 1992). The homogeneous mixture under consideration is that of acetone (L), heptane (H) and benzene (I). In this case there is only one binary azeotrope formed between acetone and heptane (93% acetone, 7% heptane). Benzene, the intermediate boiler, is used as entrainer for the separation of the acetone - heptane azeotrope. Figure 2.1 shows the residue curve map of this ternary mixture (001 class according to the classification by Matsuyama and Nishimura, 1977).

Figure 2.2 depicts the separation sequence and information about the azeotropic column. The feed composition and flows, the number of trays and the distillate, bottom, reflux and reboil flow rates are identical for both steady states. Figures 2.3 and 2.4 shows the two different stable steady state profiles reported by Laroche et al. (1990, 1991, 1992). In the first case (Figure 2.3) the column yields 99% acetone (L) at the top and 95% heptane (H) at the bottom while in the second case (Figure 2.4),

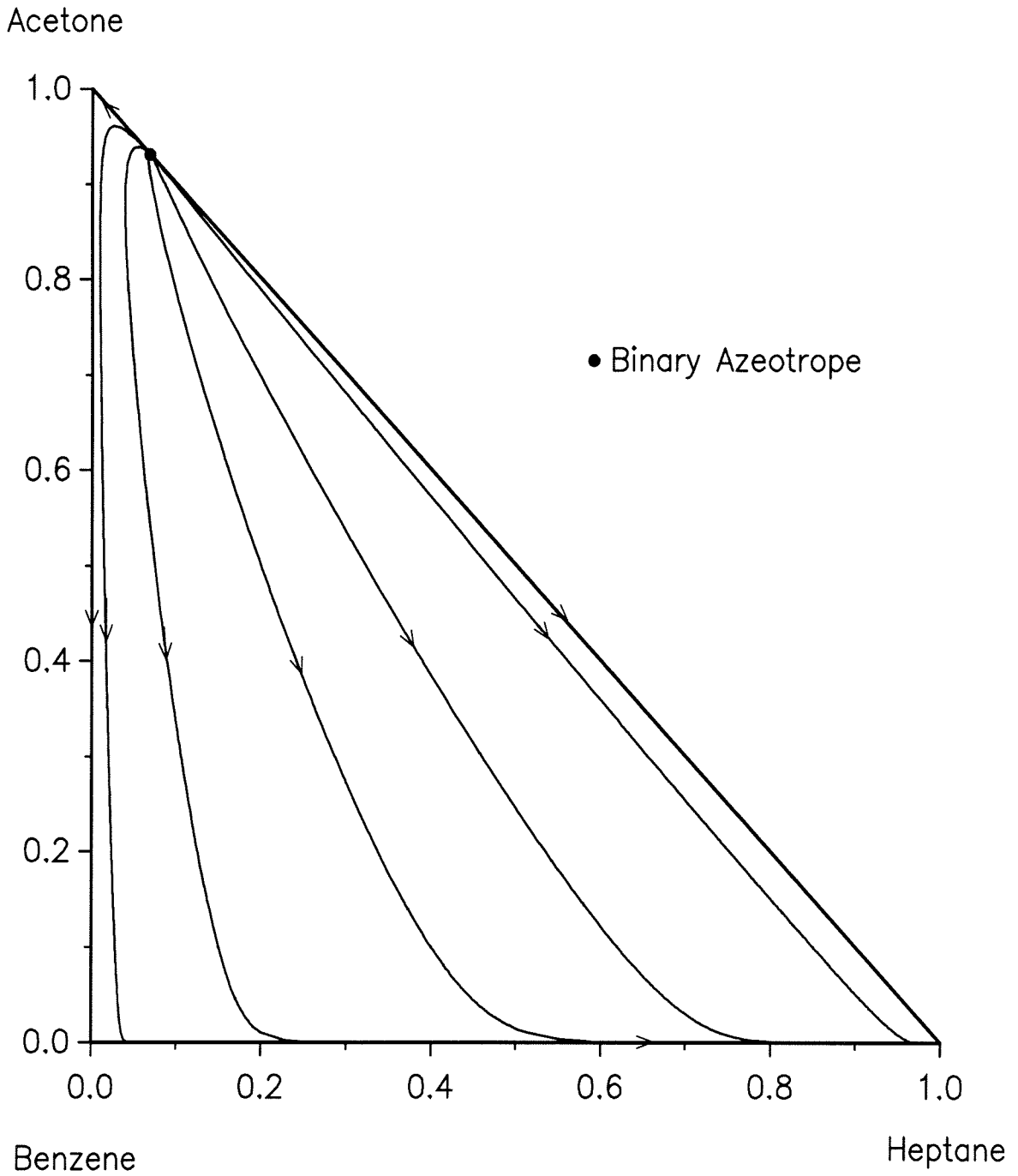


Figure 2.1: Acetone - heptane - benzene residue curve diagram.

<u>Concentration</u>	<u>Entrainer feed</u>	<u>Azeotropic feed</u>
Acetone (L)	0.0	0.90
Heptane (H)	0.0	0.10
Benzene (I)	1.0	0.0

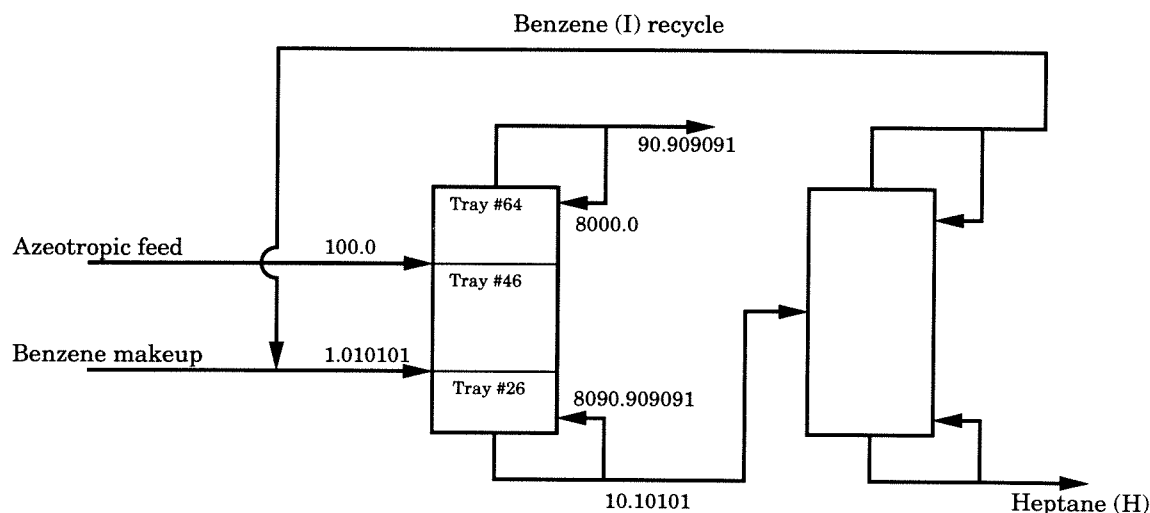


Figure 2.2: The acetone - heptane - benzene separation sequence.

the top product is a mixture of 93% acetone and 7% heptane (azeotropic mixture).

In this column, the reflux to feed and the reflux to distillate flow ratios are very high - in the order of 100. Table 2.1 summarizes simulation results with different reflux and associated reboil flows. All other column parameters are kept constant at their values shown in Figure 2.2. Table 2.1 shows that only one stable steady state exists for reflux flows less than 6600 while two stable steady states are observed for any higher reflux. Actually, no matter how large a reflux flow was used, two stable steady states were always found. This result suggests that this type of multiplicity may also occur at infinite reflux. This observation simplifies the study of multiplicities significantly since at infinite reflux column profiles coincide with residue curves.

Moreover, the column shown in Figure 2.2 has 64 theoretical trays which is quite a large number. This suggests that this multiplicity may occur in columns with a large number of trays (infinite number of trays in the limit). Columns at infinite reflux and with an infinite number of trays are obviously a special case of infinite-reflux columns which simplifies our analysis even further.

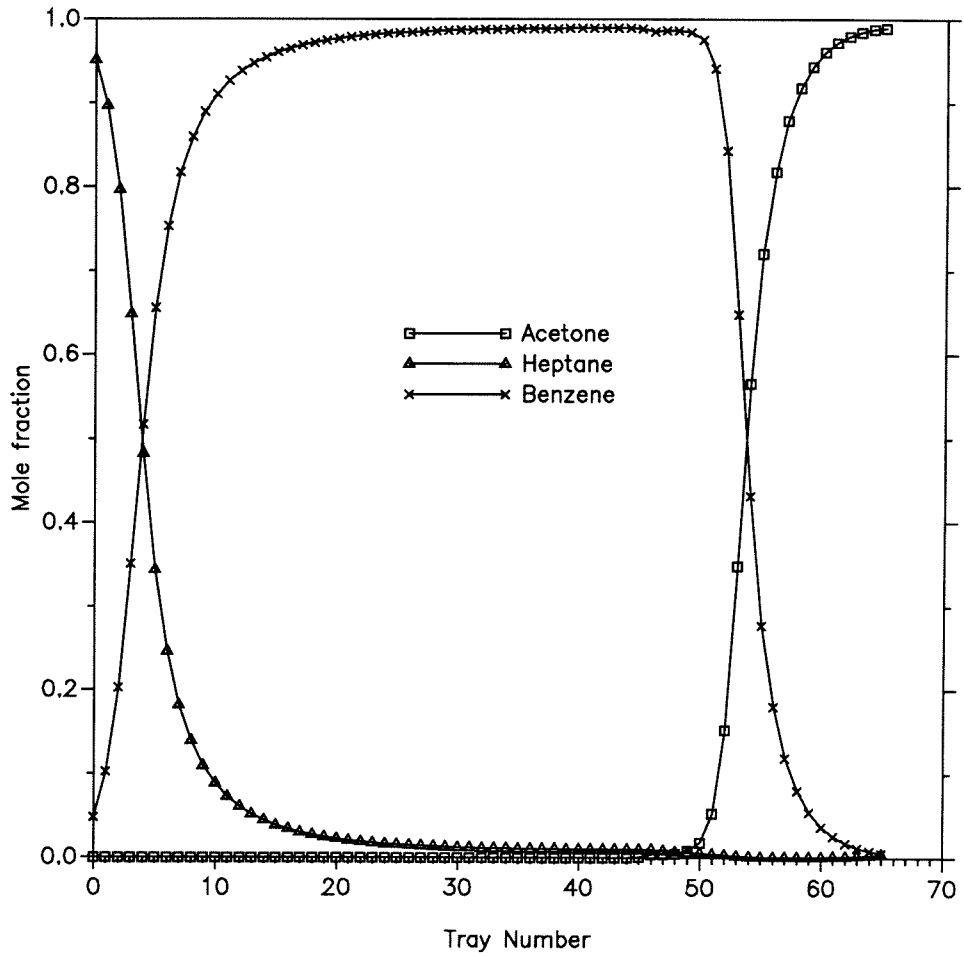


Figure 2.3: Acetone - heptane - benzene column composition profile. High conversion steady state.

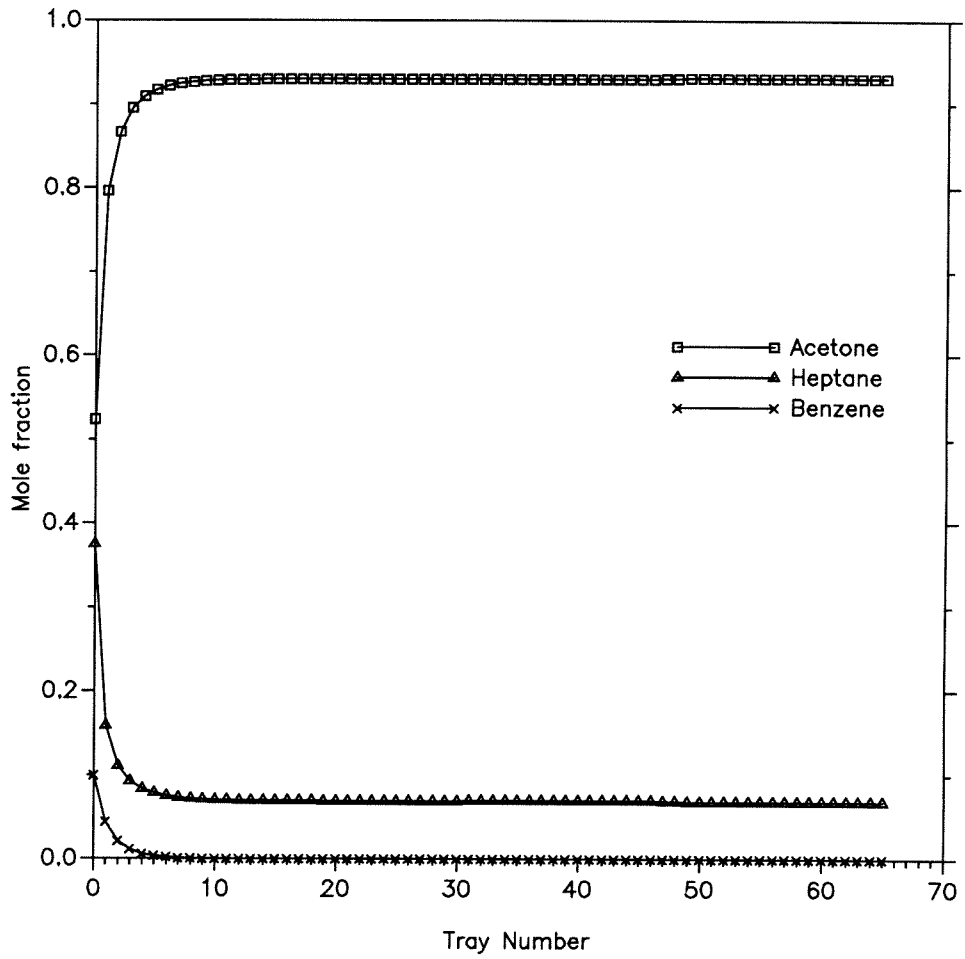


Figure 2.4: Acetone - heptane - benzene column composition profile. Low conversion steady state.

Table 2.1: Acetone mole fraction in the distillate for various reflux flows.

R (kmol/min)	First stable profile	Second stable profile
500	0.93	---
1000	0.93	---
5000	0.93	---
6500	0.93	---
6600	0.93	0.99
7000	0.93	0.99
8000	0.93	0.99
10000	0.93	0.99
20000	0.93	0.99
100000	0.93	0.99

2.3.1 Existence of Multiple Steady States

In this section we study in detail the ∞/∞ case. We use a 001 class ternary mixture to illustrate the analysis of this situation. Figure 2.5 shows the residue curve map of this type of ternary mixture. In this diagram, there is only one minimum boiling binary azeotrope between the light (L) and the heavy (H) component. The azeotrope is an unstable node, the light and the intermediate pure component corners are saddles and the heavy-component corner is a stable node. All residue curves start from the azeotrope and end at the heavy component corner; there are no interior distillation boundaries in this diagram and hence the whole triangle forms a single distillation region.

At infinite reflux, column profiles coincide with residue curves. In the special case of columns with an infinite number of trays there is one additional requirement: The column profile should include a pinch point. There are four candidate pinch points in the residue curve map shown in Figure 2.5, namely the three pure component corners

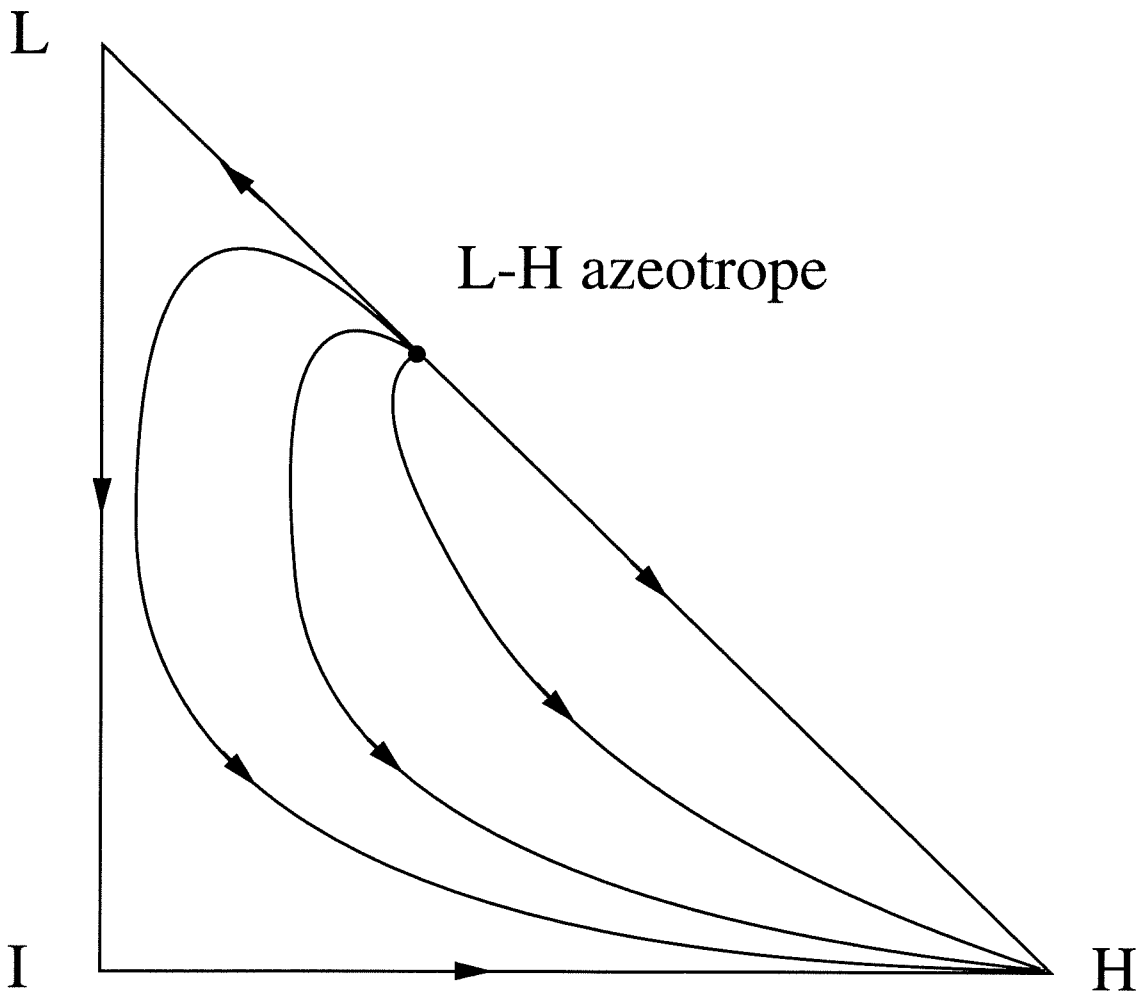


Figure 2.5: Residue curve diagram of a 001 class ternary mixture.

and the azeotrope. Therefore, in the ∞/∞ case, the only acceptable columns belong to one of the following types:

- I. Columns whose distillate composition is that of the azeotrope (unstable node). In this case, the column profile starts from the azeotrope (top of the column), follows a residue curve and ends at an arbitrary point on the same residue curve (bottom product).
- II. Columns whose bottom product composition is pure heavy component (stable node). In this case, the column profile starts from an arbitrary point in the composition triangle, follows the residue curve that passes through this starting point and ends at the heavy component corner (bottom product).
- III. Columns whose composition profiles run along the edges of the triangle and contain at least one of the saddle corners (light and intermediate component corners). In this case, the top and bottom products lie on the edges of the triangle.

In the ∞/∞ case, given a feed composition and a feed flowrate F , the only unspecified parameter is the distillate flow rate D (the bottom flow rate is $B = F - D$ from the overall material balance). In order to find whether multiple steady states can occur (i.e. whether different column profiles correspond to the same value of D) we find all possible composition profiles by tracking the distillate and bottoms in the composition triangle, starting from the column profile with $D = 0$ and ending with the column profile with $D = F$. That is, we perform a bifurcation study (continuation of solutions) using the distillate flow as the bifurcation parameter. This task can be achieved because in the ∞/∞ case a continuation of solutions can be carried out based on physical arguments only. The light component mole fraction in the distillate x_{DL} is recorded along this “continuation path.” The analysis that will follow can be applied to any feed composition but just for simplicity, we assume a feed that lies on the line connecting the azeotrope and the corner I. Therefore, $F = L + I + H$ and $L/(L + H)$ equals the azeotropic composition of the light component.

If $D = 0$ then $B = F = L + I + H$ and therefore the composition of the bottom product coincides with that of the feed F . Hence the bottom product composition is an interior point of the composition triangle (i.e. it does not lie on an edge). The only acceptable column profile (as defined above) that ends (bottom product) at an interior point of the triangle is the one that starts (top of the column) from the azeotrope and follows the residue curve that the bottoms composition lies on. This is a type I column profile. Figure 2.6a shows the column profile for $D = 0$. Therefore, in this case, $x_{DL} = L/(L + H)$, the azeotropic composition.

Using this as a starting profile, we will find all possible type I column profiles for the given feed. Since, for this type of profile, the top of the column coincides with the azeotrope, the material balance line is a segment of the line connecting the azeotrope, the feed and the intermediate component corner (for this particular choice of feed composition). Therefore the bottom composition (B) can be any point on the line segment between the feed F and the intermediate component corner (I). Figure 2.6b illustrates a type I column profile with the aforementioned characteristics. As B moves along the FI line segment from F to I the line BF continuously lengthens. Therefore, according to the lever material balance rule, the bottoms flow decreases monotonically from the initial F to I while the distillate flow will increase monotonically from initially 0 to $L + H$. The composition of L in the distillate (x_{DL}) for all type I column profiles is kept constant and equal to the azeotropic composition $L/(L + H)$. Therefore, a column profile of type I (similar to that of Figure 2.6b) exists for $0 < D < H + L$.

Figure 2.6c shows the profile with the bottoms composition B located at the intermediate component corner (I) and the distillate composition located at the azeotrope. In this case, $D = H + L$ and $B = I$. Both B and D lie on an edge of the composition triangle and therefore in this case the column profile belongs to type III. Using this as a starting profile, we will find all possible type III column profiles for the given feed.

In this type of profiles, both D and B must lie on the edges of the triangle. There exist two alternative routes: B should move along either the IL edge or the IH edge.

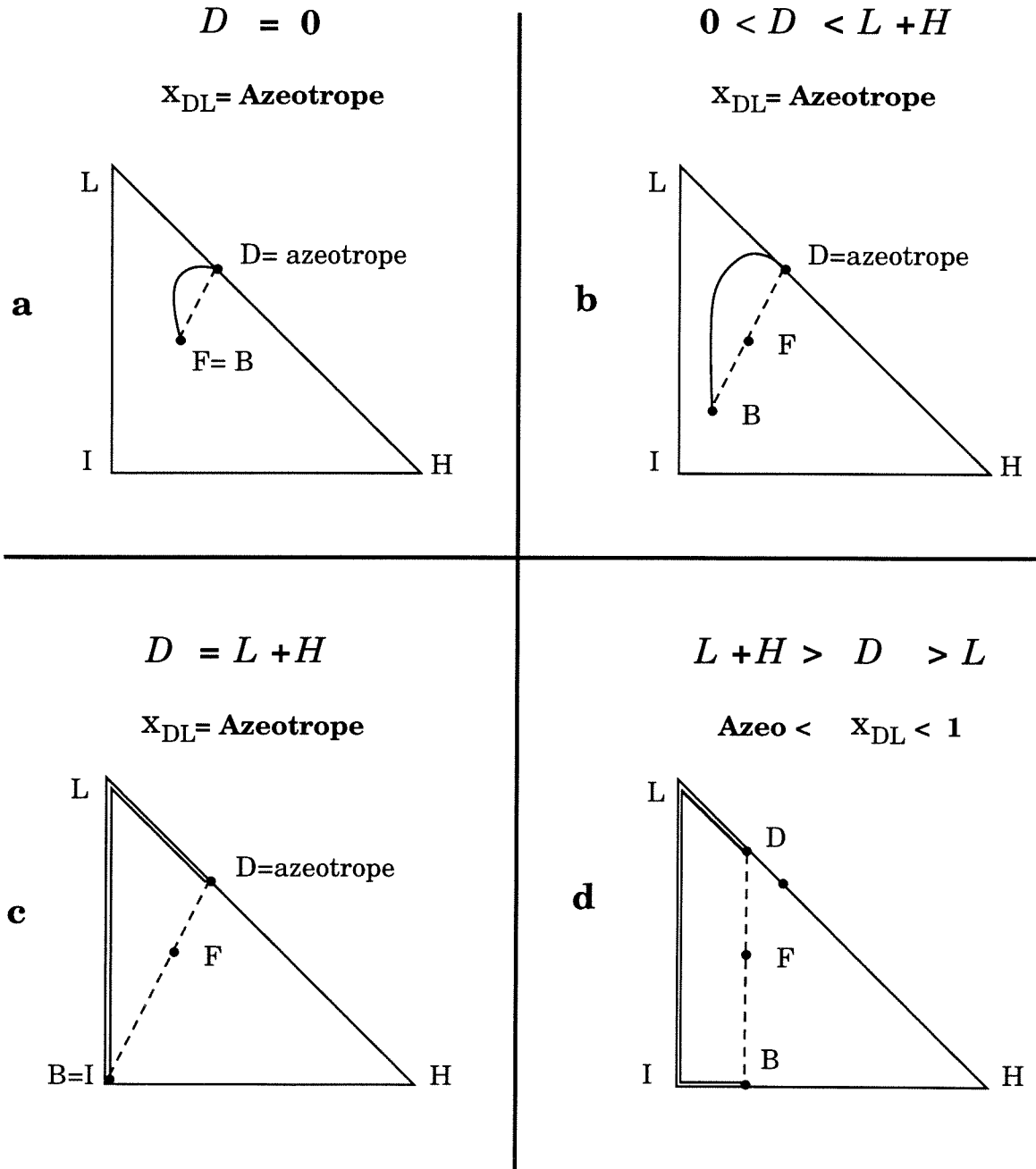


Figure 2.6: a-d. Column profiles with infinite number of trays at infinite reflux.

In the first case, the material balance implies that D has to move on the line segment between the azeotrope and the heavy component corner (H). This is not allowable though because there is no residue curve connecting D and B. In the second case, D has to move along the line segment between the azeotrope and the light component corner while B lies on the IH edge. In this case, there exists a residue curve connecting B and D.

Figure 2.6d illustrates such a column profile. Since D lies on the LH edge the composition of the intermediate component I in the distillate is zero and therefore the whole amount of I fed into the column is recovered in the bottom product. Because B lies on the IH edge, there exists some amount of heavy component in the bottom product while the whole amount of L fed is recovered entirely in the distillate. Therefore $B > I$ and consequently $D < H + L$. As D moves along the LH side from the azeotrope to the light component corner, the amount of the heavy component in the distillate decreases and consequently the distillate flow decreases monotonically from $L + H$ to L (when D is located at the light component corner). Therefore, a column profile of type III similar to that shown in Figure 2.6d exists for $L + H > D > L$. Since all the light component fed is recovered in the distillate, $x_{DL} = L/D$. Therefore along this part of the continuation path, the light component concentration in the distillate increases monotonically from $L/(L + H)$ to 1.

Figure 2.6e shows the profile with the distillate composition D located at the light component corner (L). In this case $D = L$ and $B = I + H$. As B moves further along the IH side towards the H corner, D moves along the LI edge towards the corner I. Figure 2.6f illustrates such a type III column profile. In this case, D contains no heavy component, some amount of the intermediate component and all the light component fed. Consequently, B contains no light component, some amount of the intermediate component and all the heavy component fed into the column. As B moves along the IH edge towards the heavy component corner the bottom product flow decreases monotonically from the initial $I + H$ to H (when B is located at the H corner). Consequently along this part of the continuation path the distillate flow increases monotonically from L to $L + I$. Therefore a column profile of type III similar to that

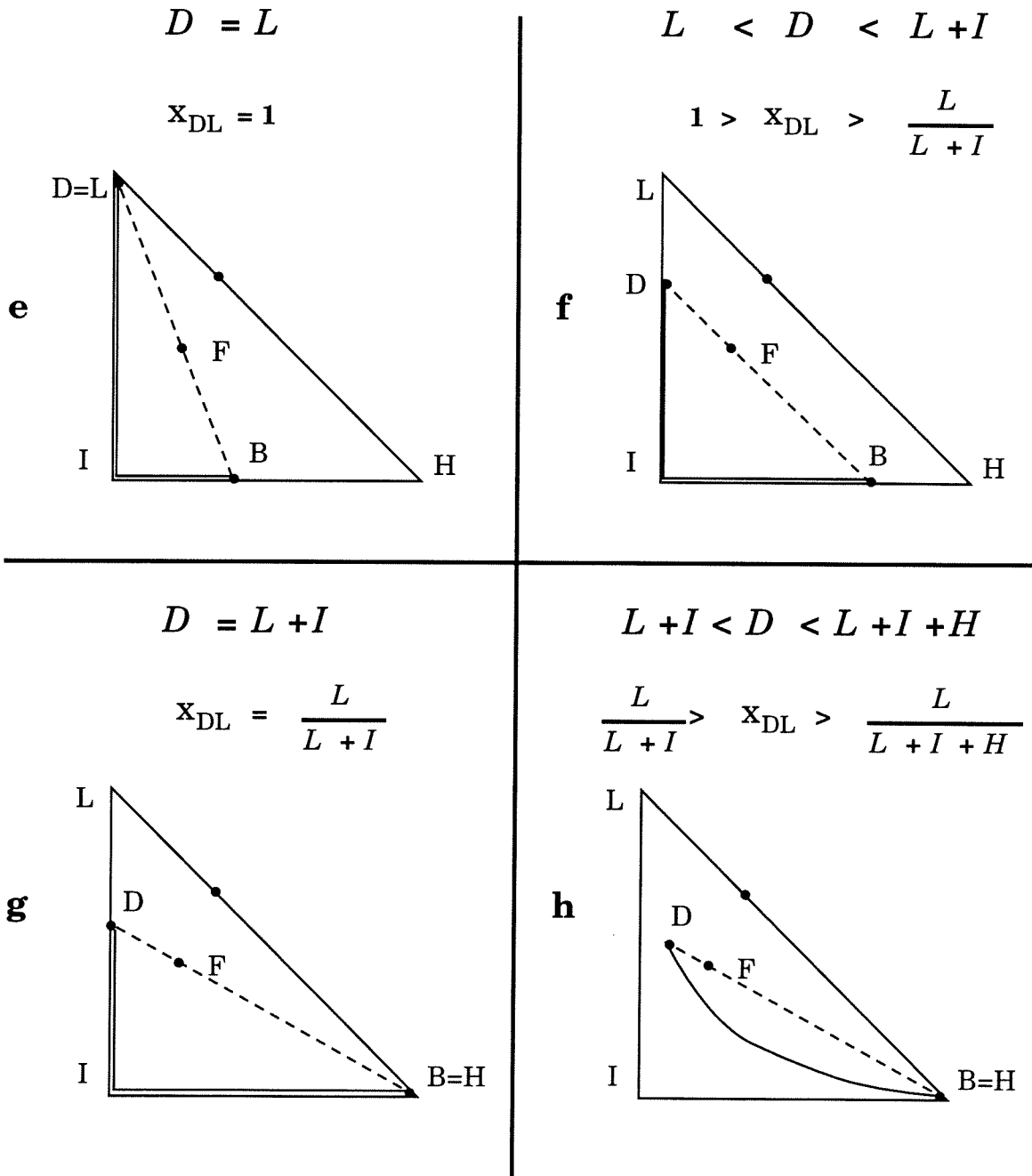


Figure 2.6: e-h. Column profiles with infinite number of trays at infinite reflux.

shown in Figure 2.6f exists for $H < D < I + H$. Along this part of the continuation path, $x_{DL} = L/D$ and hence x_{DL} decreases monotonically from 1 to $L/(L + I)$.

Figure 2.6g shows the column profile with the bottoms composition B located at the heavy component corner (H). In this case $B = H$, $D = L + I$ and $x_{DL} = L/(L + I)$. B is not allowed to move along the HL edge because a residue curve connecting B and D does not exist. Therefore all type III profiles have been found. The last case to be examined is the type II profiles. In this case the bottoms product composition is 100% heavy component (H corner). Therefore, the material balance line lies on the line connecting the feed F and the heavy component corner H. Hence, the distillate composition D can be any point on this line between the feed F and the LI edge. Figure 2.6h shows a type II column profile with the aforementioned characteristics. As D moves towards F, the length of DF decreases. Therefore, according to the lever material balance rule, the distillate flow increases monotonically from the initial $I + L$ to $I + L + H (= F)$ while the bottoms flow decreases from H to zero. Therefore a column profile of type II similar to that shown in Figure 2.6h exists for $I + L < D < I + L + H = F$. Along this part of the continuation path, the composition of L in the distillate decreases from $L/(L + I)$ to $L/(L + I + H)$ according to the rule $x_{DL} = L/D$. Finally, the endpoint of this exhaustive search for all possible column profiles is the column profile with $D = F$, $B = 0$ and $x_{DL} = x_{FL}$.

Now, we put all these pieces together by recording x_{DL} vs. D in a diagram (Figure 2.7). In the beginning as D increases from zero to $L + H$, x_{DL} remains constant at $L/(L + H)$ (the azeotropic composition). Then D decreases from $L + H$ to L while $x_{DL} = L/D$ and therefore increases from $L/(L + H)$ to 1. Then D increases again from L to $L + I$ and finally to F while $x_{DL} = L/D$ and hence decreases from 1 to $L/(L + I)$ and finally to L/F (the feed composition). For illustrative purposes only, in Figure 2.7 we draw two separate curves, ce and eh, although they are actually coinciding ($x_{DL} = L/D$). Points a - h in Figure 2.7 correspond to the column profiles shown in Figures 2.6a - 2.6h. Figure 2.7 shows that for D between L and $L + H$ there exist three steady states (points 1 - 3):

- Point 1 always corresponds to a column profile of type I like the one depicted

Three Steady States exist for
 $L + H > D > L$

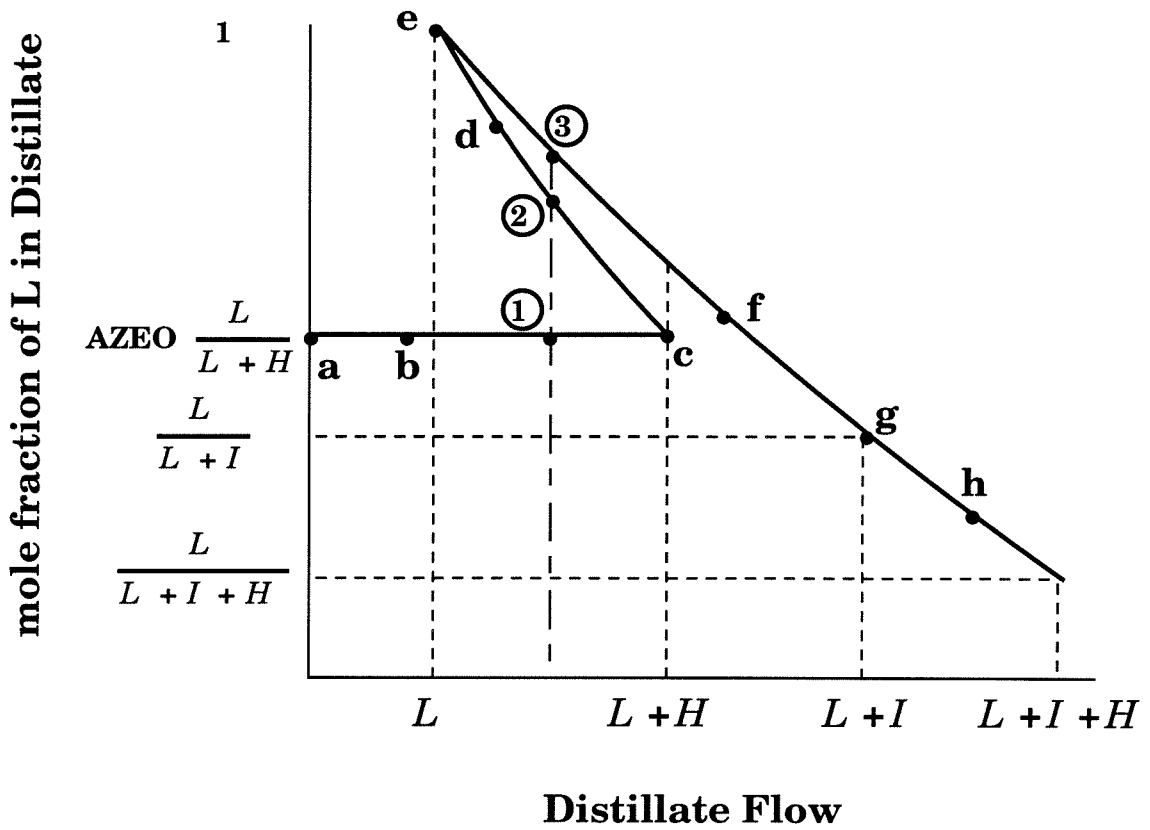


Figure 2.7: Mole fraction of L in the distillate along the continuation path.

in Figure 2.6b.

- Point 2 always corresponds to a type III column profile where the distillate composition lies on the line segment between the azeotrope and L (similar to Figure 2.6d).
- For point 3 there are two cases:
 - If $I < H$ and $D > L + I$ then point 3 corresponds to a type II column profile (similar to that of Figure 2.6h).
 - In the case that $I > H$ (Figure 2.7) as well as in the case that $I < H$ but $D < L + I$, point 3 corresponds to a type III column profile where the distillate composition lies on the LI edge (similar to that in Figure 2.6f).

In our analysis, a special choice of feed composition has been used. It is very simple to apply the same procedure to any feed composition and prove that for any feed composition inside the composition triangle three steady states exist. Therefore, for this class of residue curve diagrams, namely the 001 class, three steady states exist for any feed composition. Moreover, in this case the existence of multiplicities is independent of the thermodynamic model used to describe the vapor - liquid equilibrium.

Given any ternary mixture, its residue curve diagram and a feed composition, it is very simple to conclude whether multiple steady states can occur in the ∞/∞ case by applying the procedure described above. Next, we examine the key issues that lead to the existence of these multiple steady states.

2.3.2 Analysis

In the previous section, we tracked a “path” generating all possible column profiles starting from the column profile with $D = 0$ (type I) and ending at the column profile with $D = F$ (type II). In the beginning D increases, then decreases and then increases again. The key feature that brought about the multiple steady states is that

in a segment along this “path” D decreased. Therefore, in order to find rules for the existence of multiple steady states, we have to first answer why D decreased along the continuation path.

In this section, we assume that distillation boundaries are straight lines (this assumption will be dropped later). Therefore, any distillation region containing n ($n \geq 3$) singular points is an n -polygon. In every distillation region there is one unstable node (the origin of all residue curves in the region), one stable node (the endpoint of all residue curves in the region) and $n-2$ saddles. Finally, we assume that F is an interior point of a distillation region. It is easy to show that for feeds on a straight distillation region boundary, D cannot decrease along the continuation path. This is the case for any feed located on the edges of the triangle (binary feeds) in Figure 2.5.

Using arguments similar to those in the previous section, it is easy to show that along the continuation path, first we track all possible type I column profiles, then those of type III and last all type II column profiles. Moreover, again using the arguments which were discussed in the previous section, it can be proven that:

Fact 1 *Along the continuation path, D increases monotonically as we track all type I and type II column profiles.*

Therefore, a decrease in D can only occur as we track the type III column profiles, i.e., columns whose composition profiles run along the edges of the distillation region where F is located and contain at least one of the saddle singular points. In this case, the top and bottom products lie on the edges of the distillation region. Next we will show the following:

Fact 2 *Along the continuation path, D increases monotonically for all type III column profiles that contain only one saddle singular point.*

Figure 2.8 shows a column profile (DsB) that contains only one saddle point (s). The lines ds and sb are distillation region boundaries. The arrows on ds and sb show the direction of the residue curves; this direction coincides with the direction of the continuation path. $D'sB'$ is another, “later,” column profile along this path. We examine what happens to D as we move from DsB to $D'sB'$.

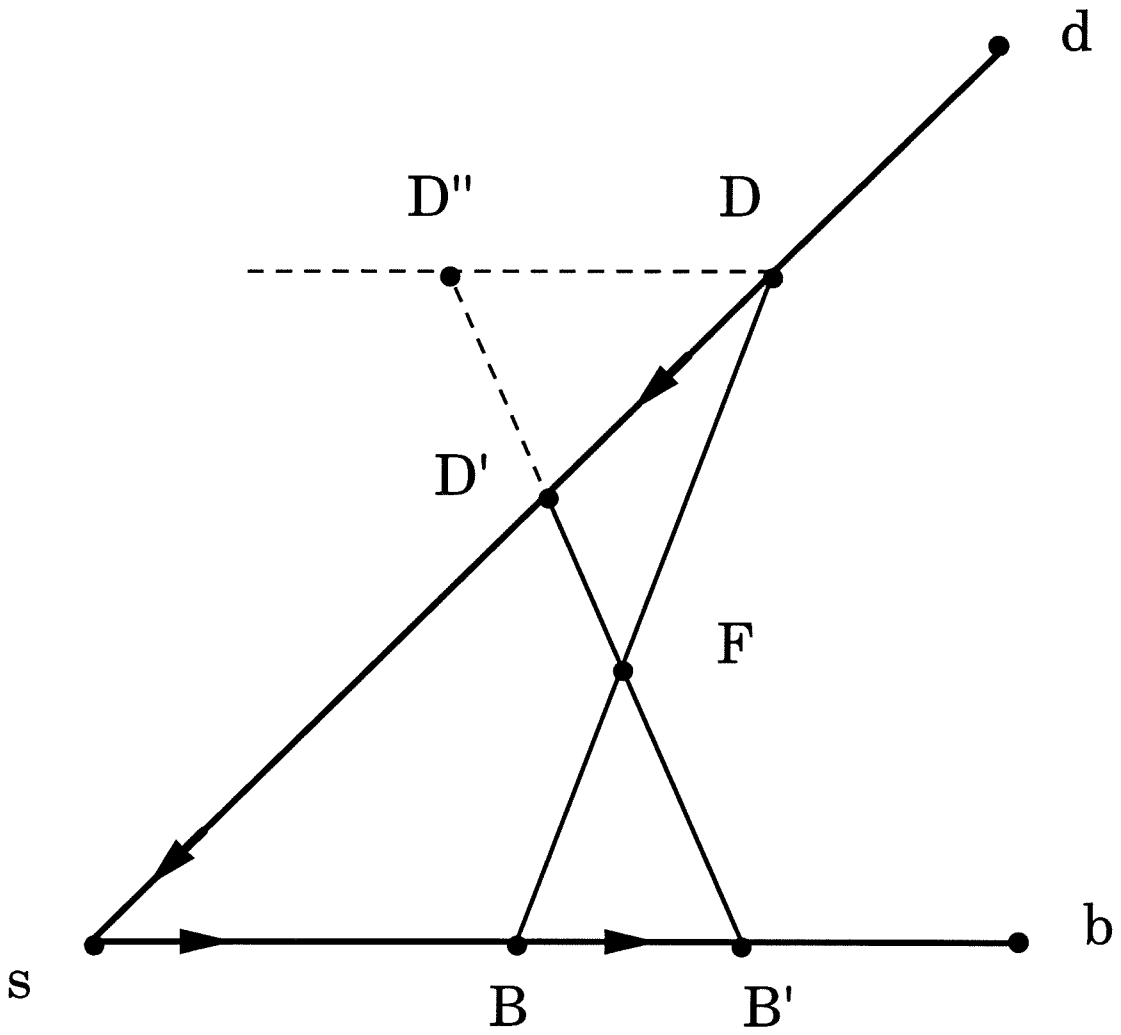


Figure 2.8: D increases monotonically for column profiles that contain only one saddle singular point.

Draw the line that is parallel to BB' and passes through D . Name D'' the point where this line intersects the $D'B'$ line. By construction, $FB/DF = FB'/D''F$. Since $D''F > D'F$ then $FB/DF < FB'/D'F$. Therefore by the lever material balance rule, we conclude that D increases along the continuation path. This result is independent of the angle dsb , and therefore D increases monotonically for all type III column profiles that contain only one saddle singular point. Q.E.D.

Note that fact 2 is equivalent to the following:

Fact 3 *A decrease in D can only occur as we track type III column profiles that contain at least two saddles.*

Two consequences of fact 3 are:

- (1) If multiplicities exist, one of the multiple steady state profiles will contain at least two saddles.
- (2) A necessary condition for the existence of this type of multiplicities is that the residue curve diagram contains at least two neighboring saddles.

The situation of at least two neighboring saddles arises in 77 out of the 113 possible residue curve diagrams (as classified by Matsuyama and Nishimura, 1977). Among the residue curve diagrams that do not contain two neighboring saddles are the ideal case (000 class) and the case of a heavy entrainer that does not introduce any additional azeotropes (100 class) which are depicted in Figure 2.9. Note also that no more than three steady states can exist in the case of two neighboring saddles while for certain feed compositions it is possible that more than three steady states exist in the case of more than two neighboring saddles.

However, the condition of at least two neighboring saddles is not sufficient for the existence of multiple steady states. There are two additional requirements.

Geometry of the Distillation Boundaries

The existence of multiplicities depends on the geometry of the distillation boundaries that form the two saddles. Figures 2.10a and 2.10b illustrate two cases of two

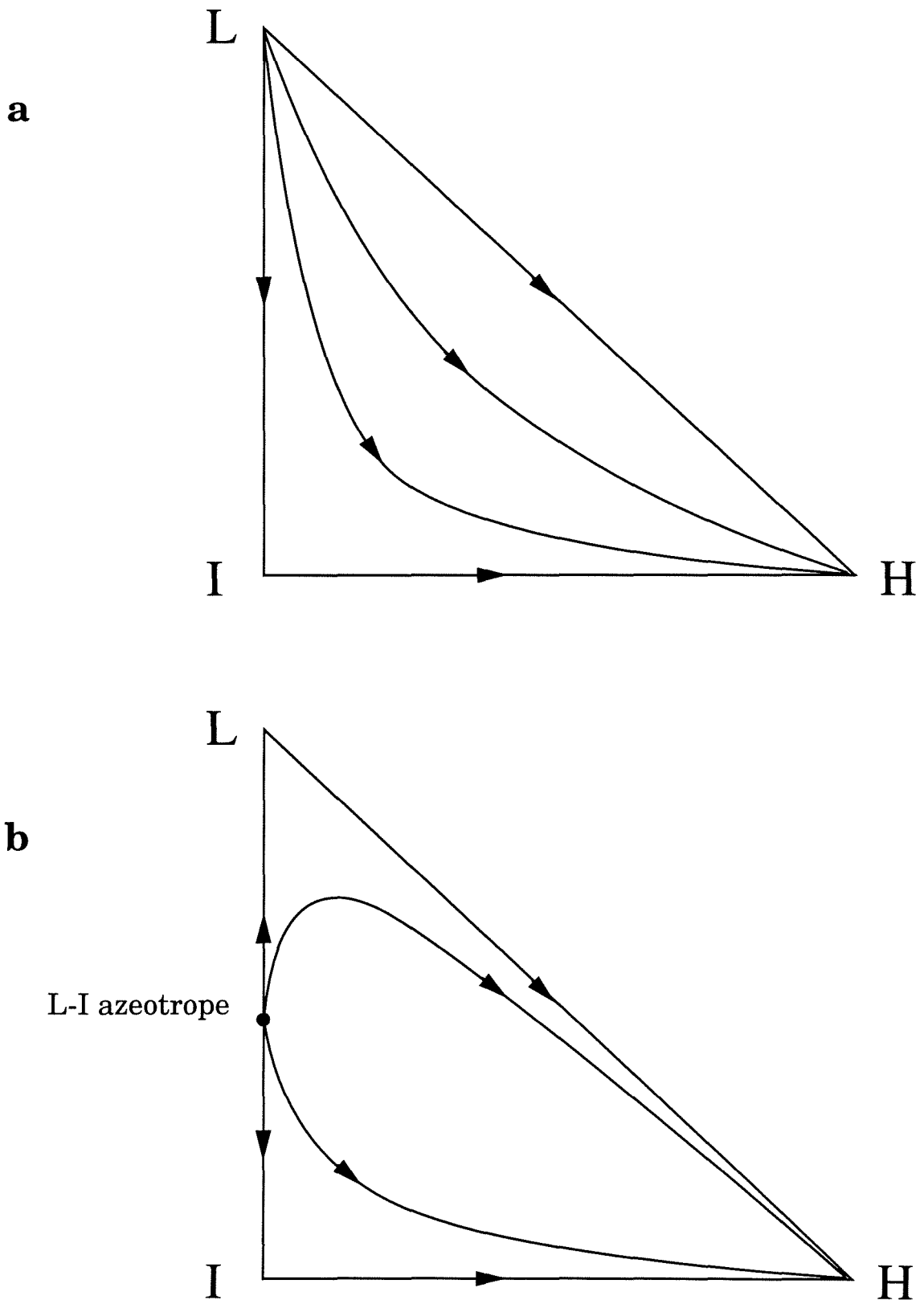


Figure 2.9: Residue curve diagrams of a. a 000 class b. a 100 class ternary mixture.

neighboring saddles. The only difference between the two is the orientation of the ds distillation boundary. In order to check if D increases or decreases along the continuation path, the procedure used for the proof of fact 2 is applied.

In Figure 2.10b, the line from D that is parallel to BB' crosses the $D'B'$ line segment while it does not cross it in Figure 2.10a. Hence in Figure 2.10a, $D''F > D'F$ while $D''F < D'F$ in Figure 2.10b. As a result D increases in Figure 2.10a whereas D decreases in Figure 2.10b. Therefore multiple steady states exist only for the situation depicted in Figure 2.10b. Note that the existence of multiple steady states depends on the relative position of the boundaries ds and $s'b$ while the location of the ss' boundary does not play any role. If the boundaries ds and $s'b$ are parallel then D remains constant along this part of the continuation path. Therefore, in this case there exists an infinite number of profiles with different product compositions for a constant distillate flow D .

In summary, for the existence of multiplicities it is required that (*geometrical condition*): As we move along the continuation path from D to D' and accordingly from B to B' , the line that passes from D and is parallel to BB' crosses the $D'B'$ line segment.

Appropriate Feed Composition

Even if a residue curve diagram contains two neighboring saddles with the appropriate geometry (as described above) for the existence of multiplicities, there might be some feed compositions for which multiple steady states do not exist. Figure 2.11 shows a residue curve diagram that belongs in the 231 class. In this diagram there are two distillation regions. In the lower region there are three saddles (two of them neighboring) while in the upper region there is only one saddle. Therefore if the feed composition lies in the upper region, a unique steady state exists for each value of D . However, placing the feed in the lower region is not sufficient for the existence of multiple steady states.

As it can be seen from Figure 2.11, ab and Ic form the only pair of boundaries that enables the existence of multiple steady states. Hence, the only feed compositions

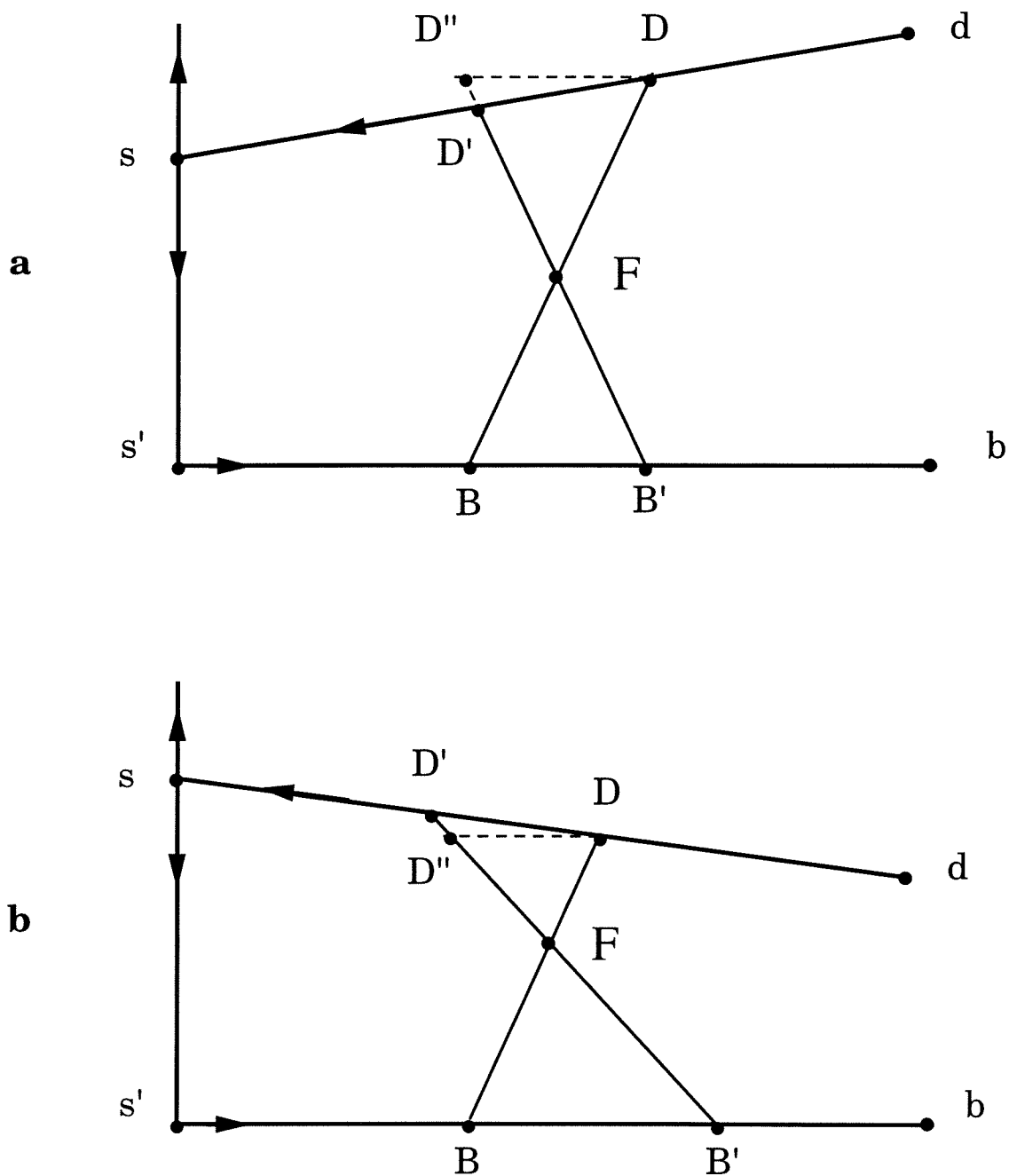


Figure 2.10: Geometry of the distillation region boundaries. a. D increases b. D decreases along the continuation path.

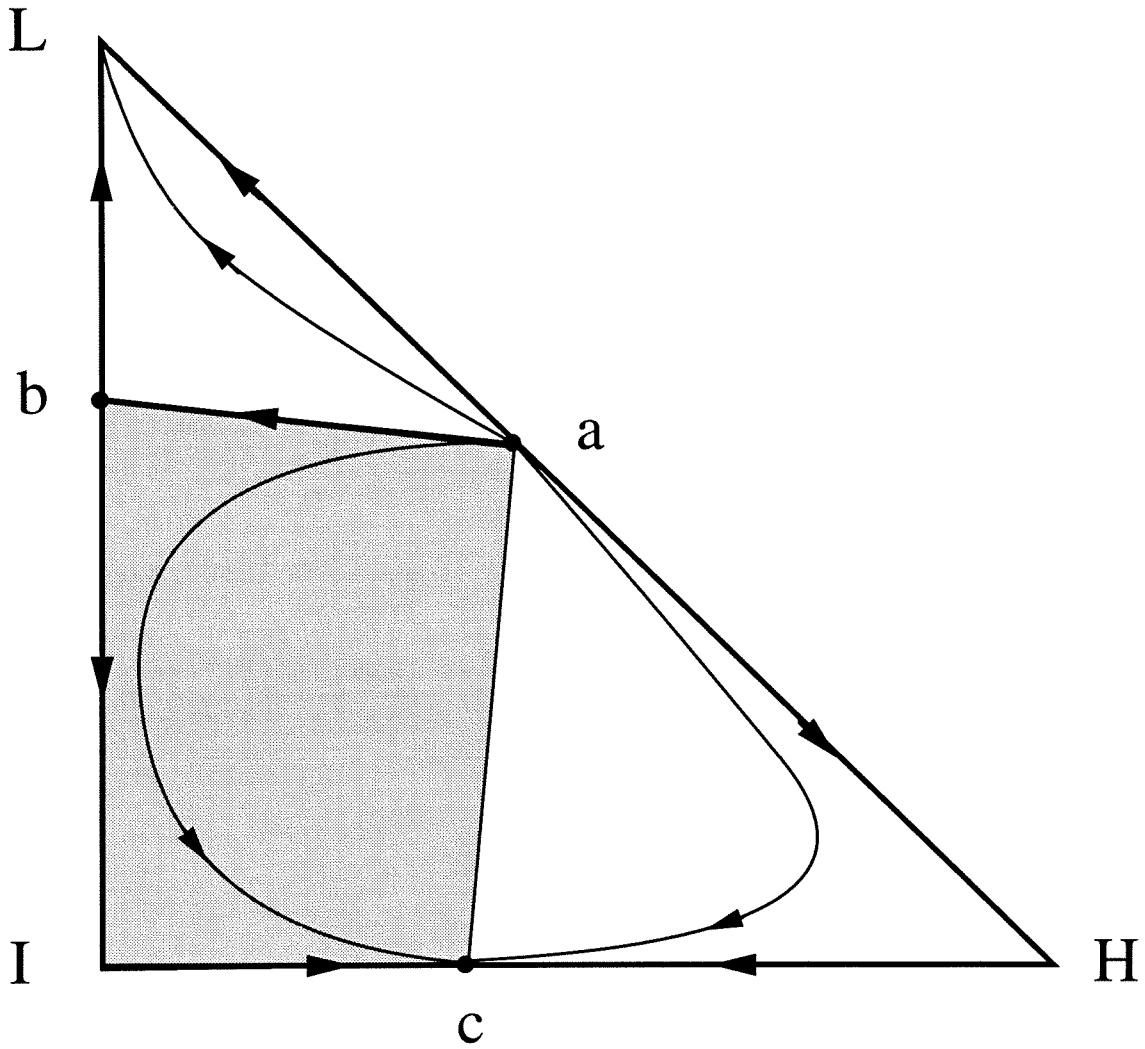


Figure 2.11: Residue curve diagram of a 231 class ternary mixture and the appropriate feed region.

that will exhibit multiple steady states are those that can be separated in a distillate lying on ab and a bottom product lying on Ic for some value of D . Therefore, multiple steady states exist for any feed located in the convex hull formed by ab and Ic (shaded region in Figure 2.11).

In summary, multiple steady states exist only for the feed compositions that lie in the convex hull formed by a pair of distillation region boundaries that satisfy the geometrical condition described above.

Summary

In this section we studied the ∞/∞ case for a ternary mixture under the assumption of straight line boundaries. We found a necessary condition for the existence of multiplicities (at least two neighboring saddles). Furthermore, the conditions developed above for the geometry of the boundaries and the appropriate feed compositions constitute a necessary and sufficient condition for the existence of multiple steady states in ∞/∞ case.

Although we assumed that the line connecting two singular points (distillation boundary) is straight, fact 1 is independent of the shape of the boundary. Moreover, the discussion about the geometry of the distillation region boundaries and the appropriate feed compositions can be generalized to curved boundaries. This is the topic of the next section.

2.3.3 Curved Boundaries

Distillation region boundaries that do not coincide with the sides of the composition triangle are often curved and in some cases highly curved. The curvature of the boundary may affect the region of feed compositions that lead to multiplicities because the geometry of the boundaries is changed. This is illustrated by Figure 2.12. This figure is similar to Figure 2.11 with the difference that the interior boundary ab is curved. However, the location of the azeotropes in the composition triangle is the same in both figures. The following interesting result can be easily shown: if multiple

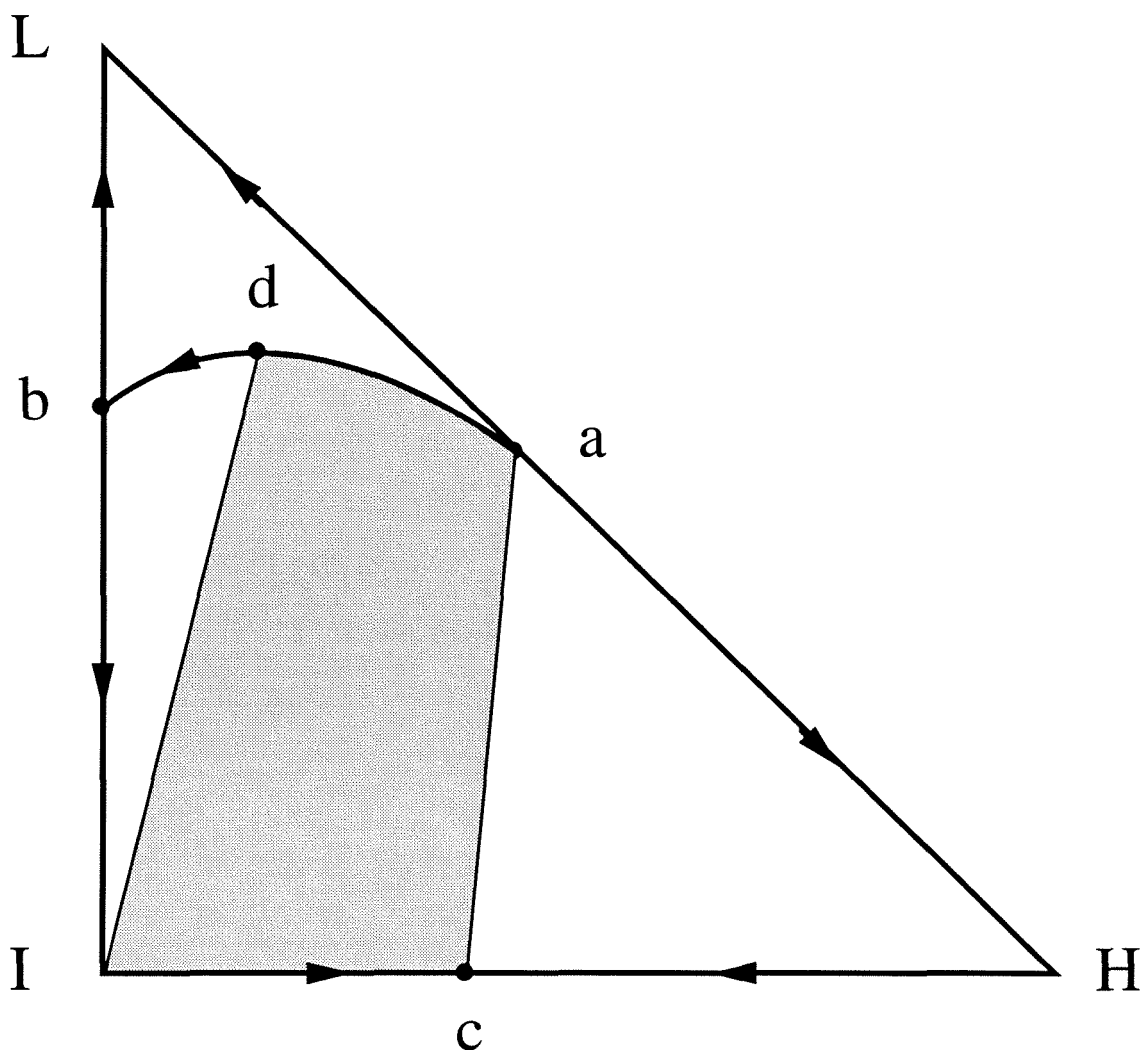


Figure 2.12: The curvature of the boundary affects the appropriate feed region.

steady states exist under the straight boundaries assumption, then, assuming that the azeotropic compositions do not change, these multiplicities still exist even if the boundaries are curved, although the appropriate feed region is changed.

Point d is the point on the boundary ab where the tangent to the boundary is parallel to Ic . It is apparent that the boundary segment ad and the boundary Ic satisfy the geometry requirement for the existence of multiplicities while bd and Ic do not. Therefore, in this case the appropriate feed location is inside the convex hull formed by ad (not ab) and Ic (shaded region in Figure 2.12).

In the previous section we concluded that the occurrence of two neighboring sad-

dles is a necessary condition for multiplicities when boundaries are straight. This is not true in the general case of curved boundaries, because highly curved boundaries can function as “pseudo-saddles” and therefore can induce multiplicities.

Figure 2.13 shows a residue curve diagram belonging to the 021 class. In this figure there is a highly curved boundary that separates the composition triangle in two distillation regions. In each region there are two routes which go from the unstable node to the stable node along the region boundaries (a total of four routes, namely $a \rightarrow L \rightarrow I$, $a \rightarrow H$, $a \rightarrow b \rightarrow I$, $a \rightarrow b \rightarrow H$). In the right region there is only one saddle singular point and in the left region there are two saddles but they are not neighboring. Therefore, if the boundary running from a to b were a straight line, there would not exist multiplicities for this mixture. The boundary ab is curved enough so that there exists a point c on it where the tangent to the boundary is parallel to the IH edge.

Now, the geometrical condition can be applied to check for multiplicities. Note that the distillate and bottoms compositions should lie on the same route and therefore we only have to check the geometrical condition along the four routes mentioned above. Also note that the type III column profile with an infinite number of trays should contain a saddle singular point and therefore this constitutes an additional restriction.

The $a \rightarrow b \rightarrow H$ route contains one saddle point (b). The restriction due to the infinite number of trays implies that the geometrical condition should be checked only for columns whose distillate lies on ab and whose bottom product lies on bH (i.e. columns with distillate and bottom product lying on ab are not permitted in the infinite number of trays case). If the distillate lies on cb then the geometrical condition is not satisfied for any bottoms product on bH . However, if D lies on ac then for any B on bH the geometrical condition is satisfied. Figure 2.14 shows the continuation path of all possible column profiles for a given feed. The ratio FB / DF and therefore D decreases as D moves from a to c and hence multiplicities exist. Similarly, for the $a \rightarrow b \rightarrow I$ route, the condition for multiplicities is satisfied if D lies on ac and the bottoms composition is any point on Ib . Note that the geometrical

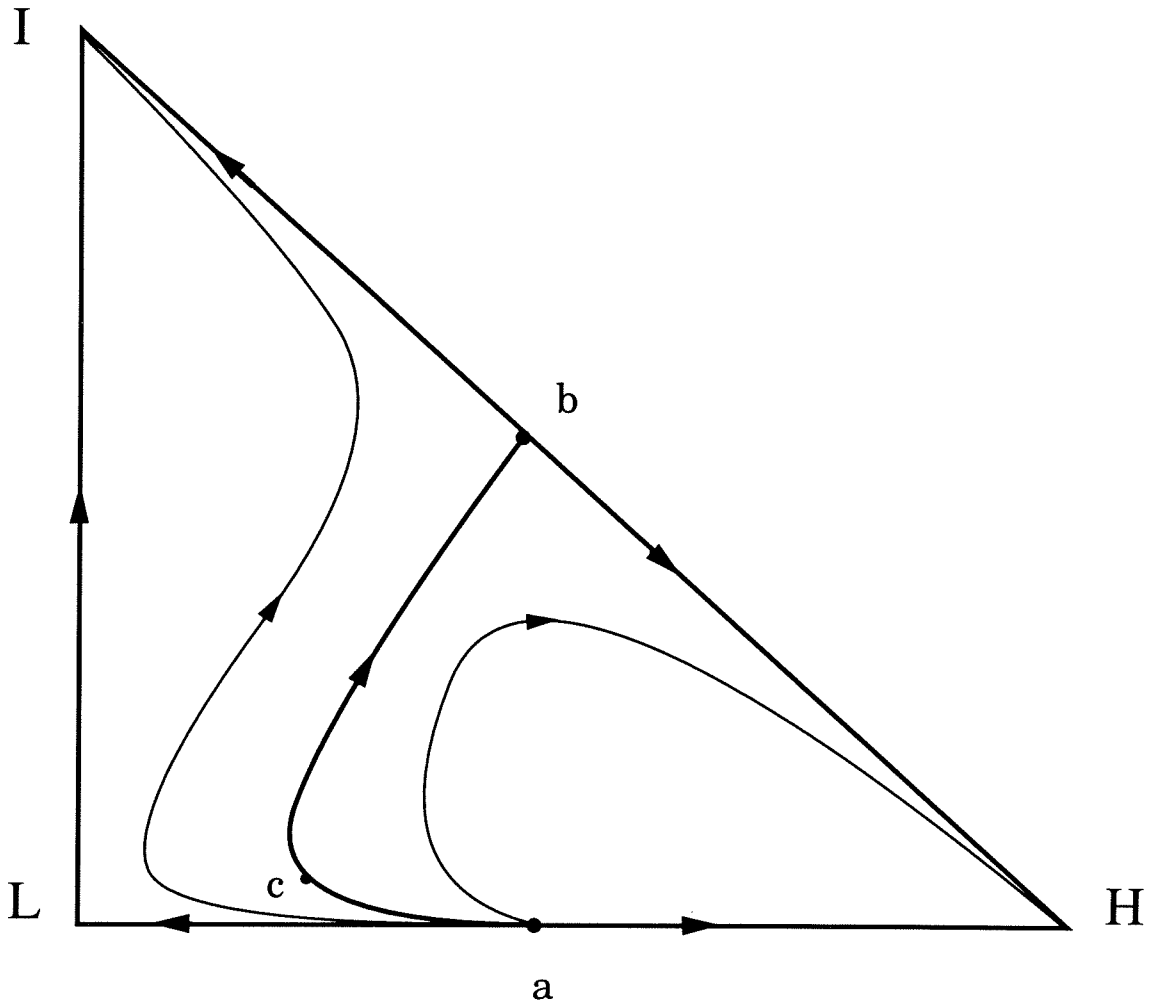


Figure 2.13: Residue curve diagram of a 021 class ternary mixture that contains a highly curved boundary.

condition is not satisfied for any D' but only for D' sufficiently close to D . Also note that the geometrical condition is not satisfied for the other two routes. Therefore multiplicities exist for this mixture for feed compositions which can be separated into a distillate lying on ac and a bottom product lying on Ib or bH , i.e., for feeds located in the convex hull formed by ac and IH .

In the case examined above, provided D lies on ac , the geometrical condition is satisfied for *any* B on IH . This is due to the fact that IH is a straight line. The most general case where both D and B lie on curved boundaries is illustrated by Figure 2.15. In this figure, point e is the location on ab where the tangent to the ab boundary is parallel to the tangent to the bc boundary at point c . Similarly, f is the point on bc where the tangent to the bc boundary is parallel to the tangent to the ab boundary at point a . For some D on ab , there exist *some* B on bc that satisfy the geometrical condition. In general, for each D on ae there exists a *different set* $S_B(D)$ of bottoms compositions that satisfies the geometrical condition. For example if D is located at point a then $S_B(D)$ is the boundary segment fc while if D is located at e the $S_B(D)$ is just the point c . Hence for each D the appropriate feed composition is the convex hull formed by D and $S_B(D)$. Therefore, the feed compositions that exhibit multiplicities lie in the union of all the convex hulls formed by D and the corresponding $S_B(D)$. In Figure 2.15 the appropriate feed region is shaded and it is clear that it does not coincide with the convex hull formed by ae and fc .

However, the aforementioned definition of the appropriate feed region is not absolutely accurate because it does not cover some rare cases that may arise, for example, when the boundaries contain inflexion points. In these cases, $S_B(D)$ may contain an inflexion point and/or it may consist of more than one non-connected boundary segments. Hence, for each D the appropriate feed composition is the union of the areas enclosed by D and each boundary segment that belongs to $S_B(D)$ (not the convex hull formed by D and $S_B(D)$). Accordingly, the feed compositions that exhibit multiplicities lie in the union of all the areas enclosed by D and each boundary segment that belongs to the corresponding $S_B(D)$. Since the above accurate definition of the appropriate feed region is much more complicated than the previous one (involving

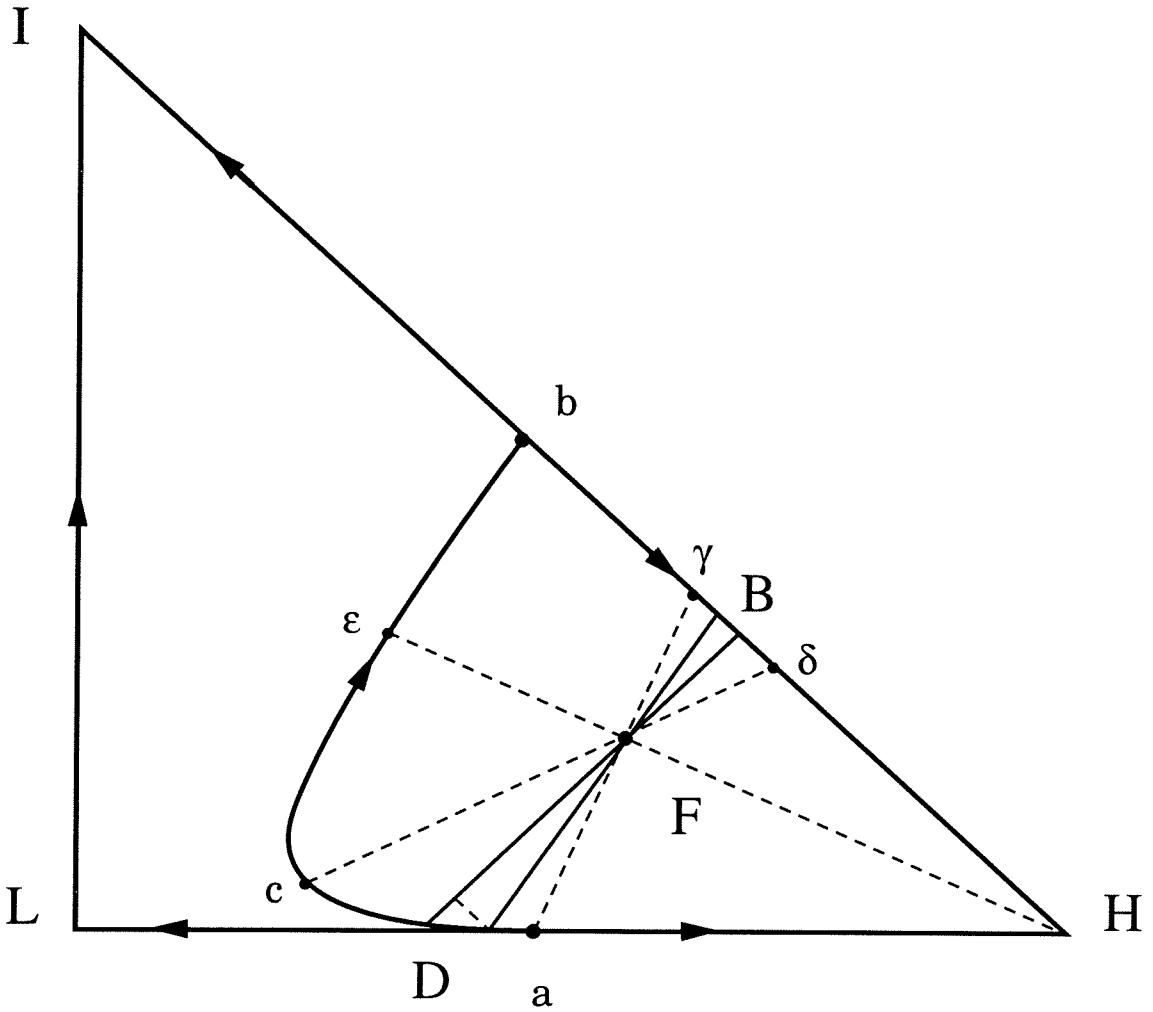
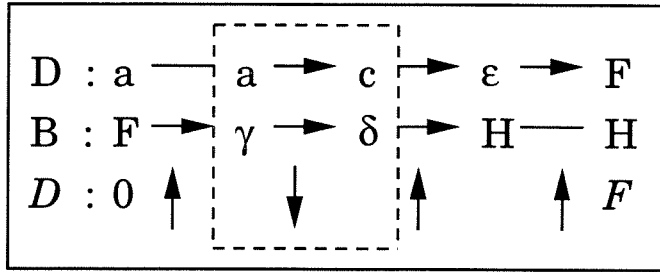


Figure 2.14: Highly curved boundaries can induce multiplicities.

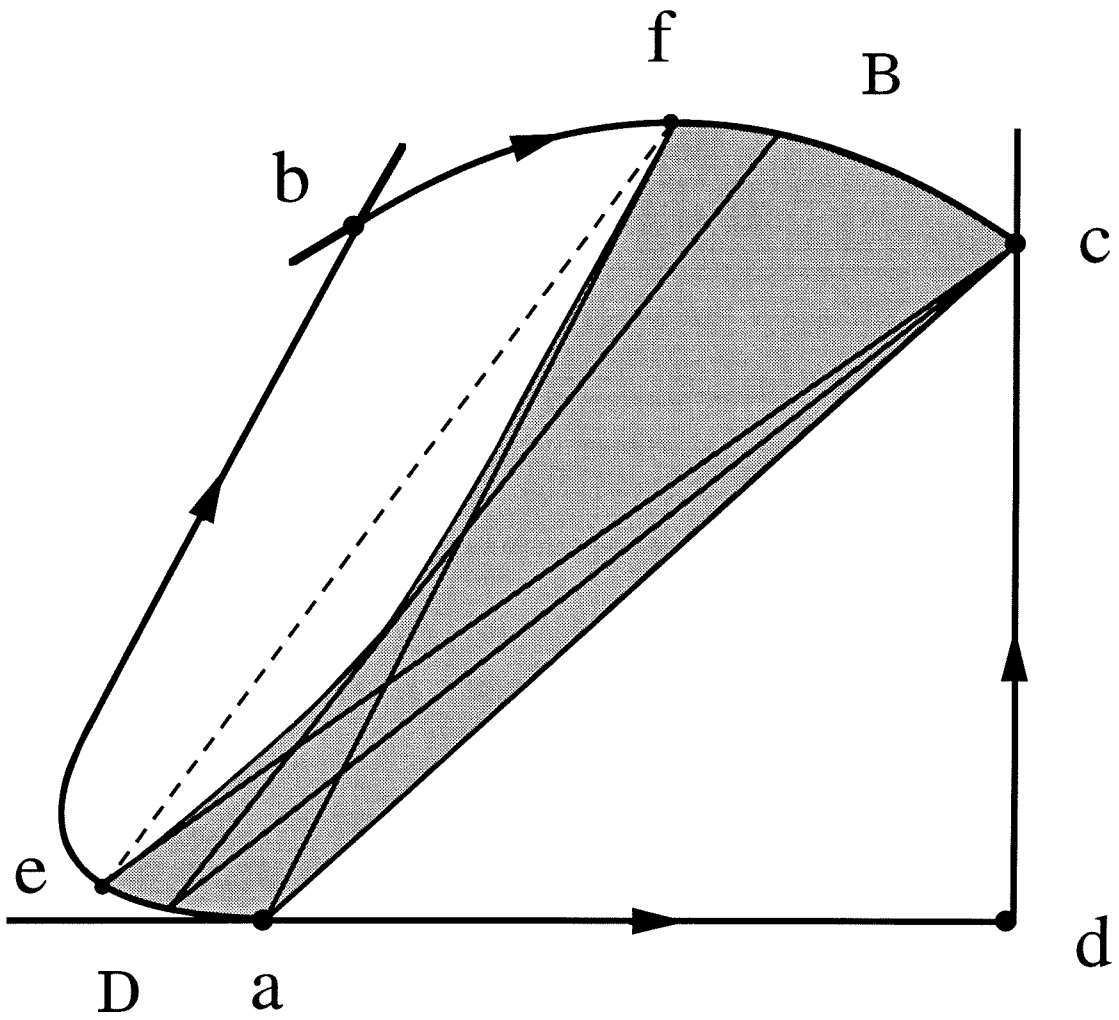


Figure 2.15: The appropriate feed region in the case of two curved boundaries.

the convex hulls), the latter will be used in the following.

2.3.4 A Degenerate Case

A different type of multiplicity occurs when the feed is located on the straight line connecting the unstable node with the stable node of a distillation region. Figures 2.16a and 2.16b show two such cases. Figure 2.16a shows the residue curve diagram of a nonazeotropic ternary mixture. The feed F is located on the LH edge of the triangle and hence $F = L + H$ (binary feed). It is very easy to show that as we track the continuation path starting from the column profile with $D=0$ and ending at the column profile with $D=F$, the distillate flow D increases monotonically, D and B always lie on LH and actually the whole column profiles lie on LH (binary profiles). However, some alternative profiles exist when $D=L$. In this case, the distillate composition D is located at the light component corner L and the bottoms composition B is located at the heavy component corner H . Since all residue curves originate from L and end at H , there exists an infinite number of alternative column profiles when $D=L$. Except for the binary profile, the rest of the profiles seem somewhat strange since they correspond to feeding a ternary column with a binary mixture (L and H) which is sharply separated into its constituents while the third intermediate component is “trapped” in the column.

The situation is similar (but somewhat less strange since the feed is a ternary mixture) in Figure 2.16b depicting a residue curve diagram belonging in the 222-m class. An infinite number of column profiles exists when D is located at the ternary azeotrope and B at a pure component corner. This type of multiplicity (infinite number of profiles with the same product compositions for a specific distillate flowrate) may be similar to the ones reported by Kienle and Marquardt (1991) and Helfferich (1993). The practical implications of the degenerate type of multiplicities reported here are unclear, i.e., we don’t know whether (1) these multiplicities are an artifact of the ∞/∞ case and therefore do not exist for finite columns at finite reflux or (2) some finite number of multiple steady states still exist for finite columns at finite reflux.

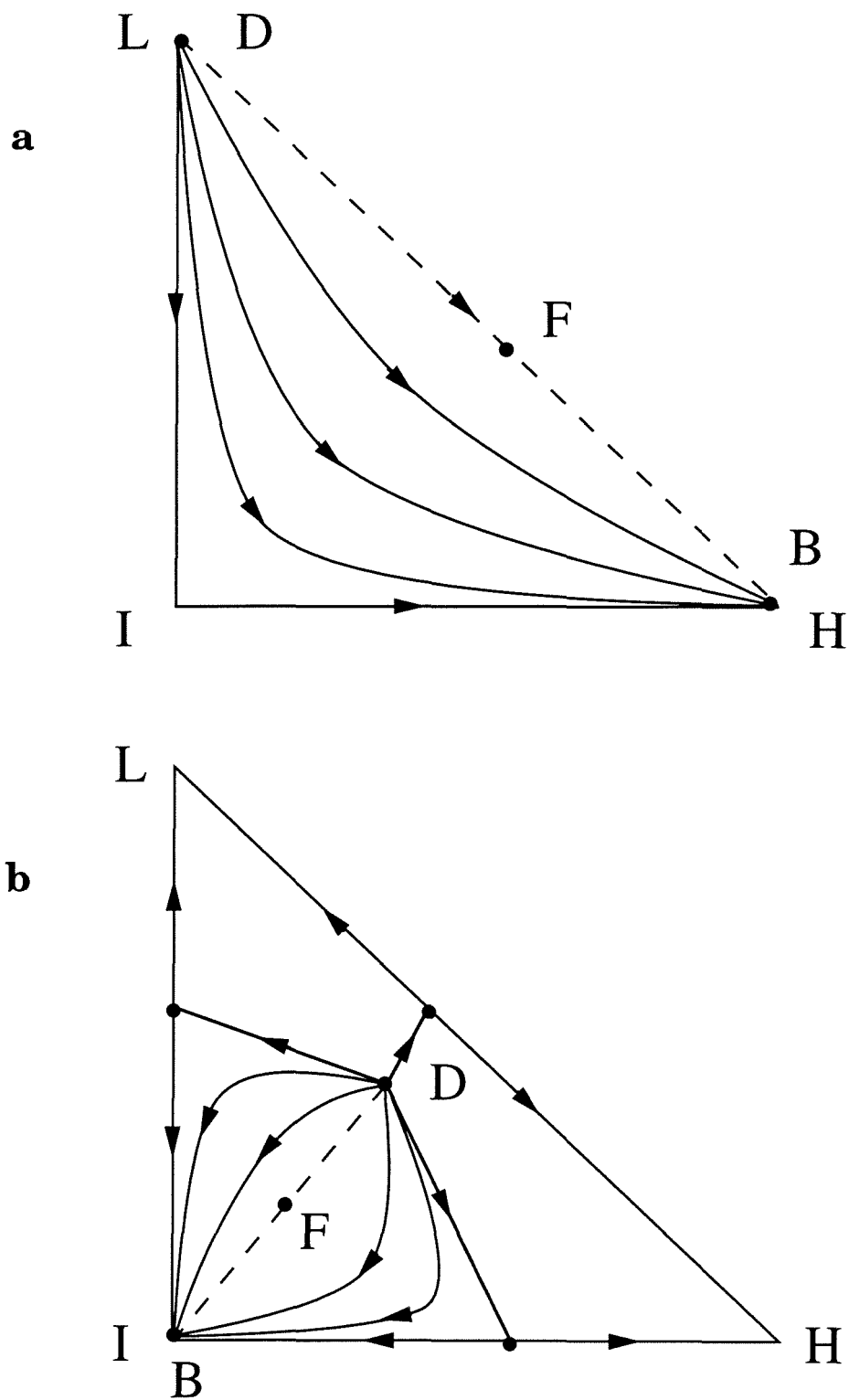


Figure 2.16: Degenerate multiplicities for (a) a 000 class and (b) a 222-m class ternary mixture.

Hence, a more thorough investigation of this topic is needed.

2.3.5 Summary

In this part we examined in detail the existence of multiple steady states in the ∞/∞ case of a ternary mixture. More specifically, we answered the following questions: Given a ternary mixture and its residue curve diagram,

- (1) find whether multiple steady states exist for some feed composition and
- (2) locate the feed composition region that lead to these multiple steady states.

The necessary and sufficient geometrical condition for the existence of multiple steady states (question 1) is summarized in the following:

The continuation path is defined as the path generating all possible column profiles starting from the profile with $D=0$ and ending at the profile with $D=F$. Multiple steady states occur when D decreases along this path. This can be checked by the following procedure: Pick a distillate D and a bottom product B , both located on some distillation region boundaries and such that the column profile that runs from D to B along the distillation region boundaries contains at least one saddle singular point (type III column profile). Now pick D' and B' sufficiently close to D and B respectively and such that the column profile from D' to B' is a "later" profile along the continuation path. For the existence of multiple steady states it is required that: As we move along the continuation path from D to D' and accordingly from B to B' , the line that passes from D and is parallel to BB' crosses the $D'B'$ line segment.

The condition for the appropriate feed region (question 2) is summarized in the following:

Pick a distillate D . Find the set of all bottom products such that the geometrical condition is satisfied for the picked D . Name this set $S_B(D)$. For the chosen D the appropriate feed composition is the convex hull formed by D and $S_B(D)$. Pick another distillate and repeat. In general, for each distillate there exists a different set of bottoms compositions that satisfies the geometrical condition. Therefore, the feed

compositions that lead to multiple steady states lie in the union of all the convex hulls formed by D and the corresponding $S_B(D)$.

2.4 Finite Reflux and Finite Number of Trays

The ∞/∞ case is the limiting case of high reflux and a large number of trays. Therefore, if the geometrical condition is satisfied for a given residue curve diagram then multiplicities will exist for some sufficiently large finite reflux and finite number of trays. However, the inverse is not true. The geometrical condition is only a sufficient condition for the existence of multiplicities when the reflux and the number of trays are finite. At infinite reflux, the column profiles coincide with residue curves. This is not true at finite reflux. Moreover, column profiles at finite reflux depend on the location and the number of the feed streams. Therefore, the residue curve map cannot be used for the study of the finite reflux and finite number of trays case.

In this section, first we present steady state bifurcation results for the mixture acetone (L) - heptane (H) - benzene (I-E) which show that the prediction for the existence of multiple steady states in the ∞/∞ case carries over to columns operating at finite reflux and with a finite number of trays. We further show that, although the predictions were made in the ∞/∞ case, it does not mean that multiple steady states do not exist for realistic operating conditions (low reflux and number of trays). However, apart from the fact that the ∞/∞ case predictions carry over, the results presented here should not be generalized because they are specific to the particular example. The column characteristics are depicted in Figure 2.17. In this column, a mixture of 90% acetone and 10% heptane (the azeotropic composition is 93% acetone and 7% heptane) is separated using benzene as the entrainer. Acetone is recovered in the distillate while the bottom product (heptane and benzene) is fed to the entrainer recovery column (Figure 2.2) from which heptane is recovered and benzene is recycled to the azeotropic column. For this example, the distillate, reflux and entrainer flows as well as the number of stages are treated as parameters. The bifurcation calculations were conducted with AUTO, a software package developed by Doedel (1986). Liquid

<u>Concentration</u>	<u>Entrainer feed</u>	<u>Azeotropic feed</u>
Acetone (L)	0.0	0.90
Heptane (H)	0.0	0.10
Benzene (I-E)	1.0	0.0

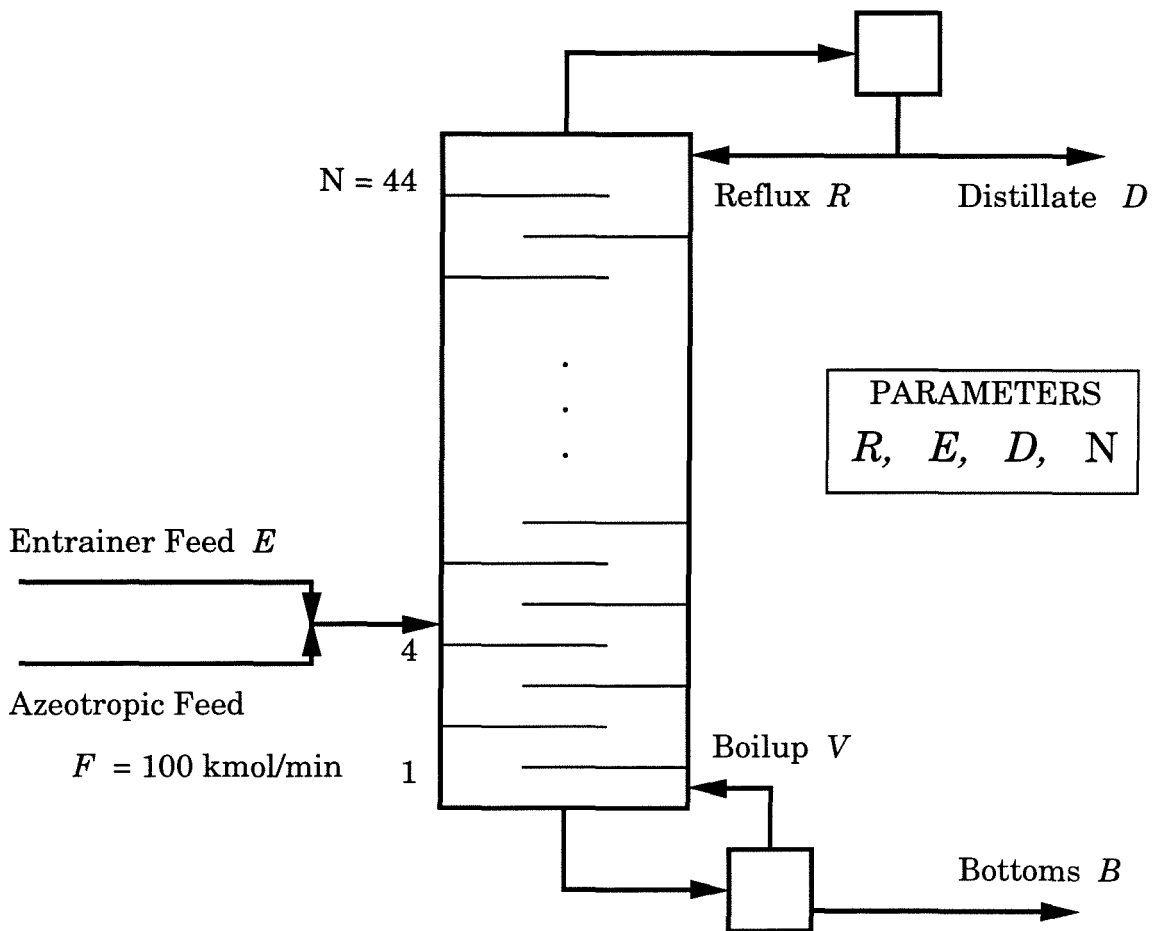


Figure 2.17: Acetone (L) - heptane (H) - benzene (I-E) azeotropic column.

activity coefficients are calculated using the Van Laar equation (multiple steady states were also obtained using the Wilson equation but they are not presented here).

2.4.1 Varying the Distillate Flow

Figure 2.18 shows typical bifurcation diagrams with the distillate flow as the bifurcation parameter for the column depicted in Figure 2.17 with $E/F = 1$ and various R . If R is low enough ($R/F = 2$), a unique steady state is calculated by the continuation algorithm. For higher values of R ($R/F = 4, 10, 50$), multiple steady states exist for some D . In these cases, a unique stable steady state exists for low D . D increases until the continuation algorithm reaches the first limit point. Beyond that point an unstable steady state is calculated (dashed curve). Along this part of the continuation path x_{DL} increases while D decreases until the second limit point is encountered. Beyond the second limit point, D increases again and a second stable steady state is calculated. Hence, two stable and one unstable steady states exist for distillate flows between the two limit points (multiplicity region); a unique stable steady state exists otherwise.

Note the similarity of those continuation paths with the continuation path we tracked in the ∞/∞ case (Figure 2.7). Also note that in Figure 2.18 the multiplicity region expands as the reflux flow increases. Figures 2.19a and 2.19b show the reflux - distillate multiplicity region for two different entrainer feed flows. As the reflux decreases, the multiplicity region becomes more narrow and at some point the multiplicities vanish. Note that, although those multiple steady states were predicted at infinite reflux, they still exist at very low reflux values. Note also that, since the overall feed does not lie on the line connecting the azeotrope with the pure benzene (I) corner, the distillate flow multiplicity interval of this column in the ∞/∞ case is not between L and $L+H$ (90 and 100 kmol/min) but between 90 and 96.6 ($=90/0.93$) kmol/min. Moreover, the column has only 4 trays in the lower section and therefore some discrepancy from the ∞/∞ case prediction is expected. In addition, note that the column with $E=1$ kmol/min is much closer to the infinite reflux and infinite re-

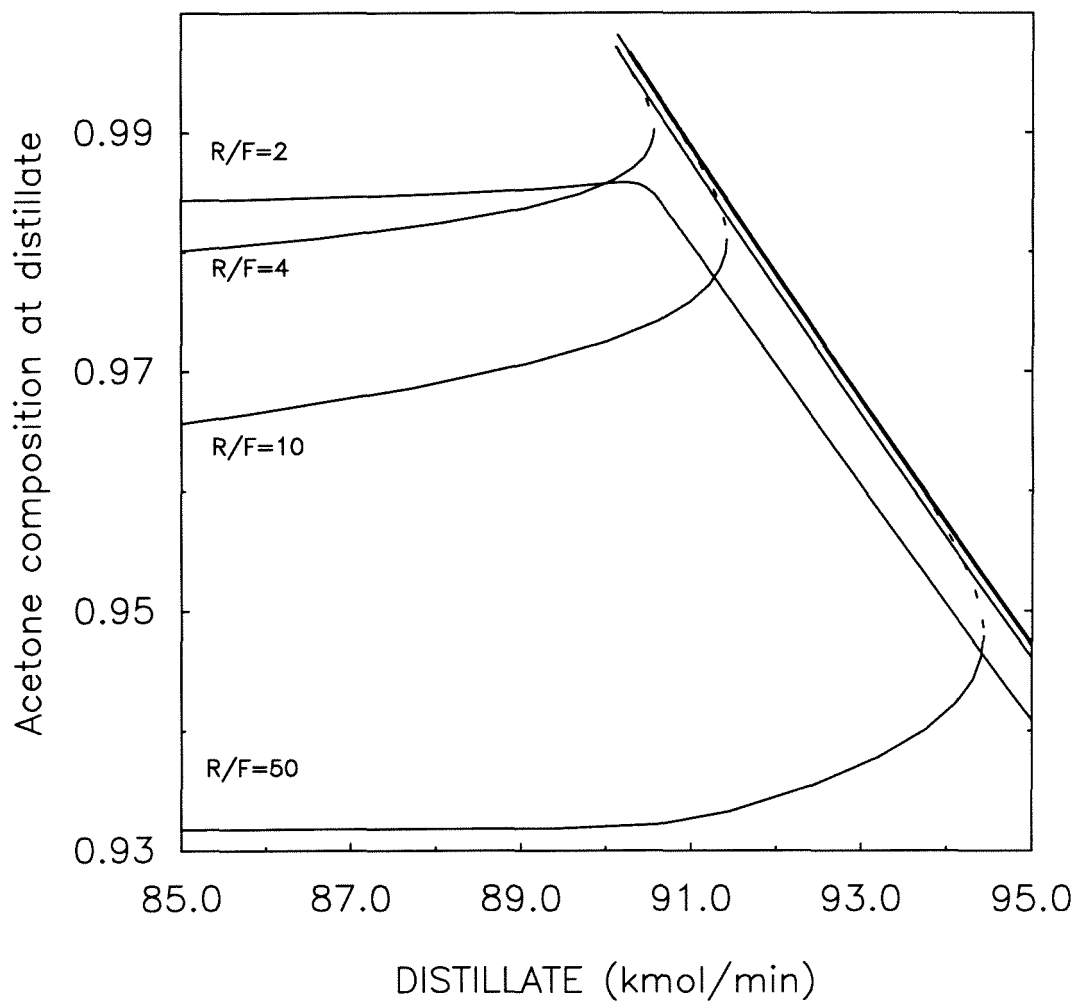


Figure 2.18: Bifurcation diagrams for a column with $N=44$ trays, $E/F = 1$ and various R/F . The distillate flow is the bifurcation parameter.

boil condition than the column with $E=200$ kmol/min. The above explains why the distillate multiplicity region at high reflux in Figure 2.19a ($E=1$ kmol/min) is much closer to the ∞/∞ case prediction than the corresponding region of Figure 2.19b ($E=200$ kmol/min).

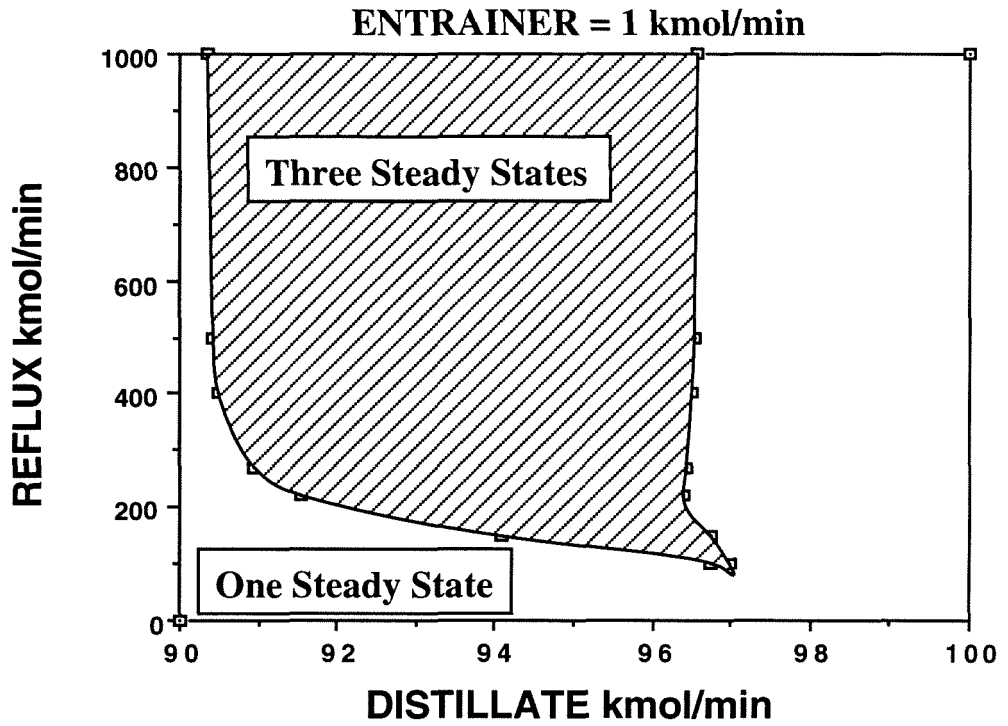
2.4.2 Varying the Entrainer and Reflux Flows

In these studies, the column depicted in Figure 2.17 is used with the distillate flow fixed at 90.9 kmol/min. The bifurcation calculation results are summarized in Figure 2.20. The four pictures at the bottom of Figure 2.20 show typical bifurcation diagrams with the entrainer feed flow as the bifurcation parameter for various fixed reflux flows. At very low reflux, a unique stable steady state exists for all entrainer feed flows. As the reflux increases, three multiple steady states appear for some entrainer feed flow interval. Like in the case where the distillate flow is the bifurcation parameter, there is just one continuation path with two limit points. For entrainer flows between the two limit points, three steady states exist. The dashed curve depicts the unstable steady state. The entrainer flow range between the two limit points expands as reflux increases. Figure 2.21 shows the actual bifurcation diagram for $R = 500$ kmol/min.

The six pictures on the right side of Figure 2.20 show typical bifurcation diagrams with the reflux flow as the bifurcation parameter for various entrainer flows. Contrary to the cases where the entrainer and the distillate flows are the bifurcation parameters, there are generally two separate continuation paths in each diagram. One of them expands along the whole range of reflux from zero to infinity. Along this path, a stable steady state is calculated. The second path generally extends to infinite reflux but vanishes at some finite reflux flow (limit or turning point). Along this second path, one stable and one unstable steady state are calculated.

At high entrainer flows, the second (two-steady-state) path lies below the single steady state path while the situation is reversed at low entrainer flows. Therefore, at high entrainer flows the unstable state is “connected” to the low conversion stable

a



b

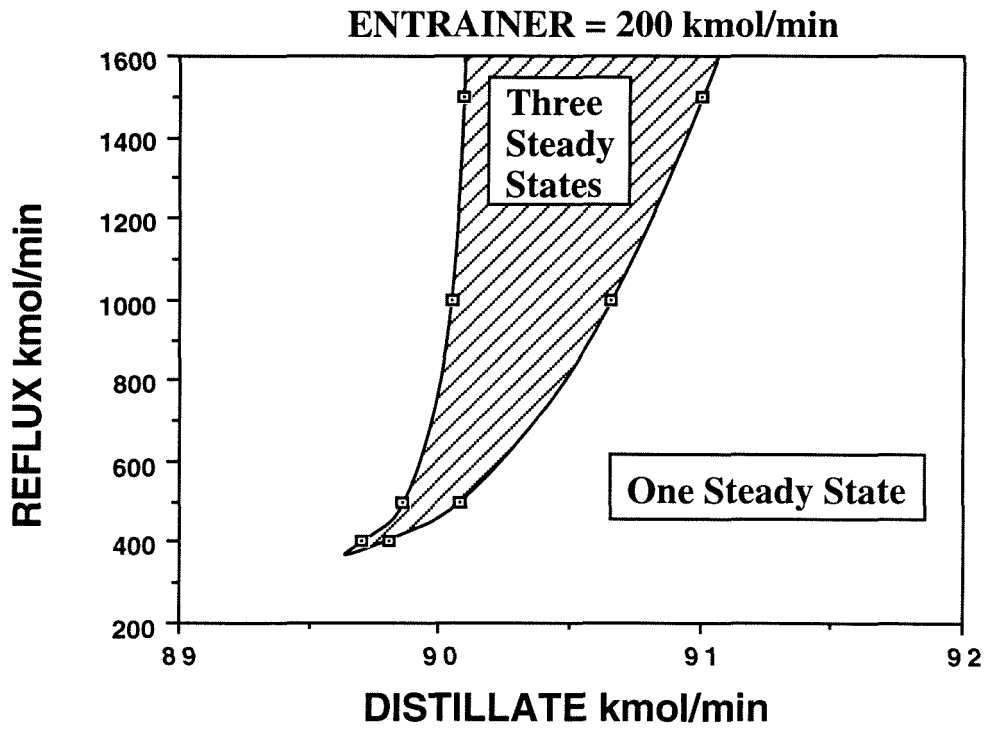


Figure 2.19: Reflux - distillate multiplicity regions.

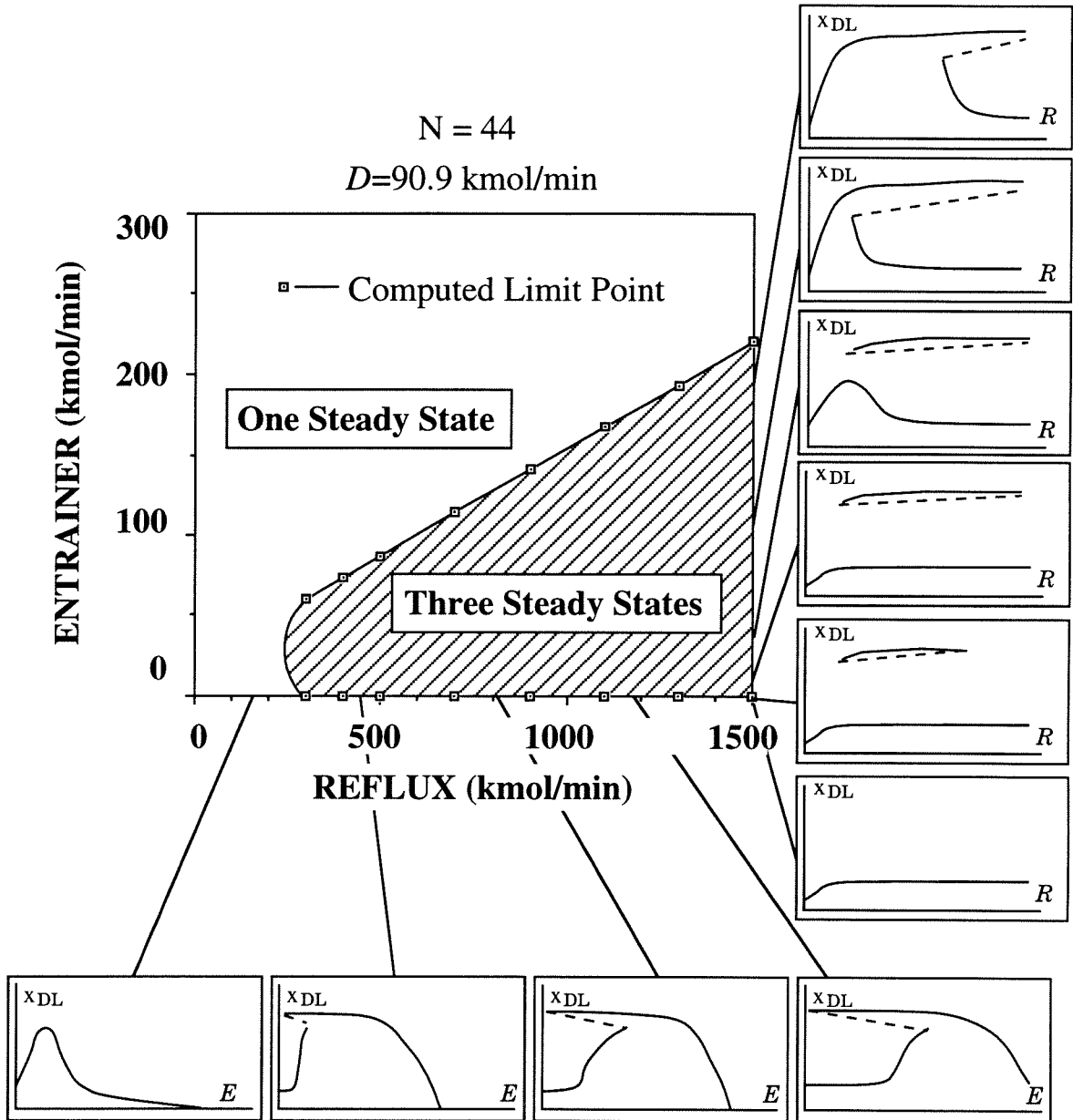


Figure 2.20: Entrainer - reflux multiplicity region and typical bifurcation diagrams with the entrainer and reflux flows as the bifurcation parameters.

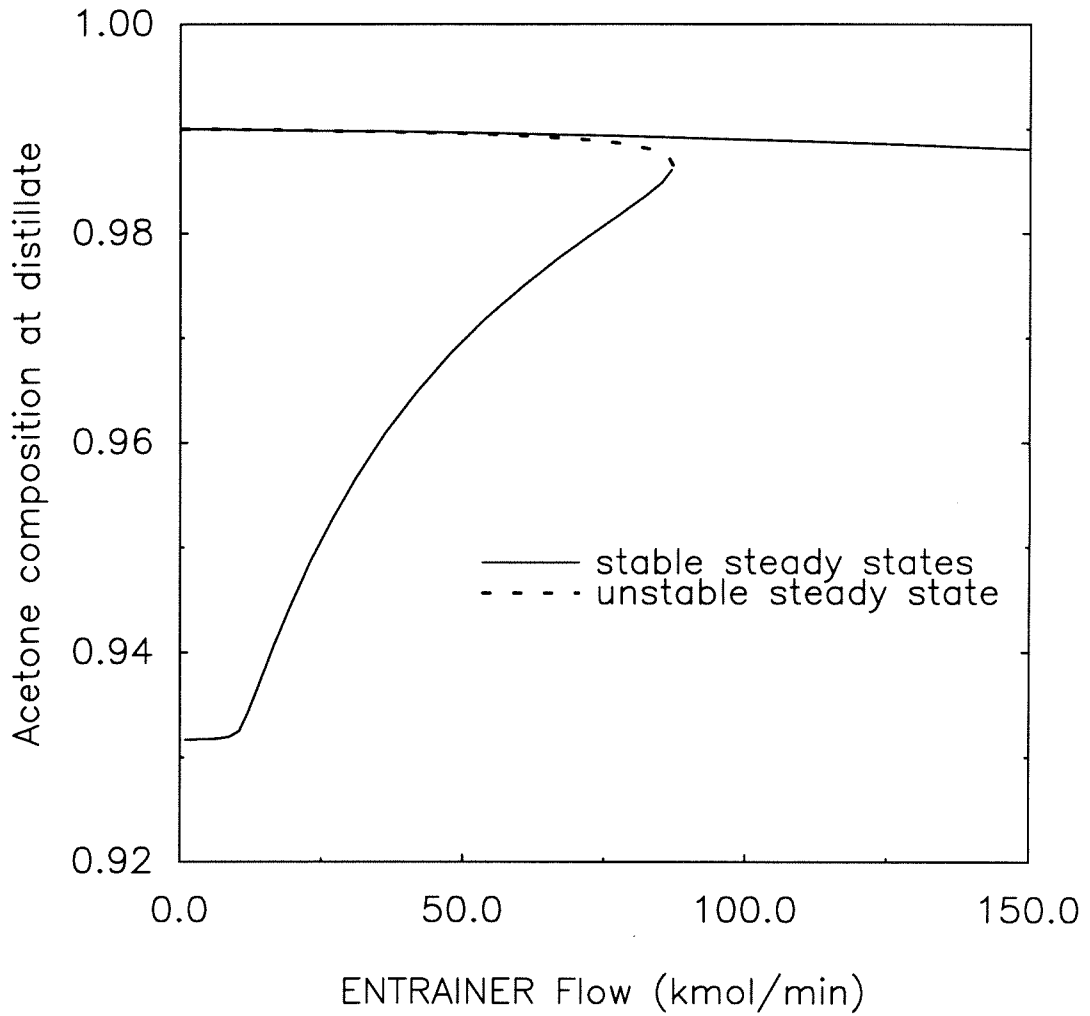


Figure 2.21: Bifurcation diagram for a column with $N=44$ trays, $R=500$ kmol/min and $D=90.9$ kmol/min. The entrainer feed flow is the bifurcation parameter.

state whereas at low entrainer flows it is “connected” to the high conversion stable state. Hence, three steady states exist for reflux flows above the limit point while a unique stable steady state exists for reflux flows below that limit point. Moreover, as the entrainer flow is decreased the limit point of the two steady state path moves to lower reflux values. The above characteristics can be seen in the upper four pictures on the right of Figure 2.20. Figure 2.22 shows the actual bifurcation diagram for $E = 80 \text{ kmol/min}$.

At very low entrainer flows, the two-steady-state path does not extend to infinite reflux and a second limit point appears at high reflux. At even lower entrainer flows, the two steady state path disappears and a unique steady state exists throughout. The above are illustrated by the two lower pictures on the right of Figure 2.20.

Finally, the central picture of Figure 2.20 shows the entrainer-reflux multiplicity region. The multiplicity region expands as reflux is increased. Note that multiplicities persist for low entrainer and reflux flows which is the region of operation in practice.

2.4.3 Effect of the number of trays

In the first part of this chapter we have shown that multiplicities exist for columns with an infinite number of trays. Doherty and Perkins (1982) proved that multiplicities cannot exist for single-staged “columns.” It is expected then, that multiplicities vanish as the number of trays decreases below some critical number.

The effect of decreasing the number of stages is depicted via bifurcation diagrams where the distillate and reflux flows are fixed and the entrainer flow is the bifurcation parameter. Figure 2.23 shows four such diagrams for columns similar to the ones depicted in Figure 2.17, i.e., with the feed location fixed on tray 4 and different number of stages N . Three steady states exist for some very narrow entrainer flow interval for the columns with 23 and 22 trays while multiplicities vanish for the 21 and 15 tray columns. Figure 2.24 shows the entrainer - reflux multiplicity region for three columns with 44, 33 and 23 stages and fixed distillate flow. It is apparent that the multiplicity region for the 23 tray column is very narrow. Moreover, no

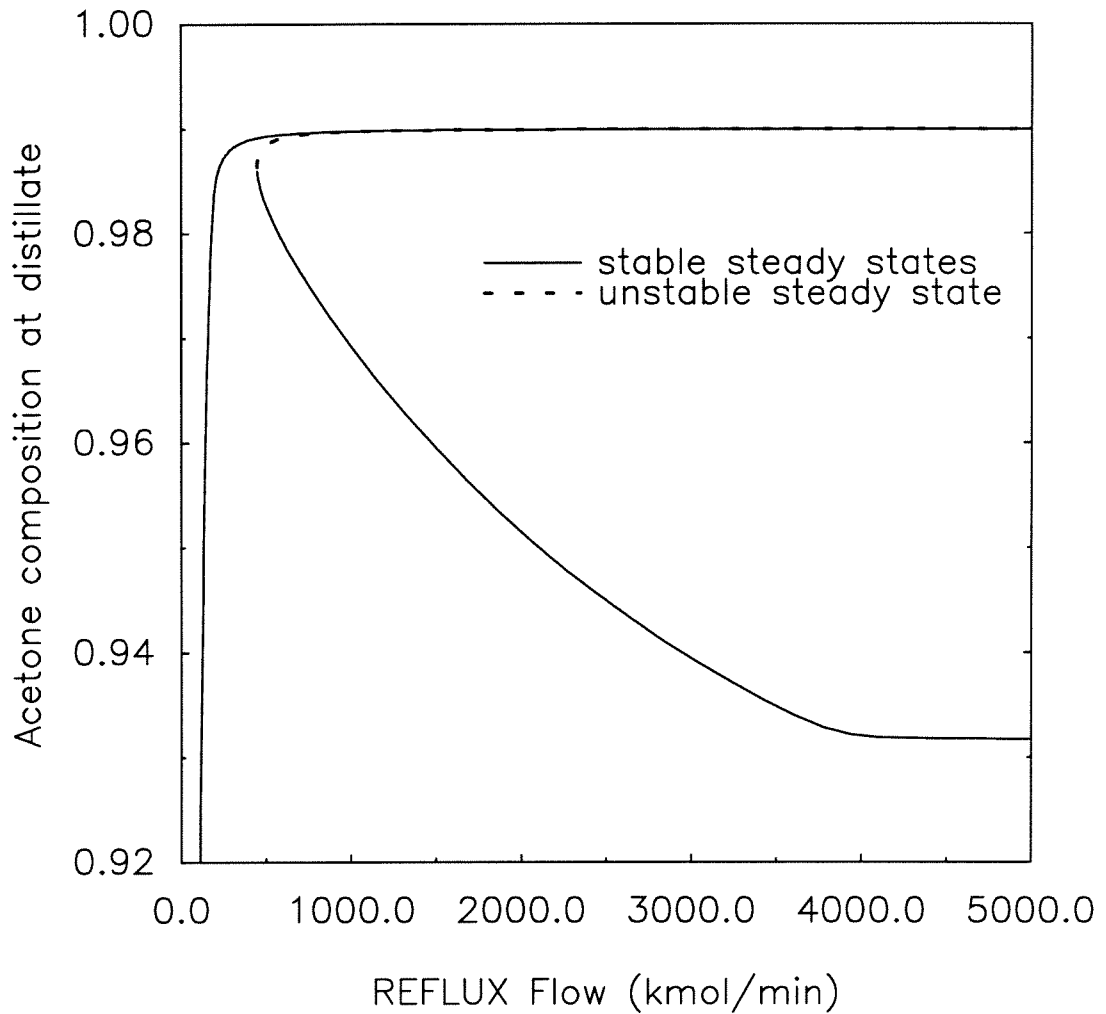


Figure 2.22: Bifurcation diagram for a column with $N=44$ trays, $E = 80$ kmol/min and $D = 90.9$ kmol/min. The reflux flow is the bifurcation parameter.

multiplicities were found for columns with less than 22 trays. Therefore, multiplicities vanish for columns with number of stages below some critical value. However, the relationship between the number of stages and the location of the multiplicity region in the entrainer - reflux plane is not clear.

2.4.4 Curved Boundaries

In this subsection we present an example which illustrates that highly curved boundaries can induce multiplicities. The ternary mixture under consideration is that of acetone (L), methanol (H) and chloroform (I) also studied by Kienle et al. (1992). The corresponding residue curve diagram is shown in Figure 2.25. It belongs to the 311-s residue curve diagram class. There are three binary azeotropes (a,b,c) and one saddle ternary azeotrope (s) in this diagram.

The interior residue curve boundaries (Figure 2.26) divide the composition triangle in four distillation regions and therefore there are eight routes (two for each region) from an unstable node to a stable node along the distillation region boundaries. Note that none of the routes contains two neighboring saddles and that sa is the only boundary that is highly curved and therefore might induce multiplicities.

There exist two routes that contain sa, namely $c \rightarrow s \rightarrow a$ and $b \rightarrow s \rightarrow a$. Now check the geometrical condition by tracking each route in the proper direction (the proper direction is the direction of the continuation path, i.e., the one that starts with the distillate located at the unstable node and ends with the bottoms located at the stable node). It is very simple to show that the distillate flowrate increases monotonically for the $c \rightarrow s \rightarrow a$ route. In contrast, the geometrical condition is satisfied for some feed locations as we track the $b \rightarrow s \rightarrow a$ route. The shaded region in Figure 2.26 depicts the appropriate feed composition region for which multiplicities will be observed in the ∞/∞ case.

The above findings are supported by simulation results for a column with 30 trays, $D/F = .5$, $R/F = 100$, a feed composition of 26.5% acetone, 23% methanol and 50.5% chloroform, a feed flowrate of 100 kmol/min and a feed tray located at stage 14.

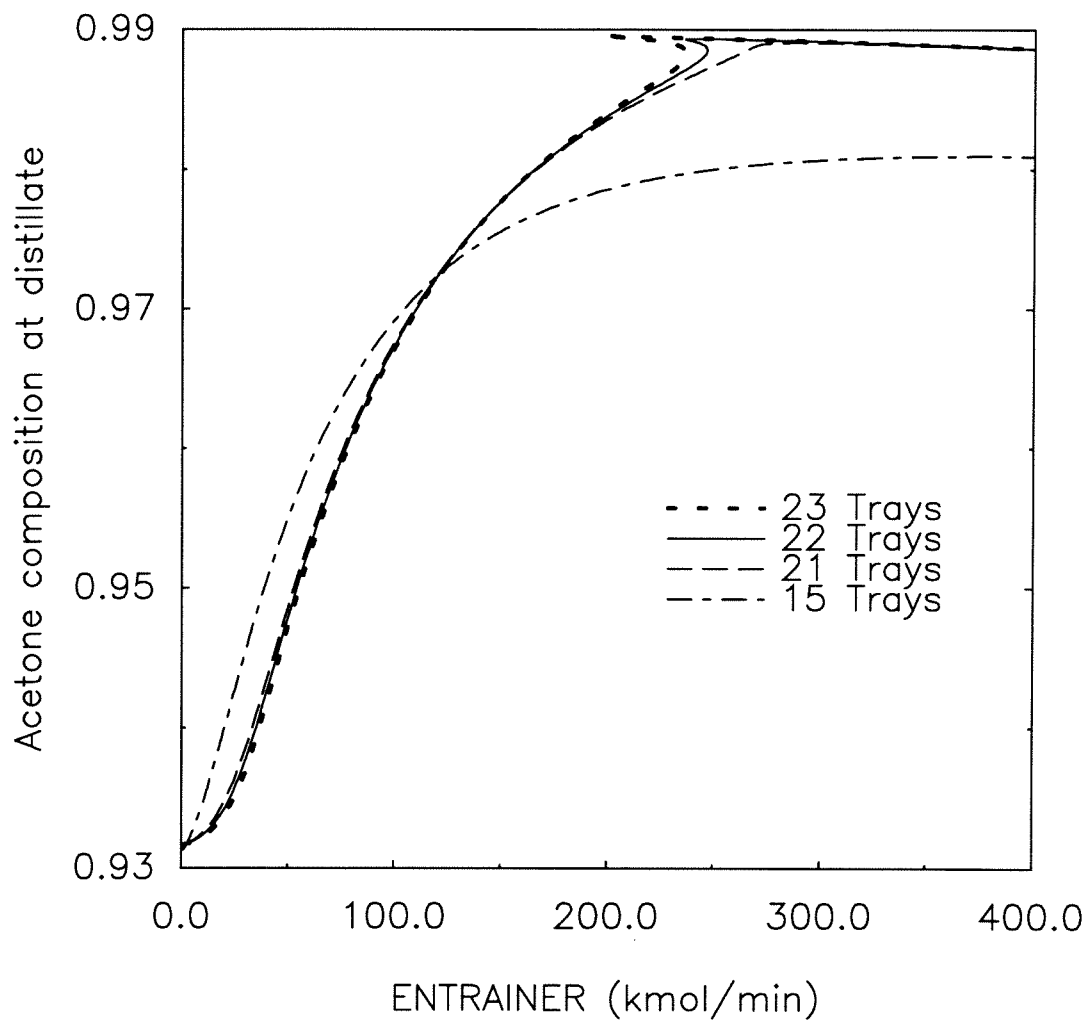


Figure 2.23: Vanishing multiplicity in small columns with $R = 1500$ kmol/min and $D = 90.9$ kmol/min.

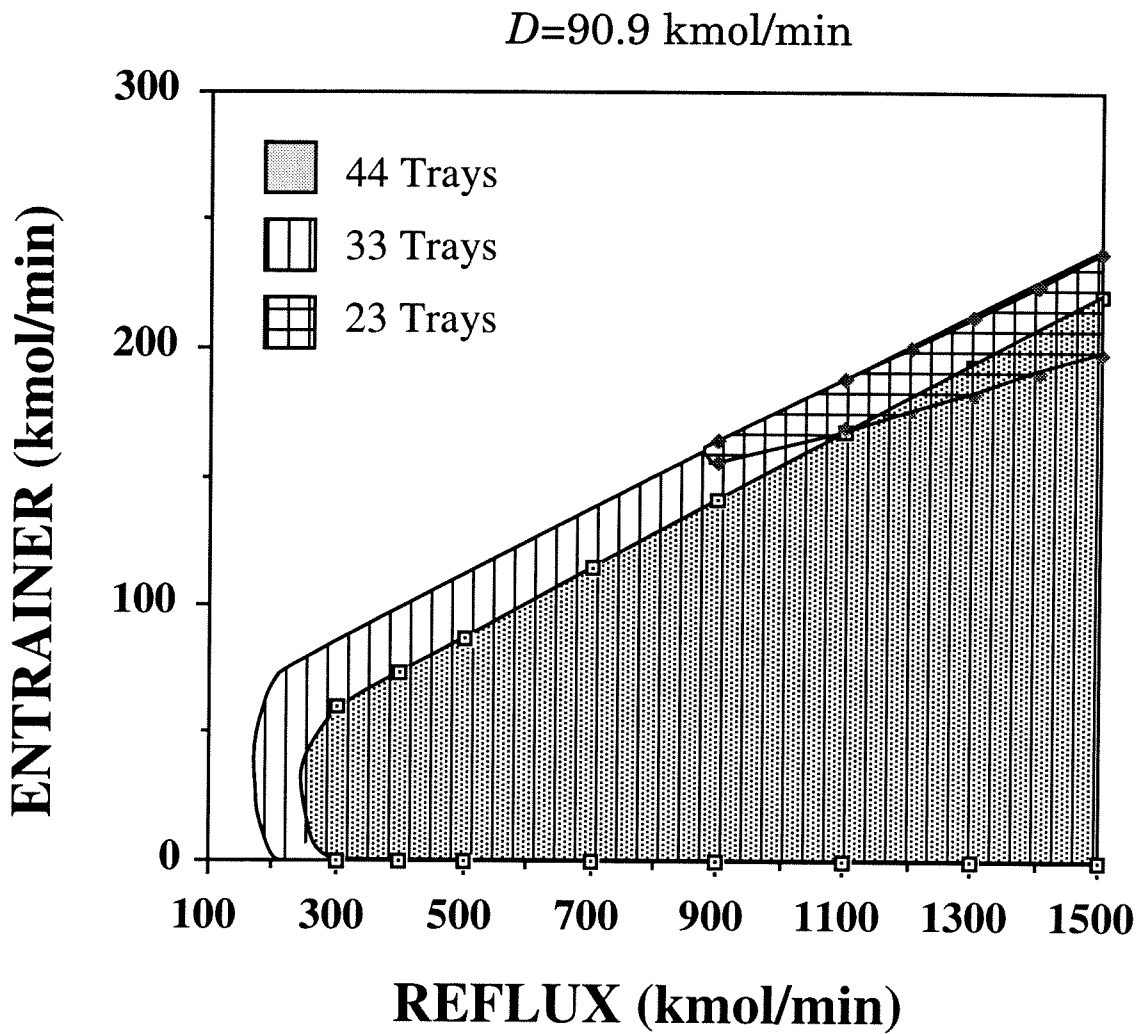


Figure 2.24: Entrainer - reflux multiplicity region variation with the number of trays.

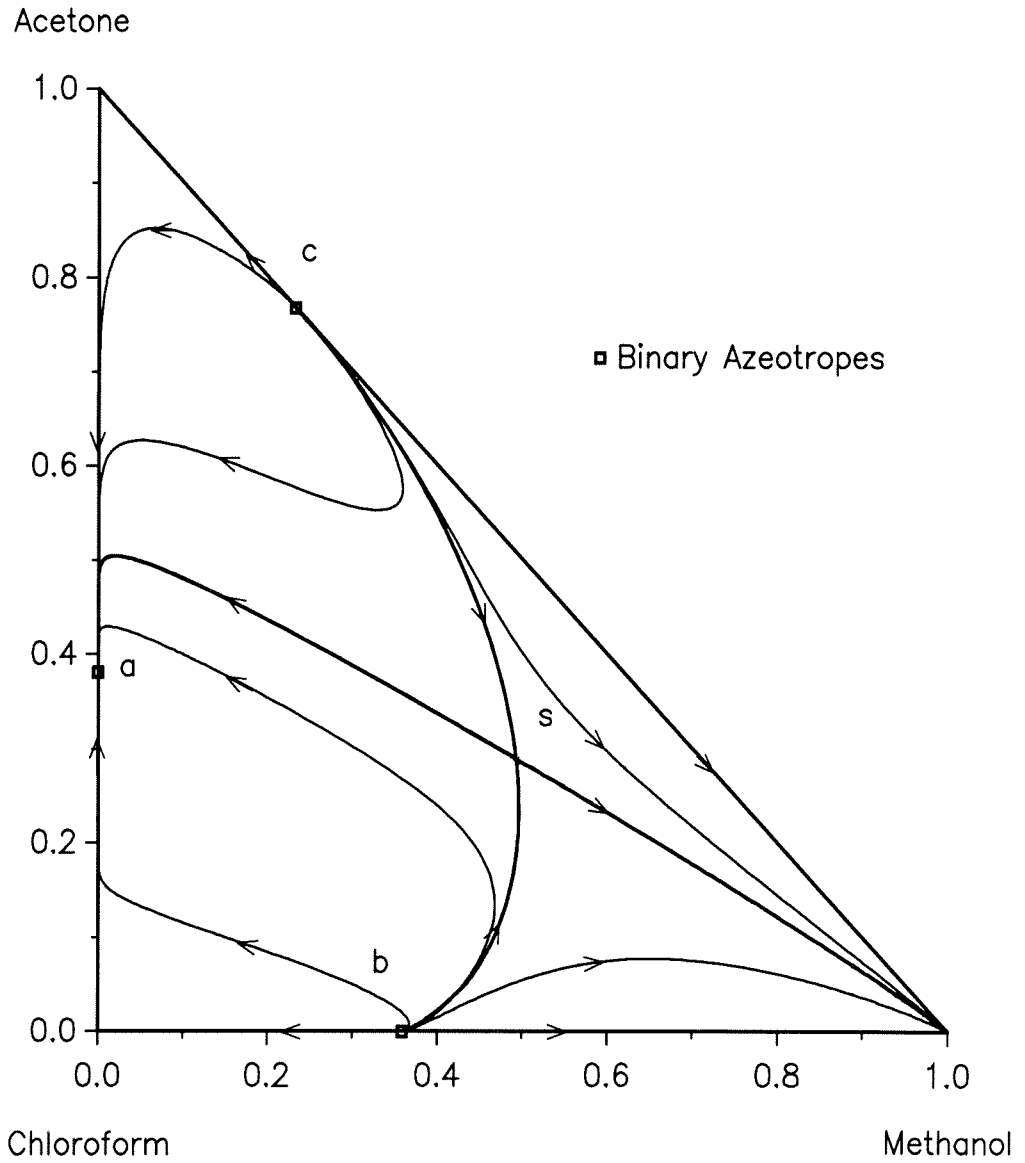


Figure 2.25: The acetone - methanol - chloroform residue curve diagram.

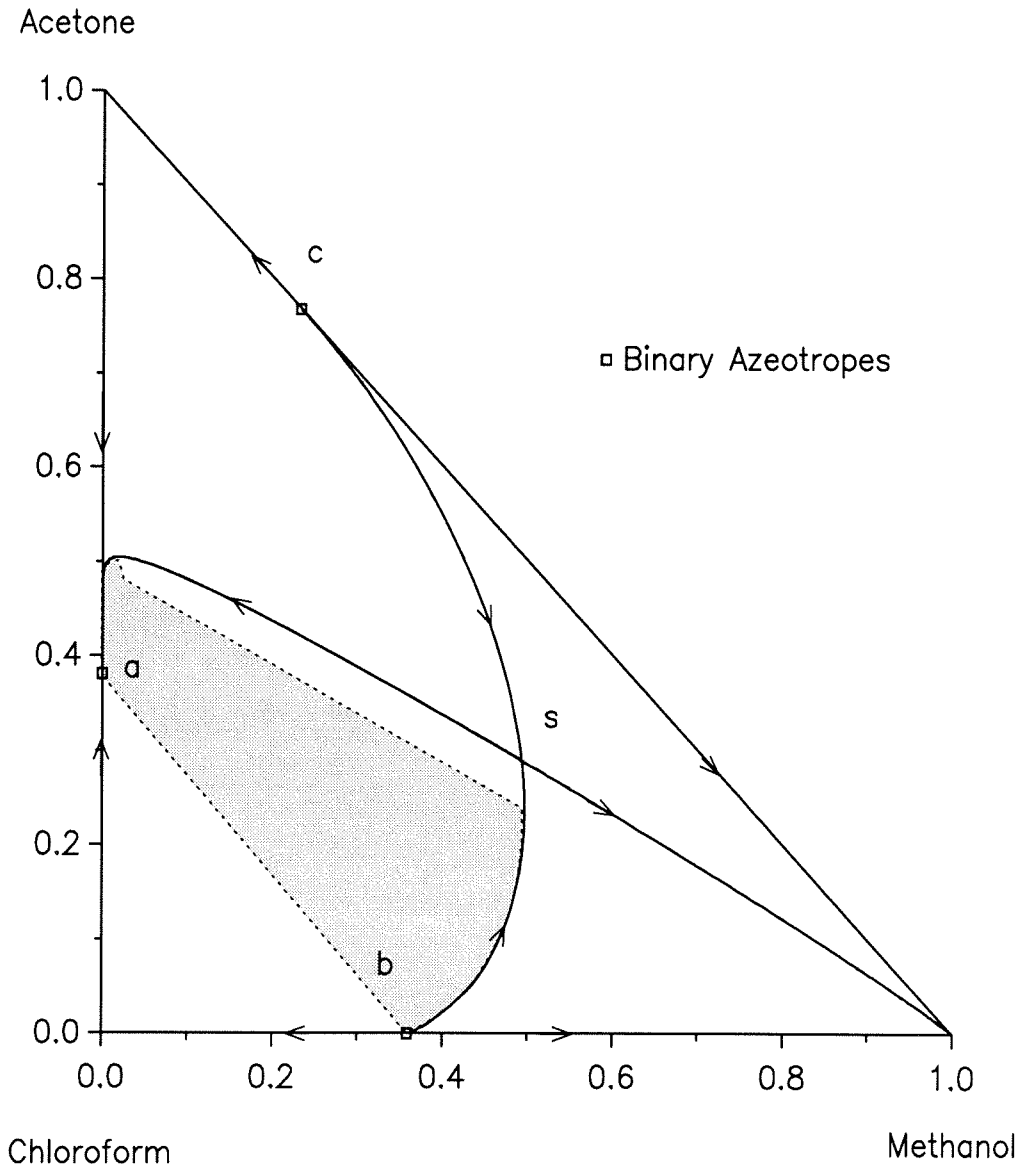


Figure 2.26: The four distillation regions and the appropriate feed region in the acetone - methanol - chloroform composition triangle.

Figures 2.27, 2.28 and 2.29 show the three different column profiles (two stable and one unstable) with the above specifications. Figure 2.30 shows the location of the three profiles relative to the distillation region boundaries in the composition triangle. Note that the column operates at high reflux but not at infinite reflux and does not have an infinite number of trays. Hence, it is expected that the column profiles do not exactly follow the residue curve boundaries. Figure 2.31 shows bifurcation diagrams with the distillate flow as the bifurcation parameter for $R/F = 1, 5$ and 100 . The three steady states persist for reflux to feed ratios as low as 1.

Finally, a note on the use of different liquid activity coefficient models. Using the one-parameter regular solution model, the residue curve diagram obtained is very similar to the one obtained with Van Laar (Figure 2.25), i.e., the *sa* boundary is highly curved. Using the two-suffix Margules model, the *sa* boundary is again highly enough curved but the curvature is not as profound as in Figure 2.25. Nevertheless, simulation results showed that multiple steady states exist in this case, too. Contrary to the previous cases, the boundaries do not seem to be curved enough when using the Wilson equation. However, caution should be taken in all such cases because the curvature of the boundary close to the boundary end points (singular points) may change dramatically and hence there might exist a small boundary segment that enables the existence of multiple steady states. Also note that this does not necessarily mean that the appropriate feed region is small. This situation was observed for the mixture isopropanol (I) - toluene (H) - methanol (L) (021 class, see Figure 2.13) using the Wilson equation. Simulation and bifurcation study results showed that the observed multiple steady states were due to the high curvature of the boundary very close to the methanol (L) - toluene (H) azeotrope.

2.5 Effect of the VLE model

The geometrical sufficient condition for the existence of multiplicities at finite reflux is based on arguments about the distillation region boundaries at infinite reflux. In general, the orientation and the curvature of those boundaries depends on the specific

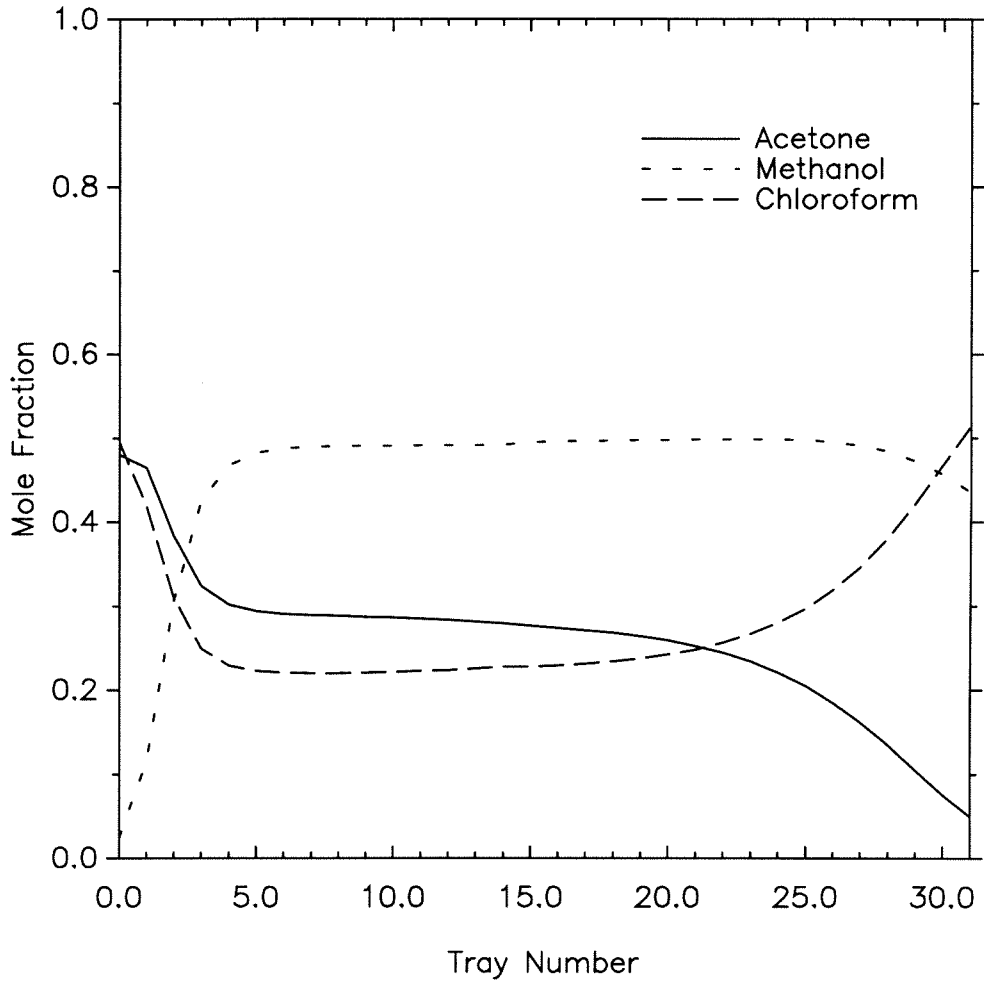


Figure 2.27: First stable profile of a column with $N=30$ trays, $E/F = .5$ and $R/F = 100$.

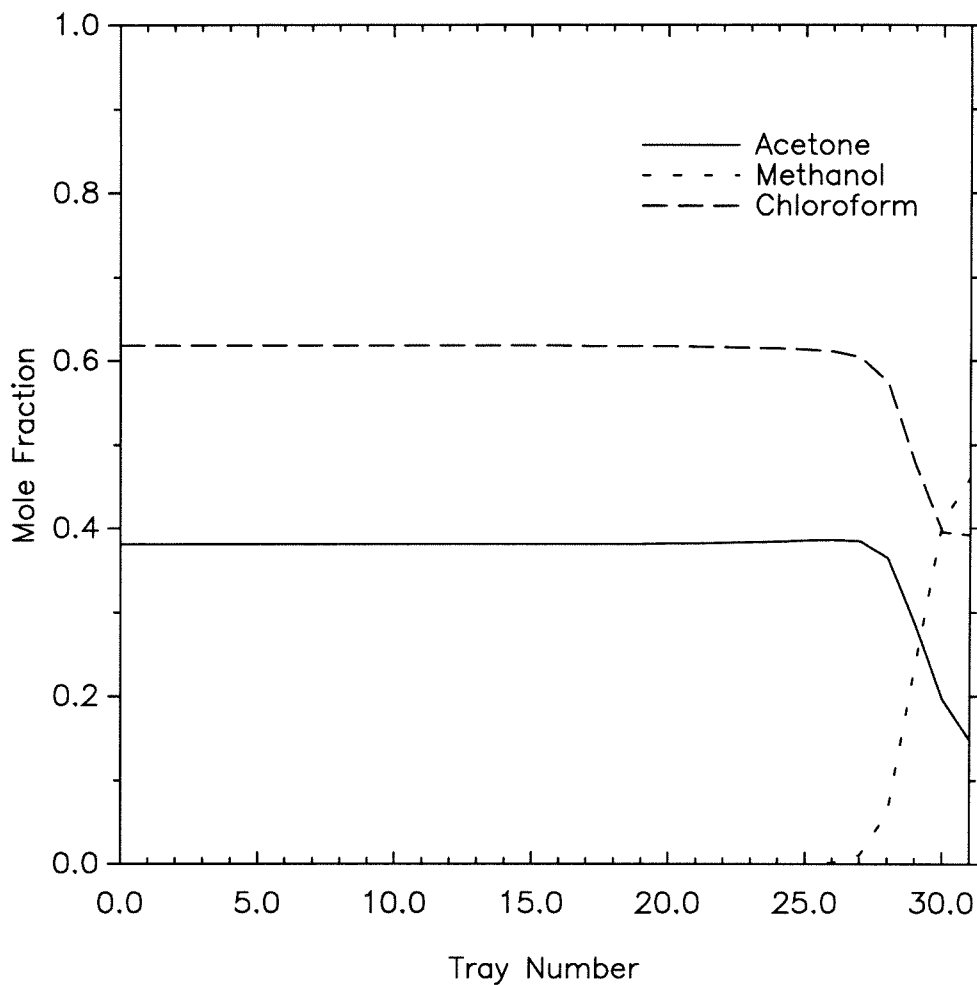


Figure 2.28: Second stable profile of a column with $N=30$ trays, $E/F = .5$ and $R/F = 100$.

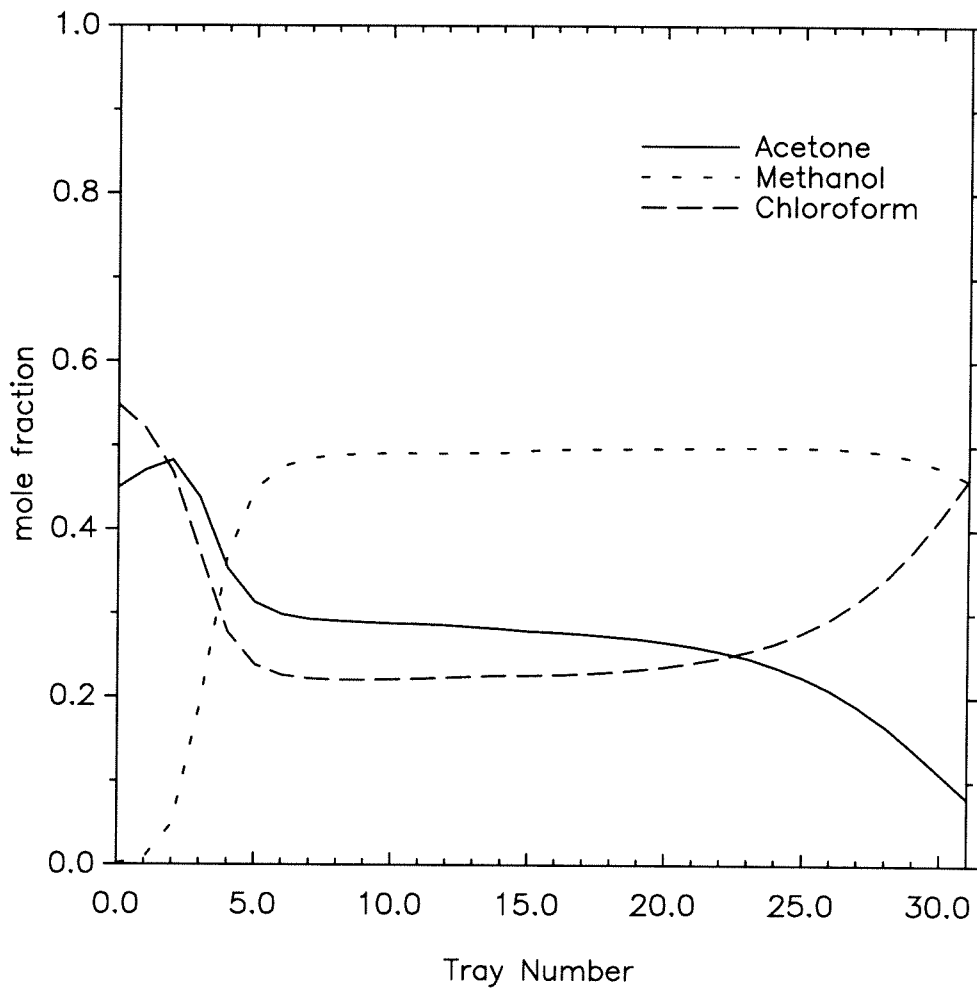


Figure 2.29: Unstable profile of a column with $N=30$ trays, $E/F = .5$ and $R/F = 100$.

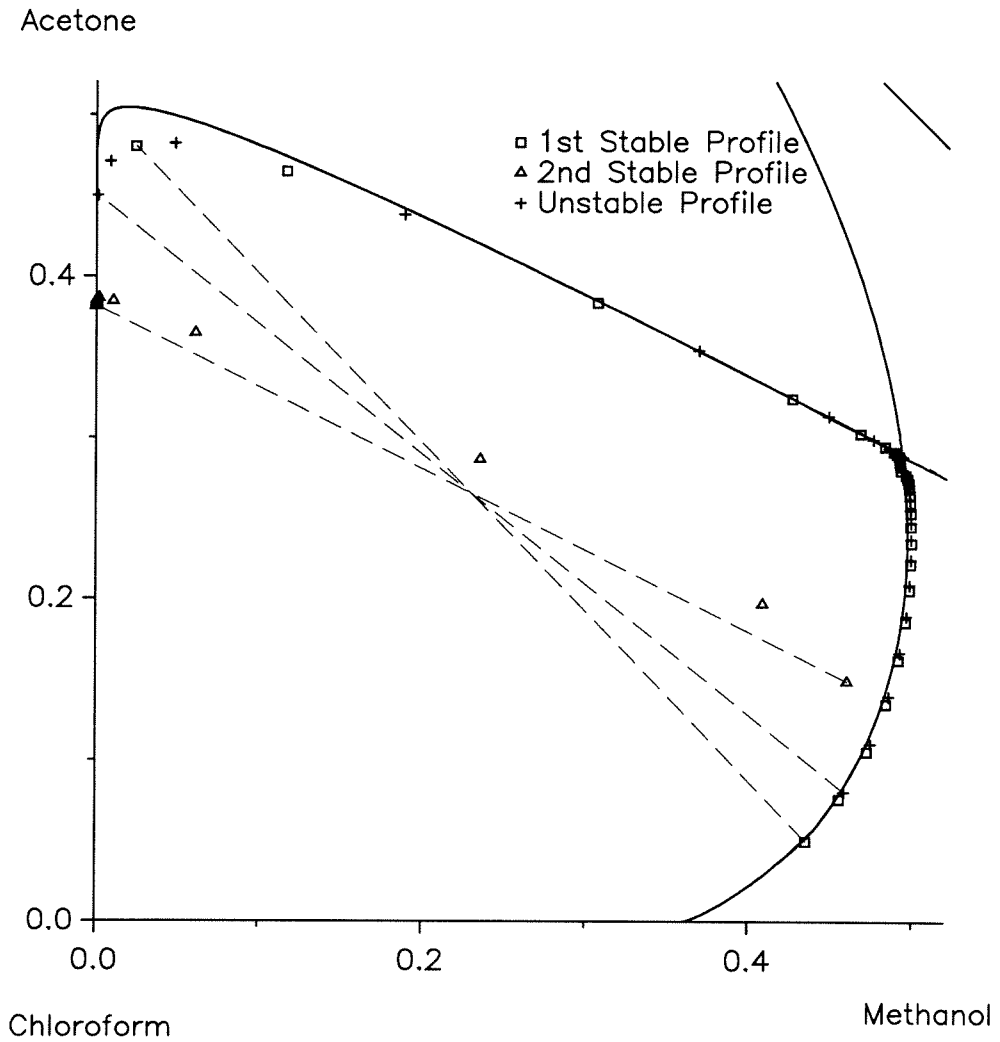


Figure 2.30: The three steady states of the acetone - methanol - chloroform column with $N=30$ trays, $E/F = .5$ and $R/F = 100$. in the composition triangle.

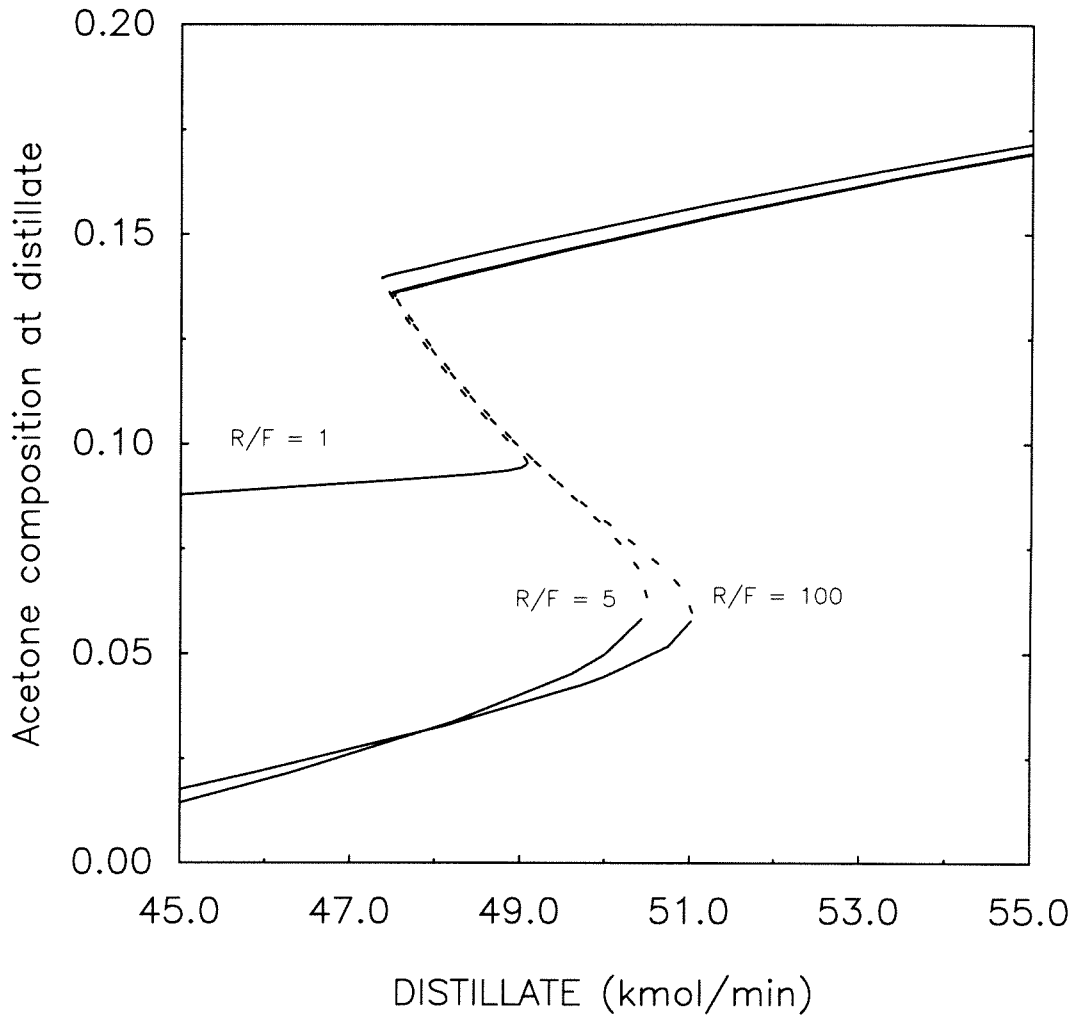


Figure 2.31: Bifurcation diagrams for the acetone - methanol - chloroform column with $N=30$ trays and various R/F . The distillate flow is the bifurcation parameter.

thermodynamic model used. Therefore it is expected that switching from one VLE model to another may affect the existence of multiplicities

- quantitatively only, i.e., multiplicities still exist but there are different appropriate feed composition regions, distillate - reflux multiplicity regions etc.
- qualitatively, i.e., multiple steady states exist using one model while they do not exist using another one.

For example, in the acetone - heptane - benzene case (001 class) multiple steady states exist in the ∞/∞ case for any feed composition inside the composition triangle, regardless of the specific thermodynamic model used. This independence from the thermodynamic model is inherent in any 001 class residue curve diagram. However, quantitative differences between the models exist for the entrainer - reflux and distillate - reflux multiplicity regions. On the other hand, when the existence of multiplicities depends on the orientation and/or the curvature of some interior residue curve boundaries, it is possible that multiple steady states exist when using one thermodynamic model while they do not exist when using another model.

Out of the 113 residue curve diagram classes, we identified 77 that contain two neighboring saddles. In 41, among those 77 classes, multiple steady states exist in the ∞/∞ case independent of the thermodynamic model used, while in the remaining 36 classes the existence of multiplicities depends on the geometry of the residue curve boundaries and hence on the thermodynamic model. The existence of multiple steady states due to highly curved boundaries, however, is possible for any residue curve diagram that contains an interior residue curve boundary. The type of multiplicities discussed here cannot occur in the 000 (nonazeotropic mixture) and 100 (heavy entrainer) classes and it is highly unlikely that it occurs in the 020 (light entrainer) class because it would require a very strange boundary shape.

Using a databank with information on the azeotropic (or zeotropic) behavior of binary mixtures, we found 3700 ternary mixtures belonging in the 001 or 002-m classes, 340 ternary mixtures belonging in the 003 or 004-M classes and 275 ternary mixtures belonging in the 103 or 104-M or 203-m classes. All 7 classes are among

the 41 that give rise to multiplicities independent of the geometry of interior residue curve boundaries. Note, however, that this is the result of a preliminary rough search which, for example, does not exclude ternary mixtures with two liquid phases.

Finally, a note on the fact that the geometrical condition is not necessary for the existence of multiple steady states in the finite reflux case. Finite reflux boundaries are not as rigorously defined as infinite reflux ones. It is known that the shape of the distillation boundaries changes with reflux. Therefore, it may be possible that multiplicities exist at some range of finite reflux flows (due to some “distorted” boundaries) while the geometrical condition is not satisfied for infinite reflux boundaries. The above can cause another discrepancy observed for different thermodynamic models.

2.6 Effect on Design and Operation

In this section we briefly discuss the effect of multiplicities on the distillation column design and operation. In separation flowsheet synthesis procedures, the calculation of the achievable product sets is commonly one of the first steps. It is apparent that if multiple steady states exist, there are subsets of the achievable product sets which correspond to unstable steady states. Hence, these subsets are qualitatively different from the rest of the achievable product sets since they are not really achievable without stabilizing control.

Next we examine the problem of avoiding the multiplicity region (i.e., operating in the single steady state region) and meeting the product specifications (defined later). Here, the number of stages and the entrainer flow are fixed while the distillate and reflux are the design parameters. The column specifications are 99% purity of acetone in the distillate and 99% acetone recovery. By superimposing the reflux-distillate regions where the above specifications are met on the corresponding multiplicity regions (Figures 2.19a and 2.19b) we obtain Figures 2.32a and 2.32b for the two fixed entrainer flows. If $E = 1$ kmol/min (Figure 2.32a) the column specifications are only met inside the multiplicity region and therefore multiplicities cannot be avoided in this case. However, if the entrainer flow is increased to 200 kmol/min, there exists

a reflux-distillate region where the specifications are met and a unique steady state exists. Therefore, we can meet the column specifications and avoid the multiplicity region at the expense of a higher entrainer feed flow.

Finally, we examine whether it is possible to “jump” from the high conversion stable steady state to the corresponding low conversion stable steady state under a feed composition disturbance while operating in the multiplicity region. In some sense, we examine whether it is necessary to operate in the single steady state region. Here, the column has 44 trays, the entrainer flow is 1 kmol/min, the reflux flow is 1000 kmol/min and no control action is used (open-loop behavior). The feed originally contains 90% acetone and 10% heptane and under these conditions three steady states exist. The column originally operates at the high conversion state (99% acetone in distillate). From time zero to 6000 seconds the feed composition is changed to 91% acetone and 9% heptane. Note that under these conditions a single (low conversion) stable steady state exists. Finally, at time 6000 seconds the feed composition is changed back to its original value. Figure 2.33 shows that the column profile “jumps” from the high conversion state to the low conversion state (93.17% acetone in distillate) because of the feed composition disturbance. The calculations were repeated for smaller disturbance time intervals (1000, 2000, 4000 seconds) but this time the acetone composition returned to its original 99% purity. Therefore, it seems that for this particular design it is relatively difficult to “jump” from one stable profile to the other and hence, this result disputes whether it is necessary to operate in the single steady state region.

However, the material presented in this section is just a brief illustration of the implications of multiplicities on column design and operation and a more thorough investigation of this subject is needed.

2.7 Conclusions

In this chapter we study multiple steady states in ternary homogeneous azeotropic distillation. First we examine in detail the infinite reflux and infinite number of trays

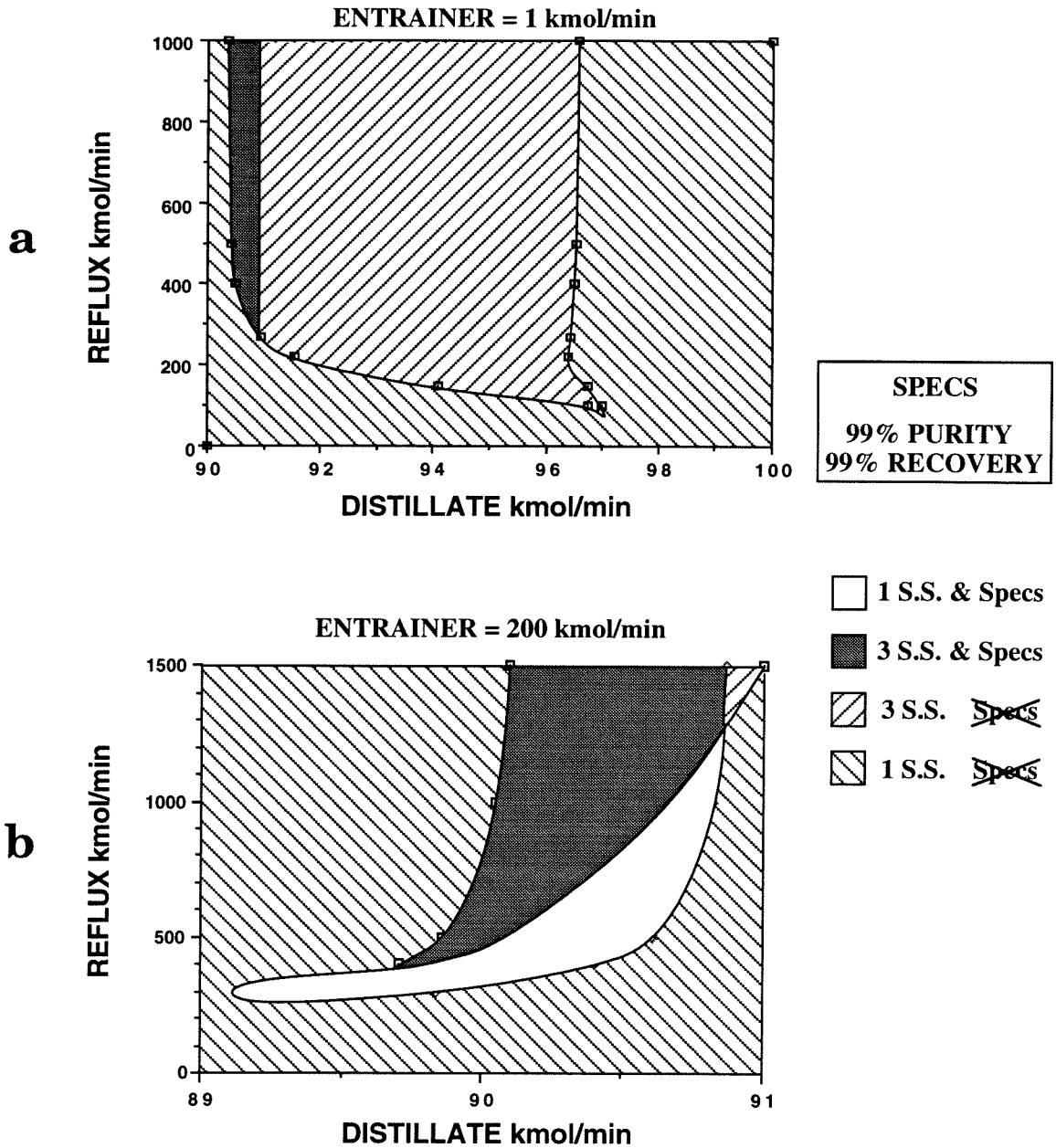


Figure 2.32: Reflux - distillate multiplicity and specifications regions.

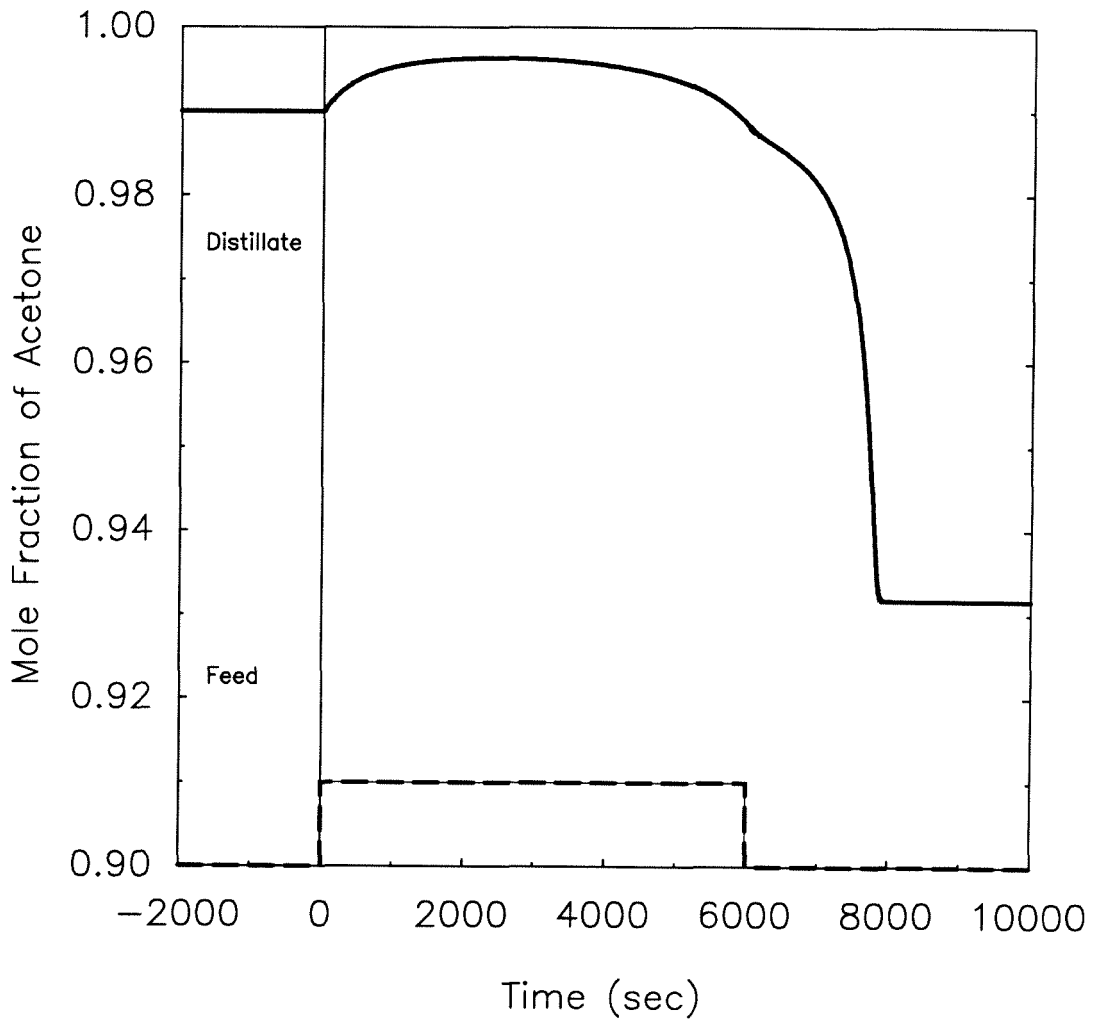


Figure 2.33: Open-loop dynamical behavior under a feed composition disturbance.

(∞/∞) case. We present a systematic procedure which determines whether multiplicities exist for any given residue curve diagram and feed composition. Through this procedure we answered the following questions:

Given a ternary mixture and its residue curve diagram, we can for the ∞/∞ case

- (1) find whether multiple steady states exist for some feed composition and
- (2) locate the region of feed compositions that lead to these multiple steady states.

We derive (1) the necessary and sufficient geometrical condition for the existence of multiple steady states and (2) the condition the feed compositions must satisfy to lead to multiple steady states. A few other important results are the following:

In the case of straight boundaries we found that two neighboring saddles is a necessary condition for the existence of multiplicities.

If multiple steady states exist under the straight boundaries assumption, then, assuming that the azeotropic compositions do not change, these multiplicities still exist even if the boundaries are curved, although the appropriate feed region is changed.

Highly curved boundaries (pseudosaddles) can induce multiple steady states.

For columns operating at finite reflux the geometrical condition is only a sufficient condition for the existence of multiple steady states. We use an example to show that the prediction for the existence of multiple steady states in the ∞/∞ case carries over to columns operating at finite reflux and with a finite number of trays. We further show that, although the predictions were made in the ∞/∞ case, it does not mean that multiple steady states do not exist for realistic operating conditions (low reflux and entrainer feed flows and small number of trays). However, apart from the fact that the ∞/∞ case predictions carry over, the observations presented here should not be generalized because they are specific to the particular example. We also present an example which illustrates that highly curved boundaries can induce multiplicities.

We offered some comments on the effect of the thermodynamic model on the existence of multiplicities and we show that some of the results presented here do not depend on the specific thermodynamic model used. Finally, we briefly discuss the effect of multiplicities on the column design and operation. The consideration here is whether it is necessary to operate in the single steady state region (i.e. avoid the multiplicity region). A more thorough investigation of this topic is needed.

Acknowledgements: We acknowledge gratefully the financial support of the Donors of the Petroleum Research Fund administered by the American Chemical Society and of the I. S. Latsis Foundation. We also thank Prof. Skogestad (Norwegian Technical University, Trondheim) for several enlightened discussions. Finally, we thank Prof. Doherty and Jeffrey Knapp (University of Massachusetts, Amherst) for providing us thermodynamic data and subroutines.

2.8 Literature Cited

Bossen, S. B., S. B. Jorgensen, and R. Gani, "Simulation, Design, and Analysis of Azeotropic Distillation Operations," *Ind. Eng. Chem. Res.*, 1993, **32**, pp. 620-633.

Chavez, R. C., J. D. Seader and T. L. Wayburn, "Multiple Steady-State Solutions for Interlinked Separation Systems," *Ind. Eng. Chem. Fund.*, 1986, **25**, pp. 566-576.

Doedel, E., "AUTO: Software for Continuation and Bifurcation Problems in Ordinary Differential Equations," Applied Mathematics, Caltech, Pasadena, CA (1986).

Doherty, M. F., and J. D. Perkins, "On the Dynamics of Distillation Processes. I. The Simple Distillation of Multicomponent Non-reacting, Homogeneous Liquid Mixtures," *Chem. Eng. Science*, 1978, **33**, pp. 569-578.

Doherty, M. F., and J. D. Perkins, "On the Dynamics of Distillation Processes. IV. Uniqueness and Stability of the Steady State in Homogeneous Continuous Distillation," *Chem. Eng. Science*, 1982, **37**, pp. 381.

Helferich, F. G., "Multiple Steady States in Multicomponent Countercurrent Mass-Transfer Processes," *Chem. Eng. Science*, 1993, **48**(4), pp. 681-686.

Jacobsen, E. W., and S. Skogestad, "Multiple Steady States in Ideal Two-Product

Distillation,” *AIChE Journal*, 1991, **37**(4), pp. 499-511.

Kienle, A., and W. Marquardt, “Bifurcation Analysis and Steady-State Multiplicity of Multicomponent, Non-Equilibrium Distillation Processes,” *Chem. Eng. Science*, 1991, **46**(7), pp. 1757-1769.

Kienle, A., W. Marquardt, and E. D. Gilles, “Steady State Multiplicities in Homogeneous Azeotropic Distillation Processes,” AIChE Annual Meeting, Miami, 1992.

Kocach III, J. W., and W. D. Seider, “Heterogeneous Azeotropic Distillation - Homotopy-Continuation Methods,” *Comput. Chem. Eng.*, 1987, **11**(6), pp. 593-605.

Laroche, L., N. Bekiaris, H. W. Andersen, and M. Morari, “The Curious Behavior of Homogeneous Azeotropic Distillation - Implications for Entrainer Selection,” presented at the AIChE Annual Meeting, Chicago, 1990.

Laroche, L., “Homogeneous Azeotropic Distillation: Entrainer Selection,” Ph. D. Dissertation, California Institute of Technology, Pasadena, 1991.

Laroche, L., N. Bekiaris, H. W. Andersen, and M. Morari, “Homogeneous Azeotropic Distillation: Separability and Flowsheet Synthesis,” *Ind. Eng. Chem. Res.*, 1992, **31**(9), pp. 2190-2209.

Lin, W. J., J. D. Seader and T. L. Wayburn, “Computing Multiple Solutions to Systems of Interlinked Separation Columns,” *AIChE Journal*, 1987, **33**(6), pp. 886-897.

Lucia, A., and H. Li, “Constrained Separations and the Analysis of Binary Homogeneous Separators,” *Ind. Eng. Chem. Res.*, 1992, **31**, pp. 2579-2587.

Magnussen, T., M. L. Michelsen, and Aa. Fredenslund, “Azeotropic Distillation Using UNIFAC,” *Inst. Chem. Eng. Symp. Ser.*, 1979, **56**, pp. 4.2/1-4.2/19.

Matsuyama, H., and H. Nishimura, “Topological and Thermodynamic Classification of Ternary Vapor-Liquid Equilibria,” *J. Chem. Eng. Jpn.*, 1977, **10**(3), pp. 181-187.

Petlyuk, F. B., and V. S. Avetyan, “Investigation of Three Component Distillation at Infinite Reflux,” *Theoretical Foundations of Chemical Engineering* (in Russian), 1971, **5**(4), pp. 499-506.

Prokopakis, G. J., and W. D. Seider, “Feasible Specifications in Azeotropic Distillation,” *AIChE Journal*, 1983, **29**(1), pp. 49-60.

Rosenbrock, H. H., “A Lyapunov Function with Applications to some Nonlinear

Physical Systems,” *Automatica*, 1962, **1**, pp. 31-53.

Rovaglio, M., and M. F. Doherty, “Dynamics of Heterogeneous Azeotropic Distillation Columns,” *AIChE Journal*, 1990, **36**(1), pp. 39-52.

Sridhar, L. N., and A. Lucia, “Analysis and Algorithms for Multistage Separation Processes,” *Ind. Eng. Chem. Res.*, 1989, **28**, pp. 793-803.

Sridhar, L. N., and A. Lucia, “Analysis of Multicomponent, Multistage Separation Processes: Fixed Temperature and Pressure Profiles,” *Ind. Eng. Chem. Res.*, 1990, **29**, pp. 1668-1675.

Widagdo, S., W. D. Seider, and D. H. Sebastian, “Bifurcation Analysis in Heterogeneous Azeotropic Distillation,” *AIChE Journal*, 1989, **35**(9), pp. 1457-1464.

2.9 Appendix

The appendix contains information on the thermodynamic model used in the simulations presented in this chapter. Vapor - liquid equilibrium calculations are based on the following equation:

$$y_i P = x_i P_i^{sat}(T) \gamma_i(T, \underline{x})$$

where $P=1$ atm in all simulations presented here.

Vapor pressures were computed by the Antoine equation:

$$\ln P_i^{sat} = A_i + \frac{B_i}{T + C_i}$$

where T in $^{\circ}K$ and P_i^{sat} in N/m^2 . Table 2.2 contains the Antoine coefficients for the components used in the simulations.

Liquid activity coefficients were computed by the Van Laar equation:

$$T \ln \gamma_k = \sum_i A_{ki} z_i - \sum_i A_{ki} z_k z_i - \sum_{j \neq k} \sum_{i \neq k} A_{ji} \frac{A_{kj}}{A_{jk}} z_j z_i$$

where z_i is the effective volume fraction,

Table 2.2: Antoine coefficients for the components used in the simulations.

	A	B	C
Heptane	20.7664	-2911.32	-56.514
Benzene	20.7936	-2788.51	-52.360
Acetone	21.3099	-2801.53	-42.875
Methanol	23.4832	-3634.01	-33.768
Chloroform	20.865	-2696.9	-46.16

Table 2.3: Van Laar coefficients for the acetone - heptane - benzene mixture.

i \ j	Heptane	Benzene	Acetone
Heptane	0	159.20	569.40
Benzene	112.00	0	144.20
Acetone	444.80	189.60	0

$$z_i = x_i / \left(\sum_j x_j \frac{A_{ji}}{A_{ij}} \right).$$

In this model $A_{ii} = 0$, $A_{ij} = 0$ implies ideality, and if $A_{ji}/A_{ij}=0/0$ set $A_{ji}/A_{ij}=1$. Tables 2.3 and 2.4 contain the Van Laar coefficients for the mixtures acetone - heptane - benzene and acetone - methanol - chloroform respectively.

Table 2.4: Van Laar coefficients for the acetone - methanol - chloroform mixture.

i \ j	Acetone	Methanol	Chloroform
Acetone	0	205.40	-260.23
Methanol	232.00	0	597.03
Chloroform	-234.17	313.06	0

Chapter 3 Multiple Steady States in Heterogeneous Azeotropic Distillation

3.1 Introduction

A thorough review of the literature on multiplicities in distillation has been presented in chapter 2. Here we focus on the articles on multiplicities in heterogeneous mixtures. Magnussen et al. (1979) first presented simulation results that show the existence of three steady states (two stable and one unstable) for the heterogeneous mixture of ethanol - water - benzene. In these calculations (1) constant molar overflow is assumed and (2) the phase splitter is removed; instead, a second feed at the top of the column is considered (this second feed is the same for all three steady states). The multiplicities were observed with the UNIQUAC and NRTL activity coefficient models but a unique steady state was found with the Wilson equation model. On all the stages in all three profiles there is only one liquid phase. A similar multiplicity was observed for the system ethanol - water - pentane.

The results of Magnussen et al. (1979) triggered great interest in multiple steady states in distillation. The belief that heterogeneity is a possible cause for such multiple steady states directed the attention towards heterogeneous azeotropic distillation. Consequently, several articles were published where the mixture ethanol - water - benzene and especially the results of Magnussen et al. (1979) were studied extensively and where multiplicities for other heterogeneous systems were reported.

More specifically, Prokopakis et al. (1981) using a column without decanter (fixed second feed composition), the NRTL thermodynamic model and including enthalpy balances verified the three “regimes” found by Magnussen et al. (1979) but not multiplicity. For the mixture isopropanol - water - cyclohexane they report two steady states for the same specifications. In these steady states, however, the entrainer

flowrate in the boilup and the reflux flowrate and composition are held constant while the product flowrates are different. Hence these do not constitute an output multiplicity as defined above. For both mixtures they find that one of the steady states is "infeasible" in the sense that its overhead vapor composition lies outside the binodal curve and hence this profile cannot describe the profile of the column with the decanter. Again, there is no phase separation on the stages.

Prokopakis and Seider (1983a,b) using a column with decanter, the UNIQUAC thermodynamic model with binary parameters different from the ones used by Magnussen et al. (1979) and including enthalpy balances, again verified the three operating regimes, conjectured that one of them is unstable but no multiplicities were found.

Kovach and Seider (1987a,b) present simulation (homotopy-continuation) and experimental results of the mixture secondary butanol - water - dissecondary butyl ether (together with butylenes and methyl ethyl ketone impurities). Although no multiplicity is found, they locate two steady states (one with a single liquid phase on all trays and the other with two liquid phases on 70% of the trays) over a narrow range of the reflux ratios and conclude that this is consistent with the experimentally observed erratic behavior of the column. Using homotopy-continuation for the mixture ethanol - water - benzene they locate five steady states for the same specifications (output multiplicity). There is some concern whether the overhead vapor composition lies outside the binodal curve for three of the five profiles. Note that in all these calculations the condenser and the decanter are not included in the model. When they are included in the model three steady states are calculated.

Venkataraman and Lucia (1988) perform continuation studies for the ethanol - water - benzene column studied by Prokopakis and Seider (1983a) with the bottoms flow as the continuation parameter. They find three steady states over a narrow range of bottoms flow. Kingsley and Lucia (1988) show that there is a minimum tray efficiency for which these multiplicities exist. For columns with tray efficiency less than this minimum, a unique steady state exists for the whole range of bottoms flow. It is important, however, to note that the three steady states are calculated

without taking into account the presence or absence of two liquid phases on a tray (ignoring the liquid split) and hence they do not correspond to any realistic column (they can be used as the starting point of a heterogeneous distillation calculation). Kingsley and Lucia (1988) show that all these three profiles “ultimately lead to the same heterogeneous solution.” The authors were unable to produce heterogeneous multiplicities.

Widagdo et al. (1989) perform parameterization with respect to the aqueous reflux ratio for the mixture secondary butanol - water - dissecondary butyl ether (also Kovach and Seider, 1987a,b). They find three steady states over a narrow range of the aqueous reflux ratio. This multiplicity occurs when a second liquid phase appears on the top tray. A single-stage bifurcation analysis shows a unique solution and the authors suggest that other effects, such as the recycle, may be responsible.

Rovaglio and Doherty (1990) study the mixture ethanol - water - benzene using a column with decanter and different sets of parameters for the UNIQUAC model. They find three steady states for all parameter sets (including those used by Magnussen et al., 1979 and Prokopakis and Seider, 1983a,b) through dynamic simulations. For some sets two liquid phases exist on some trays, for others a single liquid phase exists on all trays. Their dynamic simulation results are consistent with the five steady states reported by Kovach and Seider (1987b).

Cairns and Furzer (1990) study the multiplicities by Magnussen et al. (1979) using the UNIFAC(VLE) model. Two of the steady states were obtained only by ignoring the phase splitting and hence they conclude that these profiles are fictitious. They also report two steady states (one again obtained by ignoring the liquid split) for the mixture ethanol - water - isooctane.

Bossen et al. (1993) study the mixture ethanol - water - benzene for a column with decanter using UNIFAC and UNIFAC(VLE). They find four steady states. In one of them, the whole profile as well as the decanter lies in the homogeneous region. The products of the other three profiles have exactly the same compositions and flowrates. The only difference between these three profiles is the location of the front of sharp ethanol and benzene composition changes. These three profiles are in good agreement

with the results of Rovaglio and Doherty (1990).

Rovaglio et al. (1993) study the multiplicities found by Rovaglio and Doherty (1990) through dynamic simulations as well as many of the previously reported multiplicities for the mixture ethanol - water - benzene. They demonstrate that although these steady states satisfy the convergence criteria “there may be small differences in the necessary make-up flowrates needed to keep these states constant and stable.” They conclude that “the problem of multiple steady states seems to be associated with the numerical aspects related to the relative small amount of feed make-up.”

The study presented here is the continuation of our previous work (chapter 2) on homogeneous azeotropic distillation. A summary of this previous work will be presented in the following.

3.2 Preliminaries

The term *heterogeneous azeotropic distillation* covers the general notion of distillation of azeotrope forming mixtures where two liquid phases exist in some region of the composition space. Usually, heterogeneous azeotropic distillation units perform the separation of a binary azeotrope into two pure components through the addition of an entrainer which alters the relative volatility of the two azeotropic constituents and enables separation by inducing liquid - liquid phase separation.

Unless stated otherwise, we use the following convention to refer to a given mixture: L (I, H respectively) corresponds to the component which has the lowest (intermediate, highest resp.) boiling point; we also denote the entrainer by E. We use the same notation in italics (*L*, *I*, *H*, *E*) to denote the corresponding flow rates of the components in the feed. The locations of the feed, distillate, bottoms, reflux and overhead vapor in the composition triangle are denoted by F, D, B, R and V respectively. Again, the corresponding flowrates are denoted by the same letters in italics (*F*, *D*, *B*, *R* and *V*).

Two widely used tools for the description of azeotropic distillation are the simple distillation residue curves (hereafter called residue curves) and the distillation lines.

Residue curves: The *simple distillation process* involves charging a still with a liquid of composition \underline{x} and gradual heating. The vapor formed, $\underline{y}(\underline{x})$, is in equilibrium with the liquid left in the still; the vapor is continuously removed from the still. A residue curve is defined as the locus of the composition of the liquid remaining at any given time in the still of a simple distillation process. Residue curves are governed by the set of differential equations (Doherty and Perkins, 1978):

$$\frac{d\underline{x}}{d\xi} = \underline{x} - \underline{y}(\underline{x}) \quad (1)$$

where \underline{x} and $\underline{y}(\underline{x})$ are the molar compositions of the liquid and vapor phase respectively, and ξ is the dimensionless warped time. Equation (1) defines the residue curves for homogeneous and heterogeneous mixtures; in the case of heterogeneous mixtures, \underline{x} is the molar composition of the overall liquid phase (Pham and Doherty, 1990).

A *distillation region* is defined as a subset of the composition simplex in which all residue curves originate from the same locally lowest-boiling pure component or azeotrope and end at the same locally highest-boiling one. The curves which separate different distillation regions are called residue curve boundaries. The term distillation region boundary (or just boundary) is used for both residue curve boundaries (interior boundaries) and the edges of the composition simplex.

Distillation lines: The definition of *distillation lines* (Zharov and Serafimov, 1975; Stichlmair et al., 1989; Stichlmair and Herguajuela, 1992), on the other hand, originates directly from the description of tray columns operating at infinite reflux. In these columns, the liquid composition of tray $n+1$ equals the composition of the vapor in equilibrium with the liquid of tray n (the tray below):

$$\underline{x}_{n+1} = \underline{y}(\underline{x}_n) = \underline{y}_n \quad (2)$$

Zharov and Serafimov (1975) define the distillation line as the set of points \underline{x} whose $\underline{y}(\underline{x})$, i.e., the vapor composition in equilibrium with \underline{x} , also lies on the same distillation line. Using the recursion formula (2) forward ($\underline{x}_n \rightarrow \underline{x}_{n+1}$) and backwards ($\underline{x}_{n+1} \rightarrow$

\underline{x}_n), a sequence of points in the composition space can be calculated (Stichlmair et al., 1989; Stichlmair and Herguiguera, 1992). By definition, all the points of this sequence lie on the same distillation line. Although it is very easy to calculate a sequence of points lying on some distillation line, the calculation of the whole distillation line is not trivial because there does not exist an explicit expression to exactly calculate the points of a distillation line between two points of a sequence. It is very common, hence, to just connect the points of a sequence by straight lines and use this as the *approximate distillation line*.

The distillation lines, as defined by Zharov and Serafimov (1975), do not cross each other. If this were not the case then there would exist two different vapor compositions in equilibrium with a single liquid composition (the composition at the intersection of the distillation lines). It is later shown that the distillation lines may only coincide in the two-liquid phase region. The approximate distillation lines, however, may cross each other. Figure 3.1 shows how two approximate distillation lines, belonging to the same or different exact* distillation lines, can cross.

From the discussion above and Figure 3.1, it should be clear that an exact distillation line is constructed by an infinite number of sequences of points calculated using equation (2), and hence there is an infinite number of approximate distillation lines associated with a single exact distillation line. Figure 3.1 shows two sequences of points, a and b , on the same exact distillation line. The composition profiles of tray columns in the composition space are obviously not continuous. The way the exact distillation lines are defined/constructed from tray column profiles explains why the exact distillation lines are continuous. It should also be clear that an exact distillation line, although continuous similarly to residue curves, is not a packed column profile. Hereafter, in illustrations of distillation line diagrams, the smooth, exact distillation lines are drawn, while in computed distillation line diagrams the approximate distillation lines, that connect the points of a sequence, are used.

*In the following, the terms distillation lines and *exact* distillation lines both refer to the lines defined by Zharov and Serafimov (1975) only (not the approximate ones). The adjective “exact” is used only when it is required to distinguish between the (exact) distillation lines and the approximate distillation lines.

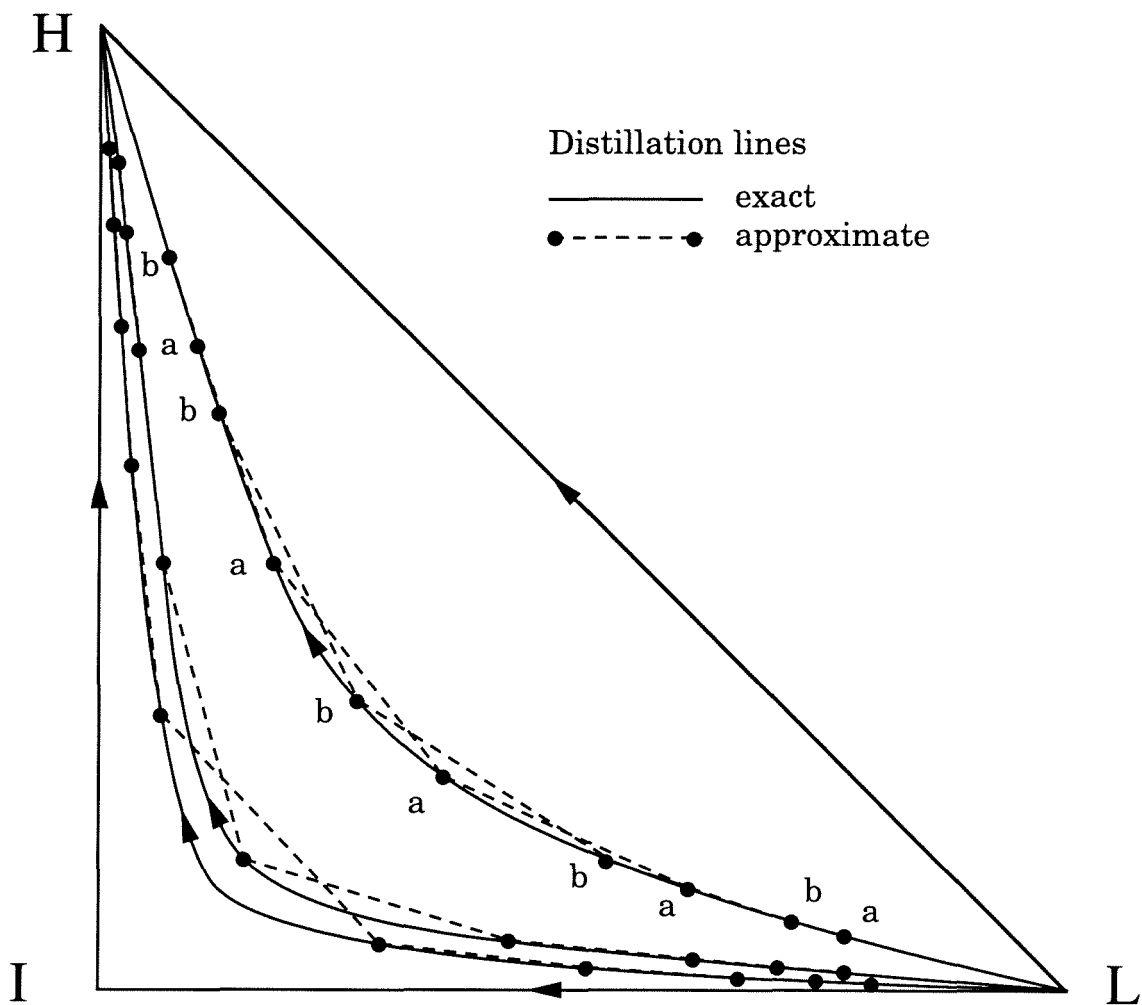


Figure 3.1: Approximate distillation lines belonging to the same or different exact distillation lines may cross. The exact distillation lines do not cross. Points a and b belong to two different sequences of points calculated using equation (2).

Zharov and Serafimov (1975) further showed that distillation lines (1) have the same singular points with residue curves and (2) behave similarly to residue curves close to singular points. Nevertheless, distillation lines do not generally coincide with residue curves. Usually, the direction opposite to that of residue curves is used for the distillation lines. In this manuscript, in order to avoid the confusion of referring to the same singular point as a stable node in residue curve diagrams and as an unstable node in distillation line diagrams, we use the direction of residue curves for distillation lines too. Figure 3.2 illustrates the residue curve, the exact distillation line and the approximate distillation line that go through a point \underline{x} in the composition triangle. The residue curve crosses the exact distillation line and is tangent to the line segment of the approximate distillation line connecting \underline{x} and $\underline{y}(\underline{x})$.

Similarly to residue curves, in the distillation line diagram there may exist distillation regions and boundaries which can be different from the regions and boundaries in the residue curve diagram. The calculation of distillation line boundaries is easier than the calculation of any other exact distillation line. The reason is that using equation (2) we can determine arbitrarily large sets of points that belong in one or the other of the two regions the boundary separates. The distillation line boundary lies between the two sets and hence a much better approximation (compared to just connecting the points of a single sequence) can be obtained.

Illustrative example: As an illustrative example throughout this chapter we use the mixture ethanol (L) - water (H) - benzene (I-E). Ethanol and water form an azeotrope which can be separated using benzene as the entrainer. Figure 3.3 illustrates the residue curve diagram of this type of ternary mixture at 1 atm. In this diagram, there are two binary homogeneous azeotropes (X and Y), one binary heterogeneous azeotrope (Z) and one ternary heterogeneous azeotrope (T). The ternary azeotrope is an unstable node, the pure components are stable nodes and the binary azeotropes are saddles. All residue curves start from the ternary azeotrope (globally lowest-boiling point) and end at one of the three pure component corners (locally highest-boiling points). There are three interior distillation boundaries in this diagram running from the ternary azeotrope to the three binary azeotropes. The boundaries separate the

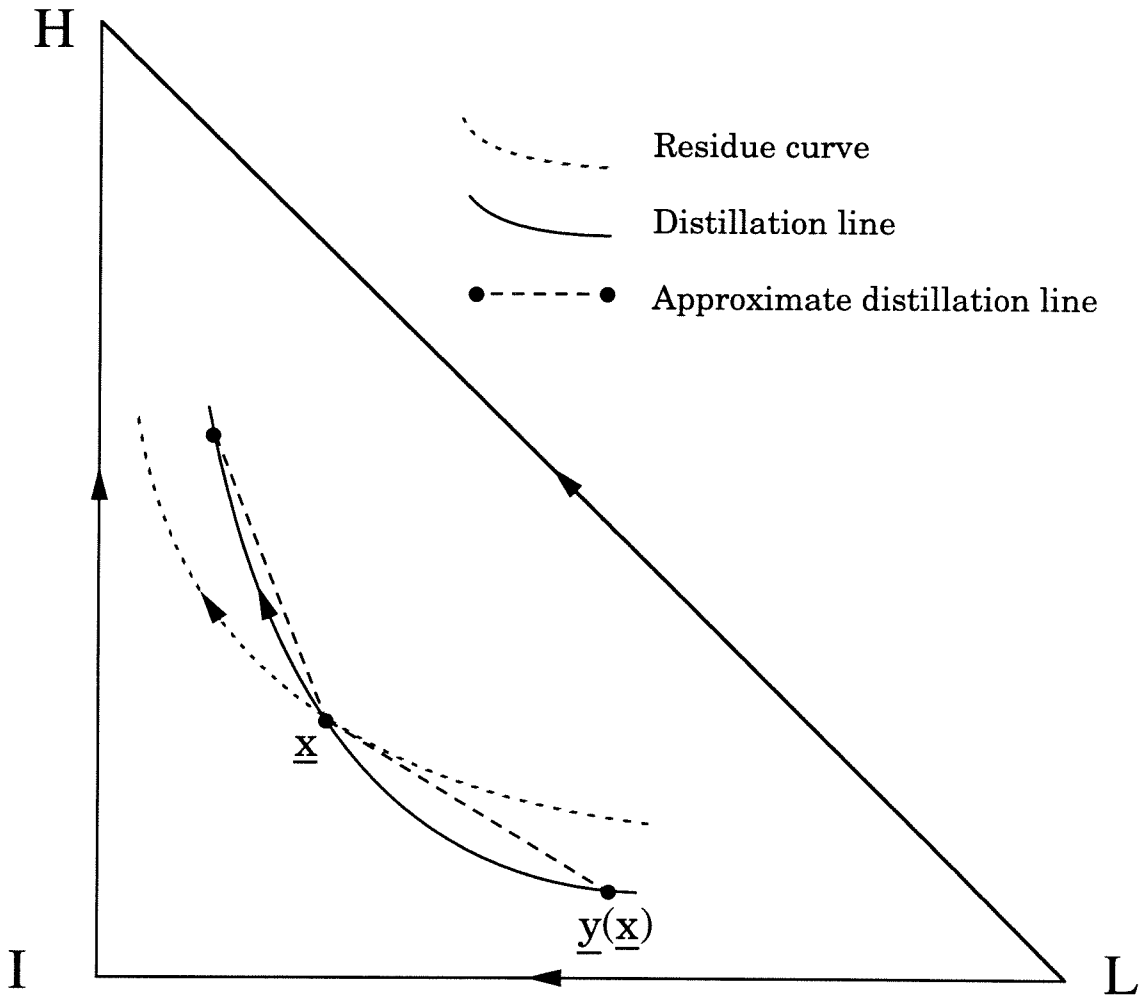


Figure 3.2: The residue curve, the distillation line and the approximate distillation line that go through point \underline{x} .

causes a singularity of the VLLE: the liquid composition in equilibrium with a vapor composition on the vapor line is not unique since it can be any point on some tie line.

Figure 3.4 illustrates the distillation line diagram for the same mixture at 1 atm. Qualitatively, the distillation line diagram is similar to the residue curve diagram of Figure 3.3. The locations of the boundaries and the distillation regions, however, are somewhat different. In the heterogeneous region, some part of the distillation line boundaries has to coincide with the vapor line (this is shown in section “Tray vs. packed columns”). Hence, the boundaries TX and TY and the vapor line coincide close to the ternary azeotrope. The point of deviation from the vapor line for each boundary is the composition of the vapor in equilibrium with the liquid at the intersection of the heterogeneous liquid boiling envelope and the boundary. The boundary TZ lies on the vapor line while the other two boundaries deviate from the vapor line at some point and therefore they do not contain point Q. This is because the boundaries do not contain the critical point C.

With this information (residue curve and distillation line diagrams and VLLE) we are able to thoroughly analyze the case of infinite reflux and infinite number of trays (or infinitely long packed columns), which we hereafter denote as the ∞/∞ case. In the following we present a general method for the study of multiplicities in the ∞/∞ case. We discuss both tray and packed columns for completeness. We illustrate this method using the mixture ethanol - water - benzene as the illustrative example. In this example, the column operates under constant atmospheric pressure, there is no pressure drop in the column, a tray efficiency of 1 is assumed and the condenser is total. We discuss the issues of tray efficiency and other condenser and reboiler types in the special topics section.

It is assumed that Figure 3.3 and Figure 3.4, describe the thermodynamic equilibrium of the mixture at 1 atm. These figures could be obtained from experimental data or using any thermodynamic model. In fact, the specific Figure 3.3 and Figure 3.4 are drawn so that they illustrate the qualitative characteristics of the following thermodynamic model: (1) Ideal vapor (2) Vapor pressures are calculated using the Antoine equation with parameters from Gmehling and Onken (1977) (3) liquid ac-

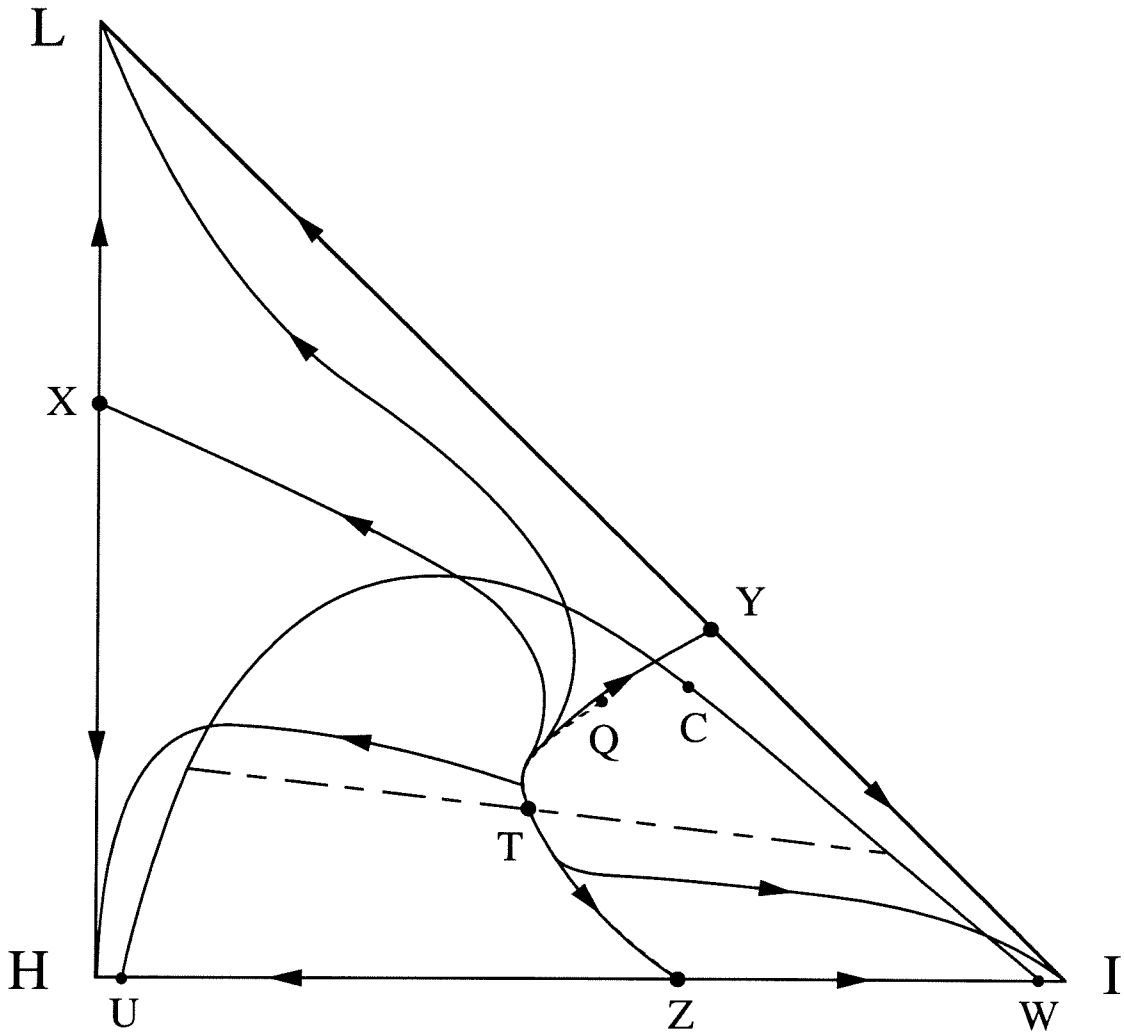


Figure 3.4: Distillation line diagram and VLE of the mixture ethanol (L) - water (H) - benzene (I-E).

tivity coefficients are calculated using the UNIQUAC equation with pure component parameters from Gmehling and Onken (1977) and binary parameters estimated from UNIFAC using Aspen Plus (1988). The appendix contains more information on the thermodynamic model as well as the Antoine and UNIQUAC parameters. Figure 3.5 and Figure 3.6 show the actual, *computed* residue curve and distillation line diagrams, respectively, using the above thermodynamic model. Note that Figure 3.3 (3.4 resp.) is simply a drawing of Figure 3.5 (3.6 resp.); they both have the same qualitative features, Figure 3.3 (3.4 resp.), however, has some important features exaggerated for illustrative purposes. Figure 3.3 and Figure 3.4 are used in the analysis of the ∞/∞ case.

In the following we summarize the results obtained in the ∞/∞ case for homogeneous mixtures (chapter 2). Although these results were derived for residue curve diagrams, we show that similar results hold for distillation line diagrams.

3.2.1 Composition Profiles in the ∞/∞ Case

Packed columns: At infinite reflux, the differential equations which describe packed columns become identical to the residue curve equations (Laroche et al., 1992). Thus residue curves coincide exactly with the liquid composition profiles of packed columns operated at total reflux. In the special case of infinitely long packed columns there is one additional requirement: The column profile should contain at least one pinch point. Pinch points at infinite reflux can only be the singular points of the residue curve diagram, i.e., the pure components and the azeotropes. Therefore, the packed column liquid composition profiles in the ∞/∞ case should follow residue curves and contain at least one pure component or azeotrope. Hence the only acceptable columns belong to one of the following types:

- I. Columns whose top liquid composition* is that of an unstable node. In this

*The top (bottom) liquid composition refers to the upper (lower) end liquid composition of the column profile without the reboiler and condenser. Therefore, the top (bottom) liquid composition does not generally coincide with the top (bottom) product composition. We discuss the effect of the reboiler and condenser on the product compositions in the special topics section.

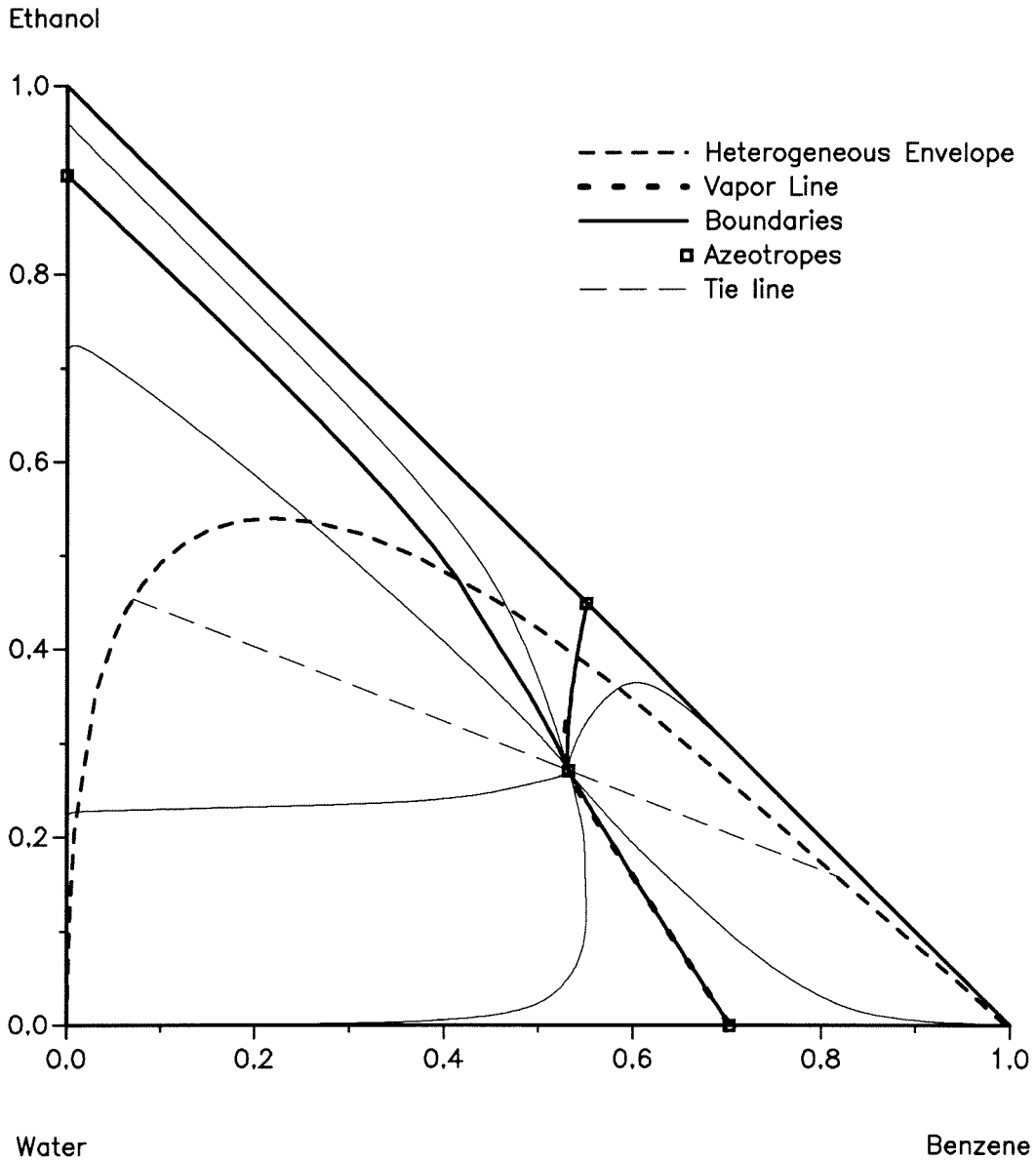


Figure 3.5: The actual, computed residue curve diagram and VLE of the mixture ethanol - water - benzene.

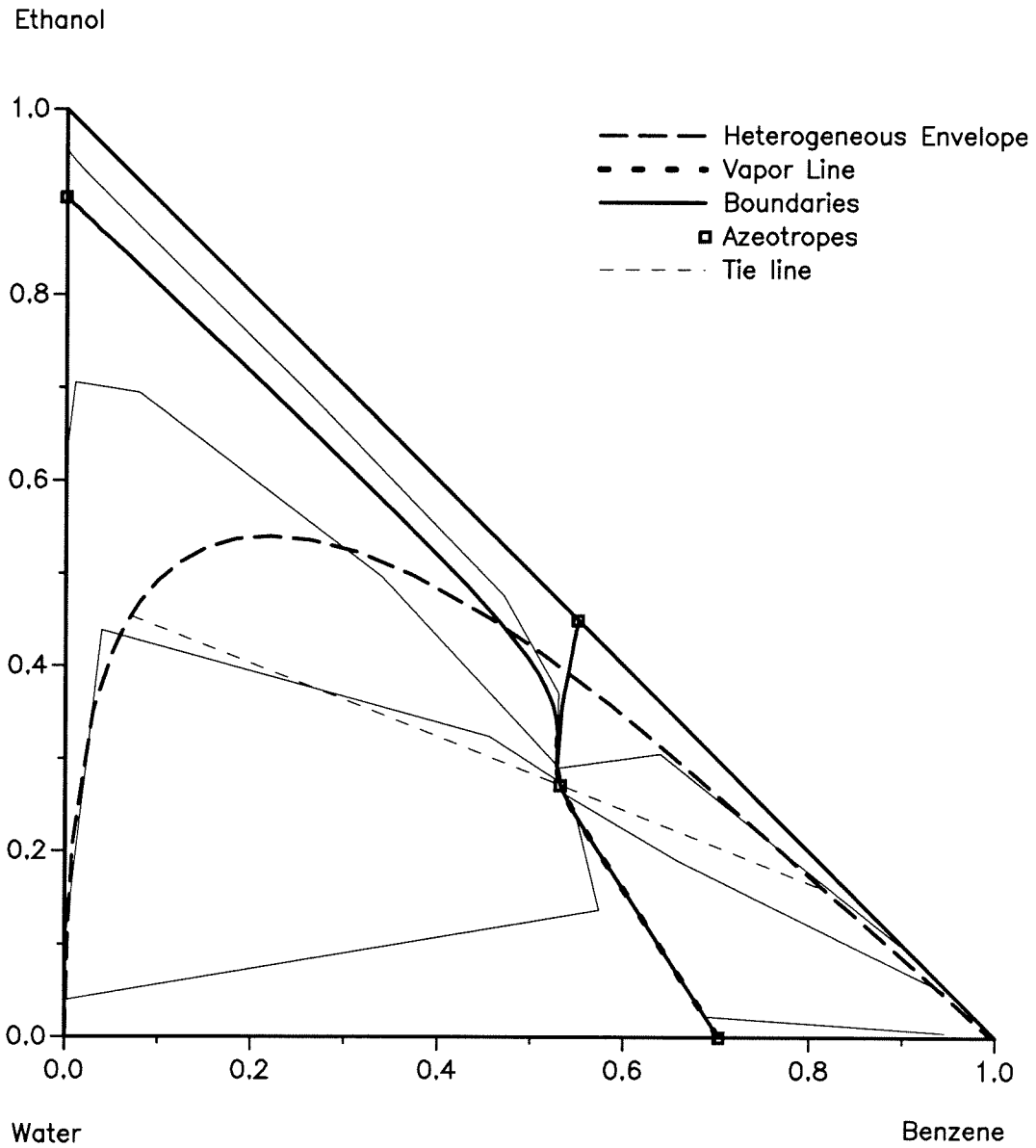


Figure 3.6: The actual, computed distillation line diagram and VLLE of the mixture ethanol - water - benzene.

case, the column liquid composition profile starts from the unstable node (top liquid composition), follows a residue curve and ends at an arbitrary point on the same residue curve (bottom liquid composition).

- II. Columns whose bottom liquid composition is that of a stable node. In this case, the column liquid composition profile starts from an arbitrary point in the composition triangle, follows the residue curve that passes through this starting point and ends at the stable node (bottom liquid composition).
- III. Columns whose liquid composition profiles run along the boundaries (edges of the triangle and/or interior boundaries) and contain at least one of the saddles. In this case, the top and bottom liquid compositions lie on the boundaries.

Figure 3.7 illustrates the three acceptable types of liquid composition profiles of packed columns for the mixture shown in Figure 3.3. The type I and II profiles contain a node singular point at one of the two ends (at the top and at the bottom resp.). The type III profiles contain an interior pinch point which can only be a saddle. Note that at any point in the column, the liquid and vapor compositions are identical (by the material balances) and hence the liquid and vapor profiles coincide.

Tray columns: Similarly, composition profiles of tray columns in the ∞/∞ case should follow distillation lines and contain at least one pinch point, i.e., pure component or azeotrope. Again there are three acceptable types of profiles similar to the ones described above; simply replace residue curves and boundaries with distillation lines and distillation line boundaries in the above. Although residue curves and distillation lines do not coincide, it is very common to consider that residue curves give a good approximation of composition profiles of tray columns at infinite reflux. In the previous chapter on homogeneous azeotropic distillation, this assumption was made. We will show later that this approximation may not be appropriate when the residue curve boundaries and the distillation line boundaries significantly deviate from each other. The effect of heterogeneity on this approximation will also be discussed later.

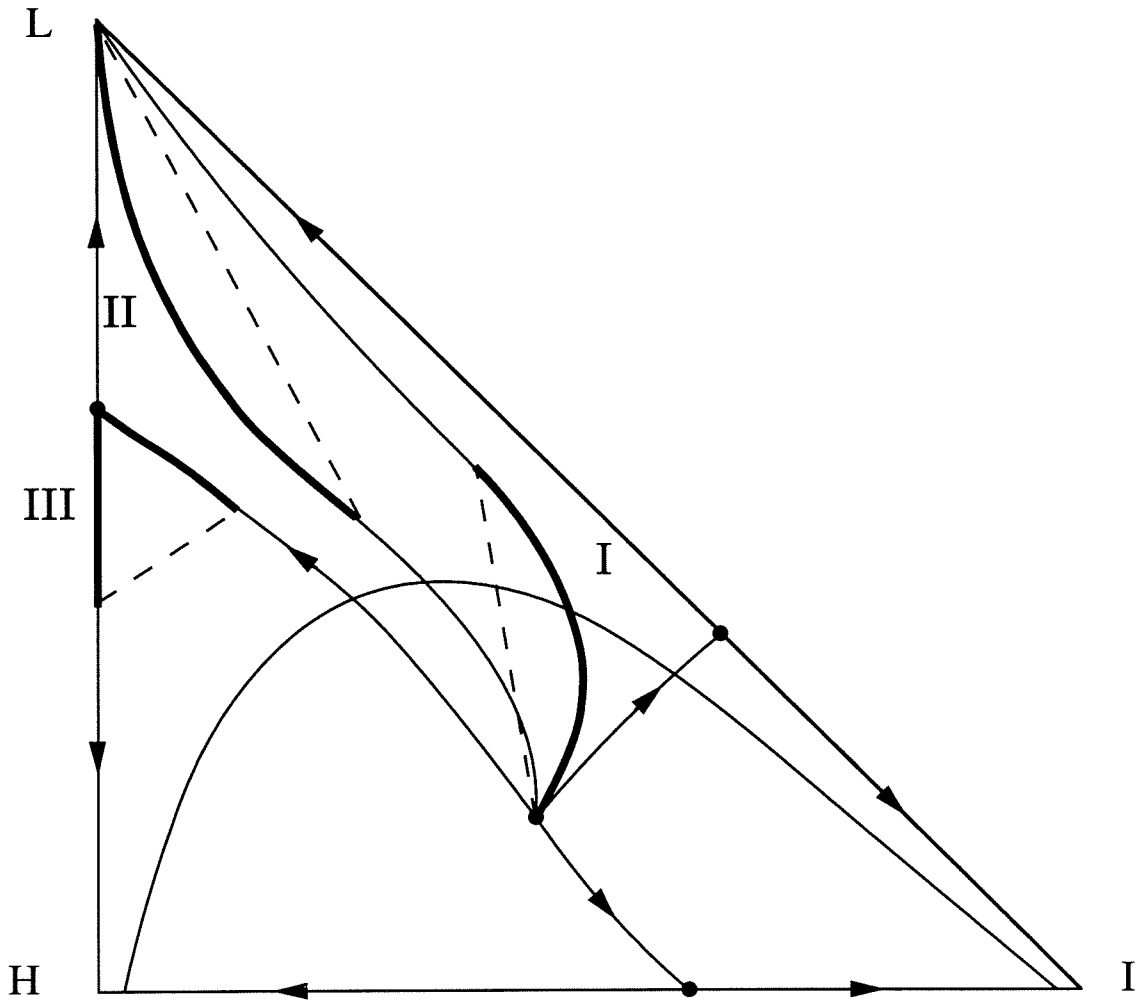


Figure 3.7: The three acceptable types of profiles in the ∞/∞ case.

3.2.2 Existence of Multiple Steady States

In the previous section we demonstrated how the column composition profiles should look in the ∞/∞ case. Using the information above and the overall material balances, we can locate the feasible distillate and bottom product compositions for any given feed. In the ∞/∞ case of a homogeneous column, given a feed composition and a feed flowrate F , the only unspecified parameter is one product flow, e.g., the distillate flow rate D (the other flow rate is specified by the overall material balance). In order to find whether multiple steady states can occur (i.e. whether different column profiles correspond to the same value of D) we find all possible composition profiles by tracking the distillate and bottoms in the composition triangle, starting from the column profile with $D = 0$ and ending with the column profile with $D = F$. That is, we perform a bifurcation study (continuation of solutions) using the distillate flow as the bifurcation parameter. This task can be achieved because in the ∞/∞ case a continuation of solutions can be obtained based on physical arguments only. Multiple steady states exist when the distillate flow varies non-monotonically along the continuation path of the bifurcation diagram and more specifically, for our continuation path choice, when the distillate flow decreases in a segment along this path. Therefore, in order to find rules for the existence of multiple steady states, we have to first find out when D decreases along the continuation path.

Some important results of our thorough analysis (chapter 2) are the following: Along the continuation path, D increases monotonically as we track all type I and type II column profiles. Therefore, a decrease in D can only occur as we track the type III column profiles, i.e., columns whose composition profiles run along distillation region boundaries and contain at least one of the saddle singular points. We further show that the existence of multiplicities depends on the relative position (geometry) of the distillation region boundaries, and hence the location of the distillation boundaries is the only information required to conclude on the existence of multiplicities.

Using the results of this analysis we derive the necessary and sufficient geometrical condition for the existence of multiple steady states which is summarized in the

following:

Geometrical, necessary and sufficient multiplicity condition: The continuation path is defined as the path generating all possible column profiles starting from the profile with $D=0$ and ending at the profile with $D=F$. Multiple steady states occur when D decreases somewhere along this path. This can be checked by the following procedure: Pick a distillate D and a bottom product B , both located on some distillation region boundaries and such that the column profile that runs from D to B along the distillation region boundaries contains at least one saddle singular point (type III column profile). Now pick D' and B' sufficiently close to D and B respectively and such that the column profile from D' to B' is a “later” profile along the continuation path. For the existence of multiple steady states it is required that: As we move along the continuation path from D to D' and accordingly from B to B' , the line that passes from D and is parallel to BB' crosses the $D'B'$ line segment (Figure 3.8).

We further show that the existence of multiplicities depends on the feed composition and we locate the feed composition region that leads to multiple steady states. The condition for the appropriate feed region is summarized in the following:

Appropriate feed region condition: Pick a distillate D . Find the set of all bottom products such that the geometrical condition is satisfied for the picked D . Name this set $S_B(D)$. Note that $S_B(D)$ is always part of a distillation region boundary and that in some rare cases, $S_B(D)$ may contain an inflexion point and/or it may consist of more than one non-connected boundary segments. Draw the straight line segments connecting D with the end points of each boundary segment that belongs to $S_B(D)$. For the chosen D , the appropriate feed composition is the union of the areas enclosed by each boundary segment that belongs to $S_B(D)$ and the corresponding straight line segments connecting D with the end points of the boundary segment of $S_B(D)$. Pick another distillate D and repeat. In general, for each distillate D there exists a different set of bottoms compositions, $S_B(D)$, that satisfies the geometrical condition. Therefore, for any given mixture, the feed compositions that lead to multiplicities lie in the union of all the areas enclosed by each boundary segment that belongs to

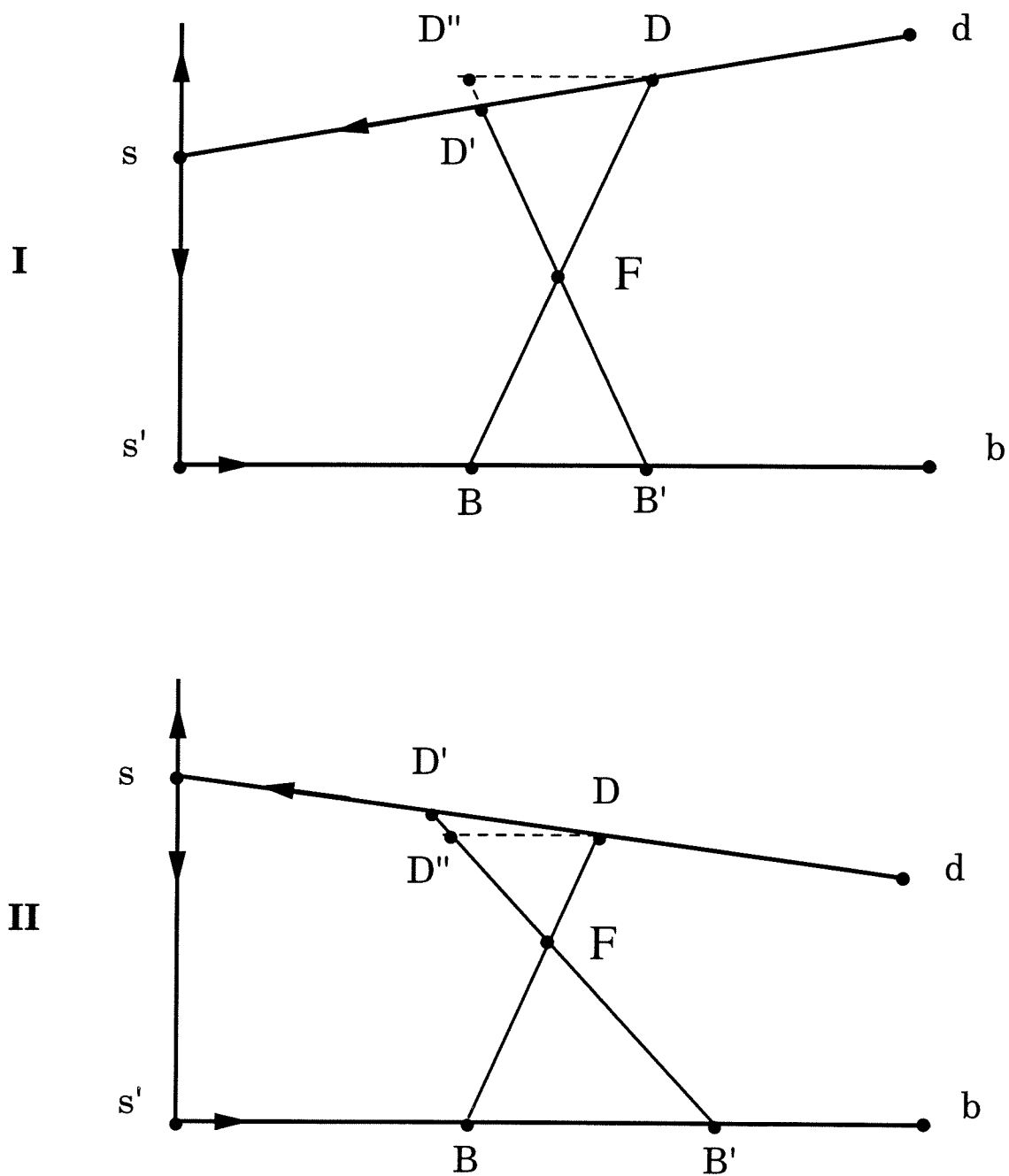


Figure 3.8: The geometrical multiplicity condition is I. not satisfied (D increases along the continuation path) II. satisfied (D decreases along the continuation path).

some $S_B(D)$ and the corresponding straight line segments connecting the distillate D associated to $S_B(D)$ with the end points of the boundary segment of $S_B(D)$.

Figure 3.9 illustrates the appropriate feed region condition. The geometrical condition is satisfied for distillate compositions D on the boundary segment ad . For any D on the boundary segment ad , the set $S_B(D)$ is the straight line segment Ic . Hence, for any D on the boundary segment ad , the appropriate feed region is the triangle Dlc . Therefore, the appropriate feed region for this mixture is the union of all these triangles, i.e., the shaded area $adlc$. Note that, for the mixture shown in Figure 3.9, the set $S_B(D)$ (1) consists of just one, straight line boundary segment and (2) is the same for all distillate compositions D that satisfy the multiplicity condition. The appropriate feed region condition described above covers the general case of $S_B(D)$ consisting of more than one, curved boundary segments and being different for each D .

The above results have been originally derived for residue curve diagrams. It is obvious that similar results hold for distillation line diagrams by simply substituting residue curve boundaries with distillation line boundaries. Using the above results, we are able to study the existence of multiple steady states in the ∞/∞ case for mixtures that exhibit two liquid phases. We will perform this task in two steps: First for packed and tray columns without decanter and then for columns with decanter.

3.3 Columns without decanter

In the homogeneous case, the composition of the distillate is that of the stream drawn from the top of the column. This is also the case when no decanter is used in heterogeneous azeotropic distillation. Hence the techniques developed for homogeneous azeotropic distillation can be directly applied in this case. In particular, the case of heterogeneous mixtures using *packed* columns without decanter is identical to the one studied in the previous chapter on homogeneous azeotropic distillation. We study packed columns first.

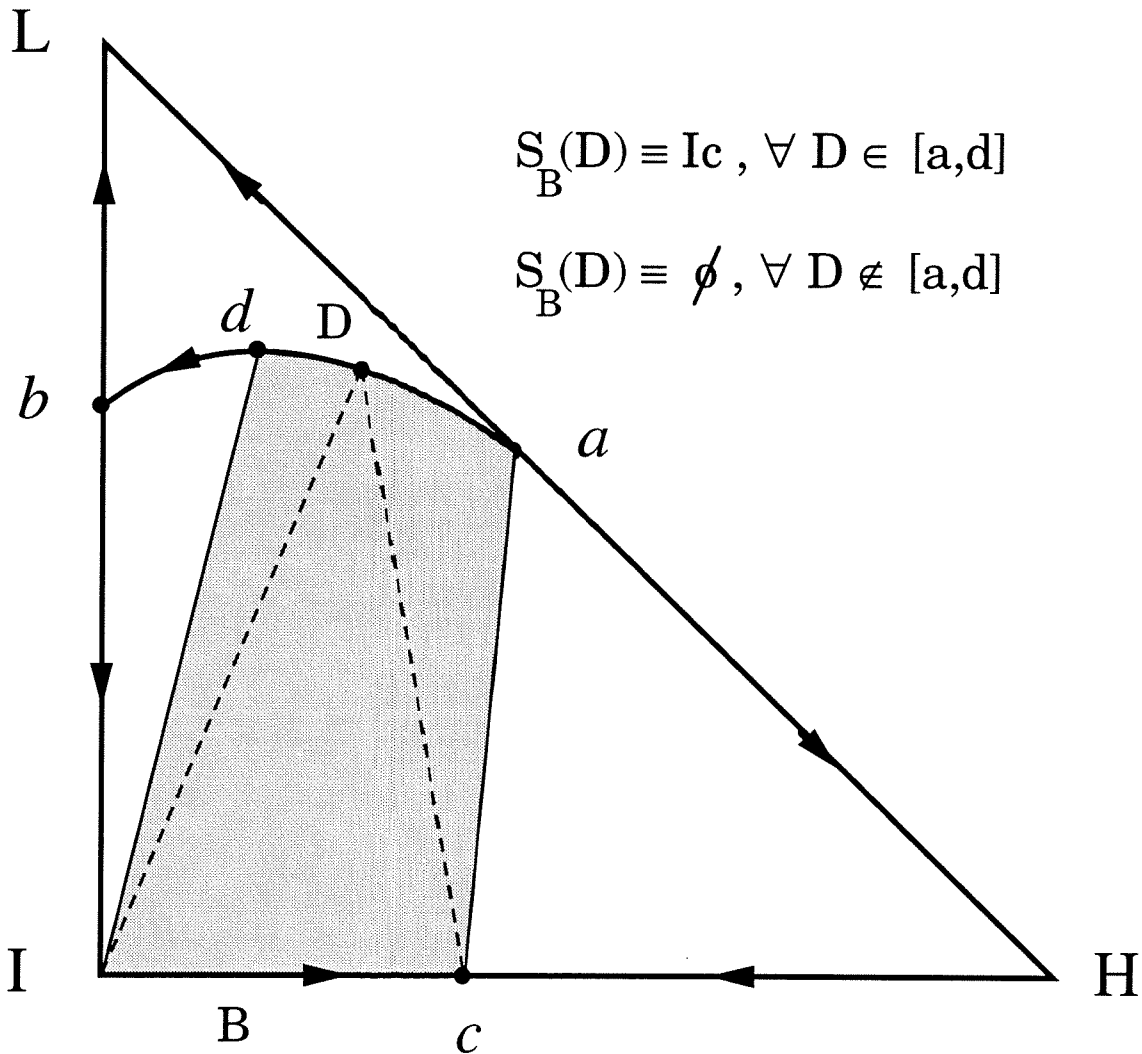


Figure 3.9: For any D on the boundary segment ad , the appropriate feed region is the triangle DIc . For this mixture, the region of feed compositions that lead to multiplicities is the union of all these triangles, i.e., the shaded area $adIc$.

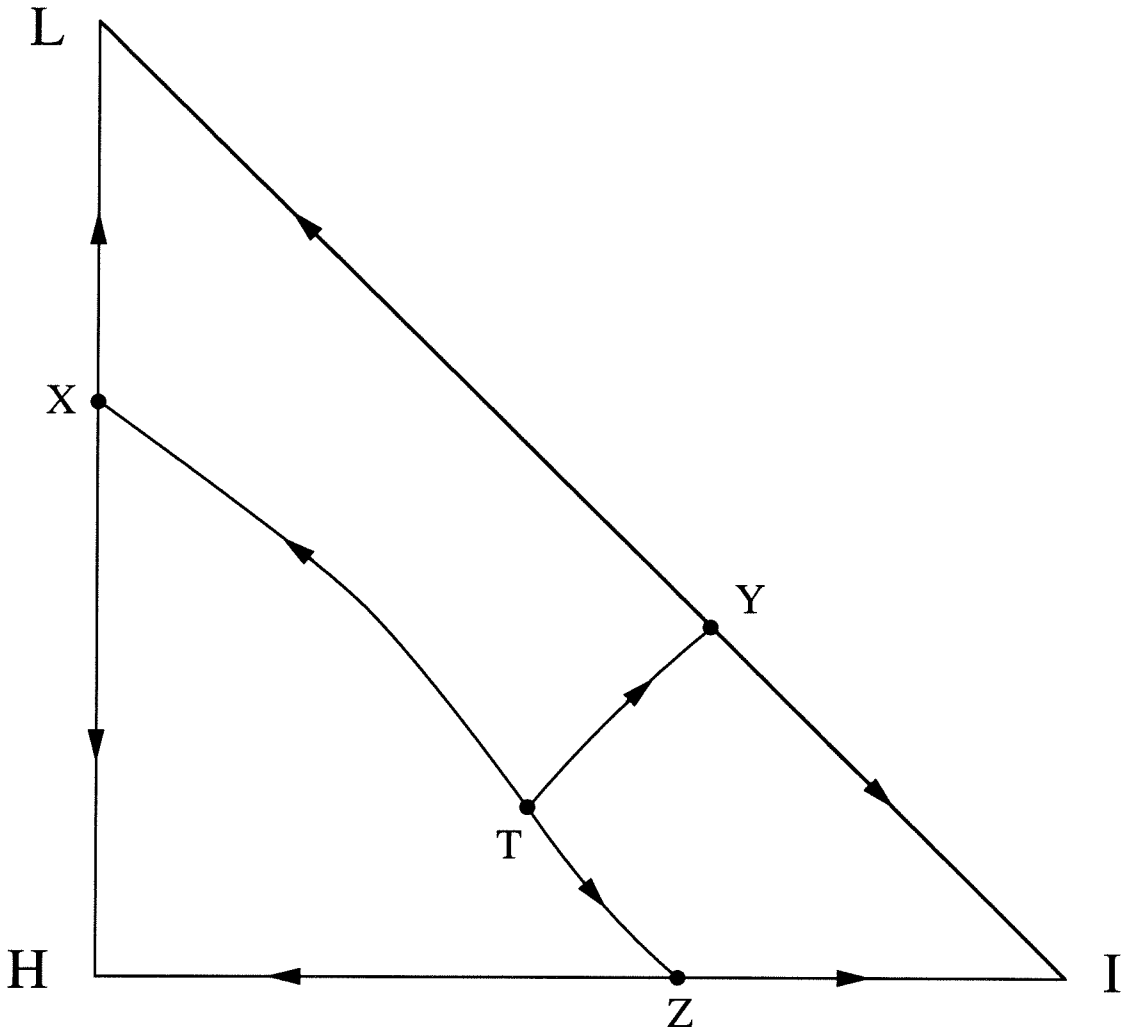


Figure 3.10: Packed columns without decanter: No multiplicities.

Packed columns: The only information required in this case is the residue curve boundaries as shown in Figure 3.10. The computation of the residue curve boundaries obviously requires VLLE information. As soon as Figure 3.10 is obtained, however, no other VLLE information (vapor line, heterogeneous envelope, etc.) is required and hence the mixture depicted in Figure 3.10 can be treated as if it were a homogeneous mixture belonging to the 222-m class according to the classification by Matsuyama and Nishimura (1977).

In each of the three regions, there are two routes which go from the unstable node to the stable node along the region boundaries (a total of six routes, namely $T \rightarrow X \rightarrow L$, $T \rightarrow X \rightarrow H$, $T \rightarrow Y \rightarrow L$, $T \rightarrow Y \rightarrow I$, $T \rightarrow Z \rightarrow I$, $T \rightarrow Z \rightarrow H$). Note that the distillate and

bottoms compositions should lie on the same route and therefore we only have to check the geometrical condition along the six routes mentioned above. All routes contain only one saddle singular point. Since the type III profile of an infinitely long column should contain at least one saddle, it is apparent that for any route the distillate may only lie on the interior boundary while the bottoms may only lie on the edge of the triangle.

It is only for these locations of D and B that the geometrical condition needs to be checked. The condition is even further simplified since the line BB' (see the geometrical condition above) may only lie on some edge of the triangle. Moreover, for this type of residue curve diagram, the distillate of type III profiles along the continuation path will move along one of the interior boundaries *monotonically* in the direction from T towards the other end of the boundary. The geometrical condition for this particular type of residue curve diagram can be then simplified to the following: For the existence of multiple steady states it is required that (1) some line parallel to the LH edge intersects the interior boundary TX more than once, or (2) some line parallel to LI intersects TY more than once, or (3) some line parallel to IH intersects TZ more than once.

In applying the geometrical condition, caution should be taken close to the boundary end points (singular points) because the curvature of the boundary may change dramatically in the neighborhood of a singular point and hence there might exist a small boundary segment that enables the existence of multiple steady states. For mixtures belonging to the 222-m class the geometrical condition cannot be satisfied close to any binary azeotrope no matter what is the orientation of the boundary. Close to T, on the other hand, the interior boundaries (as well as the vapor line) are tangent to the direction of the eigenvector associated with the smallest absolute eigenvalue of the linearized equation (1) at point T (principal eigendirection). Depending on the orientation of the principal eigendirection and on the side from which each boundary approaches T, the geometrical condition may or may not be satisfied. In Figure 3.10, the geometrical condition is not satisfied for any interior boundary and therefore no multiplicities exist for packed columns.

Tray columns: Similarly, for tray columns, we only have to check the aforementioned simplified geometrical condition for the interior distillation line boundaries which are shown in Figure 3.11. Points a and b in Figure 3.11 are defined as the points of TX where the tangent to the boundary is parallel to the LH edge. The condition is not satisfied for the boundaries TY and TZ, it is satisfied, however, for the boundary TX. By applying the geometrical condition in its original form, it is easy to show that the distillate flowrate decreases along the continuation path for distillate compositions located on the ab segment of the boundary TX and bottoms located at any point on the LH edge. Therefore, the set $S_B(D)$ is the edge LH for any D on ab . Hence, the shaded region in Figure 3.11 depicts the feed composition region that leads to multiple steady states.

We will next track the whole continuation path (as described above) for a tray column with the feed composition F shown in Figure 3.12. The feed is homogeneous and lies in the lower left distillation region where T is the unstable node and H the stable node. The light component mole fraction in the bottoms x_{BL} is recorded along the continuation path. Figure 3.12 also depicts the feasible distillate and bottoms compositions (D and B) in the composition triangle and Table 3.1 shows the location of D and B , the distillate flowrate D changes, the light component mole fraction in the bottoms x_{BL} and the type of the column profile along the continuation path. In summary, the continuation path goes as follows:

We start with the type I profile with the distillate D at the ternary azeotrope T and the bottoms B at the feed F . Hence, $D = 0$ and $x_{BL} = x_{FL}$. Then, we track all type I profiles. The distillate D for all profiles lies on T while the bottoms B lies on the straight line Fd by the material balance. Along this part of the continuation path both D and x_{BL} increase.

Next, we track all type III profiles with the distillate D for all profiles on the vapor boundary TX and the bottoms B on the LH triangle edge. As D moves from T to a , B moves from d to e and hence x_{BL} decreases while D increases. It is very simple to show using the lever material balance rule that D decreases as D moves from a to b . At this part of the continuation path, B moves from e to f and hence x_{BL} decreases.

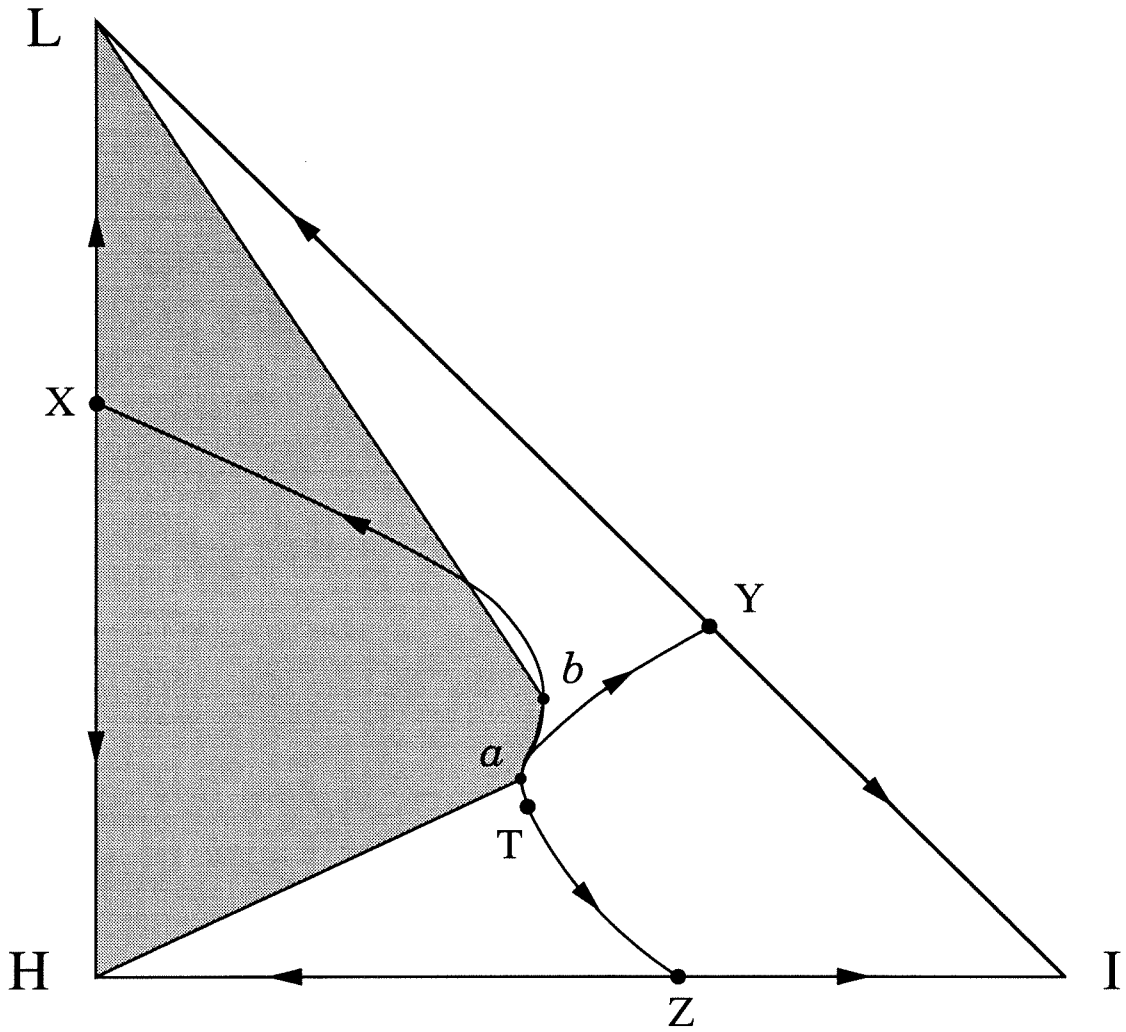


Figure 3.11: Tray columns without decanter: multiplicities for feeds in shaded region.

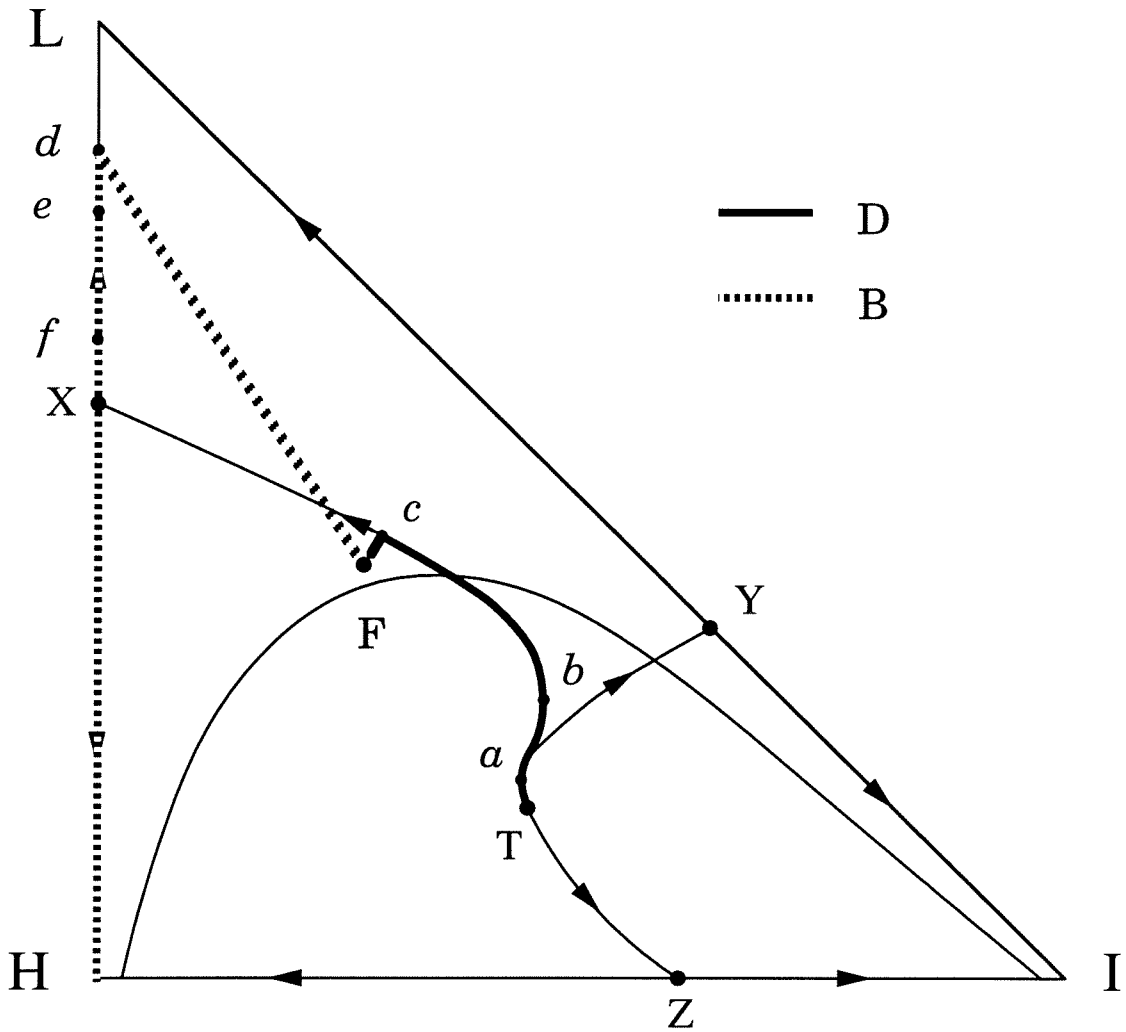


Figure 3.12: Tray columns without decanter: the continuation paths for D and B.

Table 3.1: Information along the continuation path for tray columns without decanter.

profile type	heterogeneous			homogeneous				
	I	III	III	III	II			
D	T	T	a	b	c	F		
B	F	d	e	f	H	H		
D	0	↑	↑	↓	↑	↑	F	
x_{BL}	x_{FL}	↑	↓	↓	↓	0	—	0

Then, as D moves from b to c , B moves from f to H and hence x_{BL} decreases while D increases. Note, that beyond some point along this last part of the continuation path, the column profile becomes totally homogeneous (some part of the profile was in the heterogeneous region before).

Finally, we track all type II profiles. The bottoms B for all profiles lies on H while the distillate D lies on the straight line cF by the material balance. Along this part of the continuation path D increases (reaching F at the end point) while x_{BL} remains constant $x_{BL} = 0$. Figure 3.13 shows a sketch of the bifurcation diagram of x_{BL} vs. the bifurcation parameter D . It is apparent that for some distillate flowrate range, three steady states exist. Hence, for the mixture under consideration, there exists a qualitative difference between packed and tray columns.

3.3.1 Tray vs. packed columns

If the residue curve boundaries are straight lines then the corresponding distillation line boundaries are also straight lines and they coincide with the residue curve boundaries. In this case, the study of multiplicities gives identical results for both packed

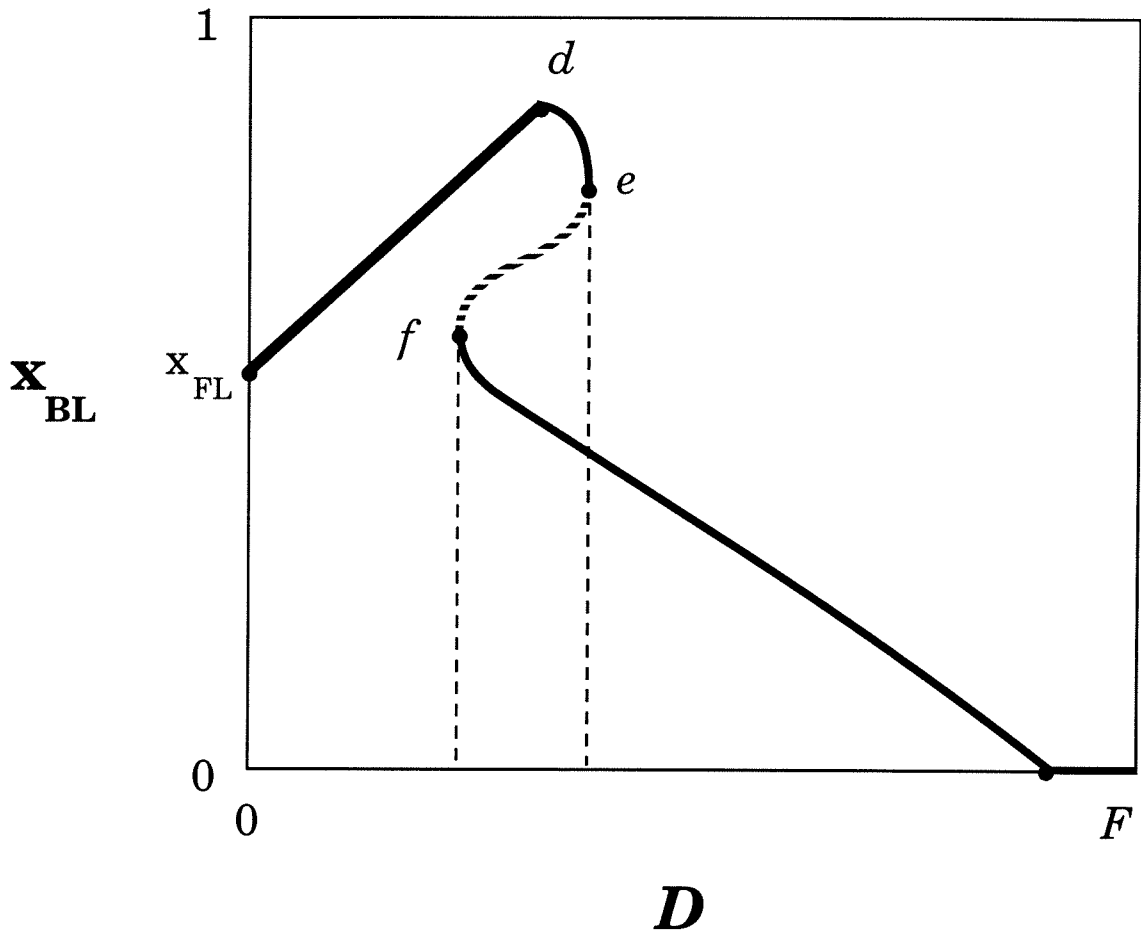


Figure 3.13: Bifurcation diagram of the mole fraction of L in the bottoms vs. the distillate flow for tray columns without decanter.

and tray columns. This was the case with the homogeneous mixture acetone - heptane - benzene studied in chapter 2 where the edges of the composition triangle were the only boundaries.

In the case of curved boundaries, however, some discrepancy between the residue curve and distillation line boundaries is expected. At a first level, this discrepancy results in some *quantitative* differences between packed and tray columns, i.e., differences in the appropriate feed region, the range of distillate flow where multiplicities exist etc. Because residue curve diagrams are much easier to calculate, it is commonly assumed that they provide a good approximation of tray columns as well. In the previous chapter on homogeneous azeotropic distillation, we used only residue curve diagrams for the theoretical study of multiplicities while the simulations were conducted for columns with trays. A very good agreement between the theory and the simulations was obtained even for residue curve diagrams with highly curved boundaries where tray column profiles may significantly deviate from residue curves.

The study of the mixture ethanol - water - benzene, however, showed that *qualitative* differences are also possible. Note that qualitatively different results may also be obtained for homogeneous mixtures. Also note that the curvature of a boundary is not the only measure of the discrepancy between residue curve and distillation line boundaries. The local “difficulty” of a separation, the “distance” between a liquid and a vapor composition in equilibrium plays a role, too. The more “difficult” a separation is, i.e., the smaller is the distance between \underline{x} and $\underline{y}(\underline{x})$, the smaller is the difference between the residue curve and distillation line boundaries. It is not easy, however, to identify the mixtures where qualitative differences occur between the predictions using the residue curve boundaries and the behavior of tray columns. This is particularly true for homogeneous mixtures although we are not aware of any mixture exhibiting such qualitative differences.

Next we show (1) why the difference between the residue curve and distillation line boundaries can be much more profound for heterogeneous mixtures and (2) how the VLLE, in particular the vapor line, can give us an indication when to expect qualitative differences between packed and tray columns. Note that the above state-

ment is not in conflict with the fact that heterogeneous columns without decanter and homogeneous columns are treated identically regarding multiplicities.

It was mentioned above that the residue curve diagram of the heterogeneous mixture depicted in Figure 3.10 could also be the residue curve diagram of a homogeneous mixture belonging to the 222-m class. This is not true, however, for the distillation line diagram of the same mixture, i.e., Figure 3.11 cannot be the distillation line diagram of any homogeneous mixture. In Figure 3.11 both distillation line boundaries TX and TY lie on the vapor line close to T and they share a common part. Boundaries for homogeneous mixtures cannot coincide at some segment and then divert. This can only happen for mixtures exhibiting two liquid phases and it is due to the singularity of the VLLE: the vapor compositions in equilibrium with the liquid compositions of the *two-dimensional* two-liquid phase region lie on the *one-dimensional* vapor line.

In fact, all distillation lines (not the boundaries only) inside the heterogeneous region have to coincide with some part of the vapor line. This can be easily shown using equation (2): consider a tray with liquid composition in the heterogeneous region; then by (2) the liquid composition of the tray above, as well as of all the trays on top of that, will lie on the vapor line. Therefore, for heterogeneous mixtures distillation line boundaries may significantly deviate from the corresponding residue curve boundaries because they have to follow part of the vapor line. Hence, the vapor line gives an indication of the geometry of some part of the distillation line boundaries which can be useful for the prediction of multiplicities of tray columns.

For heterogeneous mixtures similar to ethanol - water - benzene, in particular, it is very probable that some distillation line boundary will significantly deviate from the corresponding residue curve boundary because there are 3 residue curve boundaries running from T to each binary azeotrope and only 2 directions to approach T along the vapor line. The vapor line in Figure 3.3 lies close to the residue curve boundaries TY and TZ, but far from the third residue curve boundary TX. Note however that this is not the key feature that leads to multiplicities for tray columns; it is the geometry of the vapor line and in particular the turn from the left to the right of the

top end of the vapor line. Figure 3.14 shows the same mixture (Figure 3.3) with a slightly different vapor line that runs close to TZ and TX. From Z to Q, the vapor line runs continuously from the right to the left. In this case, it is highly probable that, similarly to packed columns, no multiplicities exist for tray columns (since parts of the vapor line coincide with only parts of the distillation line boundaries we cannot be absolutely sure).

3.3.2 Summary

In this section we studied the ∞/∞ case of packed and tray columns without decanter for mixtures that may exhibit two liquid phases. We presented the accurate geometrical condition for the existence of multiplicities for the aforementioned cases as well as for packed and tray homogeneous columns. We discussed the differences between packed and tray columns, between residue curve and distillation line boundaries and the role of the vapor line for heterogeneous mixtures. Since residue curve boundaries are easier to calculate than distillation line boundaries, we derived guidelines on when it is justified to use residue curve boundaries for the study of multiplicities of tray columns.

These guidelines are: (1) For homogeneous mixtures: residue curve boundaries provide a good approximation except when the boundaries are highly curved (although we are not aware of any mixture where the approximation fails). (2) For heterogeneous mixtures: on one hand, residue curve boundaries inside the two-liquid phase region may provide a very poor approximation of distillation line boundaries. On the other hand, the vapor line gives an indication of the geometry of the distillation line boundaries in the two phase region. Hence, the combination of residue curve boundaries and the vapor line can be used for the qualitative prediction of multiplicities of tray columns (Figure 3.3 and Figure 3.14). If this prediction is different from the one for packed columns, then it is suggested that the distillation line boundaries should be used for detailed results on multiplicities of tray columns.

A final note on the significance of this section. Although a column *with decanter*

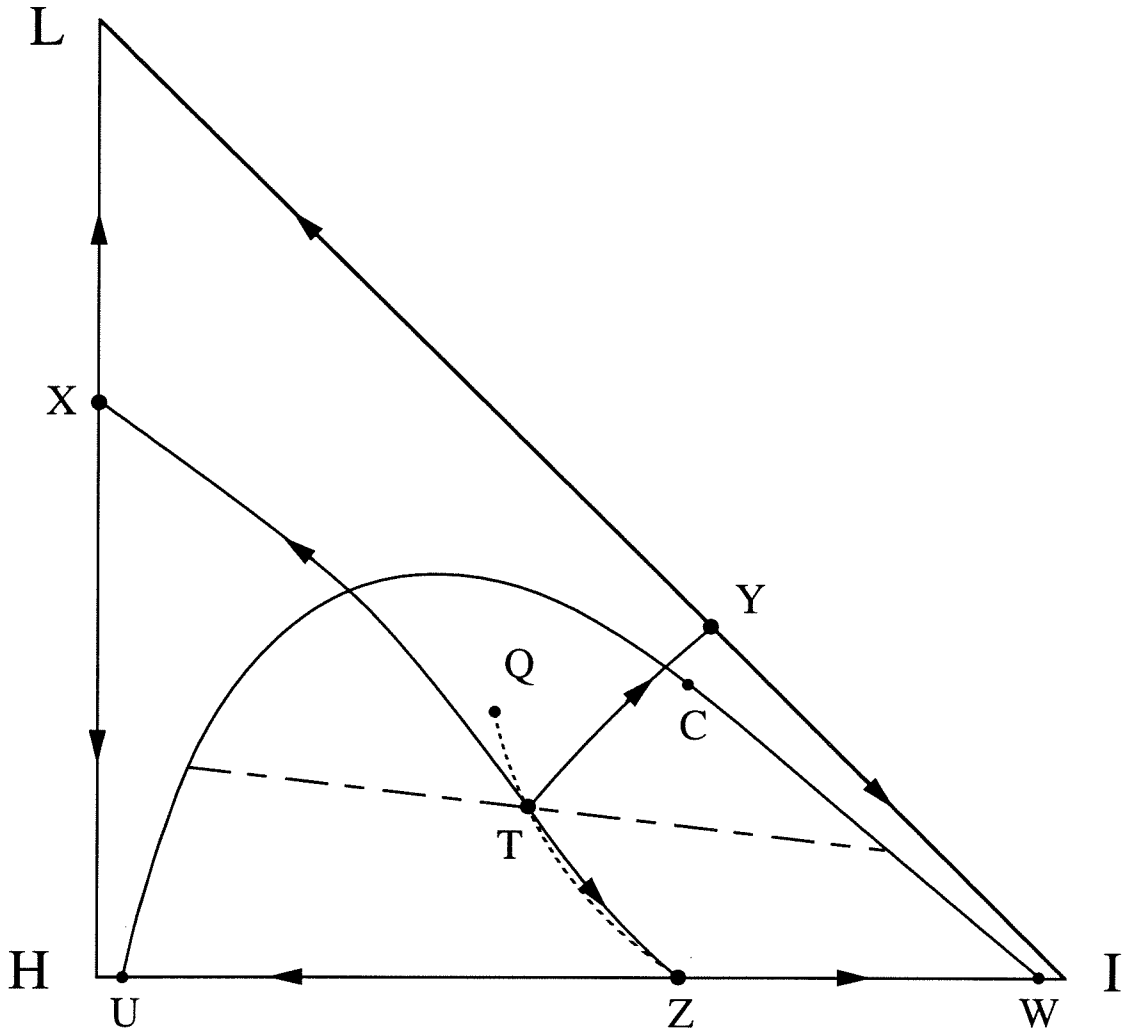


Figure 3.14: The residue curve boundaries and the vapor line can be used for the qualitative predictions of multiplicities in tray columns without decanter. For the mixture shown, the different vapor line suggests that no multiplicities exist for tray columns without decanter.

is required for the separation of the mixture ethanol - water - benzene (illustrative example), there exist other heterogeneous mixtures where a column without decanter is needed to achieve separation, e.g., ethanol - water - ethyl ether. More importantly, however, this section's analysis provides necessary information for the study of the far more common case of heterogeneous columns with decanter: the location of the feasible compositions of the stream drawn from the top of the column and consequently the overall composition of the liquid that settles in the decanter.

3.4 Columns with decanter

The existence of two liquid phases in the decanter at the top of a heterogeneous azeotropic distillation column in the ∞/∞ case adds another parameter to the problem. The column with the decanter is depicted in Figure 3.15. The overhead vapor V is fed to a total condenser and the resulting liquid settles in the decanter. The overall distillate flow is composed of two liquid streams with compositions those of the two liquid phases in equilibrium. The two stream flows, D_1 and D_2 , are the independent parameters in this case and $D = D_1 + D_2$. In general, $\underline{x}_D \neq \underline{x}_V$ and $\underline{x}_D \neq \underline{x}_R$. Since the column operates at infinite reflux ($R/D \rightarrow \infty$ and $V/D \rightarrow \infty$) the compositions of R and V are the same ($\underline{x}_R = \underline{x}_V$) and hence the residue curve and distillation line models accurately describe the column profiles of packed and tray columns with decanter respectively. For specific choices of D_1 and D_2 it is possible to have $\underline{x}_D = \underline{x}_R = \underline{x}_V$ and hence columns without decanter are a special case of columns with decanter. When \underline{x}_V lies outside the heterogeneous liquid region there is no phase separation in the decanter and hence the column becomes identical to the column without decanter.

In this framework, the first step will be to locate the feasible overhead vapor V, distillate D and bottoms B regions for the column with decanter shown in Figure 3.15. In the case of columns without decanter a feasible column (1) has to belong to one of the three acceptable column profile types (restriction on the location of B and D) and (2) D, F and B have to lie in this order on a straight line (material balance).

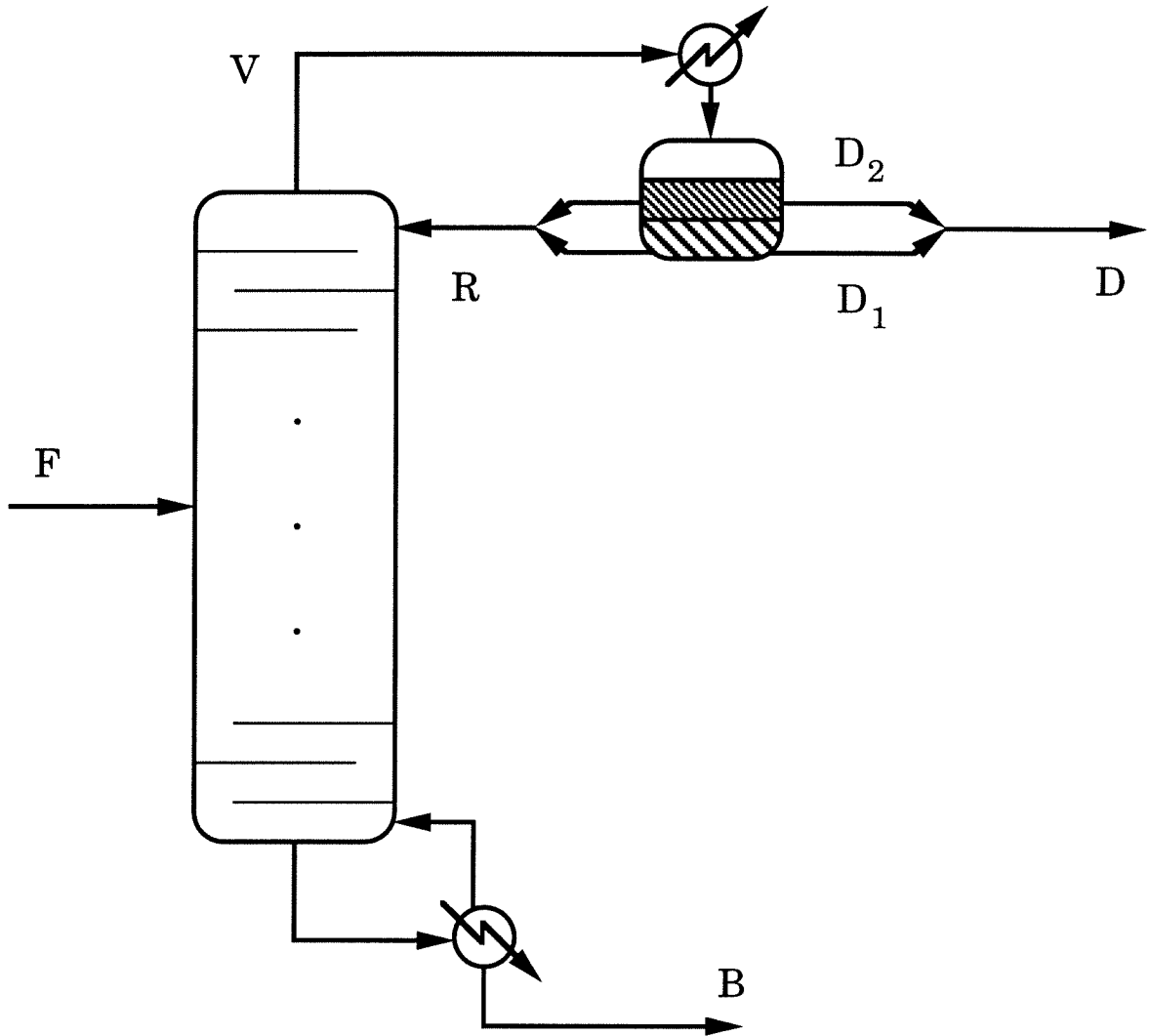


Figure 3.15: Column with decanter

The situation is slightly different for columns with decanter. The material balance condition is obviously the same, but the condition imposed by the acceptable profile types restricts the location of B and V, not D. We proceed then as follows: for each profile type (1) we locate the acceptable V and B (this is just from the definition of the profile types and hence the feed location is not considered at this stage); (2) for the acceptable V found, we locate the possible D that can be drawn from the decanter; (3) the feasible D and B, then, are the pairs of the previously located sets that satisfy the material balance and finally (4) from the feasible D we can locate the corresponding feasible V region. We apply the above procedure for the feed F shown in Figure 3.16 for a packed column. The feed composition is again located at the lower left distillation region.

We start with the type I profiles. In these profiles, V may only lie at the ternary azeotrope T while B can be any point in the composition triangle. Since V lies in the heterogeneous region, the distillate D can be any point on the tie line ab that goes through T. From the material balance, we find that the feasible B region is the quadrangle $FcLd$ and the feasible D lies on the tie line ab (aFc and bFd are straight lines). The feasible regions are shown in Figure 3.16.

Next, the type III profiles. For columns without decanter, it was shown that the distillate may only lie on an interior boundary (e.g. TX) while the bottoms may only lie on the corresponding edge of the triangle (e.g. LH). Similarly, for columns with decanter, V may lie on an interior boundary while B may only lie on the corresponding edge of the triangle. If V lies on TZ, then B has to lie on IH and the material balance cannot be satisfied. If V lies on TY (Figure 3.17) then B has to lie on LI and hence for the material balance to be satisfied the distillate D has to lie somewhere on the left of the straight line LF. Let f and e be the points where the LF straight line intersects the heterogeneous liquid boiling envelope and the aTb tie line respectively. Let g be the point where the tie line from f intersects the boundary TY. Then, the feasible D lies in the $afea$ part of the heterogeneous region, the feasible B on the Lc line segment and the feasible V on the gT part of the boundary TY.

If V lies on TX (Figure 3.18) then B has to lie on LH and hence for the material

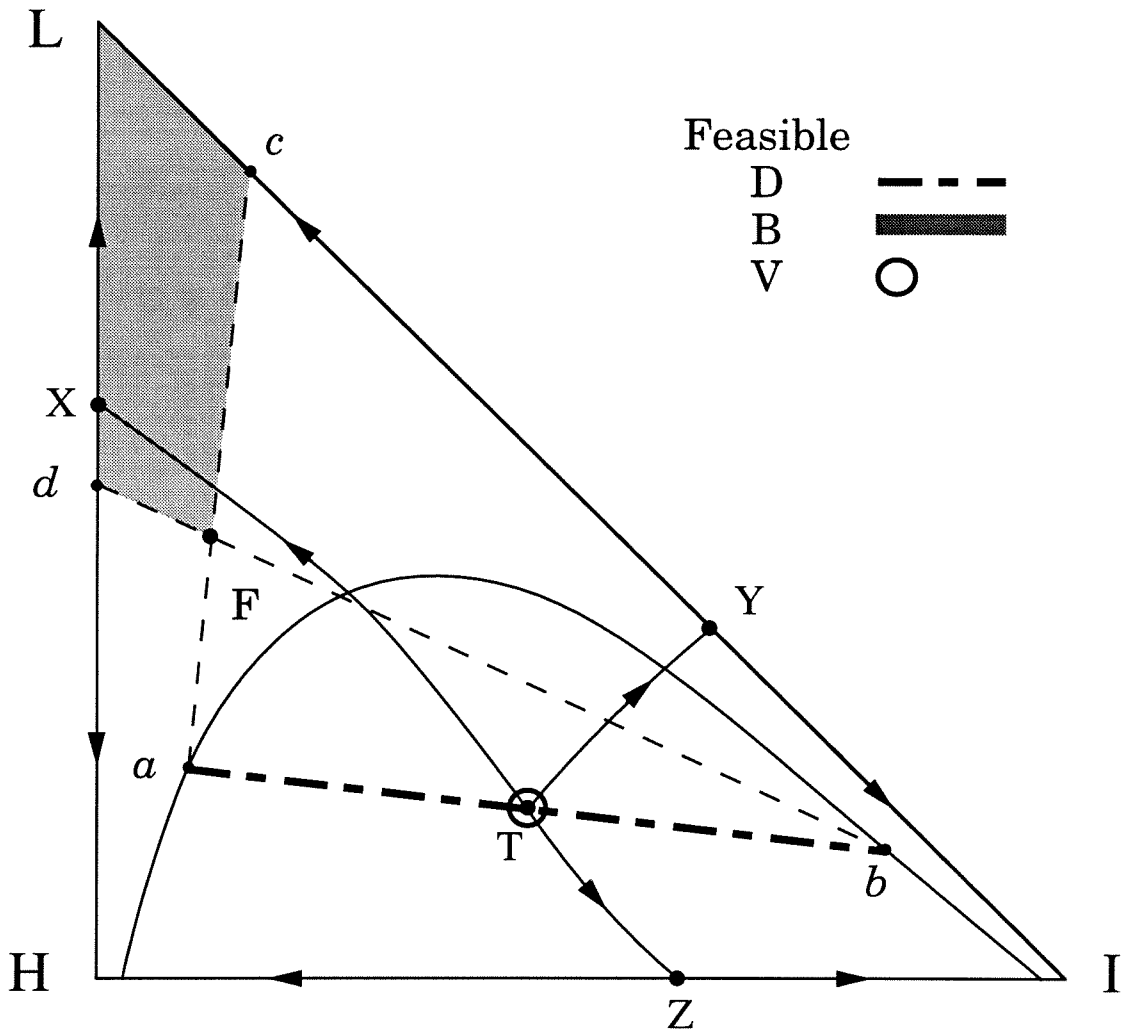


Figure 3.16: The feasible overhead vapor V, distillate D and bottom product B regions for a packed column with decanter and given feed F in the ∞/∞ case for type I profiles.

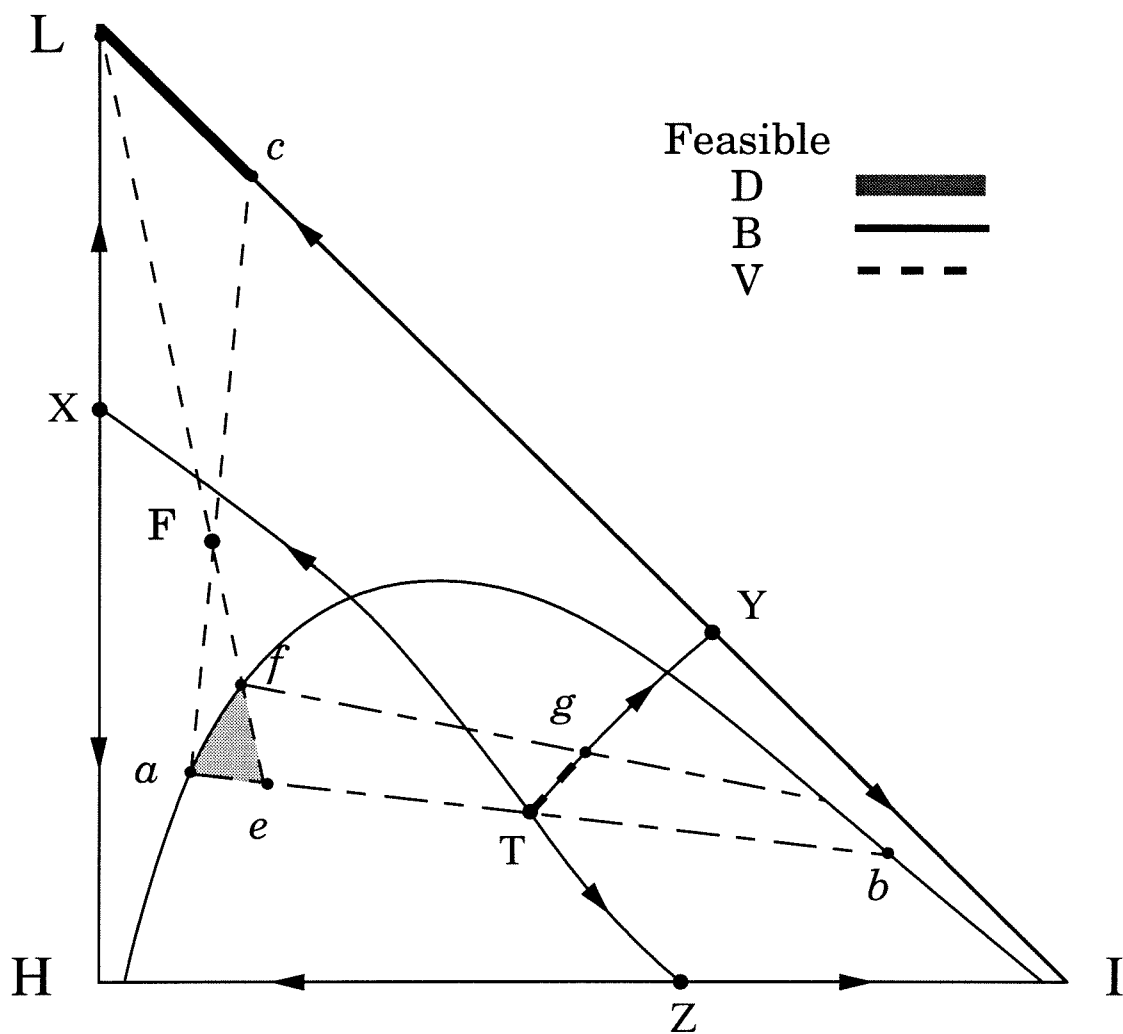


Figure 3.17: The feasible overhead vapor V, distillate D and bottom product B regions for a packed column with decanter and given feed F in the ∞/∞ case for type III profiles with V on TY.

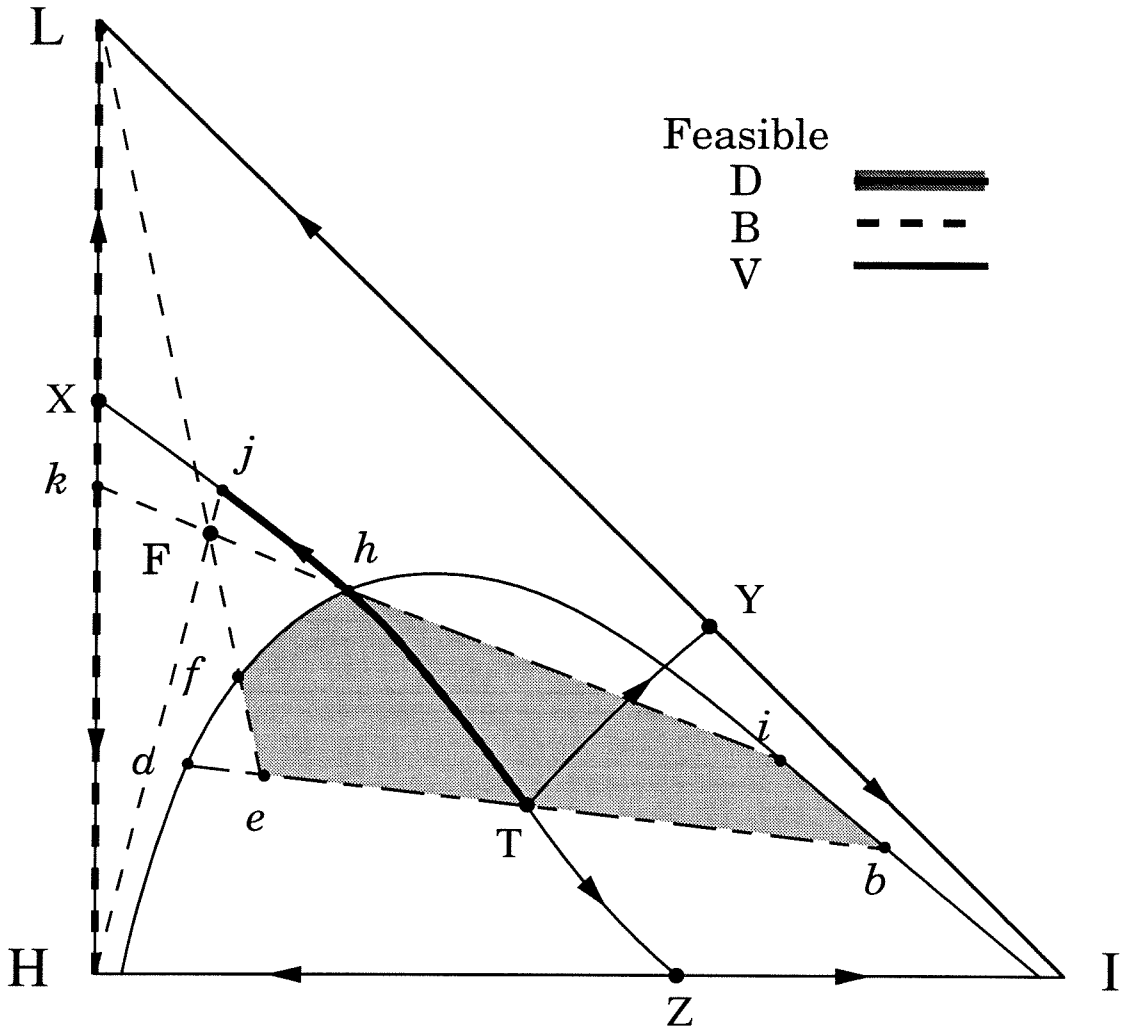


Figure 3.18: The feasible overhead vapor V , distillate D and bottom product B regions for a packed column with decanter and given feed F in the ∞/∞ case for type III profiles with V on TX .

balance to be satisfied the distillate D has to lie somewhere on the right of the straight lines LF and HF . Let h and j be the points where the TX boundary intersects the heterogeneous envelope and the HF straight line respectively. Let hi be the tie line from h . If V lies on jh then the feasible D also lies on jh and the feasible B on Hk (hFk is a straight line). If V lies on hT then the feasible D lies in the $efhibe$ part of the heterogeneous region that is shown shaded in Figure 3.18 and the feasible B lies on Lk .

Finally, in the type II profiles (Figure 3.19), the bottoms B always lies on H . Then

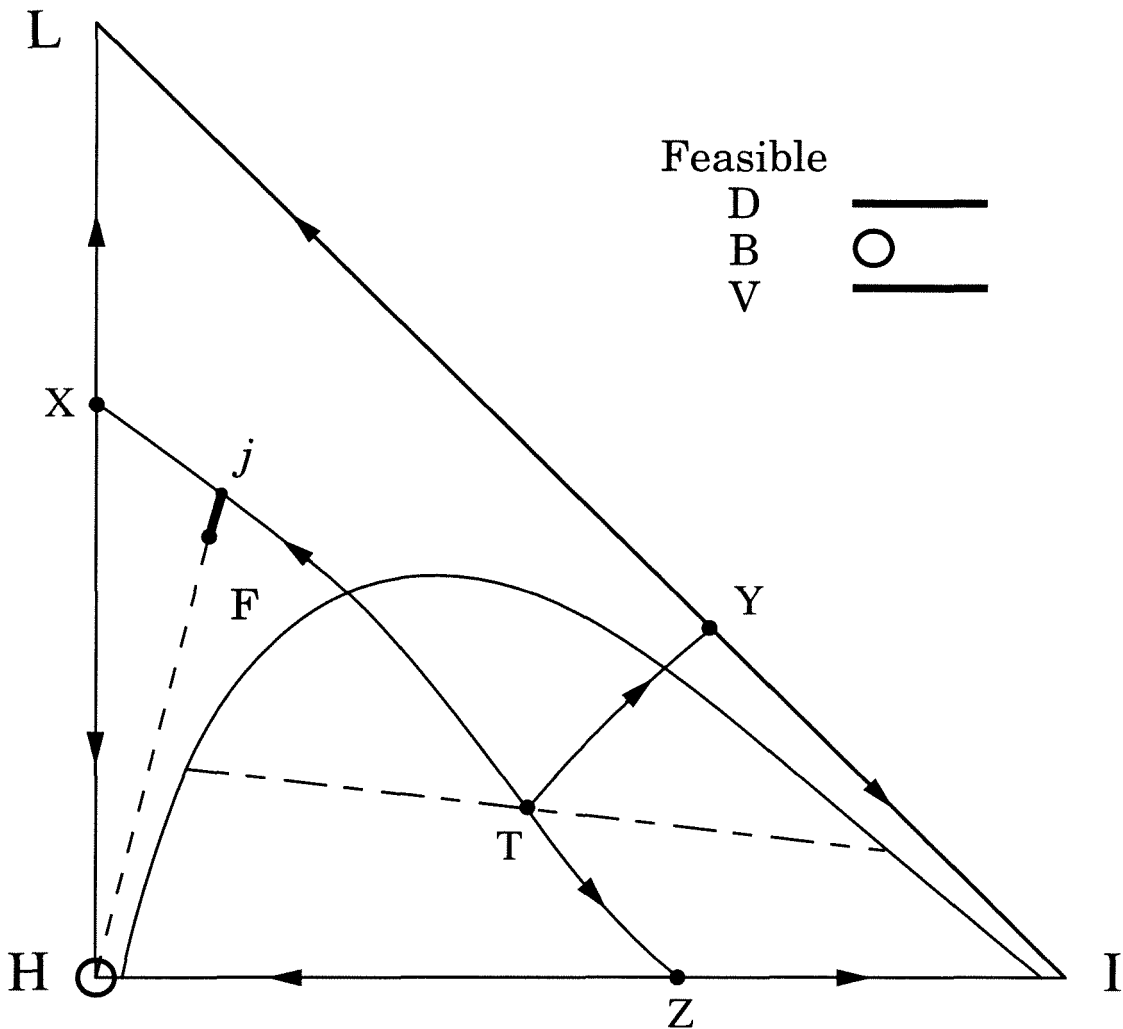


Figure 3.19: The feasible overhead vapor V, distillate D and bottom product B regions for a packed column with decanter and given feed F in the ∞/∞ case for type II profiles.

D can only be a point on the straight line Fj by the material balance. Since D lies in the homogeneous region V also lies on Fj.

Now we put all these pieces together (Figure 3.20): (1) the feasible V region is the boundary segments Tg and Tj and the straight line jF, (2) the feasible D region consists of the straight line jF, the boundary segment jh and the *abiha* part of the heterogeneous region (shaded in Figure 3.20), (3) the feasible B region consists of the LH edge, the Lc line and the FdLc quadrangle. Qualitatively similar results are obtained for tray columns using the distillation line boundaries. Some quantitative

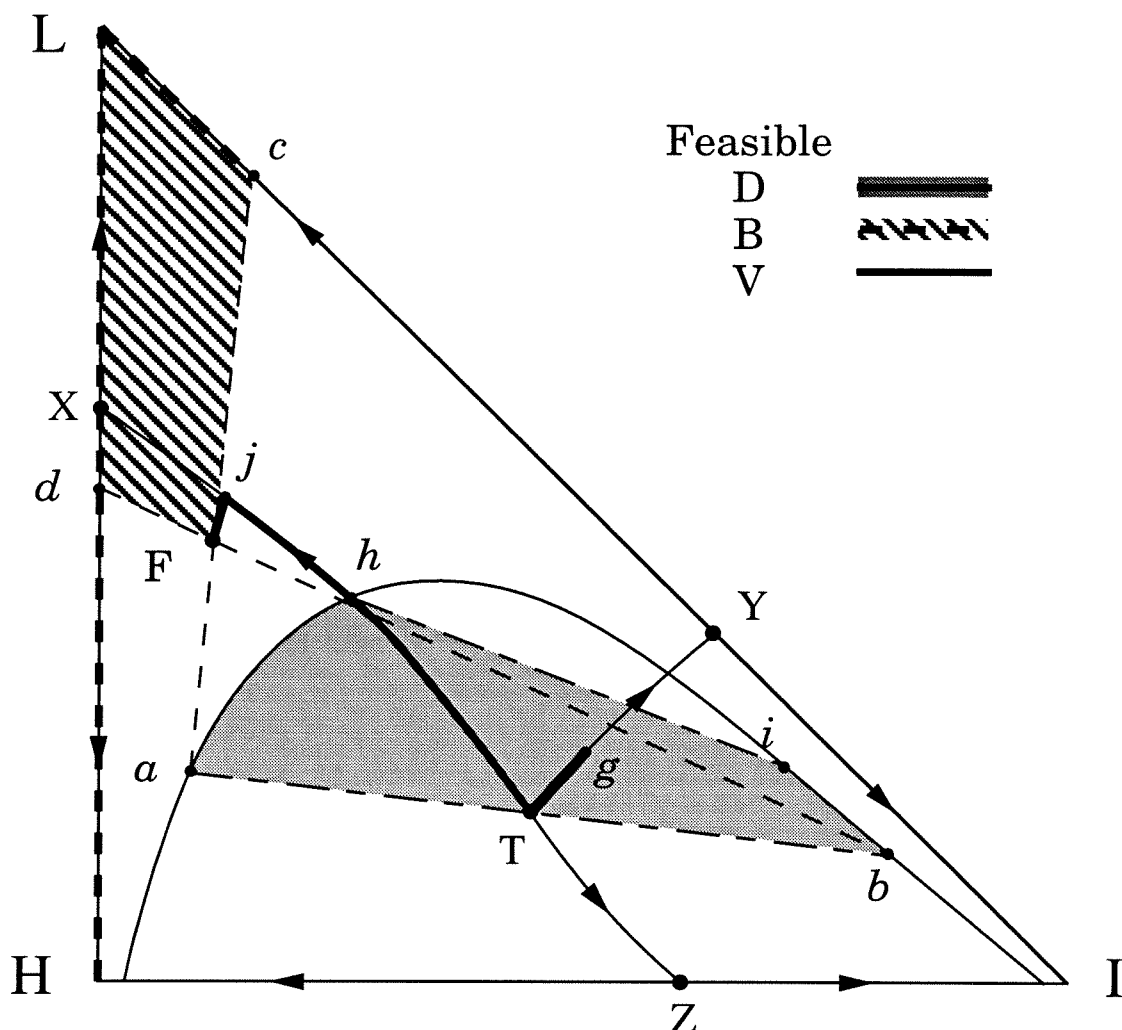


Figure 3.20: The feasible overhead vapor V, distillate D and bottom product B regions for a packed column with decanter and given feed F in the ∞/∞ case for all acceptable profiles.

differences are expected because of the different boundary locations while the shape of the vapor line does not affect the location of the feasible distillate D.

So far we considered both D_1 and D_2 as the system parameters. One can reduce the system parameters to one by imposing a “policy” on the distillate, for example, keeping the ratio D_1/D_2 constant. The most common policy used in heterogeneous azeotropic distillation for columns like the one used for the separation of the mixture ethanol - water - benzene, is to recover as distillate a portion of the entrainer-poor phase only (i.e. $D_2=0$) and recycle a mixture of the two liquid phases. Next, this

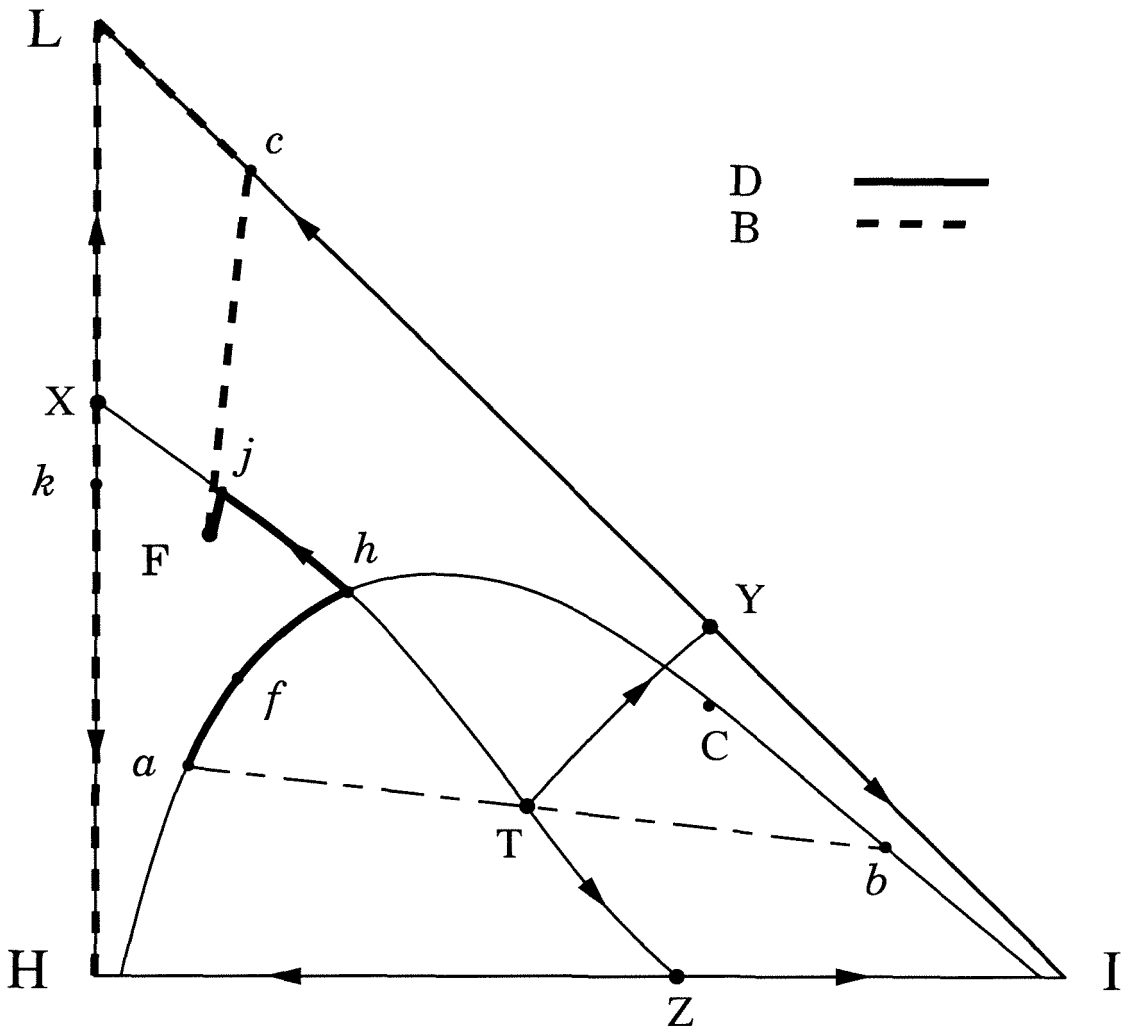


Figure 3.21: The distillate and bottoms continuation paths for packed columns with decanter and $D_2=0$.

policy is studied in detail.

Since $D_2=0$, then $D=D_1$ and hence when V lies in the heterogeneous region, the distillate may only lie on the part of the heterogeneous liquid boiling envelope on the left of the critical point. Figure 3.21 shows the distillate and bottoms composition continuation path in the composition triangle when $D_2=0$. The distillate D follows the line afh_jF and the bottoms B the line $FcLkH$. The light component mole fraction in the bottoms x_{BL} is recorded along the continuation path. Table 3.2 shows the location of D and B , the distillate flowrate D changes, the light component mole fraction in the bottoms x_{BL} and the type of the column profile along the continuation path. It is

Table 3.2: Information along the continuation path for packed columns with decanter and $D_2=0$.

profile type	heterogeneous			homogeneous		
	I	III	III	III	II	
D	a	a	f	h	j	F
B	F	c	L	k	H	H
D	0					F
x_{BL}	x_{FL}	1			0	0

very simple to show using the lever material balance rule that D decreases as D moves from f to h and accordingly B moves from L to k . Figure 3.22 shows a sketch of the bifurcation diagram of x_{BL} vs. the bifurcation parameter D . It is apparent that for some distillate flowrate range, three steady states exist. Figure 3.23 illustrates three steady state profiles with the same D .

3.4.1 Geometrical Condition and Feed Region

So far, we demonstrated how to locate the feasible product regions for a given feed when both D_1 and D_2 are used as parameters. We also showed how to locate the products continuation path in the triangle and how to construct the corresponding bifurcation diagram using the distillate flow as parameter for a given feed and a given distillate policy, $D_2=0$. Here, we answer the following questions: Given a residue curve (or distillation line) diagram and a distillate policy for columns with decanter, find if multiple steady states exist for some feed compositions and for some distillate flowrates. Locate the feed compositions that lead to multiplicities. We demonstrate

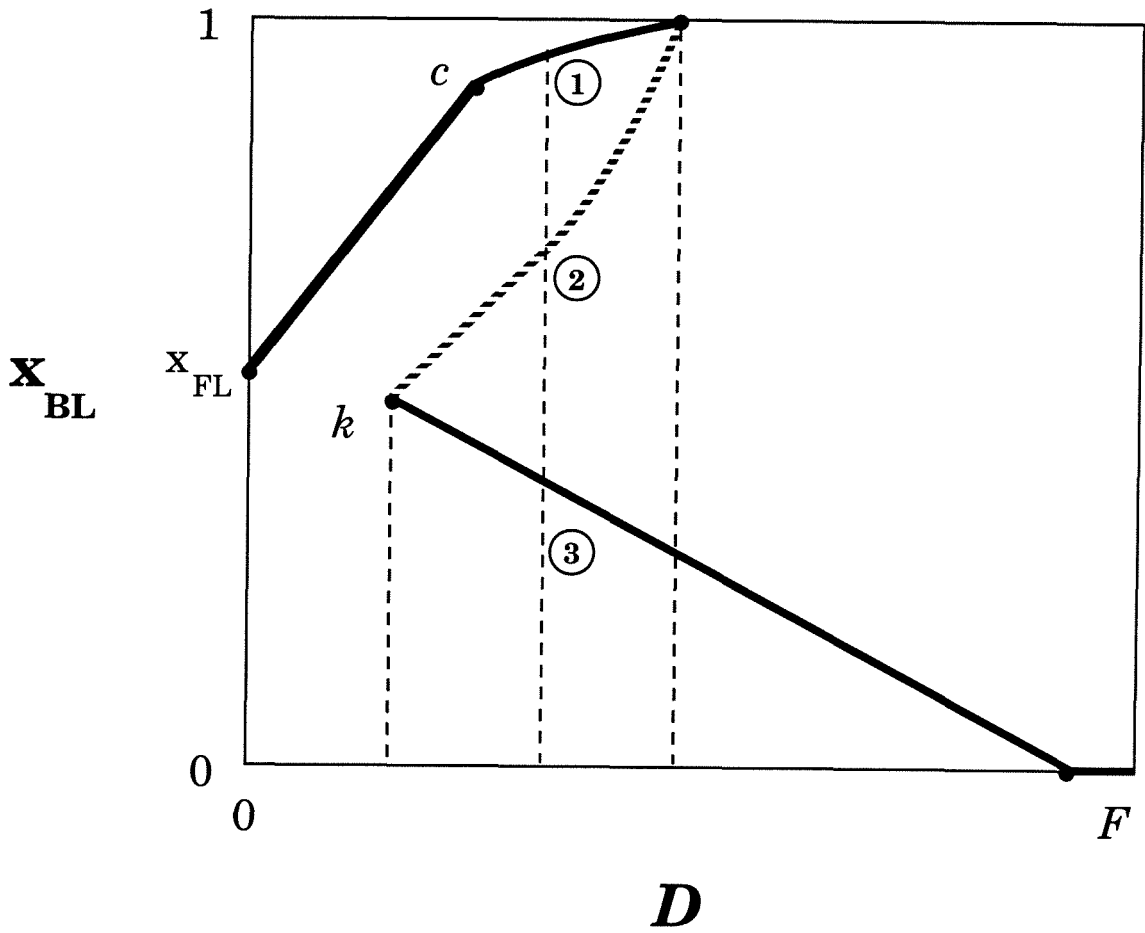


Figure 3.22: Bifurcation diagram of the mole fraction of L in the bottoms vs. the distillate flow for packed columns with decanter and $D_2=0$.

these, using the ethanol - water - benzene mixture for a packed column with decanter and distillate policy $D_2=0$.

From the discussion above, it is apparent that the key difference between columns with and without decanter is the location of the distillate continuation path. Once this path is located, the geometrical condition for the existence of multiplicities can be directly applied because it only checks if the distillate flowrate decreases along the continuation path. The information required in this case is the residue curve boundaries and the VLLE, heterogeneous envelope and tie lines, as shown in Figure 3.24. In the section of columns without decanter we located the distillate and bottoms compositions for which the multiplicity condition should be checked based solely on the knowledge of how column profiles look like in the ∞/∞ case. Therefore, these are also the locations of V (the overhead vapor stream) and B for columns with decanter. Hence, we only have to check the geometrical condition for V lying on an interior boundary and B lying on the corresponding binary edge of the triangle.

Next, we locate the distillate D when V lies on the interior boundaries under the distillate policy $D_2=0$. If V lies on TZ then D lies on aU . Let h and l be the points where the heterogeneous envelope intersects the boundaries TX and TY respectively. If V lies on TX then D lies on ahX while if V lies on TY, D lies on $ahlY$ (Figure 3.24). Now the geometrical condition can be applied for the following distillate - bottoms locations: ahX - LH, $ahlY$ - LI, aU - HI. Since the bottoms in all pairs lies on a triangle edge (similarly to columns without decanter), the geometrical condition can be simplified to the following : For the existence of multiple steady states it is required that (1) some line parallel to the LH edge intersects the distillate route ahX more than once, or (2) some line parallel to LI intersects $ahlY$ more than once, or (3) some line parallel to HI intersects aU more than once.

The conditions (2) and (3) are not satisfied. Condition (1) is satisfied, however, between a and h . By applying the geometrical condition in its original form, it is easy to show that the distillate flowrate decreases along the continuation path for distillate compositions located on the ah segment of the distillate route and bottoms located at any point on the LH edge. Therefore, the set $S_B(D)$ is the edge LH for any D on

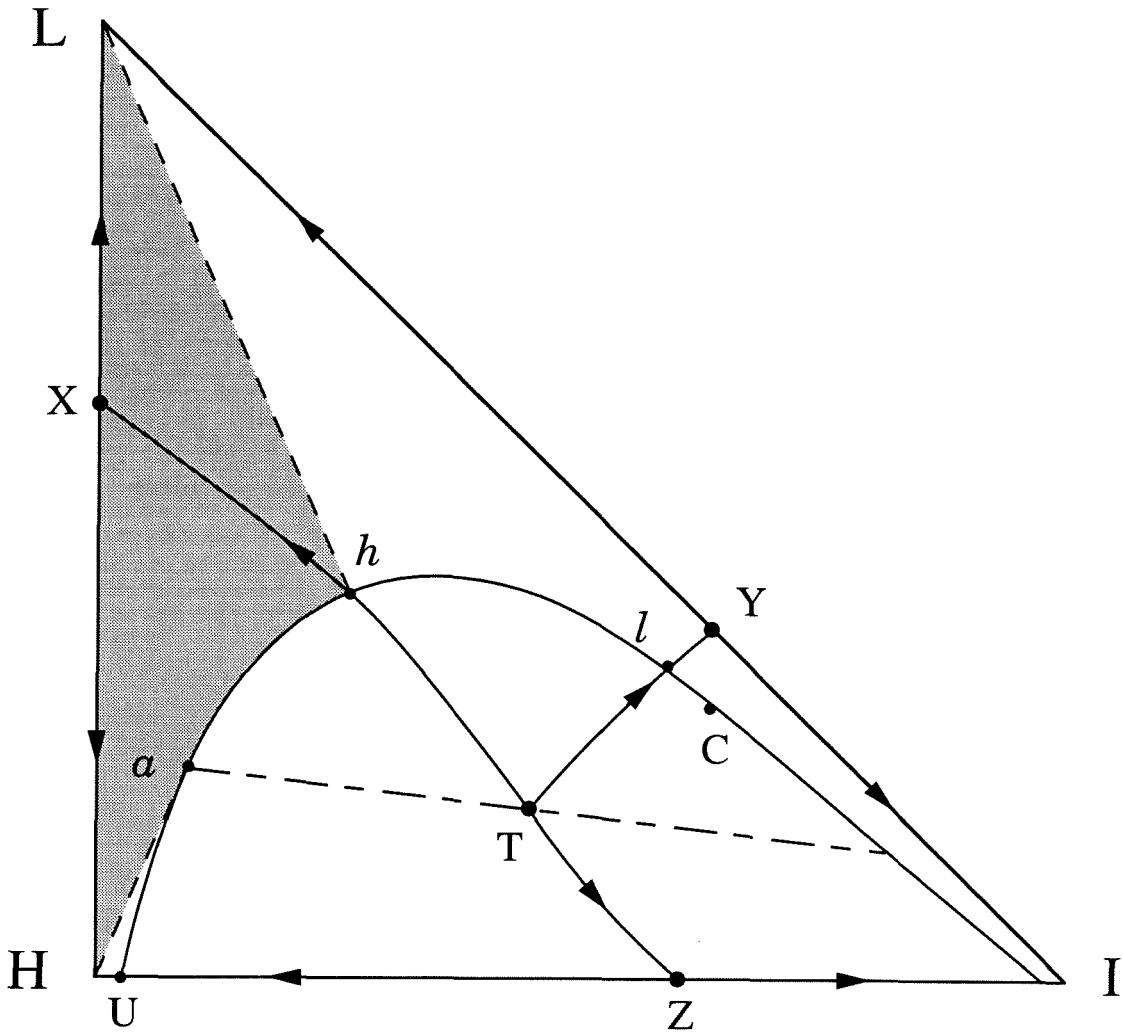


Figure 3.24: The information required to apply the geometrical condition and the feed composition region (shaded) that leads to multiplicities for packed columns with decanter and $D_2=0$.

ah. Hence, the shaded region in Figure 3.24 depicts the feed composition region that leads to multiple steady states.

3.5 Special Topics

Reboiler and other condenser types

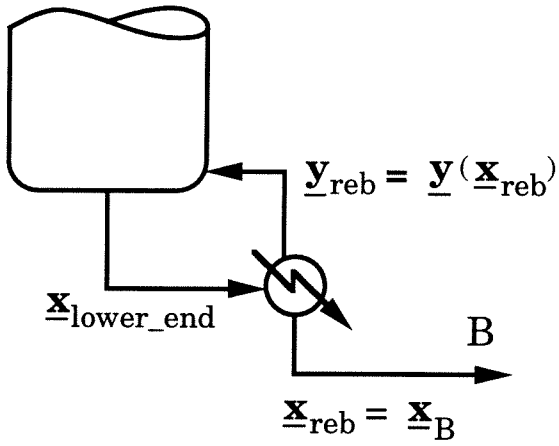
Reboiler: In the previous analysis, as well as in chapter 2, we assumed that the bottom product composition is equal to the composition of the lower end of the column profile. This is exactly correct if a total* or a thermosyphon† reboiler is used. In this case, the reboiler does not provide any additional enrichment. However, the typical reboiler type used in practice, i.e., the partial reboiler shown in Figure 3.25, is equivalent to an additional equilibrium stage. This does not affect at all the description of tray columns since the reboiler composition is just another point on the distillation line the column profile follows (Figure 3.25).

It is not exactly correct, however, in the general case of packed columns since the composition of the reboiler may not lie on the residue curve that the profile follows (Figure 3.25). Instead, the liquid leaving the reboiler is in equilibrium with the leaving vapor whose composition is equal to the one of the lower end of the packed column profile (by the material balance in the ∞/∞ case). Therefore, for packed columns with a partial reboiler, the bottom product composition \underline{x}_B is defined by the equilibrium relationship $\underline{y}(\underline{x}_B) = \underline{x}_{lower_end}$. The effect of the use of a partial reboiler (instead of a total reboiler) on the study of multiplicities of packed columns is summarized in the following.

The use of partial or total reboiler has no impact on type II column profiles. In both cases, the bottom product composition is that of a stable node and both column

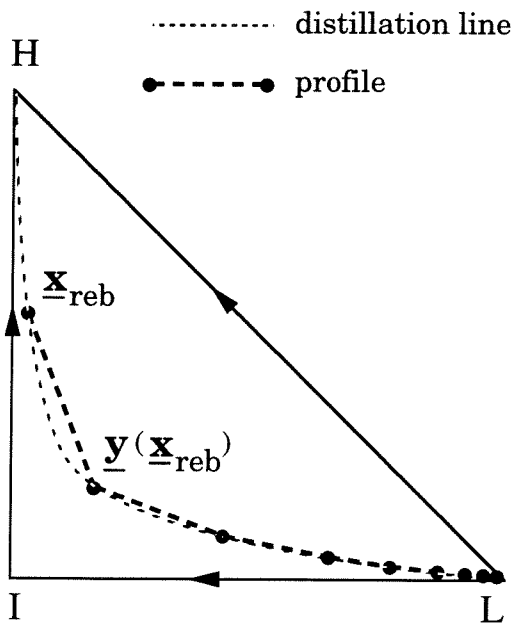
*By total reboiler we mean the equivalent of the total condenser, i.e., a unit that boils the whole amount of liquid exiting the lower end of the column; the bottoms product is some portion of the vapor formed in the reboiler.

†The bottoms product of the thermosyphon reboiler is some portion of the liquid exiting the lower end of the column. The remaining amount of liquid exiting the lower end of the column is boiled and returned to the column as boilup. The thermosyphon reboiler is identical to the total reboiler in terms of input-output stream compositions.

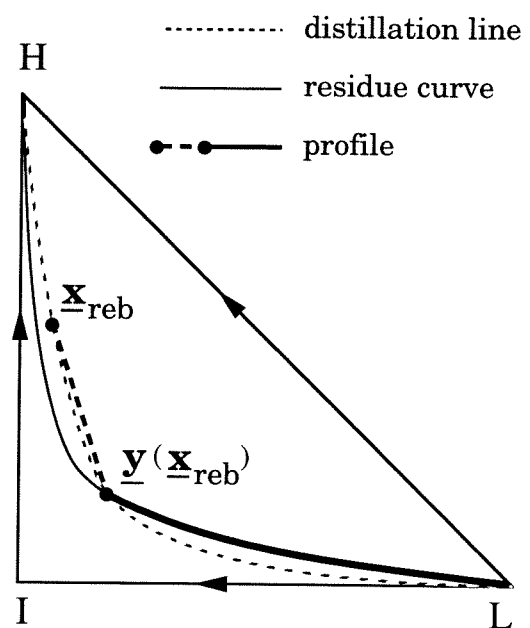


at infinite reflux:

$$\underline{x}_{\text{lower_end}} = \underline{y}_{\text{reb}}$$



tray columns



packed columns

Figure 3.25: The effect of the use of a typical, partial reboiler on the bottom product composition for tray and packed columns.

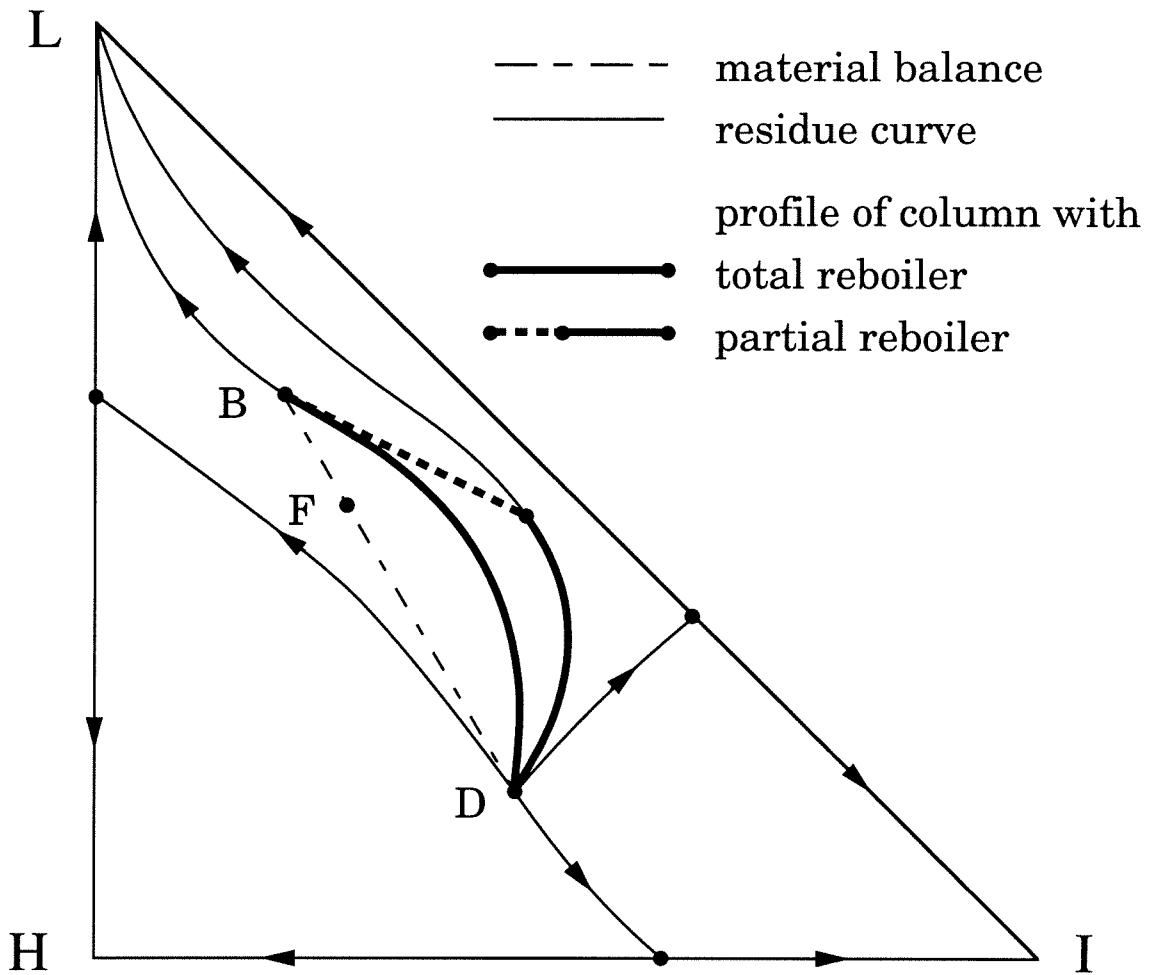


Figure 3.26: The effect of the use of a typical, partial reboiler on type I profiles of packed columns.

profiles are identical, i.e., they follow the same residue curve, for the same distillate flowrate. In type I column profiles, the feasible bottom product compositions lie on the straight line that goes through the feed F and the unstable node (Figure 3.26) independent of the reboiler type. Hence, the reboiler type does not affect the part of the product continuation path that corresponds to type I profiles. The profiles, however, of columns with the same B but different reboilers are different, i.e., they follow different residue curves, as is shown in Figure 3.26.

The use of a partial reboiler may have a significant effect on the feasible products only for type III column profiles. This effect is illustrated in Figure 3.27. In this figure, the top profile end lies on LX and the lower profile end lies on the residue

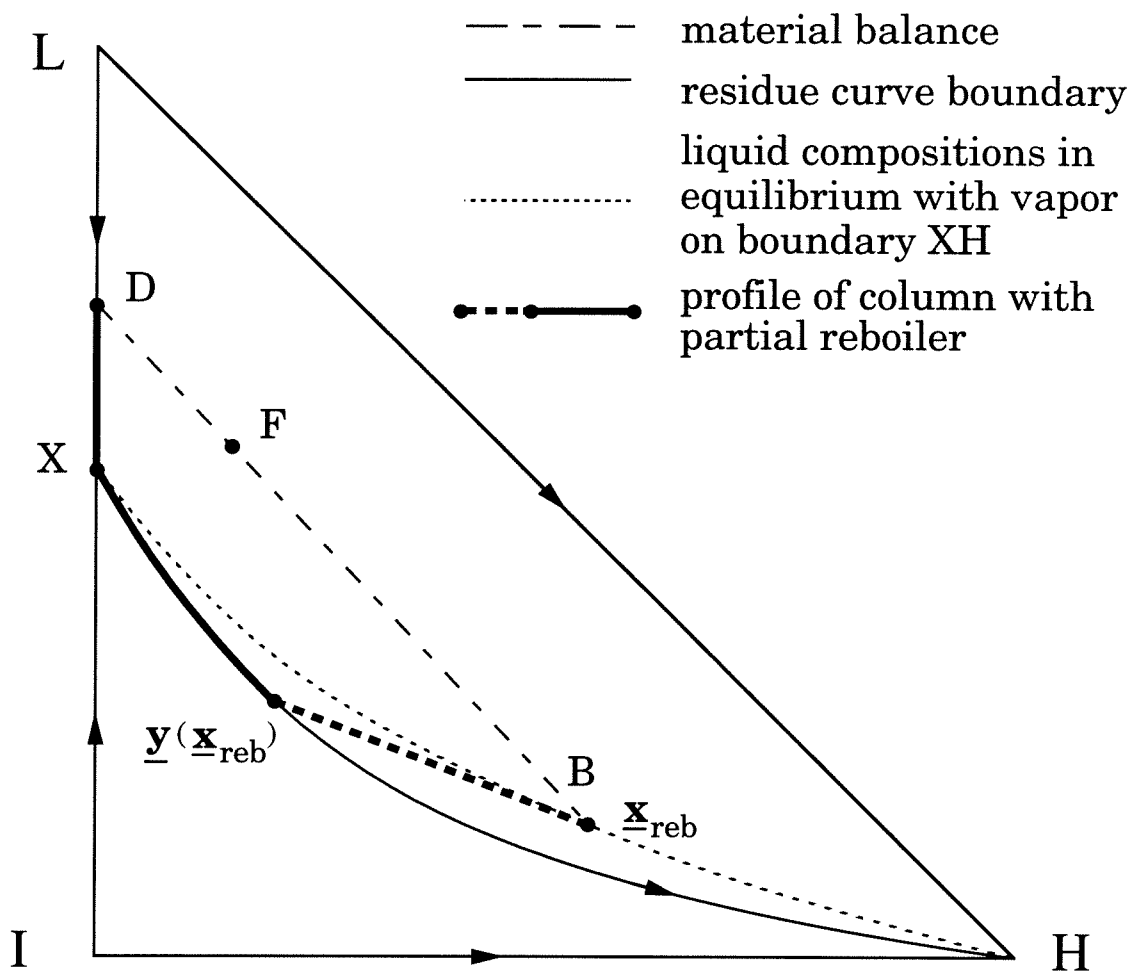


Figure 3.27: The effect of the use of a typical, partial reboiler on the bottom product composition of type III profiles of packed columns.

curve boundary XH (plain line). The curved dashed XH line is the location of the liquid compositions whose vapor in equilibrium lies on the residue curve boundary XH. If a total reboiler is used then the bottoms product composition is equal to the profile lower end composition and therefore B lies on the residue curve boundary XH. This is the case we studied in the analysis of multiplicities in the previous sections. If a partial reboiler is used, however, B will lie on the curved dashed XH line. This is the case when the use of a partial reboiler affects quantitatively and possibly qualitatively the existence of multiplicities.

Note, however, that in the special case of type III column profiles with the profile lower end lying on a straight line residue curve boundary (or a binary edge), B lies

on the boundary (or edge) regardless of the reboiler type. In this case, the plain and dashed lines of Figure 3.27 are identical. This is the case with the mixture ethanol - water - benzene. For this mixture, we have shown above that the type III profile lower ends (or equivalently the bottoms product B for columns with total reboiler) cannot lie on an interior residue curve boundary; they can only lie on a binary triangle edge. Therefore, for the ethanol - water - benzene mixture type, the use of the partial reboiler does not affect at all the multiplicity results derived above for columns with a total reboiler.

Condenser: In addition, all our analysis was made for columns with a total condenser. We can study other condenser types in a way similar to the above study of columns with different reboiler types. For example one can consider using a partial condenser and recovering as distillate only the vapor from the partial condenser. This situation is equivalent to the previous case of the partial reboiler. No difference for tray columns is expected since the partial condenser vapor composition, i.e., the distillate D, lies on the distillation line the column profile follows.

In packed columns, however, the distillate D may not lie on the residue curve the profile follows. Again, the condenser type does not affect the product continuation path that corresponds to type I and II profiles. It may have a significant effect on the feasible products only for type III column profiles. In this case, the distillate composition \underline{x}_D is defined by the equilibrium relationship $\underline{x}_D = \underline{y}(\underline{x}_{upper_end})$. Since $\underline{x}_{upper_end}$ for type III column profiles lies on residue curve boundaries, the distillate D will lie on the lines of vapor compositions in equilibrium with liquid compositions on the residue curve boundaries. Therefore, one has to calculate these lines for accurately describing packed columns with a partial condenser. These lines are depicted dashed in Figure 3.28 for the mixture ethanol - water - benzene.

Note that these dashed lines lie between the residue curve boundary and the corresponding distillation line boundary and that similarly to the distillation line boundaries, the dashed lines in Figure 3.28 coincide with some part of the vapor line in the heterogeneous region. This is why the dashed lines look similar to the distillation line boundaries although they do not generally coincide with them (unless

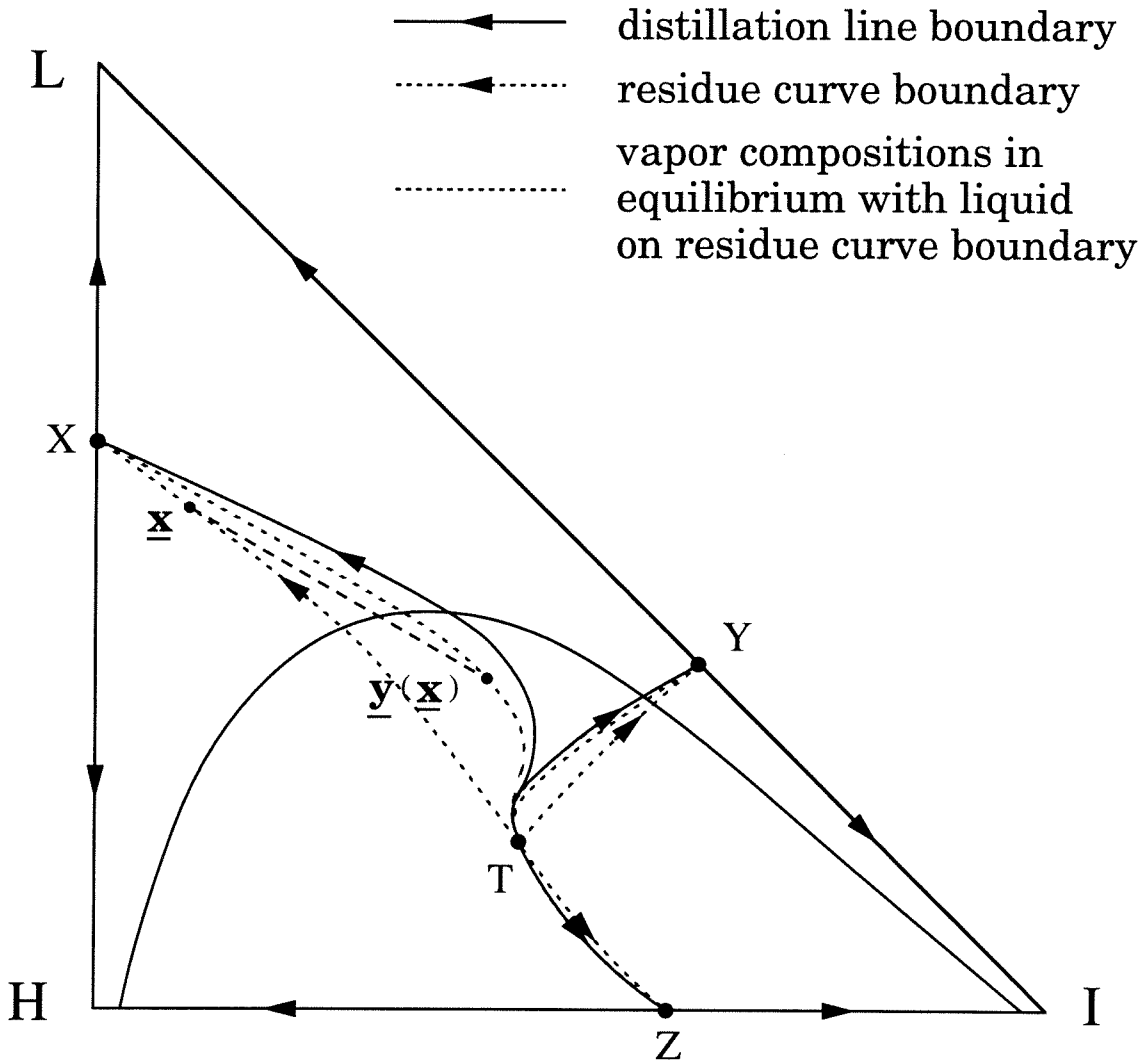


Figure 3.28: The effect of the use of a partial condenser on the feasible distillate product composition of type III profiles of packed columns without decanter.

the whole boundary lies in the heterogeneous region). By applying the multiplicity condition when D lies on the dashed lines (packed columns using a partial condenser and recovering as distillate only the vapor from the partial condenser) we conclude that multiplicities do exist. In the previous sections a unique steady state was found for packed columns with a total condenser. Therefore, for the mixture ethanol - water - benzene and for packed columns without decanter we conclude that the existence of multiplicities depends critically on the condenser type.

Recovering portions of both the liquid and the vapor phase as distillate, makes the situation similar to the previous study of columns with decanter since it adds another parameter to the problem (the liquid to vapor flow ratio recovered as distillate). For tray columns, D will lie on the *approximate* distillation line while for packed columns, D will lie between the residue curve boundary and the corresponding curve (dashed line in Figure 3.28) of vapor compositions in equilibrium with liquid compositions on the residue curve boundary. For columns with decanter, the combination of a partial condenser and a decanter can also be studied in a similar way.

Another situation very commonly encountered in practice is the use of a subcooled condenser in columns with decanter. In the ∞/∞ case, using a subcooled condenser does not affect the column profile. The only difference would be the use of the binodal curve at the temperature and pressure of the subcooled condenser (instead of the heterogeneous liquid boiling envelope used for the total condenser) to locate the distillate composition.

The examples above show that one can easily study the existence of multiplicities for many combinations of reboiler and condenser types with or without decanter; it only requires to locate the feasible product curves or regions for the various alternatives based on the ideas described above.

Tray efficiency

So far, we considered tray columns with a tray efficiency of 1. We also considered packed columns which can be regarded as tray columns with an infinitesimal tray efficiency ϵ ($\epsilon \rightarrow 0$). It is apparent that columns with tray efficiency $0 < \eta < 1$, would

“lie” somewhere in between. In fact, the corresponding distillation region boundaries would really lie between the residue curve and distillation line boundaries. Note that the fact that distillation lines coincide with the vapor line close to T is true only if $\eta = 1$. For the illustrative example studied for columns without decanter, there exists a tray efficiency value η^* such that multiplicities exist only if $\eta > \eta^*$. For columns with decanter, however, only quantitative differences are expected.

A degenerate multiplicity

In chapter 2 we showed that in the ∞/∞ case of homogeneous azeotropic distillation there exists a different, degenerate, type of multiplicity consisting of an infinite number of profiles with the same product compositions for a specific distillate flowrate. Apparently, this is not an output multiplicity; it is a case of state multiplicity, i.e., multiple steady states with the same feed and product compositions and flowrates but with different composition profiles. This type of multiplicity occurs for feeds located on the straight line connecting the unstable node with the stable node of a distillation region and for the specific distillate flowrate that places the distillate at the unstable node and the bottoms at the stable node. This is because there is an infinite number of residue curves running from the unstable node to the stable node. More specifically, for a mixture belonging in the 222-m class, this type of multiplicity occurs when D is located at the ternary azeotrope T and B at a pure component corner. The column type, packed or tray, is irrelevant for homogeneous mixtures.

The case of heterogeneous mixtures and packed columns without decanter is identical with the homogeneous case, i.e., the degenerate type of multiplicity occurs for feeds located on the straight line segments TL, TI and TH. For tray columns without decanter, however, there is a difference because a part of every distillation line (sufficiently close to T) coincides with some part of the vapor line (Figure 3.4). Hence, there is an infinite number of distillation lines that connect a point on the vapor line with a pure component corner (Figure 3.29). Note that the above does not affect the characteristics of this degenerate multiplicity; it only affects the feed region for which this degenerate type of multiplicity occurs. For tray columns, the feed region, instead

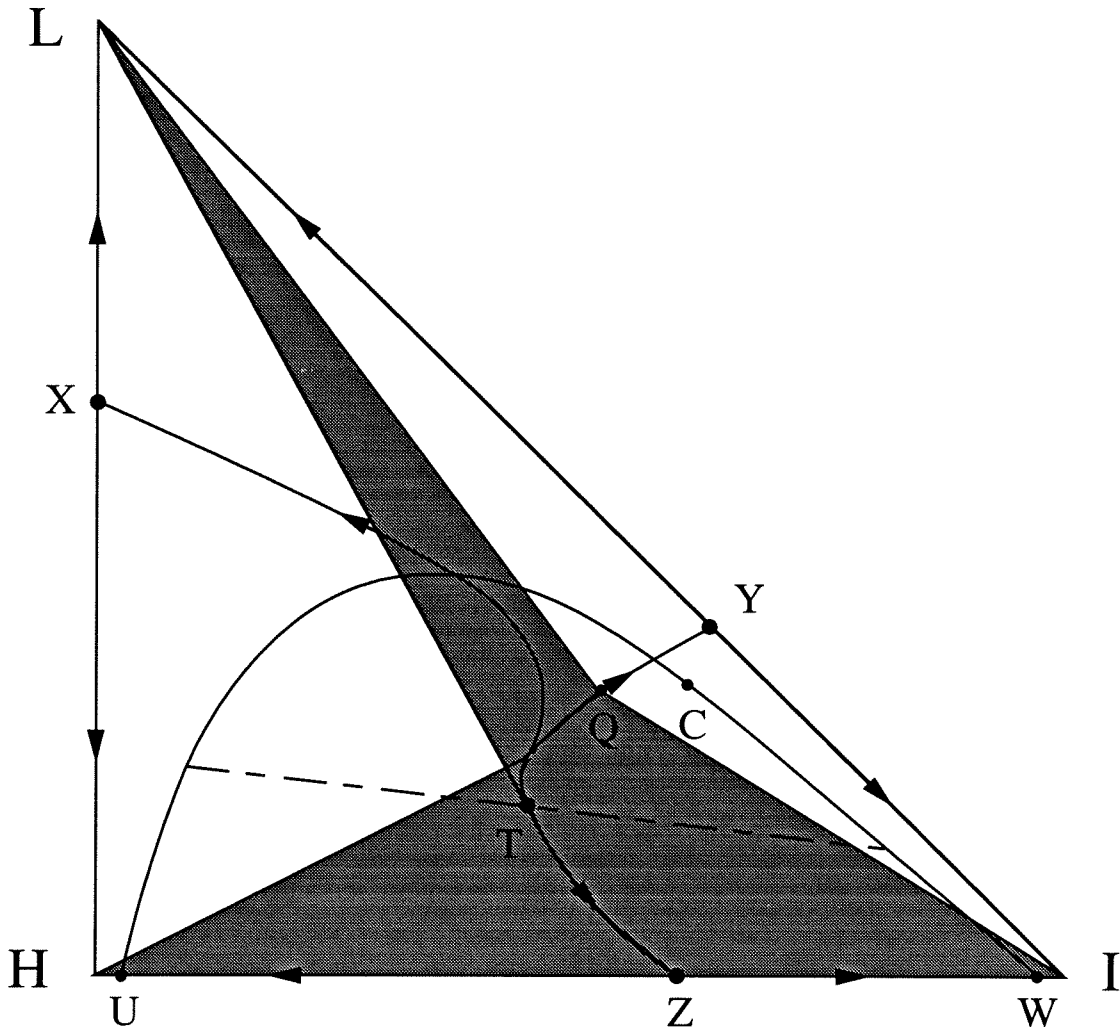


Figure 3.29: The region of feed compositions that lead to the degenerate type of multiplicity for tray columns without decanter.

of being three one-dimensional lines, is the union of the three areas enclosed by the part of the vapor line in each distillation region and the corresponding pure component vertex i.e., it is a two-dimensional region (shaded region in Figure 3.29). Note however that this two-dimensional feed region is not generic because the distillation lines do not coincide with the vapor line for columns with tray efficiency $\eta < 1$. For these columns the degenerate multiplicities occur for the feeds described above for packed columns.

The situation is different for columns with decanter and distillate policy $D_2=0$. If the bottoms is located at a stable node and the distillate D on the left part UC of

the heterogeneous envelope ($D = D_1$), then there exists an infinite number of profiles whose bottoms is the stable node and their other end, V , is located on the tie line from D . This is true for both tray and packed columns. Figure 3.30 illustrates the degenerate type of multiplicity by depicting five different tray column profiles with identical B and D . The overhead vapor V lies on the tie line from D . The composition of the liquid at the top tray is different for all five profiles. The overhead vapor V , however, is the same for the three profiles on the right because the corresponding top tray liquid compositions lie on the tie line in equilibrium with the vapor with composition the point where the tie line from D and the vapor line intersect. Note, however, that the latter phenomenon, infinite number of different column profiles with the same D , B and V , occurs only for tray columns with tray efficiency equal 1.

Hence, the degenerate type of multiplicity for columns with decanter occurs for feeds located in the union of the three areas enclosed by each one of the three pure component vertices and the corresponding part of UC that D may lie on ($L-al$, $I-UC$, $H-Uh$). This region is shown shaded in Figure 3.31. In this case, contrary to the case of tray columns without decanter, the existence of the two-dimensional feed region is generic and more specifically, independent of the tray efficiency η . This difference may help the study of the degenerate multiplicities since in the previous cases the feed had to exactly lie on a straight line that cannot be very accurately located. Another slight difference with the case of columns without decanter is that although the product compositions are the same for all the infinite number of profiles, the location of V maybe different. As it was shown before, V is the same only in some profiles of tray columns with tray efficiency equal 1.

Another important point for some future investigation of this degenerate type of multiplicity is that for the feed shown in Figure 3.21 the continuation of profiles should go through this infinity of profiles. The reason is very simple. In Figure 3.21 if B is located close to L on Lc , then the profile runs along the TYL boundary like profile 1 does in Figure 3.23. If B is located close to L on Lk , the profile runs along the TXL boundary (similarly to profile 2 in Figure 3.23). Therefore, when B is located at L and D at f (Figure 3.21) the profile should move from the TYL boundary to

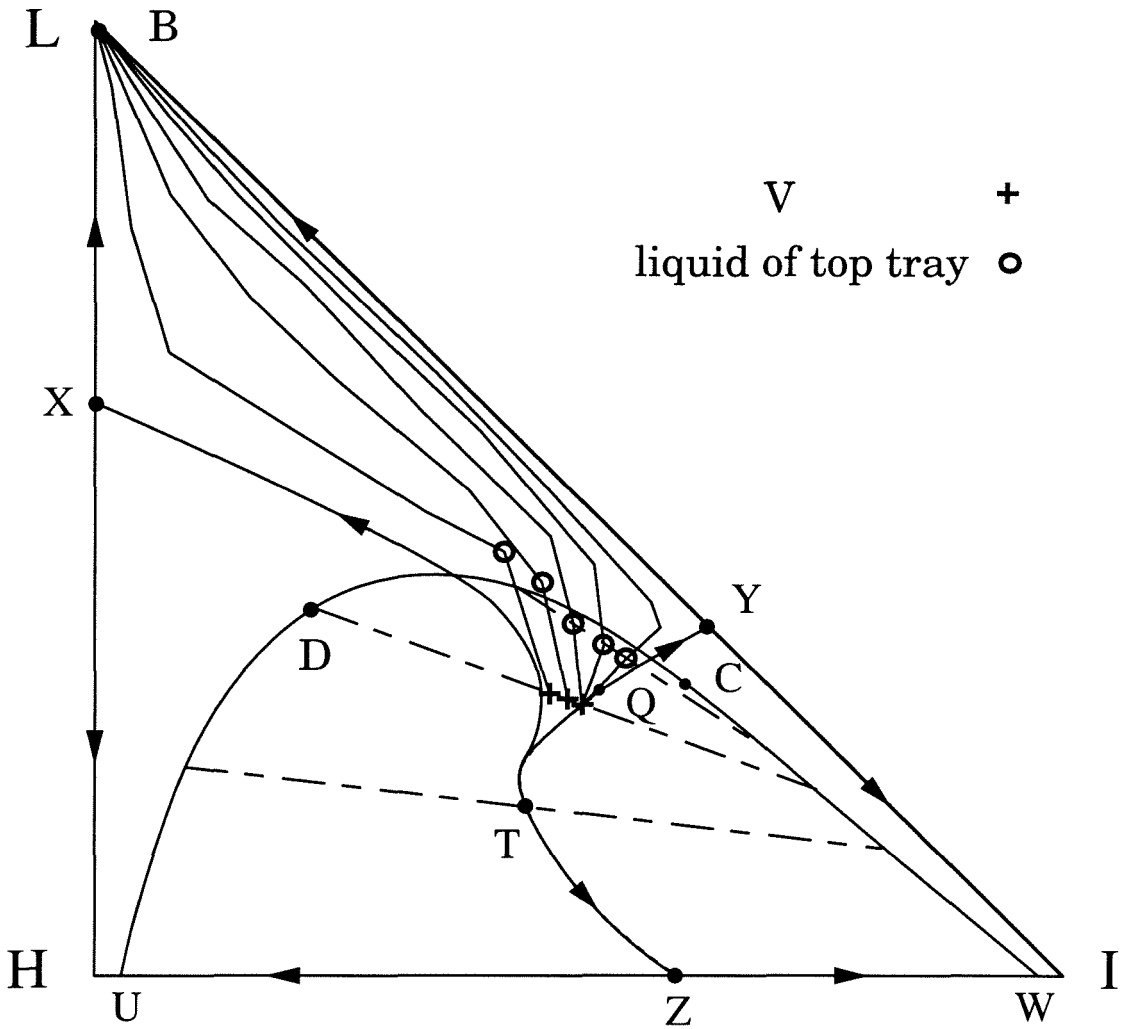


Figure 3.30: Five different column profiles with identical B and D (degenerate multiplicity) for a tray column with decanter and $D_2=0$.

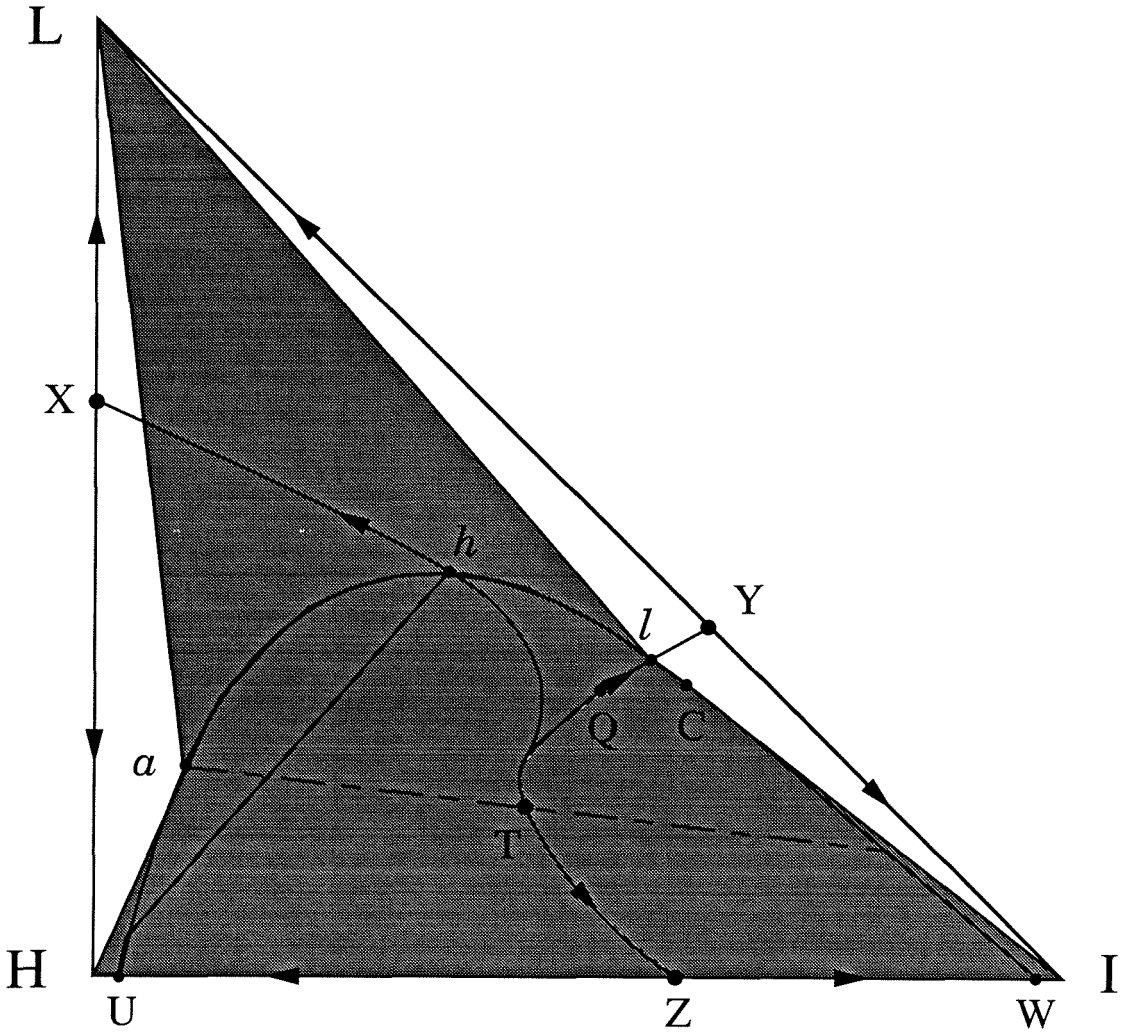


Figure 3.31: The region of feed compositions that lead to the degenerate type of multiplicity for tray columns with decanter and $D_2=0$.

the TXL boundary, i.e., it will scan the infinite number of profiles of the degenerate type of multiplicity. This phenomenon occurs for packed as well as tray columns with decanter and arbitrary tray efficiency.

This type of multiplicity (infinite number of profiles with the same product compositions for a specific distillate flowrate) may be similar to those reported by Kienle and Marquardt (1991) and Helfferich (1993)*. The practical implications of the degenerate type of multiplicity reported here are unclear i.e., we don't know whether (1) these multiplicities are an artifact of the ∞/∞ case and therefore do not exist for finite columns at finite reflux or (2) some finite number of multiple steady states still exist for finite columns at finite reflux. Hence, a more thorough investigation of this topic is needed.

Distillate policies - Discontinuity

In our study of columns with decanter we discussed the commonly used distillate policy $D_2=0$. One can define another policy by tracing an arbitrary path of D in the heterogeneous shaded region in Figure 3.20. For example, suppose that the distillate D follows the Th path along the TX boundary; the path Th defines a distillate policy that makes the column with decanter equivalent to the column without decanter. It is apparent that since the paths are defined arbitrarily, one can easily draw paths that would exhibit an arbitrary number of steady states. For example, for the feed shown in Figure 3.20, it is easy to show that if some vertical line (parallel to the LH edge) intersects the distillate path more than once then multiplicities exist. Moreover, the larger the number of the intersection points, the larger the number of the multiple steady states. Therefore, if the distillate follows a continuous-S-shaped path along a vertical line, the column will exhibit a number of steady states proportional to the number of the path S's.

We have shown that in the ∞/∞ case of columns with decanter there exist two

*Kienle and Marquardt (1991) and Helfferich (1993) investigated multiplicities in single column sections. Helfferich (1993) argues that these types of multiplicities disappear in practice (finite length column sections with finite mass-transfer rates). The implications of those multiplicities for complete distillation columns are unclear.

parameters yet to be specified: D_1 and D_2 or equivalently the distillate flowrate D and the ratio D_1/D . For the feed shown in Figure 3.20, we now want to draw the 3-D surface which depicts the light component mole fraction in the bottoms x_{BL} as a function of both the distillate flowrate D and the ratio D_1/D (bifurcation diagram with two bifurcation parameters). We derive this 3-D diagram by sketching the “cuts” of the surface for several distillate policies with constant ratio D_1/D , i.e., we draw the bifurcation diagrams with the distillate flowrate D as the only bifurcation parameter while the ratio D_1/D is fixed. We focus on the part of the bifurcation diagrams which corresponds to heterogeneous profiles.

If $D_1/D=1$ (i.e. $D_2=0$) we obtain the bifurcation diagram of Figure 3.22 which we place in Figure 3.32 at the $D_1/D=1$ plane. The line abc (Figure 3.32) corresponds to heterogeneous profiles. Along ab , x_{BL} and D monotonically increase and along bc , they both decrease. Point b marks the point of the highest x_{BL} achieved and point c denotes the end of the heterogeneous part of the bifurcation diagram. The points b' and c' are the projections of b and c on the plane $x_{BL} = 0$. Two heterogeneous steady states exist for distillate flowrates between c' and b' .

If $D_1/D=0$, it is easy to show that D will move on the bi part of the heterogeneous envelope (Figure 3.20). The line def of Figure 3.32 sketches the heterogeneous part of the bifurcation diagram of columns with distillate policy $D_1/D=0$. Along de , x_{BL} and D increase and along ef , x_{BL} decreases while D still increases. The distillate flowrate D is monotonically increasing along def and therefore, a unique heterogeneous steady state exists for columns with distillate policy $D_1/D=0$.

Using similar arguments we sketch the other two “cuts” in Figure 3.32 which show bifurcation diagrams for constant D_1/D . Now it is easy to draw the whole surface which is shown in Figure 3.32. The line be is the set of points of the highest x_{BL} achieved for every fixed D_1/D . The line cf is the end of the heterogeneous part of the bifurcation diagram for every fixed D_1/D . The lines $b'e'$ and $c'f'$ are the projections of be and cf on the plane $x_{BL} = 0$.

We can distinguish two parts of the surface shown in Figure 3.32. The surface $abeda$ is formed by the part of the “cuts” with constant D_1/D where x_{BL} and D

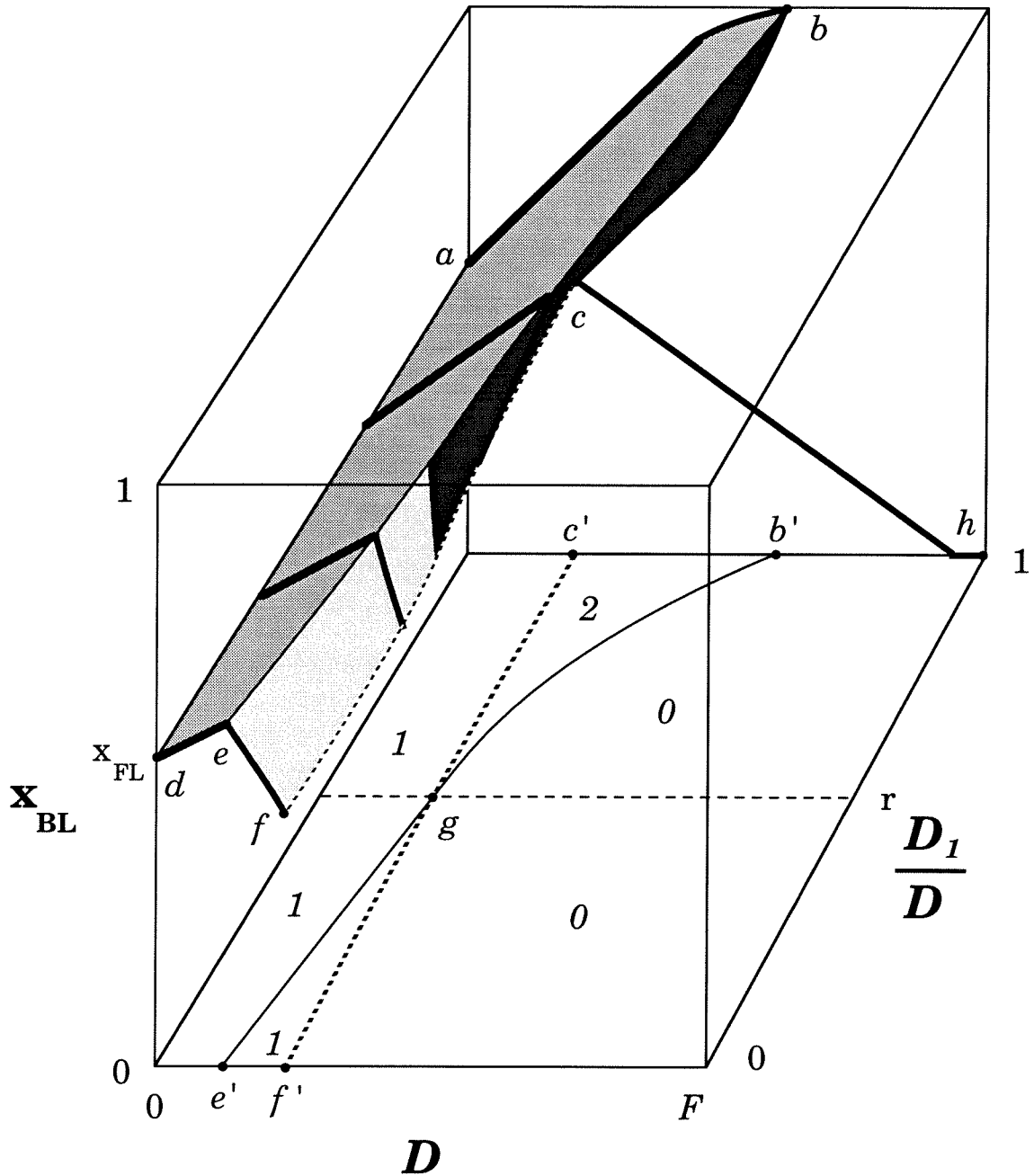


Figure 3.32: The mole fraction of L in the bottoms vs. the distillate flow and the ratio D_1/D for packed columns with decanter. Numbers in italics: the number of heterogeneous steady states in the $D - D_1/D$ parameter space.

monotonically increase until x_{BL} reaches its highest value. The second part of the surface, $bcfeb$, is formed by the part of the “cuts” of constant D_1/D where x_{BL} monotonically decreases beyond the point of the highest x_{BL} value. The dark-shaded (light-shaded resp.) portion of $bcfeb$ depicts the part of the “cuts” of constant D_1/D where the distillate flowrate D decreases (increases resp.). For simplicity, one may consider the dark-shaded part of the surface $bcfeb$ as the portion of $bcfeb$ that lies under the surface $abeda$, although this is not exactly correct.

It is apparent that the projection of the dark-shaded portion of the surface $bcfeb$ on the plane $x_{BL} = 0$ marks the parameter space region where two heterogeneous steady states exist. The region $c'b'gc'$ in Figure 3.32 depicts the approximate parameter space region of two heterogeneous steady states. Figure 3.32 also shows that if D_1/D is less than some value r , a unique heterogeneous steady state exists. Any arbitrary path of D in Figure 3.20 will correspond to a different “cut” of the surface in Figure 3.32 and depending on the shape of the “cut,” to a different number of multiple steady states.

Also note that the kF part of the bifurcation diagram of Figure 3.22 that corresponds to homogeneous profiles is placed at the $D_1/D=1$ plane in Figure 3.32 (ch line). This is obviously its “natural” location by continuity (point h of Figure 3.20 belongs to the phase 1 part of the heterogeneous boiling envelope). Any other constant D_1/D distillate policy exhibits a discontinuity at the point where the profile along the continuation path becomes homogeneous. For example, if $D_1/D=0$ the bifurcation diagram consists of the lines def (heterogeneous part) and ch (homogeneous part) of Figure 3.32 and apparently it exhibits a discontinuity (jump from f to c). A very important factor for the presence or absence of discontinuities in the bifurcation diagrams is the location of the critical point C . If C were located to the left of point h in Figure 3.21 ($D_2=0$), a discontinuity would occur between points C and h , i.e., the distillate would not be allowed to lie on Ch under the distillate policy $D_2=0$ since Ch would correspond to phase 2. In addition, the changed orientation of the tie lines would give different feasible product regions in Figure 3.20.

In the case of columns without decanter, similarly as the homogeneous case, there is no discontinuity along the continuation path and therefore, multiple steady states

exist if and only if the distillate flowrate decreases along some part of the continuation path. In the case of columns with decanter and a given distillate policy, however, we just showed that discontinuity is possible at the transition from heterogeneous to homogeneous profiles. Therefore, in this case, in addition to the aforementioned multiplicity condition, one has to check the distillate flowrate ranges of the heterogeneous and homogeneous branches of the continuation path for possible distillate flowrate overlap and consequently multiplicity.

3.6 Finite Reflux and Finite Number of Trays

The ∞/∞ case is the limiting case of high reflux and a large number of trays. Therefore, if the geometrical condition is satisfied for a given mixture then multiplicities will exist for some sufficiently large finite reflux and finite number of trays. However, the inverse is not true, i.e., there may be mixtures that exhibit multiple steady states in finite columns but these multiplicities do not exist in columns operating at the ∞/∞ conditions. Therefore, the geometrical condition is only a sufficient condition for the existence of multiplicities when the reflux and the number of trays are finite.

At infinite reflux, the column profiles coincide with residue curves or distillation lines. This is not true at finite reflux. Moreover, column profiles at finite reflux depend on the location and the number of the feed streams. Therefore, the residue curve and distillation line diagrams do not provide an accurate description of columns at finite reflux and with a finite number of trays.

In this section, we present steady state bifurcation results for the mixture ethanol (L) - water (H) - benzene (I-E) with the distillate flow D as the bifurcation parameter. These bifurcation results show (1) that the predictions for the existence of multiple steady states in the ∞/∞ case carry over to columns operating at finite reflux and with a finite number of trays and (2) that, although the predictions were made in the ∞/∞ case, it does not mean that multiple steady states do not exist for realistic operating conditions (low reflux and number of trays).

In all simulations presented here, we use a tray column with a total condenser

while the reboiler constitutes an additional equilibrium stage (partial reboiler). Constant molar overflow and a tray efficiency of 1 are assumed. Finally, the column operates under atmospheric pressure and there is no pressure drop in the column. The thermodynamic model described in the preliminaries of this chapter is used for the VLLE calculations. The tray counting starts from the reboiler (number 1) and ends at the top. The bifurcation calculations were conducted with AUTO, a software package developed by Doedel (1986). In the following, we present steady state bifurcation results for two columns, one without decanter and one with decanter.

Column without decanter:

The column characteristics are depicted in Figure 3.33 and they are similar to the column studied by Magnussen et al. (1979). The column has 27 ideal stages (including the reboiler). The reflux flow is fixed at $R=345.157$. A mixture of 89% ethanol and 11% water, is fed at stage 23 (F_1). It is assumed that the distillate D of the column in Figure 3.33 is fed to a decanter (not included in the model); the benzene-rich phase from the decanter is returned to the column. Since the decanter is not included in the model, a second stream (F_2) is fed at the top of the column (Figure 3.33) to compensate for the returned benzene-rich phase from the decanter and the benzene make-up stream. The flowrate and composition of the second feed F_2 are the same as the one Magnussen et al. (1979) specified “according to experimentally observed liquid-liquid equilibria.” The location of the overall feed ($F=F_1+F_2$) composition in the composition triangle is similar to the one illustrated in Figure 3.12. Therefore, Figure 3.13 illustrates the predicted ∞/∞ case bifurcation diagram for the column in Figure 3.33.

Moreover, in the ∞/∞ case, the distillate flowrate range where three steady states exist can be predicted. For the overall feed F of this example, this is done by calculating the distillate flowrates corresponding to points f and e of Figure 3.13, or equivalently, the distillate flowrates of columns with distillate compositions D at points a and b of Figure 3.12. The latter can be easily calculated using the lever rule for material balances, the known overall feed composition F and the location of points a and b (Figure 3.12). Note that, in locating the points a and b in the composition

	$F_1 = 100.00$	$F_2 = 45.32$
Ethanol (L)	89.00	9.90
Benzene (I)	0.00	33.62
Water (H)	11.00	1.80

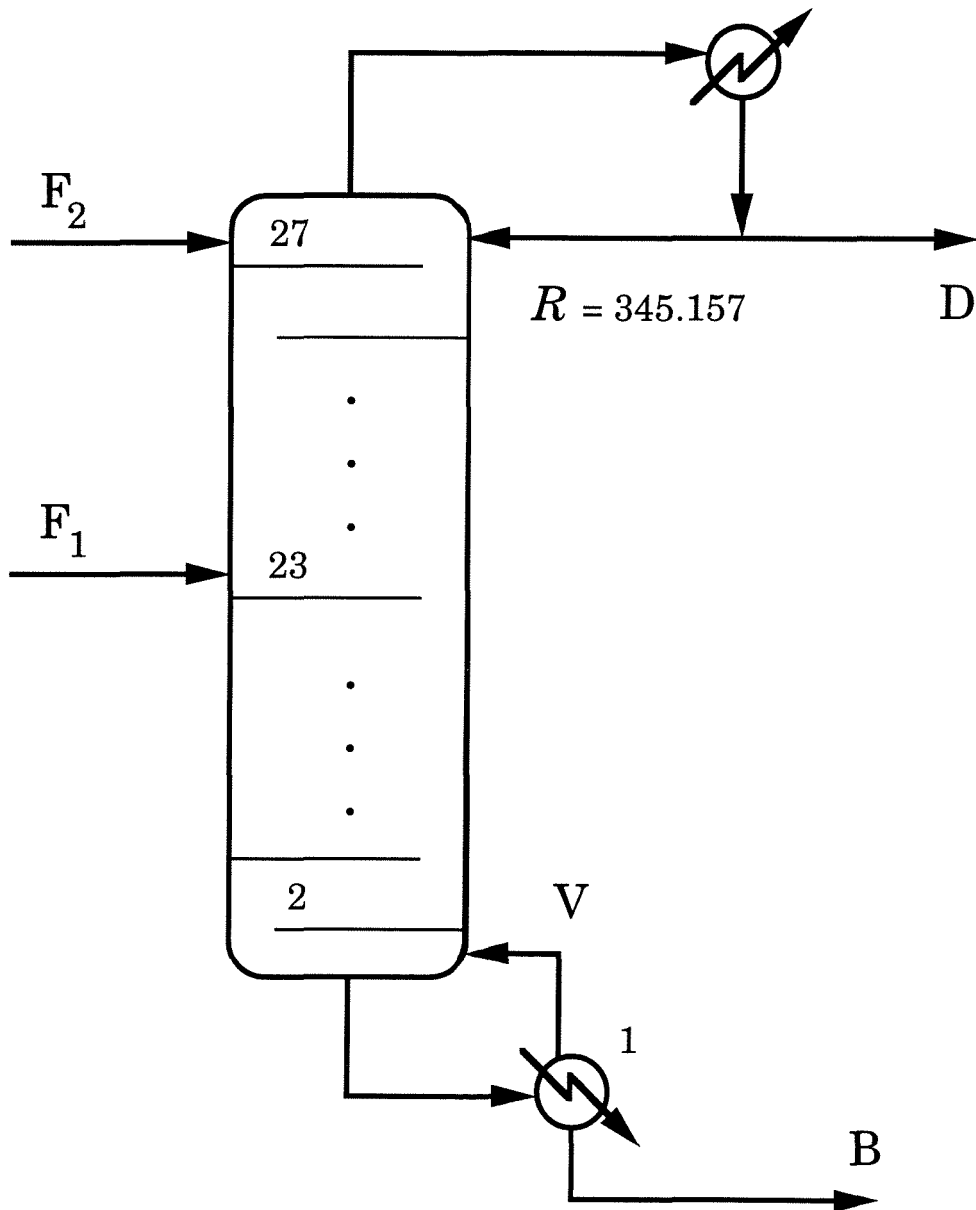


Figure 3.33: The column without decanter used in the numerical continuation calculations.

triangle, the actual, computed distillation line diagram (Figure 3.6) should be used, not the illustration (Figure 3.12). Using the lever rule for material balances it can be shown that for the overall feed F of this example, the distillate flowrates of columns with D at points a and b are equal to the benzene feed flow ($F_I=33.62$) divided by the benzene mole fraction at points a and b respectively. Using the actual, computed distillation line diagram, the benzene composition was found to be equal to 0.52793 at point a and 0.52935 at point b . Therefore, it is predicted that in the ∞/∞ case, three steady states exist for distillate flows between 63.51 and 63.68.

Figure 3.34 shows the computed bifurcation diagram with the distillate flow as the bifurcation parameter for the column in Figure 3.33. A unique stable steady state exists for low D . D increases until the continuation algorithm reaches the first limit point. Beyond that point an unstable steady state is calculated (dashed curve). Along this part of the continuation path x_{BL} decreases while D decreases until the second limit point is encountered. Beyond the second limit point, D increases again and a second stable steady state is calculated. Hence, two stable and one unstable steady states exist for distillate flows between the two limit points (multiplicity region); a unique stable steady state exists otherwise. Note the similarity of this continuation path with the continuation path we tracked in the ∞/∞ case (Figure 3.13) and of the computed multiplicity region (D between 63.06 and 63.68) and the predicted one. Some discrepancy from the ∞/∞ case prediction is expected. Finally, note that, although those multiple steady states were predicted at infinite reflux, they still exist at low reflux values ($R/F=2.4$).

Column with decanter:

The column characteristics are depicted in Figure 3.35. The column has 27 ideal stages (including the reboiler). The reflux flow is fixed at $R=508.369$. A mixture of 89% ethanol and 11% water, is fed at stage 23 (F_1). In this case, the second feed (F_2) at the top of the column is the benzene make-up stream. The location of the overall feed ($F=F_1+F_2$) composition in the composition triangle is similar to the one illustrated in Figure 3.21 and hence, Figure 3.22 illustrates the predicted ∞/∞ case bifurcation diagram for the column in Figure 3.35 with the exception that the mole

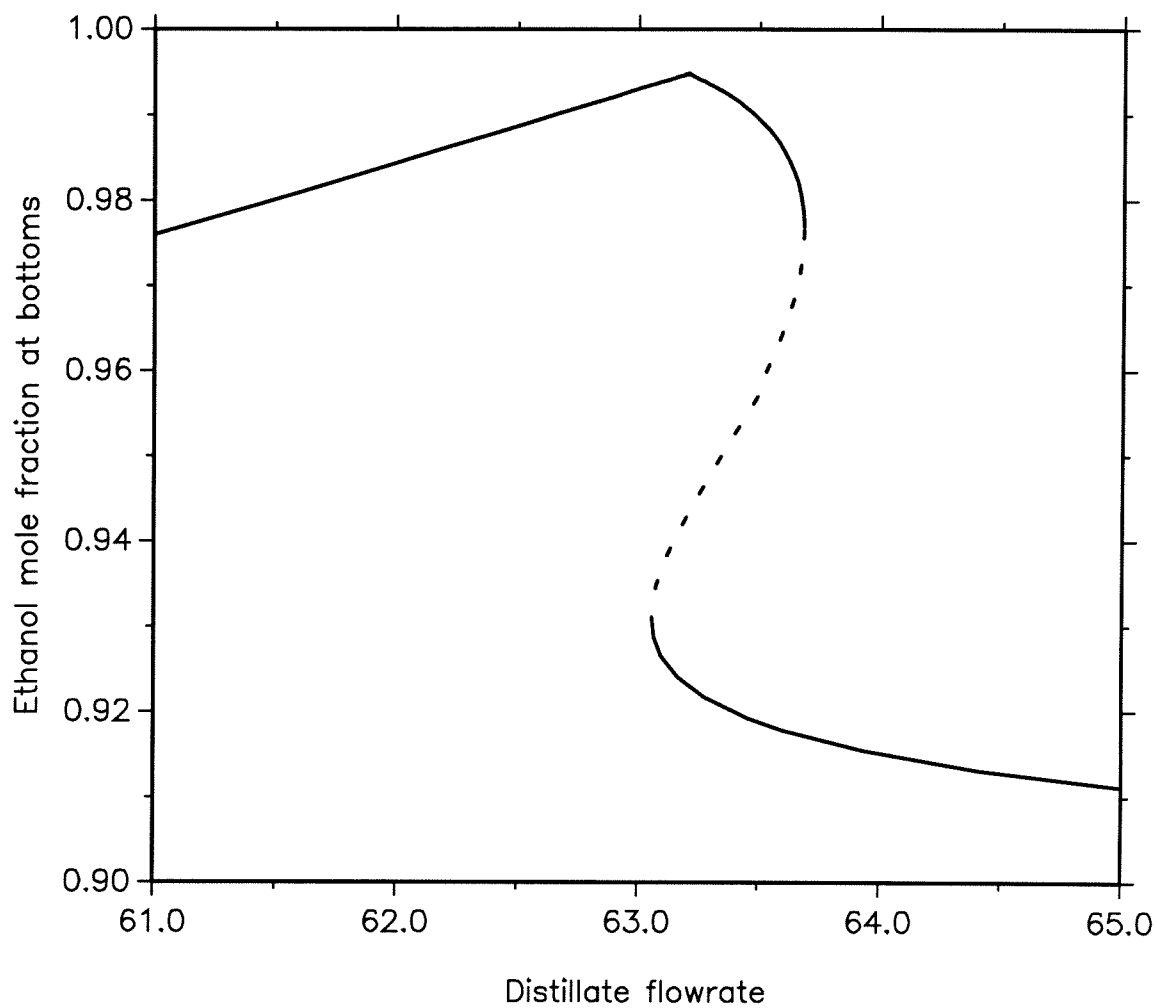


Figure 3.34: Bifurcation diagram with the distillate flow as the bifurcation parameter for the column without decanter.

fraction of ethanol at point k of Figure 3.22 is larger than x_{FL} .

Again, in the ∞/∞ case, the distillate flowrate range where three steady states exist can be predicted. For the overall feed F of this example, this is done by calculating the distillate flowrates of columns with distillate compositions D at points f and h of Figure 3.21. These can be easily calculated using the lever rule for material balances, the known overall feed composition F and the location of points f and h (Figure 3.21). Again, in locating the points f and h in the composition triangle, the actual, computed distillation line diagram (Figure 3.6) should be used, not the illustration (Figure 3.21). Using the lever rule for material balances it can be shown that for the overall feed F of this example, the distillate flowrates of columns with D at points f and h are equal to the benzene feed flow ($F_I=1.962$) divided by the benzene mole fraction at points f and h respectively. Using the actual, computed distillation line diagram, the benzene composition was found to be equal to 0.08038 at point f and 0.47067 at point h . Therefore, it is predicted that in the ∞/∞ case, three steady states exist for distillate flows between 4.17 and 24.41.

Figure 3.36 shows the computed bifurcation diagram with the distillate flow as the bifurcation parameter for the column in Figure 3.35. A unique stable heterogeneous steady state exists for low D . D increases until the continuation algorithm reaches the first limit point. Beyond that point an unstable heterogeneous steady state is calculated (dashed curve). The distillate flow D decreases along the unstable part of the continuation path until the second limit point is encountered. Note that it is purely coincidental that the second limit point appears to be on the heterogeneous stable part of the continuation path (it does not because the other component mole fractions are different). Beyond the second limit point, D increases again and a second stable, but homogeneous, steady state is calculated. Hence, two stable (one heterogeneous and one homogeneous) and one unstable (heterogeneous) steady states exist for distillate flows between the two limit points; a unique stable steady state exists otherwise. Again, note the similarity of this continuation path with the continuation path we tracked in the ∞/∞ case (Figure 3.22) and of the computed multiplicity region (D between 4.23 and 24.41) and the predicted one. Some discrepancy from

	$F_1 = 100.00$	$F_2 = 1.962$
Ethanol (L)	89.00	0.00
Benzene (I)	0.00	1.962
Water (H)	11.00	0.00

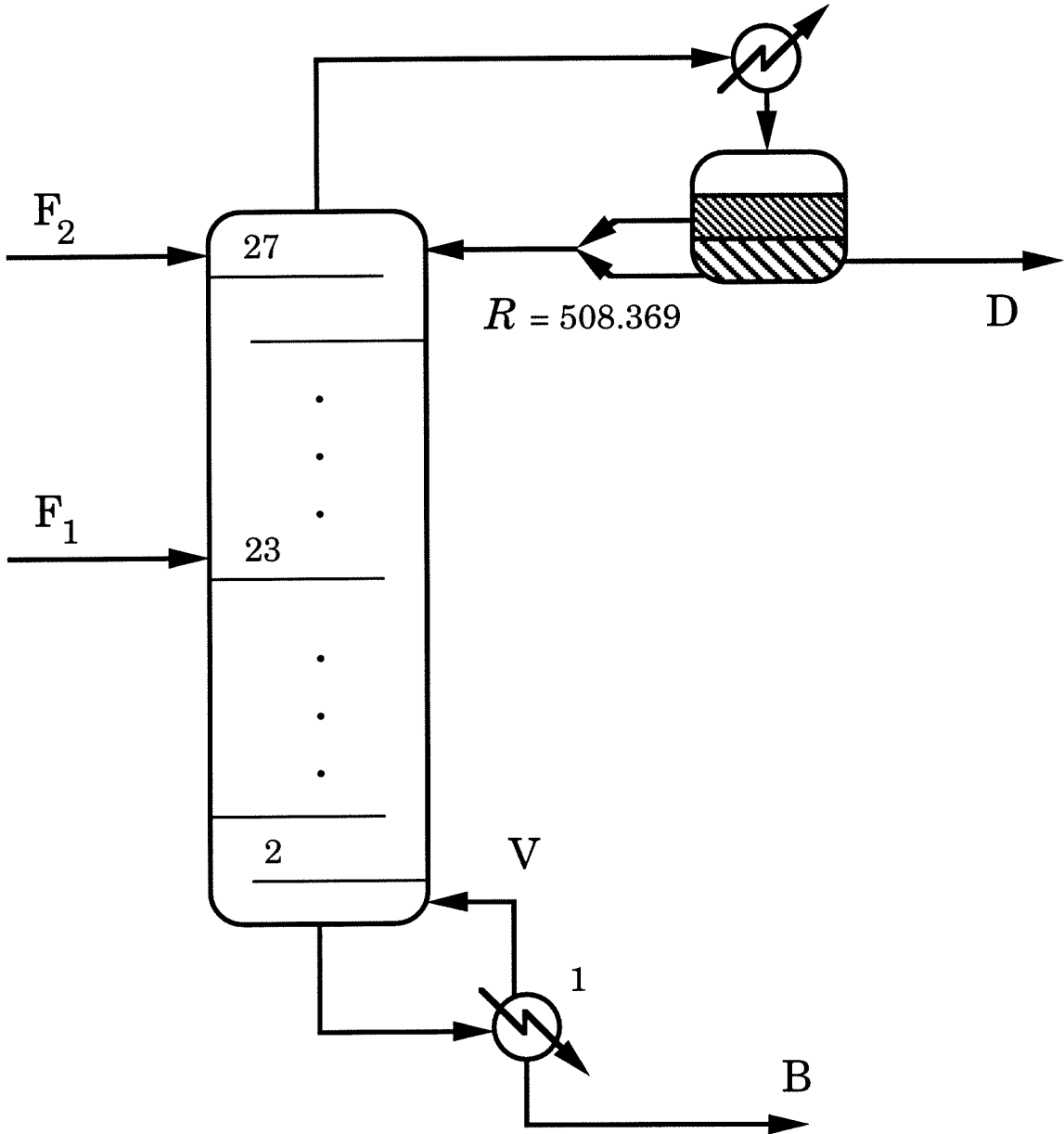


Figure 3.35: The column with decanter used in the numerical continuation calculations.

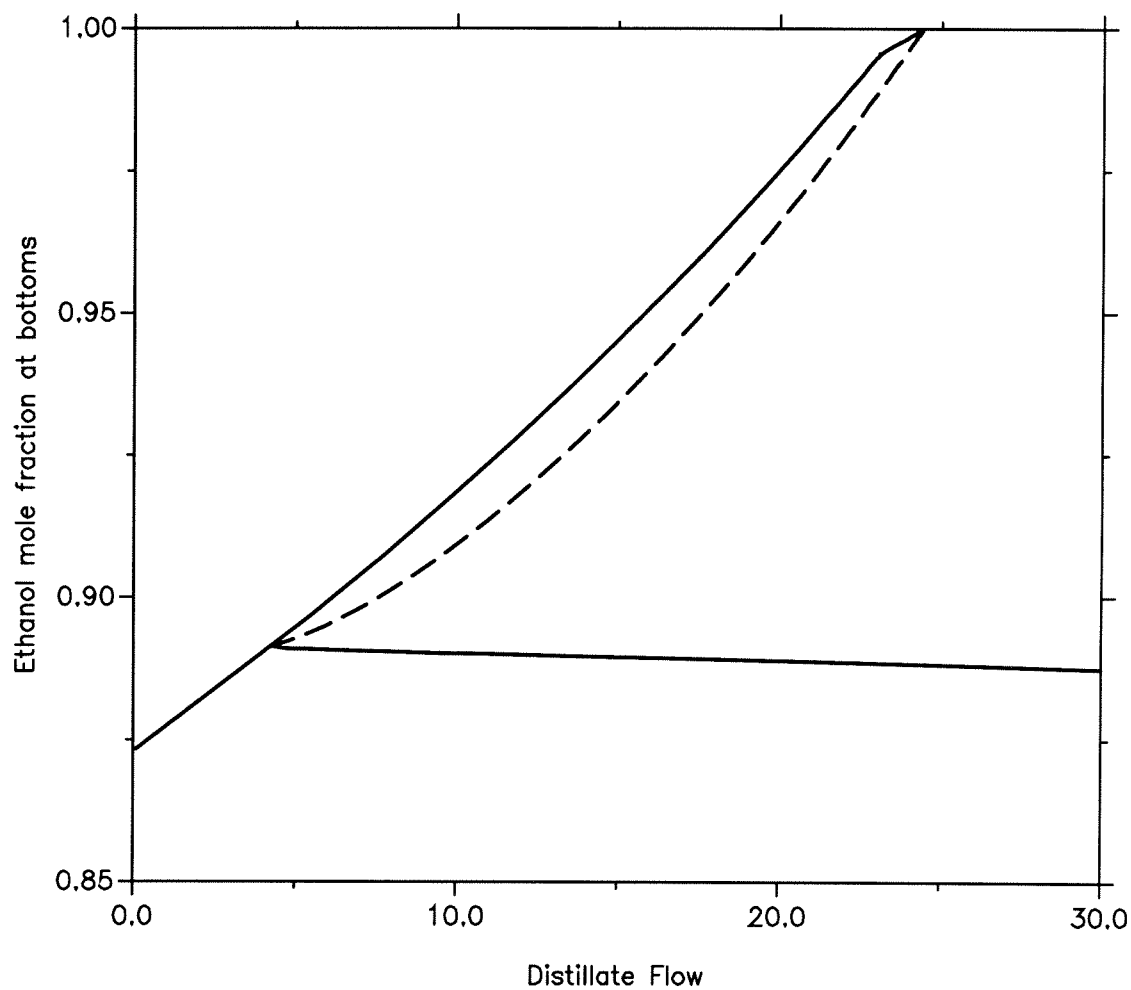


Figure 3.36: Bifurcation diagram with the distillate flow as the bifurcation parameter for the column with decanter.

the ∞/∞ case prediction is expected.

3.7 Conclusions

In this chapter we examine in detail the existence of multiple steady states in the ∞/∞ case of a ternary mixture. More specifically, we answer the following questions: Given a ternary (homogeneous or heterogeneous) mixture and its VL(L)E diagram (residue curve diagram for packed columns, distillation line diagram for tray columns),

- (1) find whether multiple steady states exist for some feed composition and
- (2) locate the feed composition region that leads to these multiple steady states.

The existence of multiplicities (question 1) can be checked by the procedure depicted in Figure 3.37 which is summarized in the following:

Locate the singular points (pure components and azeotropes) in the VL(L)E diagram. Locate the m distillation regions. In every distillation region containing k singular points, there is one unstable node, one stable node and $k-2$ saddles. For each region there exist two routes which go from the unstable node to the stable node along the region boundaries (a total of $2m$ routes).

For each route, mark the n singular points along the route as follows: point 1, the unstable node; points 2 to $n-1$, the saddles; point n , the stable node. The only eligible column profile lower end compositions along this route lie on the part between points 2 and n . This is the profile lower end route. Accordingly, the eligible column profile upper end (overhead vapor) lies on the part of the route between points 1 and $n-1$. This is the profile upper end route. These two routes define the locations of the upper and lower end column profile compositions for which the geometrical condition should be checked (type III column profiles).

Note, however, that the geometrical condition directly involves the distillate and bottom product routes which may be different from the profile upper and lower end routes depending on the type of the equipment used at the column ends (condenser, reboiler, decanter). In this chapter, we show how the distillate and bottoms routes

(associated with a given pair of upper and lower profile end routes) can be located for any equipment combination. Tables 3.3a and 3.3b show how the distillate and bottom product routes are related to the profile upper and lower end routes for some equipment types and for tray and packed columns respectively.

Finally, we define the continuation path (and its direction) as the path generating all possible column profiles starting from the profile with $D=0$ and ending at the profile with $D=F$. Multiple steady states occur when D decreases along this path. This can be checked by the following condition:

Geometrical, necessary and sufficient multiplicity condition: Pick a distillate D and a bottom product B , both located on some pair of distillate and bottoms product routes and such that (1) the line segment $D'B'$ crosses the line segment DB (to ensure that there exists a feed composition associated with both profiles) and (2) the column profile that runs from D to B along the distillation region boundaries contains at least one saddle singular point (type III column profile). Now pick D' and B' sufficiently close to D and B respectively and such that the column profile from D' to B' is a “later” profile along the continuation path. For the existence of multiple steady states it is required that: As we move along the continuation path from D to D' and accordingly from B to B' , the line that passes from D and is parallel to BB' crosses the $D'B'$ line segment.

Finally, for columns with decanter and a given distillate policy, we show that discontinuity is possible at the transition from heterogeneous to homogeneous profiles along the continuation path. In this case, in addition to the aforementioned geometrical condition, one has to check the distillate flowrate ranges of the heterogeneous and homogeneous branches of the continuation path for possible distillate flowrate overlap and consequently multiplicity.

The condition for the appropriate feed region (question 2) is summarized in the following:

Appropriate feed region condition: Pick a distillate D . Find the set of all bottom products such that the geometrical condition is satisfied for the picked D . Name this set $S_B(D)$. Note that $S_B(D)$ is always part of a distillation region boundary and

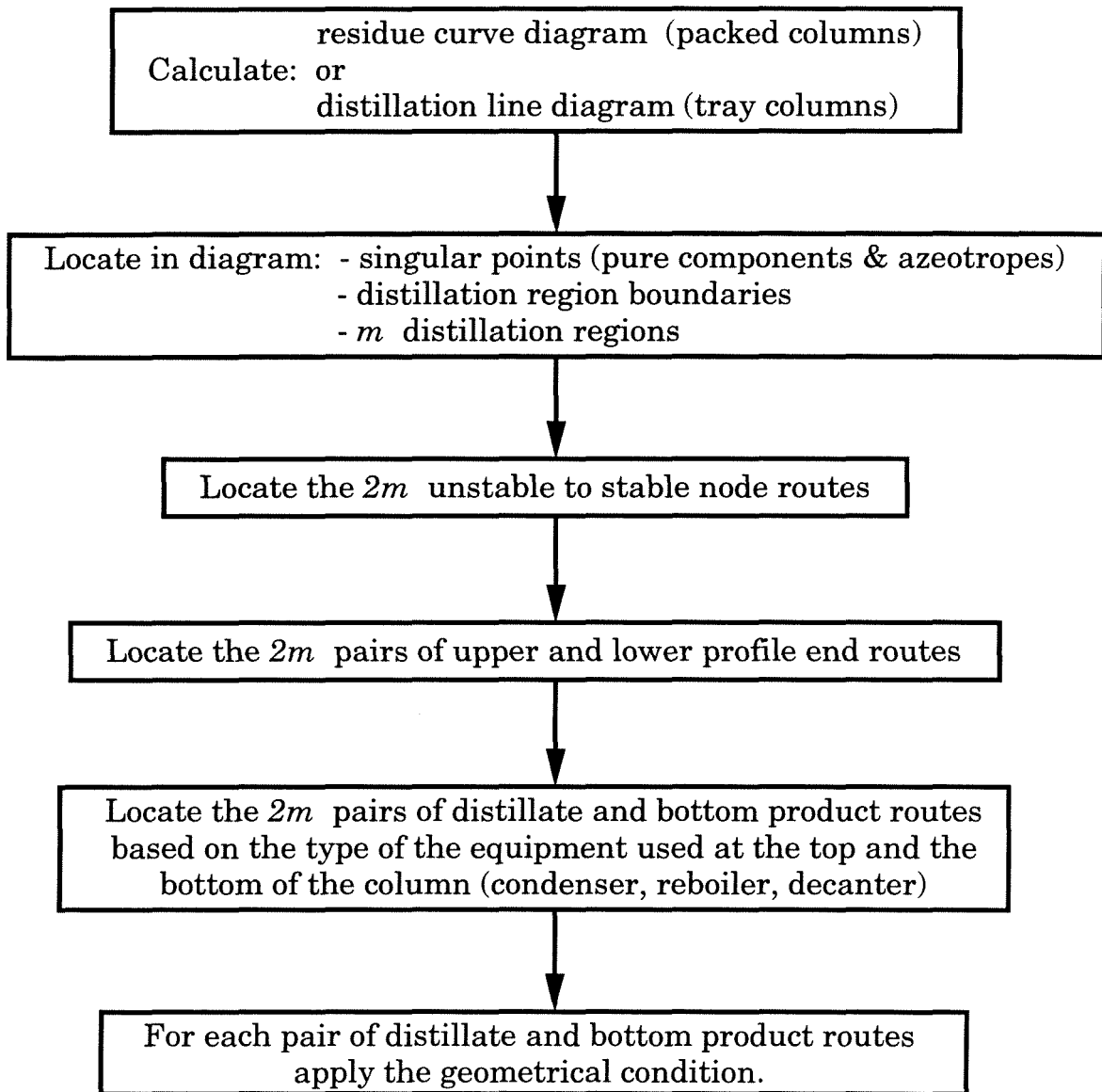


Figure 3.37: The general procedure for checking the existence of multiple steady states in the ∞/∞ case of any ternary mixture.

Table 3.3: The distillate and bottoms routes for various types of equipment (condenser/reboiler/decanter). a. tray columns b. packed columns.

a. Tray columns (tray efficiency=1)

Total Reboiler	B route = lower end route
Partial Reboiler B = liquid	
Total Condenser	D route = upper end route
Partial Condenser D = vapor	
Total (or Subcooled) Condenser & Decanter with policy $D_2=0$	D route composed of: - the homogeneous part of the upper end route & - the part of the 1st phase of the heterogeneous liquid boiling envelope (or binodal curve) that can be obtained from the phase split of the heterogeneous part of the upper end route

b. Packed columns (\approx tray columns w/ tray efficiency $\rightarrow 0$)

Total Reboiler	B route = lower end route
Partial Reboiler B = liquid	B route = line of liquid compositions in equilibrium with vapor compositions on the lower end route
Total Condenser	D route = upper end route
Partial Condenser D = vapor	D route = line of vapor compositions in equilibrium with liquid compositions on the upper end route
Total (or Subcooled) Condenser & Decanter with policy $D_2=0$	D route composed of: - the homogeneous part of the upper end route & - the part of the 1st phase of the heterogeneous liquid boiling envelope (or binodal curve) that can be obtained from the phase split of the heterogeneous part of the upper end route

that in some rare cases, $S_B(D)$ may contain an inflexion point and/or it may consist of more than one non-connected boundary segments. Draw the straight line segments connecting D with the end points of each boundary segment that belongs to $S_B(D)$. For the chosen D , the appropriate feed composition is the union of the areas enclosed by each boundary segment that belongs to $S_B(D)$ and the corresponding straight line segments connecting D with the end points of the boundary segment of $S_B(D)$. Pick another distillate D and repeat. In general, for each distillate D there exists a different set of bottoms compositions, $S_B(D)$, that satisfies the geometrical condition. Therefore, for any given mixture, the feed compositions that lead to multiplicities lie in the union of all the areas enclosed by each boundary segment that belongs to *some* $S_B(D)$ and the corresponding straight line segments connecting the distillate D associated to $S_B(D)$ with the end points of the boundary segment of $S_B(D)$.

The procedures and conditions described above constitute the fully detailed, accurate and totally general answers to the questions about the existence of multiplicities and the feed compositions that lead to these multiplicities in the ∞/∞ case. Given a mixture and its VL(L)E diagram, we show via an illustrative example how the specific VL(L)E diagram structural information can be used to simplify these conditions (unavoidably by reducing the degree of generality) to some very simple tests. We also discuss the differences between packed and tray columns, between residue curve and distillation line diagrams, the effect of tray efficiency as well as the role of the vapor line for heterogeneous mixtures. Since residue curve boundaries are easier to calculate than distillation line boundaries, we derive guidelines on when it is justified to use residue curve boundaries for the study of multiplicities of tray columns (at the expense of less quantitative accuracy).

As an illustrative example throughout this chapter we use the mixture ethanol - water - benzene. For this mixture and the specific VL(L)E model and parameters used, we derive the following conclusions regarding multiplicities in the ∞/∞ case solely based on (1) the residue curve boundaries, the heterogeneous region envelope, the distillation line boundaries and the line of vapor compositions in equilibrium with liquid compositions on the residue curve boundaries, if accurate quantitative results

are needed, or (2) the residue curve boundaries, the heterogeneous region envelope and the vapor line, if somewhat less accurate quantitative results are sufficient.

Columns without decanter: In this case, we identify that the existence of multiplicities critically depends on the location of the distillate path away from the binary edges and more specifically in the heterogeneous region. We show that the location of the vapor line is very crucial in this case. We further show that the reboiler type has absolutely no effect on the existence of multiplicities for this particular mixture class.

For tray columns with tray efficiency 1, we conclude that multiplicities exist regardless of the condenser type. For packed columns, multiplicities exist if a partial condenser is used and the distillate product consists of the vapor phase only. A unique steady state exists, however, for packed columns with a total condenser. Finally, for tray columns with a total condenser, we conclude that there exists a tray efficiency value η^* such that multiple steady states exist only if $\eta > \eta^*$.

Columns with decanter: We show that the existence of multiplicities depends on the distillate policy. The most common distillate policy for this mixture, i.e., recovering as distillate a portion of the entrainer-poor phase only ($D_2=0$) and refluxing a mixture of the two liquid phases, is studied in detail. We conclude that under this distillate policy: (1) the existence of multiple steady states is generic for this heterogeneous mixture class and therefore the presence of multiplicities does not critically depend on some specific VL(L)E characteristic as long as the basic qualitative structural properties of the VL(L)E diagram are preserved, (2) consequently, using different reboiler, condenser and column types does not qualitatively affect the existence of multiplicities although some quantitative differences are expected.

Finally, using numerically constructed bifurcation diagrams, we show that the ∞/∞ case predictions carry over to columns operating at finite reflux and with a finite number of trays. We also discuss a different, degenerate type of multiplicity (infinite number of profiles with the same product compositions for a specific distillate flowrate) whose practical implications are unclear and therefore, a more thorough investigation of this topic is needed.

Acknowledgements: We acknowledge gratefully the financial support of the Donors of the Petroleum Research Fund administered by the American Chemical Society and of the I. S. Latsis Foundation. We also thank Prof. Seider (University of Pennsylvania, Philadelphia) and Prof. Michelsen (Danish Technical University, Lyngby) for providing us thermodynamic subroutines.

3.8 Literature Cited

Aspen Plus, Release 8, Aspen Technology Inc., Cambridge, MA, 1988.

Bossen, S. B., S. B. Jorgensen, and R. Gani, "Simulation, Design, and Analysis of Azeotropic Distillation Operations," *Ind. Eng. Chem. Res.*, 1993, **32**, pp. 620-633.

Cairns, B. P., and I. A. Furzer, "Multicomponent Three-Phase Azeotropic Distillation. 3. Modern Thermodynamic Models and Multiple Solutions," *Ind. Eng. Chem. Res.*, 1990, **29**(7), pp. 1383-1395.

Doedel, E., "AUTO: Software for Continuation and Bifurcation Problems in Ordinary Differential Equations," Applied Mathematics, Caltech, Pasadena, CA, 1986.

Doherty, M. F., and J. D. Perkins, "On the Dynamics of Distillation Processes. I. The Simple Distillation of Multicomponent Non-reacting, Homogeneous Liquid Mixtures," *Chem. Eng. Science*, 1978, **33**, pp. 569-578.

Gmehling, J., and U. Onken, "Vapor-Liquid Equilibrium Data Collection," DECHEMA, Chemistry Data Series, I, Part 1, Verlag & Druckerei Friedrich Bischoff, Frankfurt, 1977.

Helferich, F. G., "Multiple Steady States in Multicomponent Countercurrent Mass-Transfer Processes," *Chem. Eng. Science*, 1993, **48**(4), pp. 681-686.

Kienle, A., and W. Marquardt, "Bifurcation Analysis and Steady-State Multiplicity of Multicomponent, Non-Equilibrium Distillation Processes," *Chem. Eng. Science*, 1991, **46**(7), pp. 1757-1769.

Kingsley, J. P., and A. Lucia, "Simulation and Optimization of Three-Phase Distillation Processes," *Ind. Eng. Chem. Res.*, 1988, **27**(10), pp. 1900-1910.

Kovach III, J. W., and W. D. Seider, "Heterogeneous Azeotropic Distillation -

Homotopy-Continuation Methods,” *Comput. Chem. Eng.*, 1987a, **11**(6), pp. 593-605.

Kovach III, J. W., and W. D. Seider, “Heterogeneous Azeotropic: Experimental and Simulation Results,” *Comput. Chem. Eng.*, 1987b, **11**(6), pp. 593-605.

Laroche, L., N. Bekiaris, H. W. Andersen, and M. Morari, “Homogeneous Azeotropic Distillation: Separability and Flowsheet Synthesis,” *Ind. Eng. Chem. Res.*, 1992, **31**(9), pp. 2190-2209.

Magnussen, T., M. L. Michelsen, and Aa. Fredenslund, “Azeotropic Distillation Using UNIFAC,” *Inst. Chem. Eng. Symp. Ser.*, 1979, **56**, pp. 4.2/1-4.2/19.

Matsuyama, H., and H. Nishimura, “Topological and Thermodynamic Classification of Ternary Vapor-Liquid Equilibria,” *J. Chem. Eng. Jpn.*, 1977, **10**(3), pp. 181-187.

Pham, H. N., and M. F. Doherty, “Design and Synthesis of Heterogeneous Azeotropic Distillations - II. Residue Curve Maps,” *Chem. Eng. Science*, 1990, **45**(7), pp. 1837-1843.

Prausnitz, J. M., R. N. Lichtenthaler, and E. G. Azevedo, “Molecular Thermodynamics of Fluid-Phase Equilibria,” pp. 238-240;262-264, Prentice-Hall, Englewood Cliffs, NJ, 1986.

Prokopakis, G. J., W. D. Seider, and B. A. Ross, “Azeotropic Distillation Towers with Two Liquid Phases,” *Foundations of Computer-aided Chemical Process Design*, pp. 239-272, R. S. H. Mah, and W. D. Seider, eds., AIChE, New York, 1981.

Prokopakis, G. J., and W. D. Seider, “Feasible Specifications in Azeotropic Distillation,” *AIChE Journal*, 1983a, **29**(1), pp. 49-60.

Prokopakis, G. J., and W. D. Seider, “Dynamic Simulation of Azeotropic Distillation Towers,” *AIChE Journal*, 1983b, **29**(6), pp. 1017-1029.

Rovaglio, M., and M. F. Doherty, “Dynamics of Heterogeneous Azeotropic Distillation Columns,” *AIChE Journal*, 1990, **36**(1), pp. 39-52.

Rovaglio, M., T. Faravelli, G. Biardi, P. Gaffuri and S. Soccol, “The Key Role of Entrainer Inventory for Operation and Control of Heterogeneous Azeotropic Distillation Towers,” *Comput. Chem. Eng.*, 1993, **17**(5/6), pp. 535-547.

Stichlmair, J. G., J. R. Fair, and J. L. Bravo, “Separation of Azeotropic Mixtures

via Enhanced Distillation," *Chem. Eng. Prog.*, 1989, (1), pp. 63-69.

Stichlmair, J. G., and J. R. Herguijuela, "Separation Regions and Processes of Zeotropic and Azeotropic Ternary Distillation," *AIChE Journal*, 1992, **38**(10), pp. 1523-1535.

Venkataraman, S., and A. Lucia, "Solving Distillation Problems by Newton-like Methods," *Comput. Chem. Eng.*, 1988, **12**(1), pp. 55-69.

Widagdo, S., W. D. Seider, and D. H. Sebastian, "Bifurcation Analysis in Heterogeneous Azeotropic Distillation," *AIChE Journal*, 1989, **35**(9), pp. 1457-1464.

Zharov, V. T., and L. A. Serafimov, "Physicochemical Fundamentals of Simple Distillation and Rectification" (in Russian), pp. 160-168, Khimia, Leningrad, 1975.

3.9 Appendix

The appendix contains information on the thermodynamic model used in this chapter. Vapor - liquid equilibrium calculations are based on the following equation:

$$y_i P = x_i P_i^{sat}(T) \gamma_i(T, \underline{x})$$

where $P=1$ atm in this chapter.

Vapor pressures were computed by the Antoine equation:

$$\ln P_i^{sat} = A_i + \frac{B_i}{T + C_i}$$

where T in $^{\circ}K$ and P_i^{sat} in *atm*. Table 3.4 contains the Antoine coefficients given by Gmehling and Onken (1977) for the components used in this chapter.

Liquid activity coefficients were computed by the modified UNIQUAC model. The exact form of the modified UNIQUAC model used here is given in equations (6.11-11)-(6.11-22) and (6.15-9)-(6.15-12) in Prausnitz et al. (1986).

Table 3.5 contains the UNIQUAC parameters R , Q and Q' for the pure components ethanol, water and benzene given by Gmehling and Onken (1977). Note that $Q=Q'$. Table 3.6 contains the UNIQUAC binary parameters a_{ij} in $^{\circ}K$ (equation 6.11-17 in

Table 3.4: Antoine coefficients for the components used in the chapter.

	A	B	C
Ethanol	12.0455965	-3667.705	-46.966
Benzene	9.2080465	-2755.642	-53.989
Water	11.9514465	-3984.923	-39.724

Table 3.5: UNIQUAC pure component parameters used in this chapter.

	R	Q	Q'
Ethanol	2.1055	1.972	1.972
Benzene	3.1878	2.4	2.4
Water	0.92	1.4	1.4

Table 3.6: UNIQUAC binary parameters a_{ij} in °K for the ethanol - benzene - water mixture.

i \ j	Ethanol	Benzene	Water
Ethanol	0	-43.0334	-32.9976
Benzene	384.892	0	903.800
Water	203.843	362.300	0

Prausnitz et al., 1986) for the mixture ethanol - water - benzene used in this chapter; the UNIQUAC binary parameters a_{ij} were estimated from the UNIFAC model using the Aspen Plus (1988) property parameter estimation option.

Chapter 4 ∞/∞ Predictions and Implications for Design, Synthesis and Simulation.

4.1 Introduction

In chapters 2 and 3, we presented a thorough study of the existence of such multiple steady states in ternary homogeneous* and heterogeneous azeotropic distillation. They provided a simple physical explanation and developed graphical predictive rules for the occurrence of these multiplicities based solely on the VL(L)E of the ternary mixture. These results were obtained by the thorough analysis of the case of infinite reflux and infinite number of trays (or infinitely long packed columns), which we hereafter denote as the ∞/∞ case. In chapters 2 and 3, we also showed that the prediction of the existence of multiple steady states in the ∞/∞ case has relevant implications for columns operating at finite reflux and with a finite number of trays.

The implications of these multiplicities for distillation simulation, design and operation are numerous and can be critical for design decisions. The existence of multiple solutions may cause problems in simulations, e.g., a higher convergence failure rate. Furthermore, the computation of only one solution may also result in misleading conclusions and decisions regarding the separation under consideration caused by disregarding some eligible, and possibly, attractive solutions.

Multiplicities may also cause problems in column operation and control. When two or more steady states exist for the same inputs it is possible that for some disturbance, the column profile jumps (or shifts) from the desirable - in terms of product purity - steady state to another undesirable steady state, e.g., a steady state with low product purity. Evidence of the operational problems that multiple steady

*The mixture under consideration is called homogeneous if only one liquid phase exists throughout the composition range and heterogeneous if two liquid phases exist for some compositions.

states can cause is given by Kovach and Seider (1987). Their conclusion is that the experimentally observed erratic behavior of the industrial tower they study is due to the existence of multiple steady states.

In addition, the existence of multiplicities in distillation has implications for distillation design and synthesis. This is mainly an issue of control-design interactions. The reason is that alternative designs may have different control properties. One design alternative may be much more difficult to control than another. Since we know that multiple steady states can cause control problems, it is apparent that the existence of multiplicities has several implications for design and synthesis, e.g., for the selection of the entrainer, the equipment and the separation scheme.

In this chapter, first we briefly review the ∞/∞ analysis (chapters 2 and 3). Then we present the ∞/∞ case multiplicity predictions. Finally, we demonstrate the implications of these multiplicities and predictions for column design, synthesis and simulation.

4.2 Tools and preliminaries

Two widely used tools for the description of azeotropic distillation column profiles are the residue curves (Doherty and Perkins, 1978) and the distillation lines (Zharov and Serafimov, 1975; Stichlmair et al., 1989). By drawing a number of these curves or lines in the composition space, one can construct a mixture's residue curve or distillation line diagram.

The singular points of both residue curves and distillation lines are the pure components and the azeotropes and they can be stable nodes, unstable nodes or saddles. Zharov and Serafimov (1975) showed that distillation lines (1) have the same singular points as residue curves and (2) behave similarly to residue curves close to singular points. Nevertheless, distillation lines do not generally coincide with residue curves. Usually, the direction opposite to that of residue curves is used for the distillation lines. In this chapter (like in chapter 3), in order to avoid the confusion of referring to the same singular point as a stable node in residue curve diagrams and as an unstable

node in distillation line diagrams, we use the direction of residue curves for distillation lines, too.

A distillation region is defined as a subset of the composition space in which all curves originate from the same singular point (locally lowest-boiling pure component or azeotrope) and end at another singular point, which is the same for all curves, however (locally highest-boiling pure component or azeotrope). The curves which separate different distillation regions are called distillation region boundaries. The term distillation region boundary (or just boundary) is used for both residue curve or distillation line boundaries (interior boundaries) and the edges of the composition space. Chapter 3 provides a more detailed review of residue curves and distillation lines.

Unless stated otherwise, we use the following convention to refer to a given mixture: L (I, H respectively) corresponds to the component which has the lowest (intermediate, highest resp.) boiling point; we also denote the entrainer by E. We use the same notation in italics (L , I , H , E) to denote the corresponding flow rates of the components in the feed. The locations of the feed, distillate, bottoms, reflux and overhead vapor in the composition triangle are denoted by F, D, B, R and V respectively. Again, the corresponding flowrates are denoted by the same letters in italics (F , D , B , R and V).

Figure 4.1 illustrates the residue curve diagram of the ternary homogeneous mixture acetone (L) - heptane (H) - benzene (I-E). In chapter 2, we used this mixture as the illustrative example throughout most of the ∞/∞ analysis because it belongs to the simplest class of homogeneous mixtures that exhibit multiple steady states, i.e., the 001 class according to the classification by Matsuyama and Nishimura (1977). In this diagram, there is only one binary azeotrope between the light and the heavy component, the whole composition triangle is a single distillation region and there are no distillation region boundaries. Benzene is the entrainer that enables the separation of the acetone - heptane azeotrope (93% acetone and 7% heptane). We use this diagram for the illustration of the ∞/∞ analysis.

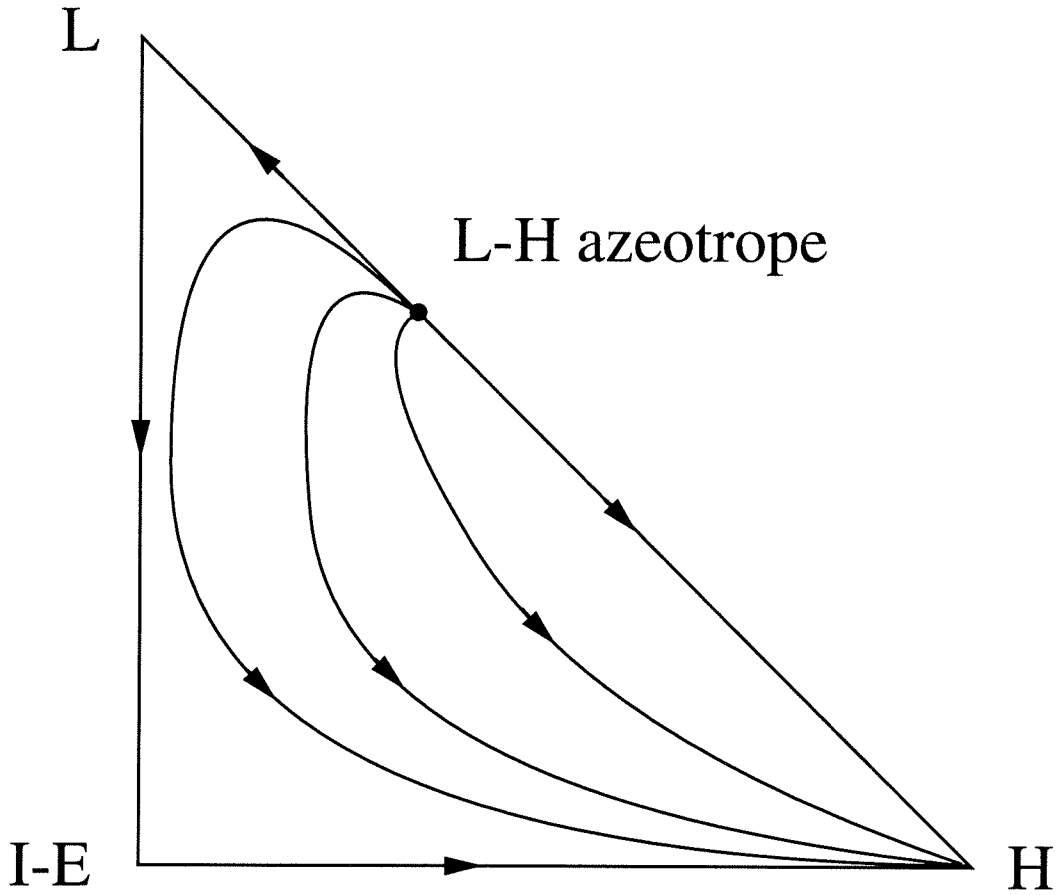


Figure 4.1: Illustration of the residue curve diagram of a ternary homogeneous mixture belonging to the 001 class, e.g., acetone (L) - heptane (H) - benzene (I-E).

4.3 ∞/∞ Analysis

In the ∞/∞ case, it is very easy to predict the column profiles with minimum computations. The ∞/∞ case analysis is performed in three steps. First we study how the column profiles look like in this limiting case of infinite reflux and an infinite number of trays. Then we determine the feasible product regions in the composition space. Finally, based on the above information, we construct a bifurcation diagram which reveals whether multiple steady states exist or not. The three basic steps of the ∞/∞ analysis presented in chapters 2 and 3 can be summarized in the following:

1. *Column profiles.* At infinite reflux, the composition profiles of packed columns coincide with some portion of residue curves (Laroche et al., 1992) while the profiles of tray columns coincide with distillation lines. Moreover, columns with an infinite number of stages (or infinitely long packed columns) should contain a pinch point. Pinch points at infinite reflux can only be the singular points of the residue curves (or distillation lines), i.e., the pure components and the azeotropes. Therefore, in the ∞/∞ case, column profiles follow residue curves (packed columns) or distillation lines (tray columns) and contain at least one singular point (pure component or azeotrope).

Hence, the only acceptable column profiles in the ∞/∞ case belong to one of the following three types: I. Columns whose top liquid composition is that of an unstable node; II. Columns whose bottom liquid composition is that of a stable node; III. Columns whose liquid composition profiles run along the boundaries (edges of the triangle and/or interior boundaries) and contain at least one saddle singular point.

2. *Feasible product regions.* In order to locate the feasible product regions, some more information is required (in addition to the ∞/∞ case profile characteristics): the equipment at the top and the bottom of the column, i.e., the type of reboiler and condenser (partial or total); whether a decanter is used or not (for heterogeneous mixtures); the product phase. Furthermore, the feed composition should be provided and finally it is obviously required that the material balances are satisfied.

Using the above information the feasible product regions can be located. Figure 4.2 shows the feasible distillate and bottoms lines for the mixture acetone - hep-

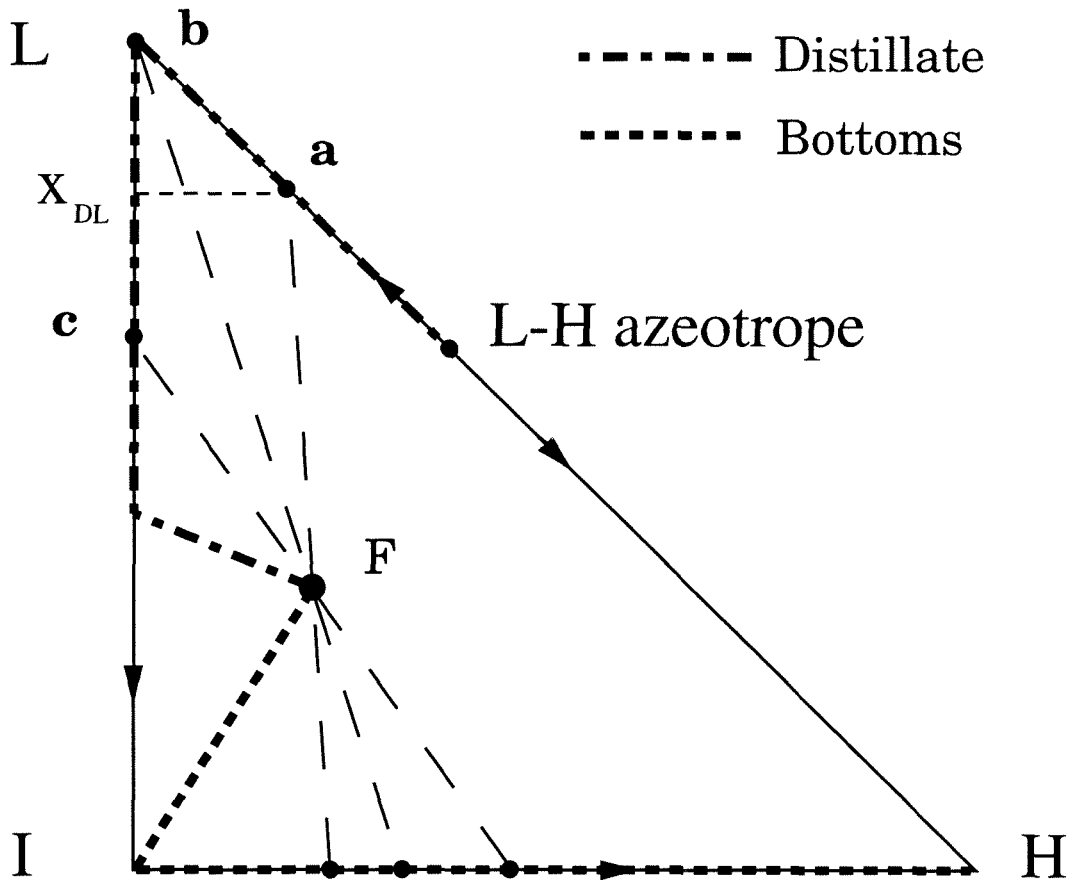


Figure 4.2: The feasible distillate and bottoms lines for the mixture acetone (L) - heptane (H) - benzene (I) and some feed F .

tane - benzene and some feed F . Note that, in the ∞/∞ case, given a feed composition and a feed flowrate F (and a distillate policy for columns with decanter, see chapter 3), the only unspecified column parameter is one product flow, e.g., the distillate flow rate D .

3. *Bifurcation diagram.* A bifurcation diagram with a product flowrate as the bifurcation parameter can be constructed by performing a continuation of solutions along the feasible product lines (continuation path). The existence of multiplicities (i.e. different column profiles corresponding to the same value of product flowrate) can be determined by examining the product flowrate along the continuation path using the lever rule. Multiple steady states exist when the product flow varies non-monotonically along the continuation path.

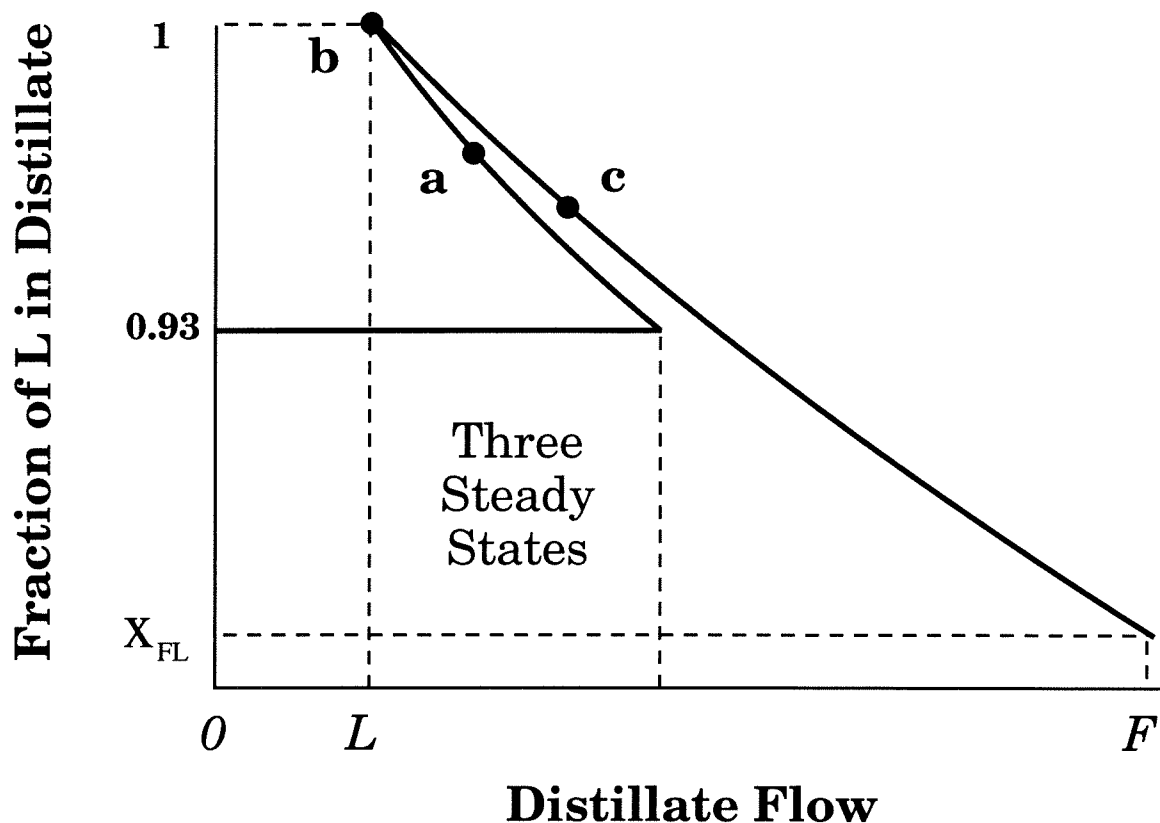


Figure 4.3: Bifurcation diagram showing the light component mole fraction in the distillate x_{DL} as a function of the distillate flow.

For example, in Figure 4.2, the distillate flowrate D associated with any feasible distillate D can be easily calculated using the lever rule for material balances. For any feasible distillate D , it is also very simple to calculate the light component mole fraction in the distillate x_{DL} . By repeating this procedure for all feasible distillate compositions, a diagram showing x_{DL} as a function of the distillate flowrate can be constructed. In other words, by tracking the distillate D along the feasible distillate line, we construct a bifurcation diagram with the distillate flow as the bifurcation parameter. The bifurcation diagram is illustrated in Figure 4.3.

There are two turning points in this diagram and three steady states exist for a range of the distillate flow. The key feature for the existence of the ∞/∞ multiplicity is that the distillate flow varies non-monotonically as we track the path of the feasible distillate compositions. We demonstrate this point by studying what happens as the

distillate D moves around the light component corner from point a to b and then c (Figure 4.2). It does not require more than just looking at Figure 4.3 and applying the lever rule for material balances to show that the distillate flowrate at points a and c is larger than the one at point b . Therefore, moving from a to b the distillate flowrate decreases and then from b to c it increases.

4.3.1 Geometrical multiplicity condition

From the above, it is clear that in order to derive rules for the existence of multiple steady states, one has to identify when the product flows vary non-monotonically along the continuation path. In chapters 2 and 3 we developed the *geometrical, necessary and sufficient, multiplicity condition* which answers the following question: Given any ternary mixture, its VL(L)E diagram and a column design (tray or packed column, condenser and reboiler types, decanter etc.), find whether multiple steady states exist for some feed composition in the ∞/∞ case. Furthermore, the *appropriate feed region condition* was developed; using this condition, the feed composition region that leads to these multiple steady states can be located.

Based on the above analysis and the developed conditions, we can predict *exactly* when multiple steady states occur in the ∞/∞ limiting case. The geometrical multiplicity condition enables the prediction of multiplicities from the structural properties of the VL(L)E diagram; and what is meant by structural properties is *not* necessarily the detailed VL(L)E diagram, but, in most cases, the character and location of singular points, the location of boundaries and the location of the two-liquid phase region for heterogeneous mixtures. It is clear that the existence of multiplicities for any mixture depends on the structural properties of its VL(L)E diagram (physical explanation).

The reader is referred to chapters 2 and 3 for more details on the ∞/∞ analysis, and in particular for the geometrical multiplicity condition and the appropriate feed region condition which are not described in this chapter.

In summary, in chapter 2 we study the existence of multiple steady states in

ternary *homogeneous* azeotropic distillation. The emphasis is on the basic development of the steps of the ∞/∞ analysis, the derivation of the multiplicity conditions and the implications of the ∞/∞ case multiplicities for columns at finite reflux and with a finite number of trays (finite case). In chapter 2 we show that the ∞/∞ multiplicities carry over to the finite case and moreover that they may exist at realistic operating conditions, that is, for small reflux and a small number of trays. Note that the geometrical condition is only a sufficient condition for the existence of multiplicities when the reflux and the number of trays are finite, i.e., multiplicities will exist for some sufficiently large finite reflux and finite number of trays but there may be mixtures that exhibit multiple steady states in finite columns, but not in columns operating at the ∞/∞ conditions.

In chapter 3 we extend the homogeneous mixture results to ternary heterogeneous mixtures but more importantly we study the ∞/∞ case in much more depth and detail by demonstrating how the ∞/∞ analysis can be applied for different column designs. More specifically, we discuss the differences between packed and tray columns, residue curve and distillation line diagrams, columns with and without decanter, columns with partial and total condenser etc. In chapter 3 we present the fully detailed, accurate and totally general geometrical multiplicity condition. Simulation results for finite columns show that the predictions carry over to the finite case.

4.3.2 ∞/∞ predictions

In summary, we list all the information that can be obtained from the analysis of the ∞/∞ case, i.e., the ∞/∞ predictions.

- 1. Existence of multiplicities:** For any ternary (homogeneous or heterogeneous) mixture and column design, we can predict whether multiplicities exist for some feed composition and some product flowrate, using the geometrical, necessary and sufficient, multiplicity condition.

- 2. Feed composition region that leads to multiplicities:** For any ternary mixture and column design, we can locate the feed compositions region that leads to

multiplicities, for some product flowrate, using the appropriate feed region condition.

3. Feasible product regions: For any ternary mixture, column design and feed composition, we can locate the feasible product regions in the composition space.

4. Bifurcation diagram construction: For any ternary mixture, column design and feed composition, we can construct a bifurcation diagram with a product flowrate as the bifurcation parameter by performing a continuation of solutions along the feasible product lines.

5. Location of turning (limit) points: For any ternary mixture, column design and feed composition, we can identify the characteristics of the VL(L)E diagram, i.e., locate the points in the composition space, responsible for the turning (limit) points of the constructed bifurcation diagram. Note that in some cases, these points in the composition space are independent of the feed composition.

6. Product flowrate multiplicity range: For any ternary mixture, column design and feed composition, we can predict the product flowrate range where multiple steady states exist. This is a direct consequence of the prediction of the location of turning points; the product flowrate multiplicity range, however, always depends on the feed composition.

7. Column composition profile: For any ternary mixture, column design, feed composition and (distillate or bottoms) product to feed ratio, we can locate the column composition profile in the composition space. Therefore, the composition profiles of multiple steady states can be predicted.

The ∞/∞ case is the limiting case of high reflux and a large number of trays. Therefore, if the geometrical condition is satisfied for a given mixture then multiplicities will exist for columns with some sufficiently large finite reflux and finite number of trays. The operating conditions where the multiplicities vanish cannot be predicted. Note that in finite columns multiplicities may be affected by column parameters, such as, the feed location and the enthalpy balances, which do not play any role in the ∞/∞ case. Nevertheless, the simulation results in chapters 2 and 3 show that the ∞/∞ multiplicities do exist for columns at realistic operating conditions. Obviously, in finite columns, some deviations from the ∞/∞ predictions are expected; the

smaller the reflux and the column length, the larger the deviations from the ∞/∞ predictions.

4.4 Implications for Design, Synthesis and Simulation

The implications of the existence of multiple steady states for distillation design, synthesis and simulation are presented in the following. We discuss the problems multiplicities may cause, how multiplicities may affect design decisions and in what ways the ∞/∞ predictions may be helpful.

Multiplicities may cause problems in column operation and control. When two or more steady states exist for the same inputs it is possible that for some disturbance, the column profile jumps (or shifts) from the desirable - in terms of product purity - steady state to another undesirable steady state, e.g., a steady state with low product purity.

In chapter 2 we present an example how this may happen for some feed disturbance for a column separating the mixture acetone - heptane - benzene (*cf.* Figure 27). By changing the feed composition from 90% acetone to 91% acetone, holding this new feed composition for a period of time and then changing it back to its original value, the column profile jumps from the high purity (99% acetone) to the low purity (93% acetone) steady state. Note, however, that this is just a single example and it should not be used to derive any general conclusions.

Some other evidence of the operational problems that multiple steady states can cause is given by Kovach and Seider (1987). They study an industrial azeotropic distillation tower that performs the dehydration of sec-butanol. They conduct simulations as well as experiments. Their conclusion is that the experimentally observed erratic behavior of this industrial tower is caused by the existence of multiple steady states.

The existence of multiple steady states raises new questions and problems for

distillation control and operation. For example: When is the control of a column operating in the presence of other steady states difficult?; What are the areas of attraction of the stable steady states?; What is the appropriate start-up strategy that would drive the column to the desired steady state?; How difficult is it to stabilize the unstable steady state? etc. These topics are not investigated in this chapter.

It is clear that multiplicities may cause some serious problems to column operation and control (erratic behavior, instabilities, start-up problems). Because of the control-design interactions, one has to take into account the effect of design on control at the level of synthesizing and designing the separation sequence. The reason is that alternative designs may have different control properties. One design alternative may be much more difficult to control than another. Since we know that multiple steady states can cause control problems, it is apparent that the existence of multiplicities in distillation has implications for distillation design and synthesis. These issues as well as the implications of multiplicities for simulation are presented in the following.

4.4.1 Entrainer selection

The problem of entrainer selection can be formulated as follows: given an azeotrope that we want to separate into its constituents, choose the entrainer that makes the separation feasible and economical. The first step of entrainer selection is usually the entrainer screening. At this step, the less promising candidate entrainers are discarded and the most promising ones are kept for further evaluation. The entrainer screening is essentially a test that determines whether a candidate has or does not have a certain set of properties. It separates the candidates set into two (or more) pools with desirable or undesirable properties.

Lets assume that we want to choose the entrainer that enables the separation of a given azeotrope and that, in addition, we want to avoid multiplicities (because of the potential control problems).

Mixture classes with multiplicities: It would be nice if we could exclude the candidate entrainers that produce VL(L)E diagrams that will always have multiplic-

ities. Using the ∞/∞ analysis, we are able to identify entire mixture classes for which the multiplicities are *inherent*. (“Inherent,” in the sense that multiple steady states exist for any mixture belonging to such classes.) It is apparent that for these classes the multiple steady states are *robust*, i.e., the multiplicities do not vanish if the VL(L)E model and/or the VL(L)E model parameters are changed, as long as the resulting VL(L)E diagram still belongs to the same class.

The 001, 002-m, 003 and 004-M are such classes (Figure 4.4). In addition, we can predict that for mixtures belonging to these classes, multiplicities exist *for any feed composition*. More specifically, three steady states exist for any feed composition and for any mixture belonging to the 001 and 003 classes; three and possibly five (for some feed compositions) steady states exist for mixtures belonging to the 002-m and 004-M classes. Using a databank with information on the azeotropic (or zeotropic) behavior of binary mixtures, we found 3700 ternary mixtures belonging to the 001 or 002-m classes and 340 ternary mixtures belonging to the 003 or 004-M classes. These classes will always exhibit multiplicities and hence all candidate entrainers that produce such VLE diagrams can be excluded from the entrainer selection search.

Mixture classes without multiplicities: It would be nice to retain all the candidate entrainers that produce VL(L)E diagrams for which multiplicities will never exist. Using the ∞/∞ analysis, we can identify entire mixture classes for which multiplicities can be *generically* excluded, i.e., there will be no multiple steady states for any mixture belonging to such class, for any feed composition, for any VL(L)E model and parameters (as long as the resulting VL(L)E diagram still belongs to the same class).

For example, the 100 and 020 (heavy and light entrainers, resp., introducing no additional azeotropes) are such classes. Figure 4.5 illustrates a heterogeneous VL(L)E diagram with the aforementioned multiplicity properties. The mixture acetic acid (H) - water (I) - propyl formate (L) belongs to this class. Therefore, for these mixture classes, multiplicities are not an issue to worry about; the candidate entrainers that produce such VL(L)E diagrams can be kept for further evaluation.

Mixture classes with multiplicities in some feed region: Finally, there

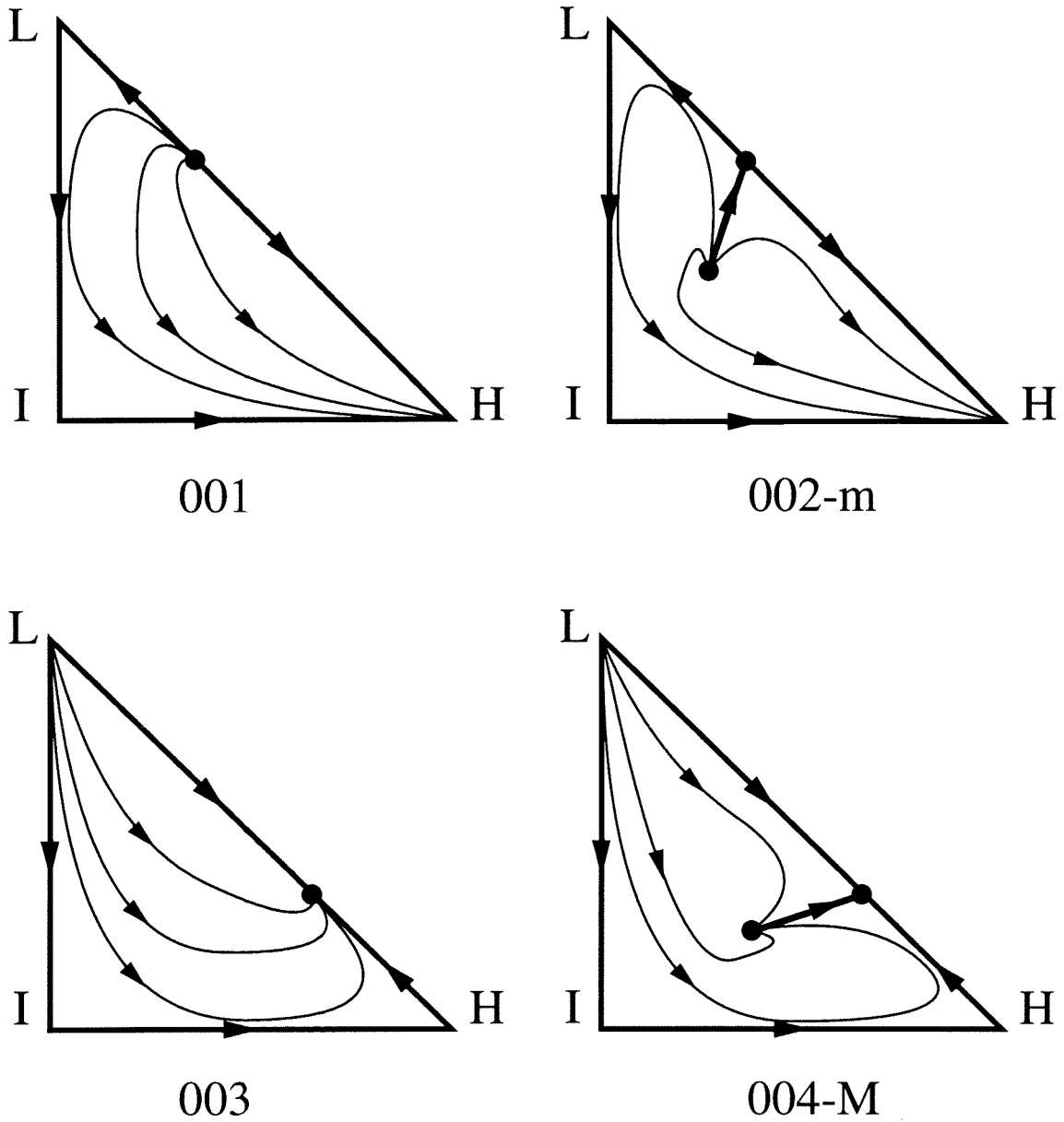


Figure 4.4: Residue curve diagrams of four mixture classes with inherent multiplicities.

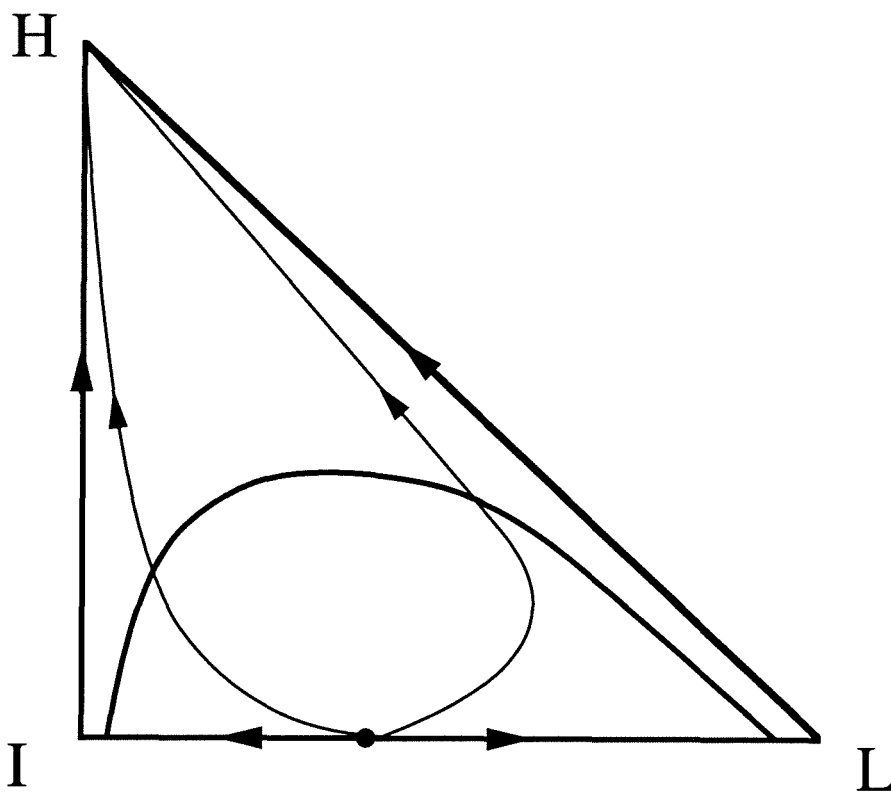


Figure 4.5: A heterogeneous VL(L)E diagram class without multiplicities.

are all the other classes where multiplicities sometimes exist, depending on the feed composition. It would be nice if we could locate the region of feed compositions for which a unique steady state exists and select (if possible) a feed composition in this region. Obviously, the ∞/∞ analysis can be very useful since one of the ∞/∞ predictions is that of the feed composition region that leads to multiplicities.

For example, Figure 4.6 illustrates the VL(L)E diagram of the heterogeneous mixture benzene (I) - heptane (H) - methanol (L). The only information needed to locate the feed region for which multiplicities occur is the distillation region boundaries and the two-liquid phase region. The shaded regions in Figure 4.6 depict the feed regions for which multiple steady states occur; Figure 4.6a for a column without decanter, Figure 4.6b for a column with decanter (and distillate consisting of a portion of the heptane-rich phase). Figure 4.7 illustrates similar results for the mixture acetone (L) - chloroform (I) - water (H).

Using the ∞/∞ analysis we can locate the feed composition region where no multiple steady states exist and immediately predict if multiple steady states exist for any given feed. It is important to note that we can obtain all this information with a minimum of numerical computations since the method is graphical. Because of that, we do not need to use any specific thermodynamic model for the VL(L)E description; instead, we can even use experimental data, if available. Note that the graphical VL(L)E data shown in Figures 4.6 and 4.7, i.e., the boundaries and the two-liquid phase regions, are illustrations of the computed VL(L)E diagrams shown in Pham and Doherty (1990a).

Obviously, in finite columns, some deviations from the ∞/∞ predictions are expected. For small enough reflux and column length, multiplicities vanish and so does the feed region for which multiple steady states occur. This, however, does not necessarily mean that the feed region “shrinks” as the operating conditions move away from the ∞/∞ case; there may be feed compositions in the neighborhood of, but outside the ∞/∞ appropriate feed region, for which multiplicities exist at some finite conditions while a unique steady state exists in the ∞/∞ case. Is this some different type of multiplicity, irrelevant to the ∞/∞ multiplicity? The proximity of

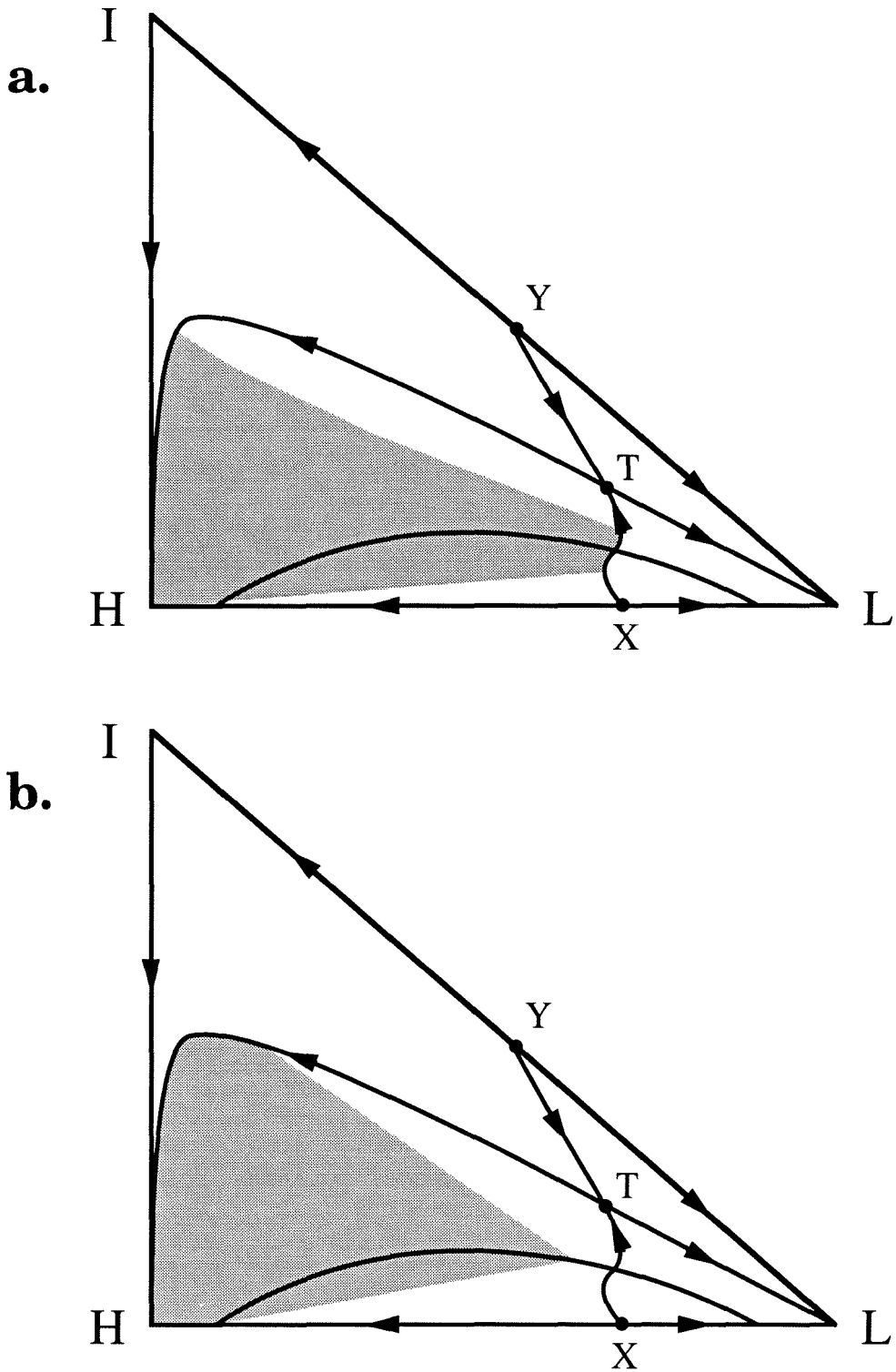


Figure 4.6: The VL(L)E diagram of the heterogeneous mixture benzene (I) - heptane (H) - methanol (L). The shaded regions depict the feed regions for which multiple steady states exist for a column a. without decanter b. with decanter

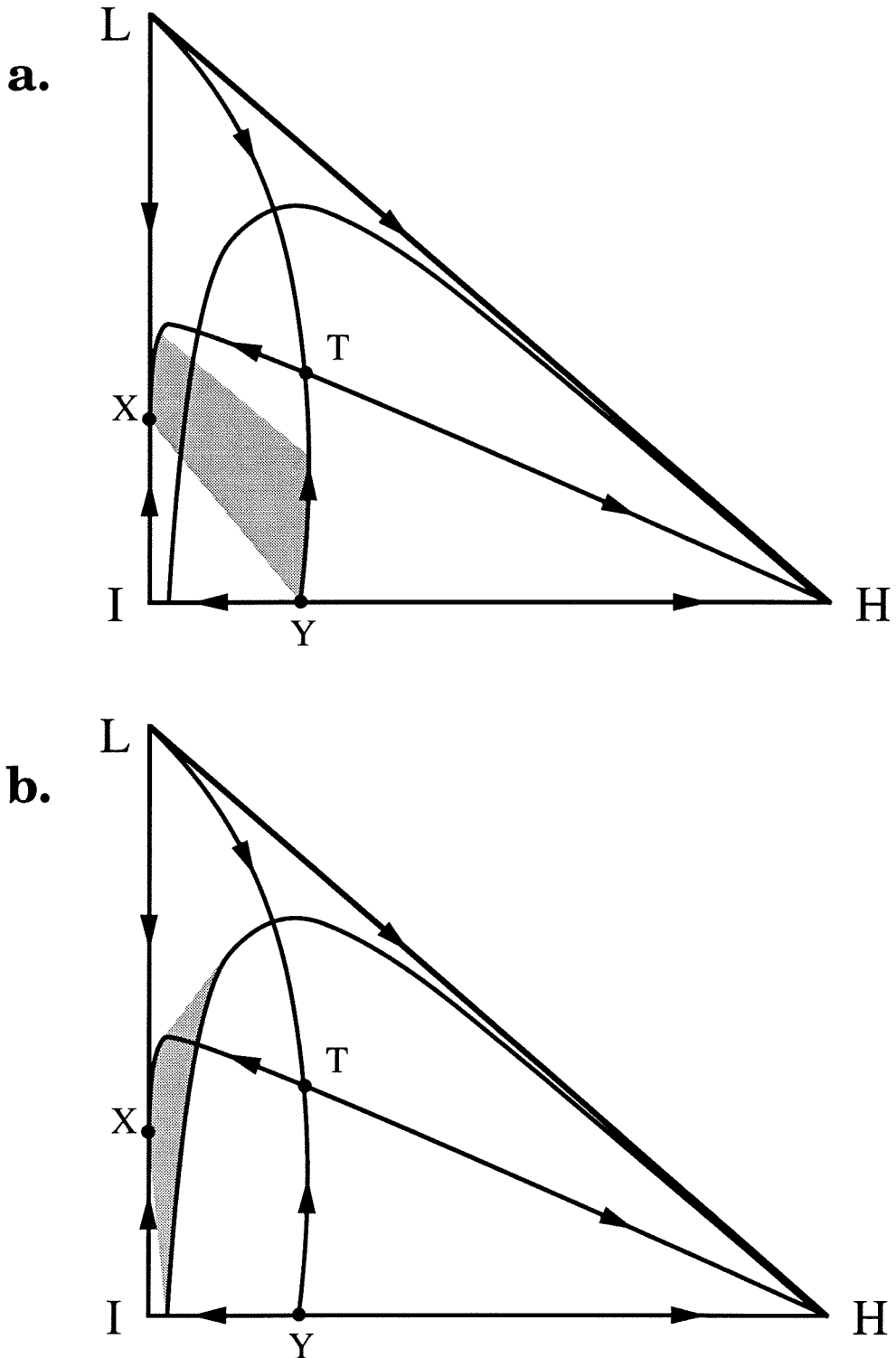


Figure 4.7: The VL(L)E diagram of the heterogeneous mixture acetone (L) - chloroform (I) - water (H). The shaded regions depict the feed regions for which multiple steady states exist for a column a. without decanter b. with decanter.

such feed compositions to the ∞/∞ appropriate feed region clearly indicates that this phenomenon happens because of the expected discrepancies between the finite and the ∞/∞ case (a boundary crossing, for example) and therefore it should not be interpreted as some different type of multiplicity.

4.4.2 Column design and separation scheme selection

The separation scheme selection is another step in any separation synthesis and design procedure. Although the separation scheme selection may involve some column design decisions, the selection of the complete and detailed column design is usually a later step in the separation sequence design. Here we assume that we want to choose the separation scheme and column design for a given separation and that, in addition, we want to avoid multiplicities.

In chapter 3 we discussed in detail the effect of different column designs (tray or packed columns, different types of condenser and reboiler, columns with or without decanter) on the existence of multiplicities. Therefore, for a given separation scheme, multiplicities may or may not exist depending on the selected column design. Moreover, since different separation schemes may require different column designs, it is apparent that multiplicities may exist for one separation scheme alternative while they do not exist for another.

Column design selection: We demonstrate the effect of the column design on multiplicities using the mixture ethanol (L) - water (H) - benzene (I-E) which was extensively studied in chapter 3. Figure 4.8a illustrates the mixture's residue curve diagram and Figure 4.8b its distillation line diagram. The two-liquid phase region is shown in both figures. The two diagrams are very similar with the exception of a small difference in one distillation boundary, TX, close to the ternary azeotrope T.

Using the ∞/∞ analysis we can immediately predict if multiplicities exist for packed or tray columns, with or without decanter for any feed composition F. For the feed F shown in Figure 4.8, we conclude the following (see chapter 3, for more details):

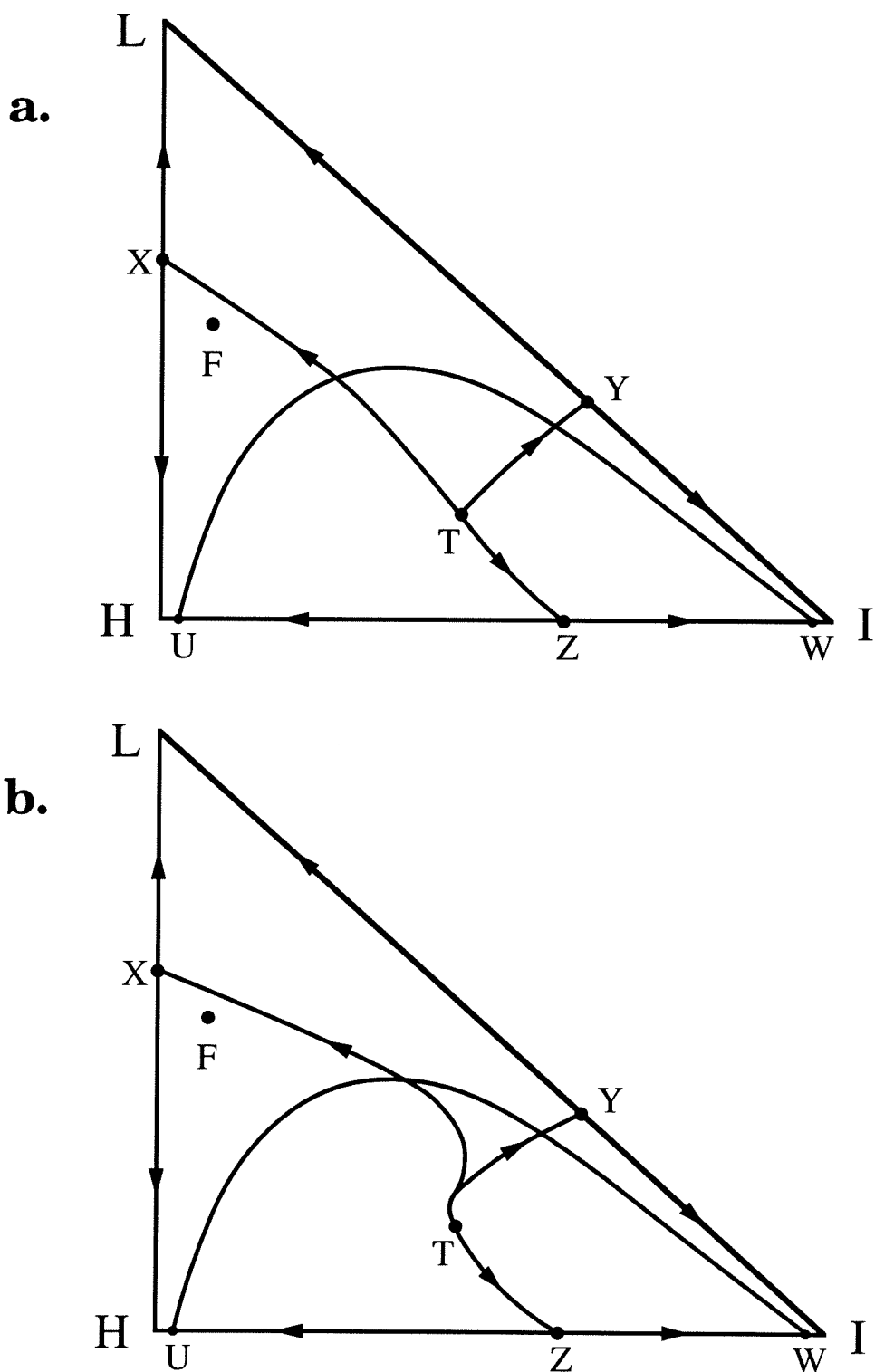


Figure 4.8: The residue curve (a) and distillation line (b) diagrams of the heterogeneous mixture ethanol (L) - water (H) - benzene (I-E).

For packed columns without decanter (Figure 4.8a), a unique steady state exists while for tray columns without decanter (Figure 4.8b) multiplicities do exist. On the other hand, for columns with decanter, using trays or packing does not make a difference; in both cases multiple steady states exist. The reason is that for columns with decanter, the different distillation boundaries do not affect the distillate product composition which will lie on the two-liquid phase region envelope for both tray and packed columns.

Therefore, for a column without decanter, we can avoid multiplicities by selecting a packed column instead of a tray column. For a column with decanter, we cannot avoid the multiple steady states.

Separation scheme selection: It is apparent that the effect of column design on multiplicities will have implications regarding the existence of multiplicities for different separation schemes. We demonstrate this using the mixture ethanol (I) - water (H) - ethyl ether (L-E). We want to separate the azeotrope between ethanol and water using ethyl ether as the entrainer. There are two alternative schemes that achieve this separation. Figure 4.9 illustrates the mixture's VLLE diagram, the two alternative flowsheets and the material balances of the two schemes in the composition triangle. Suppose that we want to choose one of the two and that we want to avoid multiple steady states.

In the first scheme, two columns are used. The first one is a column with decanter; the second one without decanter. The separation scheme works similarly as the one used for the separation of the ethanol - water azeotrope using benzene as the entrainer (Pham and Doherty, 1990b). The overall feed ($F+R$) of the first column is separated in pure ethanol at the bottoms and F_2 at the top. Note that F_2 is a portion of the water-rich phase in the decanter and that the first column reflux consists of a mixture of the entrainer-rich and the water-rich phase. The second column separates F_2 into pure water at the bottoms and R which is recycled.

The second scheme involves one column without decanter that separates the overall feed ($F+E$) into pure ethanol at the bottoms and the heterogeneous azeotrope between water and ethyl ether (H/E) at the top. The top product is fed to a de-

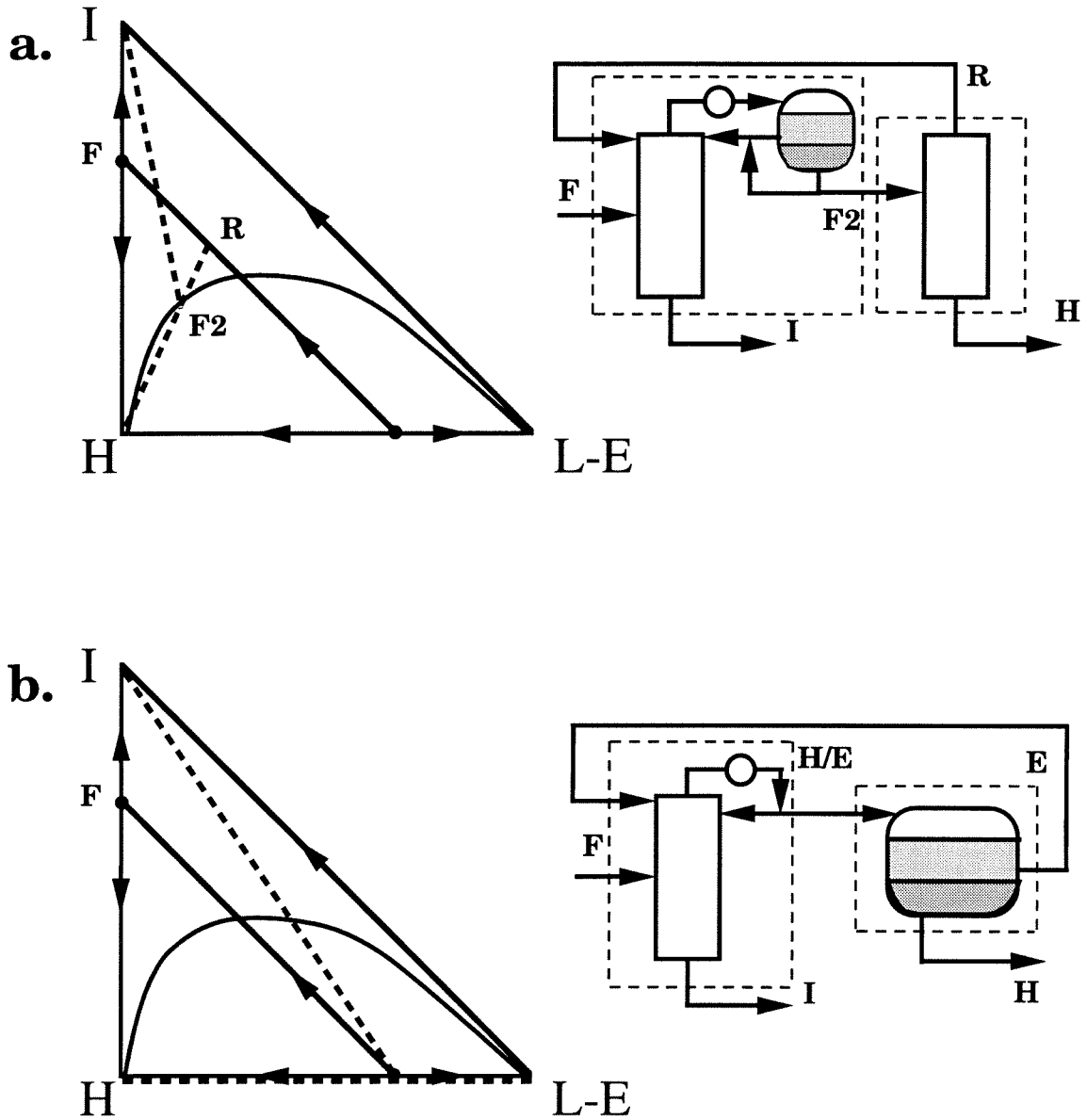


Figure 4.9: Two separation schemes for the separation of the ethanol (I) - water (H) azeotrope using ethyl ether (L-E) as the entrainer.

canter and it is separated into water and entrainer which is recycled. Note that such a scheme is not feasible in the case of the ethanol - water - benzene mixture because of the ternary azeotrope which restricts the column distillate product away from the water - entrainer binary edge.

Using the ∞/∞ analysis, we can predict that a unique steady state exists for the column of the second scheme and the second column of the first scheme. For the first column of the first scheme, however, there exists another steady state at the same operating conditions. Figure 4.10 shows the two steady state profiles (for an overall feed F' slightly off the distillation region boundary for illustrative purposes). The second steady state is homogeneous and the bottoms product is far from being the desired pure ethanol. Note that these are single column multiple steady states and have nothing to do with column interlinking. Although the homogeneous steady state does not satisfy the material balances for the first scheme, it may very well affect the column operation and control.

Therefore, since we want to avoid multiple steady states, the ∞/∞ analysis suggests that we can immediately rule out the first scheme.

4.4.3 Critical VL(L)E data - Design of experiments

It was shown above that, using the ∞/∞ analysis, we are able to identify entire mixture classes for which the multiplicities are inherent and other classes for which multiplicities can be generically excluded. For these classes the existence (or nonexistence) of multiple steady states is robust, i.e., multiplicities do not vanish (or appear resp.) if the VL(L)E model and/or the VL(L)E model parameters are changed, as long as the resulting VL(L)E diagram still belongs to the same class.

There exist, however, mixture classes for which the existence of multiplicities depends critically on some key feature of the VL(L)E. Using the ∞/∞ analysis, we can identify these key features.

The 222-m class: Figure 4.11 illustrates three residue curve (or distillation line) diagrams of mixtures belonging to the 222-m class. There are three binary azeotropes

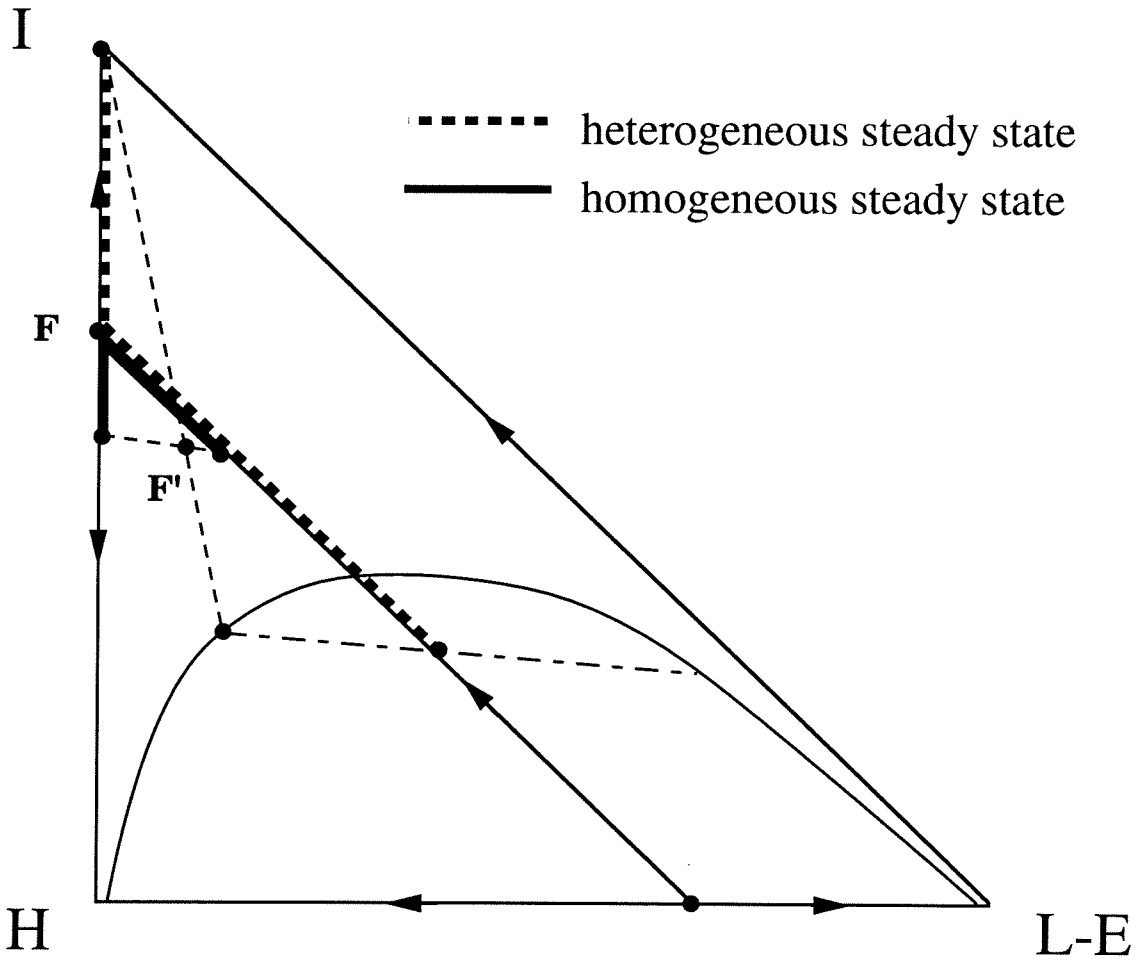


Figure 4.10: The two steady state profiles of the first column of scheme a .

(X,Y,Z), one ternary azeotrope T and three interior boundaries (TX, TY, TZ). In chapter 3 we have shown that the geometrical multiplicity condition for mixtures belonging to the 222-m class can be simplified to the following: For the existence of multiple steady states it is required that (1) some line parallel to the LH edge intersects the interior boundary TX more than once, or (2) some line parallel to LI intersects TY more than once, or (3) some line parallel to IH intersects TZ more than once.

Using the ∞/∞ analysis, it can be shown that the orientation of the boundaries near T is critical for the existence of multiplicities. More specifically, close to T, the boundaries are tangent to the principal eigendirection, the direction of the eigenvector associated with the smallest absolute eigenvalue of the linearized residue curve differential equation at point T. Depending on the orientation of the principal eigendirection at the ternary azeotrope and on the side from which each boundary approaches the ternary azeotrope, the geometrical condition may or may not be satisfied.

Figure 4.11a shows a 222-m class diagram for which a unique steady state exists. Figure 4.11b shows another diagram with a different principal eigendirection at T. In this case, multiple steady states exist for feed compositions in the shaded region. Figure 4.11c is similar to Figure 4.11a with the only exception that the boundary TY approaches T from the other side of the principal eigendirection. Contrary to Figure 4.11a, multiple steady states do exist for feed compositions in the shaded region of Figure 4.11c. Figure 4.11d shows six sections of the composition space separated by the lines parallel to LI, LH and IH that go through T. Each section is marked with one or two boundary names. Given a 222-m class mixture, multiplicities exist, if some part of a boundary lies in a section marked with the boundary's name.

Note that, although both residue curve and distillation line boundaries are tangent at T, the distillation line boundaries exhibit a higher curvature than residue curve boundaries. Using the residue curve diagram (instead of the distillation line diagram) for the study of multiplicities of tray columns for mixtures belonging to the 222-m class, may, in some cases, result in the wrong conclusion. Finally, note that, since curved boundaries can be crossed in the finite case, it is possible that, for some 222-m

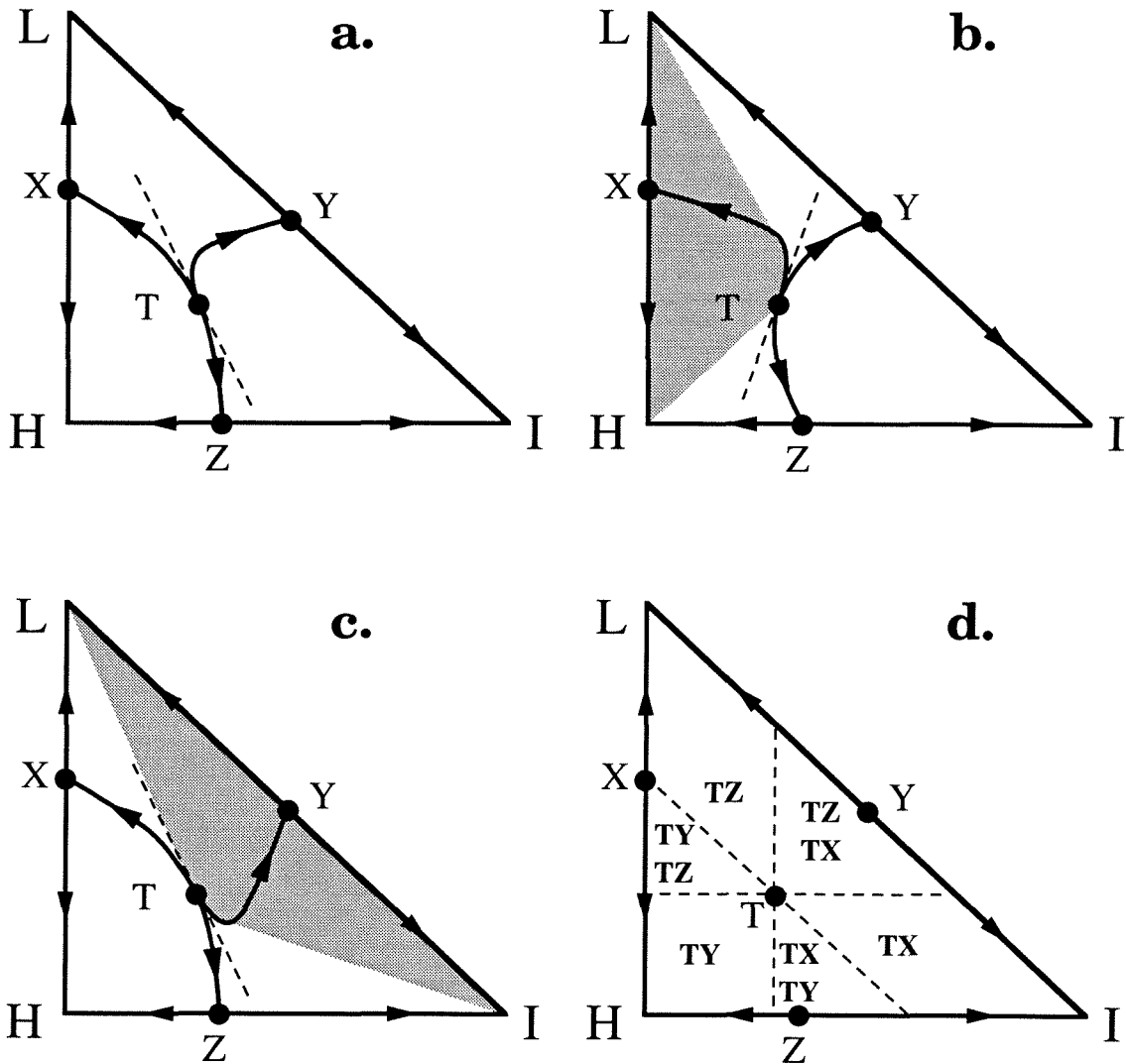


Figure 4.11: Three residue curve (or distillation line) diagrams of mixtures belonging to the 222-m class (a,b,c) and a graphical illustration of the simplified multiplicity condition for 222-m class mixtures (d). a. Unique steady state b. and c. Multiple steady states for feed compositions in the shaded regions.

mixtures, multiplicities exist for finite columns while they do not exist in the ∞/∞ case. We believe that this may explain the output multiplicities Kienle et al. (1993) have reported for several mixtures belonging to the 222-m class.

The ethanol - water - benzene mixture class: In chapter 3 we have shown that for columns without decanter, the heterogeneous mixture ethanol (L) - water (H) - benzene (I-E) can be treated as if it were a homogeneous mixture belonging to the 222-m class, i.e., the only information required is the residue curve and distillation line boundaries which are shown (together with the two-liquid phase region) in Figure 4.8. In chapter 3 we also show why the difference between the residue curve and distillation line boundaries can be much more profound for heterogeneous mixtures and how the VLLE, in particular the vapor line in the two-liquid phase region, can provide an indication when to expect qualitative differences between packed and tray columns.

In chapter 3 we find that for the mixture ethanol (L) - water (H) - benzene (I-E) and the specific thermodynamic model and parameters used, for packed columns without decanter a unique steady state exists while for tray columns without decanter multiplicities do exist. The key feature that leads to multiplicities for tray columns is the geometry of the vapor line and in particular the turn from the left to the right of the top end of the vapor line (ZQ) which is shown in Figure 4.12.

Suppose that using another VL(L)E model and/or parameters or using experimental data, the vapor line shown in Figure 4.13 is obtained. In fact, we obtained a VLLE diagram qualitatively similar to the one illustrated in Figure 4.13 for another mixture; the isopropanol (L) - water (H) - benzene (I-E) mixture. Figure 4.12 and Figure 4.13 are very similar with the exception of a small difference in the vapor line. In Figure 4.13 the vapor line runs continuously from the right (Z) to the left (Q). Using the ∞/∞ analysis we can predict that in this case, it is highly probable* that multiplicities do not exist for tray columns. This small change in the vapor line may make the difference between multiple steady states and a unique steady state.

*Since parts of the vapor line coincide with only parts of the distillation line boundaries we cannot be absolutely sure. The computation of the distillation line boundaries could provide an accurate prediction.

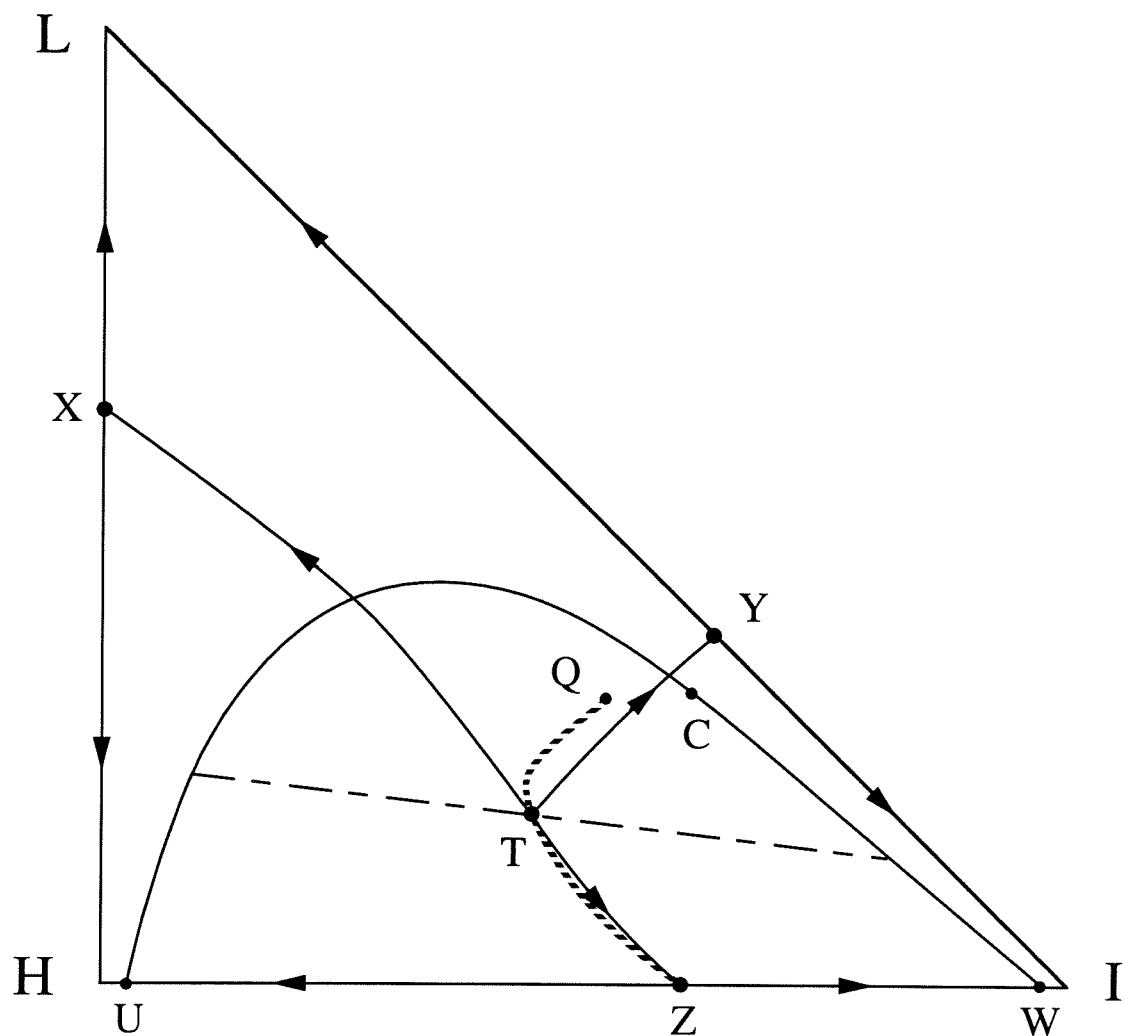


Figure 4.12: The residue curve diagram and the vapor line ZQ of the mixture ethanol (L) - water (H) - benzene (I-E).

Ambiguous azeotropes: So far, we discussed the VL(L)E ambiguity within the same mixture class, i.e., what may happen if some VL(L)E characteristic is different (1) between mixtures belonging to the same mixture class or (2) between different VL(L)E models/parameters for the same mixture provided that the resulting VL(L)E diagrams still belong to the same class. It is possible, however, that for some mixtures there exist some more fundamental ambiguity, namely ambiguity regarding the existence of azeotropes. Obviously, this means that the mixture may belong to different mixture classes depending on whether the ambiguous azeotrope exists or not. We study two cases here. We examine what may happen to the existence of multiplicities of a 001 class mixture (1) if a maximum boiling azeotrope between the light and the intermediate component is introduced and (2) if a minimum boiling azeotrope between the intermediate and the heavy component is introduced.

1. According to the experimental binary azeotropic data reported by Horsley (1973), the mixtures methanol (L) - benzene (H) - butyraldehyde (I) and methanol (L) - toluene (H) - butyraldehyde (I) belong to the 001 class. The Wilson binary parameters were estimated from the UNIFAC model using the Aspen Plus (1988) property parameter estimation option. Using these estimated Wilson binary parameters the residue curve diagrams of the two mixtures were calculated.

Figure 4.14 illustrates the qualitative characteristics of both diagrams; the calculated diagrams belong to the 401 class. Apparently, a spurious maximum boiling azeotrope (Y) between the light and the intermediate component is introduced by the VLE model and parameters. The location of this spurious azeotrope was found to be very close to the intermediate pure component corner.

Using the ∞/∞ analysis, we can predict that, independent of the locations of the azeotrope Y and the boundary YH, multiplicities do not vanish by the introduction of a maximum boiling azeotrope between the light and the intermediate component, for any 001 class mixture. For the mixtures mentioned above, the existence of multiple steady states using the estimated Wilson parameters for the VLE calculations has been verified via simulations. Note, however, that the region of feed compositions that lead to multiplicities is now restricted to the region above the YH boundary

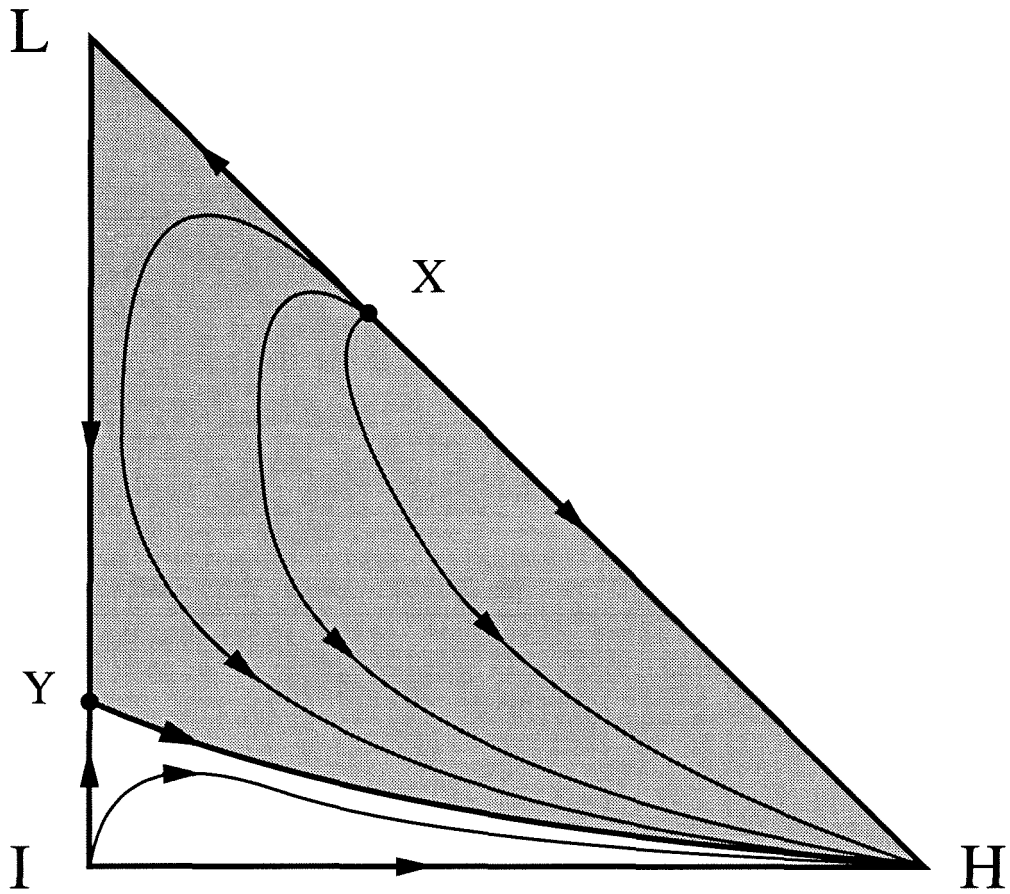


Figure 4.14: The residue curve diagram of a 401 class mixture. The shaded region depicts the feed compositions for which multiple steady states exist.

(shaded region in Figure 4.14) and that differences (with the 001 class predictions) in the column profiles are expected because of the boundary YH. Nevertheless, using the ∞/∞ analysis, we were able to predict, without any VLE diagram calculation, that an additional maximum boiling L-I azeotrope does not affect the existence of multiplicities for any 001 class mixture.

2. The experimental binary azeotropic data reported by Horsley (1973) for the mixture benzene - heptane is somewhat ambiguous. More specifically, there is a total of four references regarding the mixtures' azeotropic behavior at atmospheric pressure. Most (three) of them report that the mixture is zeotropic while one (the earliest reference) reports a minimum boiling azeotrope at 99.3% wt. benzene. We use the ∞/∞ analysis to study the consequences of the (potential) existence of such an azeotrope on the multiplicities predicted (and reported via simulations) for the mixture acetone (L) - heptane (H) - benzene (I).

Figure 4.15 shows two possible residue curve diagrams. The mixture now belongs to the 021 class. There are two binary azeotropes, X and Y, and a boundary, XY, connecting the two azeotropes. The main difference between Figure 4.15a and Figure 4.15b is the shape of the XY boundary. More specifically, in Figure 4.15a there is no straight line parallel to IH that intersects the boundary XY more than once. In Figure 4.15b, there exist such lines. For the diagram shown in Figure 4.15a, we predict that in the ∞/∞ case a unique steady state exists for any feed composition. For the diagram shown in Figure 4.15b, however, multiplicities exist for feed compositions in the shaded region. It is apparent that, in this case, the information of the existence of another azeotrope (Y) is not sufficient to draw conclusions and that the boundary has to be calculated.

In chapter 2, using several different thermodynamic models (Van Laar, Wilson) and parameter sets, we found no azeotrope between benzene and heptane. Using Aspen Plus (1988) and its physical properties option set SYSOP7, i.e., the UNIFAC liquid activity coefficient model and the Redlich-Kwong equation of state for vapor phase properties, we found that a minimum boiling azeotrope between benzene and heptane is predicted. Its molar composition is 98.82% benzene and 1.18% heptane.

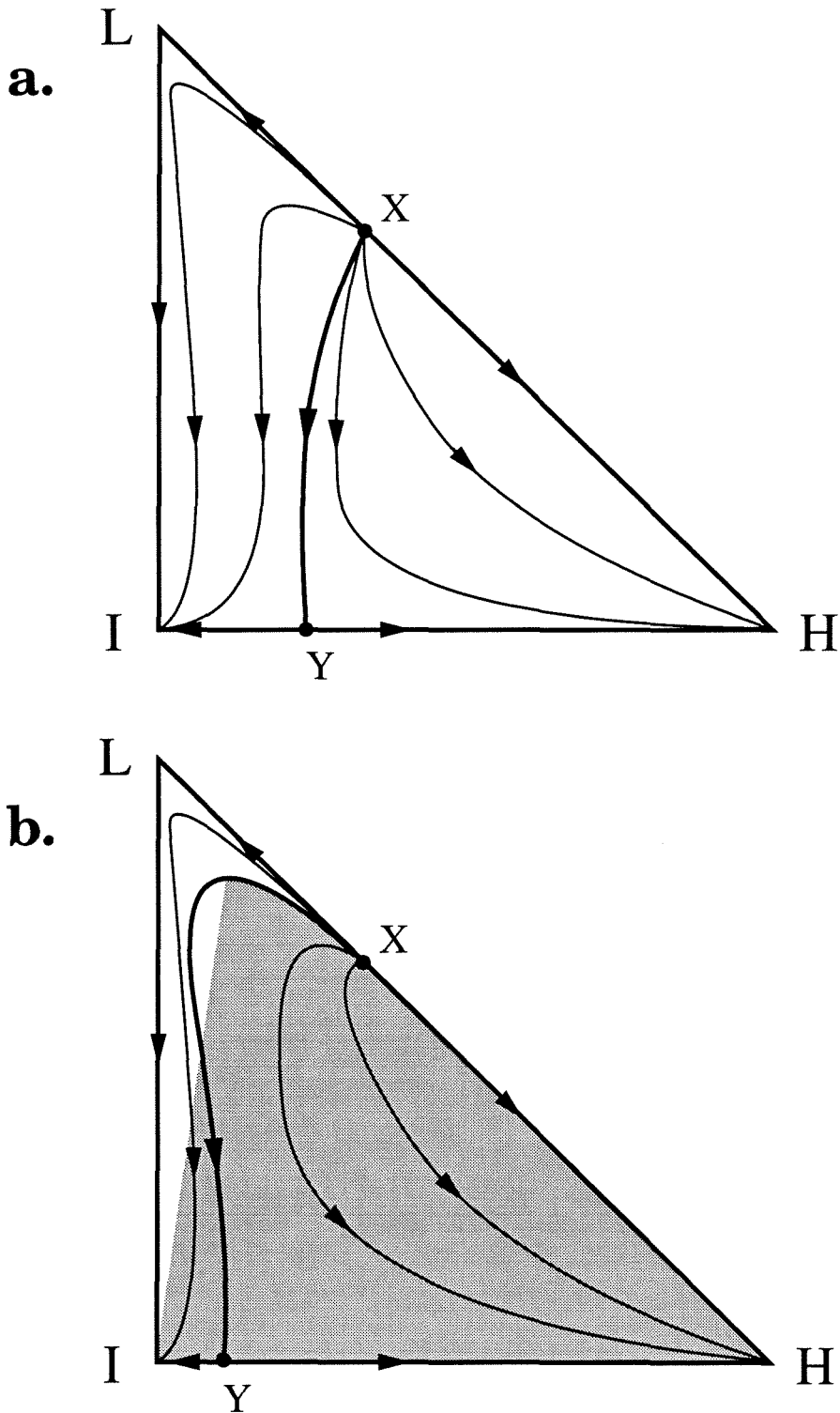


Figure 4.15: Two residue curve diagrams of mixtures belonging to the 021 class. a. Unique steady state b. Multiple steady states for feed compositions in the shaded region.

Figure 4.16 shows the location of both azeotropes and the distillation line boundary using the above physical properties set. Note how close to the triangle edges the boundary lies. It is clear that Figure 4.16 is similar to Figure 4.15b and that multiplicities exist using this physical properties set, too. Therefore, in this case, the introduction of the, potentially erroneous, minimum boiling benzene - heptane azeotrope does not affect the existence of multiple steady states (although, in principle, it could).

Design of experiments: The above examples show that apart from the mixture classes for which a unique steady state or multiple steady states are inherent and robust, there are other classes for which the existence of multiplicities is sensitive and depends critically on some key feature of the VL(L)E. Using the ∞/∞ analysis we can identify these key VL(L)E features, e.g., the eigendirection at the ternary azeotrope and the location of the vapor line.

Most importantly, however, in case there are doubts about the used VL(L)E data, using the ∞/∞ analysis one can predict if this ambiguity of the VL(L)E data may lead to erroneous conclusion about multiplicity. Note that since the method is graphical, experimental data may be used to resolve these issues. When experimental data are not available or they are insufficient, the ∞/∞ analysis gives indications on how to design the appropriate experiments to resolve whether multiplicities exist or not. For example, for the mixture ethanol (L) - water (H) - benzene (I-E), one would have to experimentally locate the part of the vapor line above the ternary azeotrope.

4.4.4 Operation

In this section, we discuss how multiple steady states may affect the operation of a column at a stable or unstable steady state from the design point of view.

Product set restrictions: Suppose that we wish to operate a column at a (open-loop) stable steady state. Apparently, when multiple steady states exist, parts of the feasible product sets correspond to unstable steady states. Therefore, for operation at a stable steady state, the feasible product set is restricted. Figure 4.17 illustrates

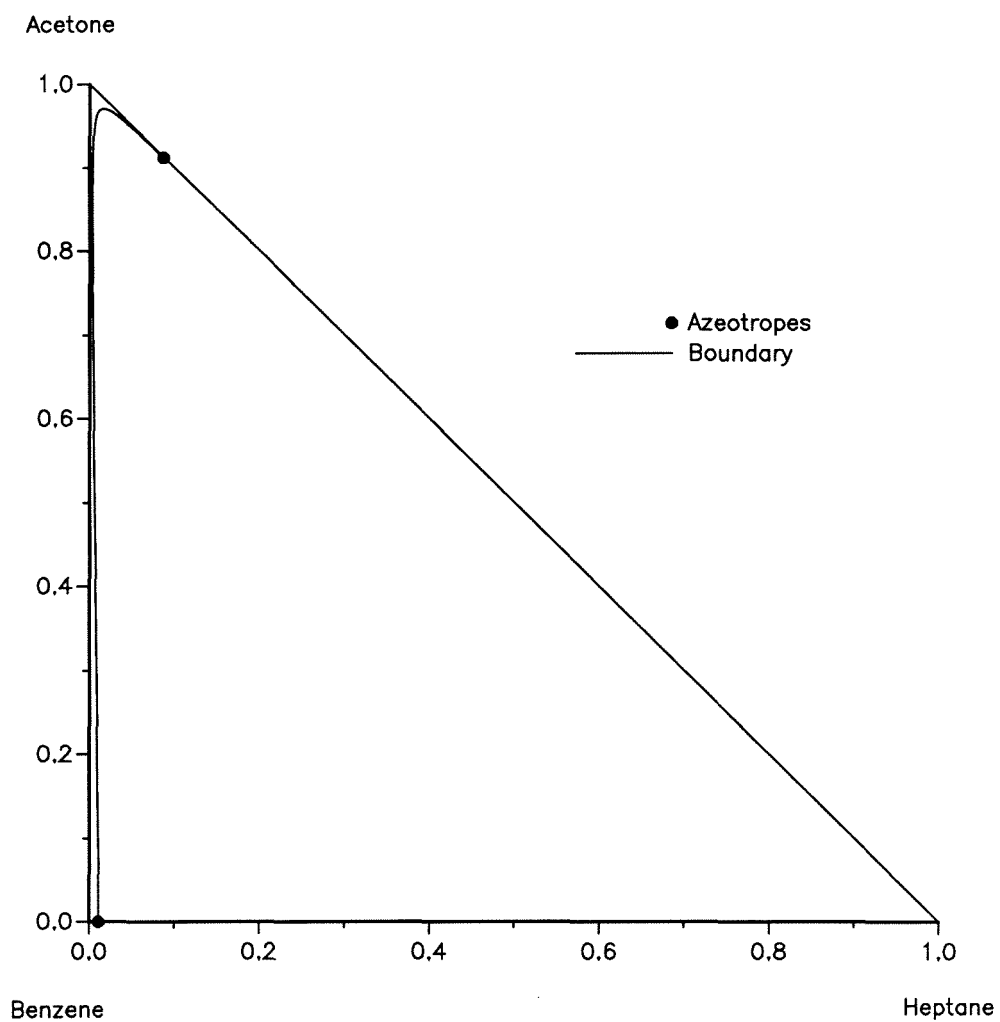


Figure 4.16: The location of the acetone (L) - heptane (H) and benzene (I) - heptane (H) azeotropes and the computed distillation line boundary using the Aspen Plus SYSOP7 physical properties set.

this for the mixture acetone (L) - heptane (H) - benzene (I-E). Figure 4.17 shows the feasible distillate and bottoms sets for a given feed F . It also shows the parts of the feasible product sets that correspond to unstable steady states. Suppose that the column has a specification of 99% acetone in the distillate. Figure 4.17 shows that, for operation at a stable steady state, benzene will be the 1% distillate impurity. In order to achieve 99% acetone and 1% heptane in the distillate or any other distillate composition lying on the acetone - heptane binary edge, between pure acetone and the azeotrope, stabilizing control action is required. It is therefore important to locate these qualitatively different product regions in the design parameter space.

Distance from instability: Suppose that again we want to operate at a stable steady state but we want to know how close to instability we are. Based on the ∞/∞ predictions, we can extract simple rules regarding the distance from instability.

For example, Figure 4.18 illustrates the VL(L)E diagram of the mixture ethanol (L) - water (H) - benzene (I-E). One of the ∞/∞ predictions is the location of turning (limit) points of the bifurcation diagram that can be constructed in the ∞/∞ case. For columns with decanter and distillate consisting of a portion of the water-rich phase and for the feed composition F shown in Figure 4.18, two turning points exist in the bifurcation diagram (chapter 3). Using the ∞/∞ analysis, these two limit points can be located along the distillate and bottoms continuation paths (feasible product lines); a total of four points (Figure 4.18), two along the feasible distillate line (points on the two-liquid phase region envelope) and the corresponding two points along the feasible bottoms line (points on the ethanol - water edge).

Note that, among the four points, the locations of the two depend on the feed composition while the locations of other two are independent of the feed F (Figure 4.18). The most interesting one is the point marked with an asterisk, which is located at the pure ethanol corner which is actually the desired product of this separation. The conclusion derived by the location of this limit point is that: the higher the ethanol purity at the bottoms, the closer is the column operation to instability.

Operation at unstable steady state: So far, we discussed the implications of multiplicities for the operation at a stable steady state. But we may not want to stay

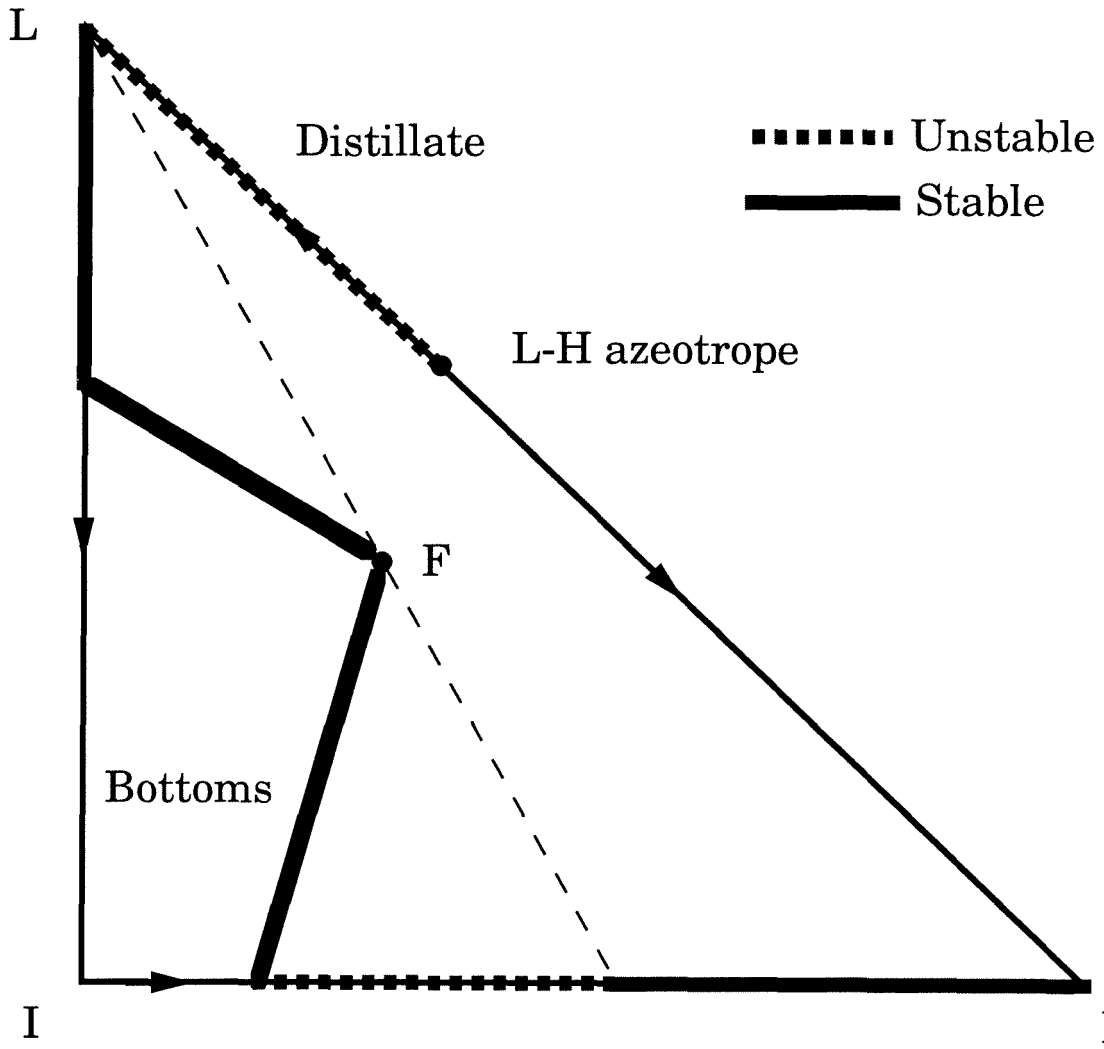


Figure 4.17: The feasible distillate and bottoms sets for a given feed F of the mixture acetone (L) - heptane (H) - benzene (I-E).

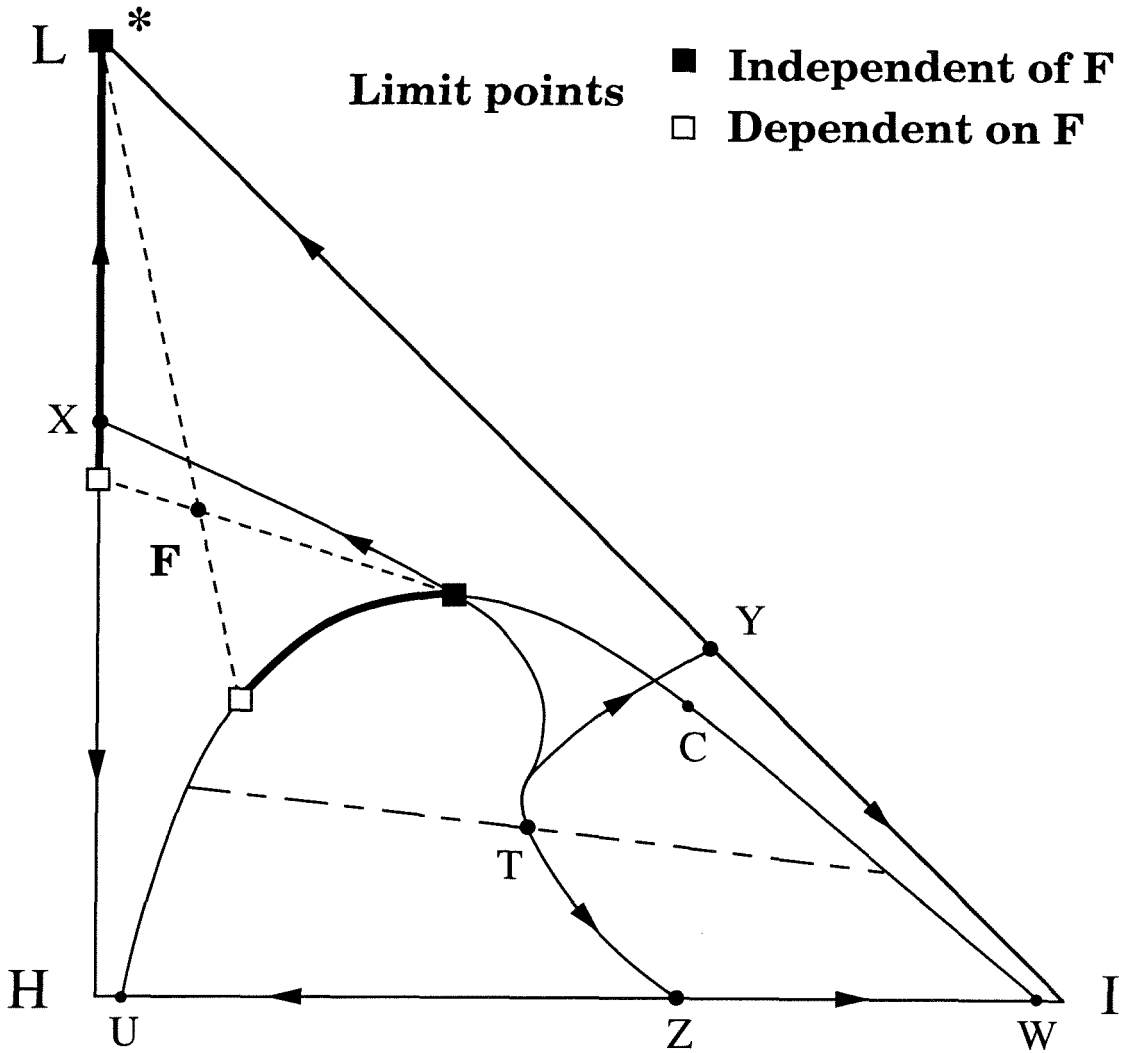


Figure 4.18: The location of the limit points along the distillate and bottoms continuation paths for the mixture ethanol (L) - water (H) - benzene (I-E).

away from the unstable steady state; we may want to operate at the unstable steady state because it may have some advantages.

For example, in the case of the ethanol (L) - water (H) - benzene (I-E) mixture. Suppose that we have the following bottoms product composition specifications:

$$x_{BL} \geq 99.5\%, \quad x_{BI} \leq 0.01\%.$$

We can achieve these specifications by operating either at a stable or at an unstable steady state. Figure 4.19 illustrates the two steady state profiles in the composition space. While the bottoms ethanol mole fraction (x_{BL}) at the unstable steady state is 99.5%, at the stable steady state, in order to satisfy the bottoms benzene mole fraction (x_{BI}) specification, the ethanol mole fraction in the bottoms should be 99.99%. This is so, because at the stable steady state the separation is limited by the benzene mole fraction specification. Since the distillate composition of the stable steady state has to lie on the ethanol - benzene edge, the bottoms ethanol mole fraction should go as high as 99.99% and hence the operation at the stable steady state may require a large reflux ratio and/or a large number of stages. Therefore, in this case, by operating at the unstable steady state the specifications may be achievable with a smaller number of trays and/or lower reflux (compared to the operation at the stable steady state).

4.4.5 Simulation

In this section we discuss something different from the issues above, an application for numerical computations. The existence of multiple solutions may cause problems in simulations, such as, a higher convergence failure rate. Furthermore, current commercial simulators cannot find multiple solutions. When multiplicities exist for a given column specification, the solution simulators calculate, using some convergence algorithm, depends on the simulator-generated or user-supplied initial column profile. The computation of only one of the solutions lurks the danger of disregarding some other eligible, and possibly, attractive solutions and it may therefore result in misleading conclusions and decisions regarding the separation under consideration.

The problem for simulations is how to pick initial profiles that will lead to the

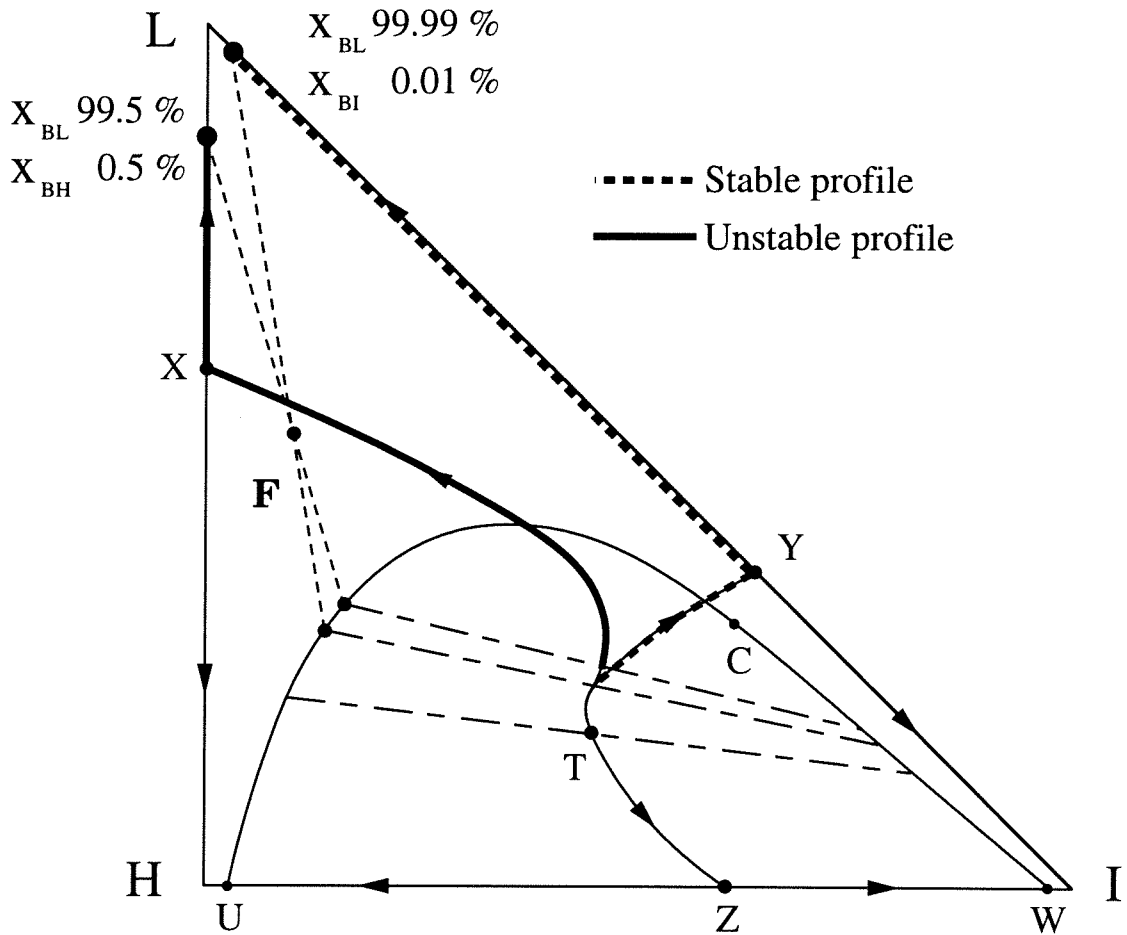


Figure 4.19: The stable and unstable steady state profiles satisfying the ethanol (L) - water (H) - benzene (I-E) column specification.

computation of specific solutions. Using the ∞/∞ analysis, we can locate the ∞/∞ case composition profiles of the multiple solutions in the composition space. For example, Figure 4.20 illustrates the three steady state profiles for the 001 class mixture acetone (L) - heptane (H) - benzene (I-E) and some given feed F. Using these as initial profiles for a computation, there is a better chance to find all the solutions. There is no guarantee, however. Therefore, the ∞/∞ analysis, apart from just “warning” about the existence of multiple solutions for some mixture, it also provides good initial profiles for simulations. Using these initial profiles, the computation of specific solutions, and possibly, a higher convergence rate and/or lower computation time may be achieved.

In the following, we present simulation results which demonstrate the computation of specific solutions by providing initial profiles based on the ∞/∞ case predictions. Aspen Plus (1988) is used for the simulation of a column separating the acetone (L) - heptane (H) azeotrope using benzene (I-E) as the entrainer. The column characteristics are depicted in Figure 4.21. Appendix A contains detailed information about the column design and specifications, the thermodynamic model used and the Aspen Plus convergence parameters. The Aspen Plus input file is also provided in Appendix A (for the readers who want to reproduce the results).

The Aspen Plus physical properties option set SYSOP7, i.e., the UNIFAC liquid activity coefficient model and the Redlich-Kwong equation of state for vapor phase properties, is used. Using this option set, all property model parameters are provided by the Aspen Plus databanks and although there exists the option of modifying the parameter values, we chose not to because we want to keep things as simple as possible.

Using the SYSOP7 physical properties set, the acetone (L) - heptane (H) azeotrope has composition 91.23% acetone and 8.77% heptane. It was shown above that using this physical properties set, a minimum boiling benzene (I) - heptane (H) azeotrope exists (at 98.82% benzene and 1.18% heptane) and therefore the ternary mixture belongs to the 021 class. Figure 4.15b illustrates the mixture’s distillation line diagram and the feed region that leads to multiplicities while Figure 4.16 shows the location of

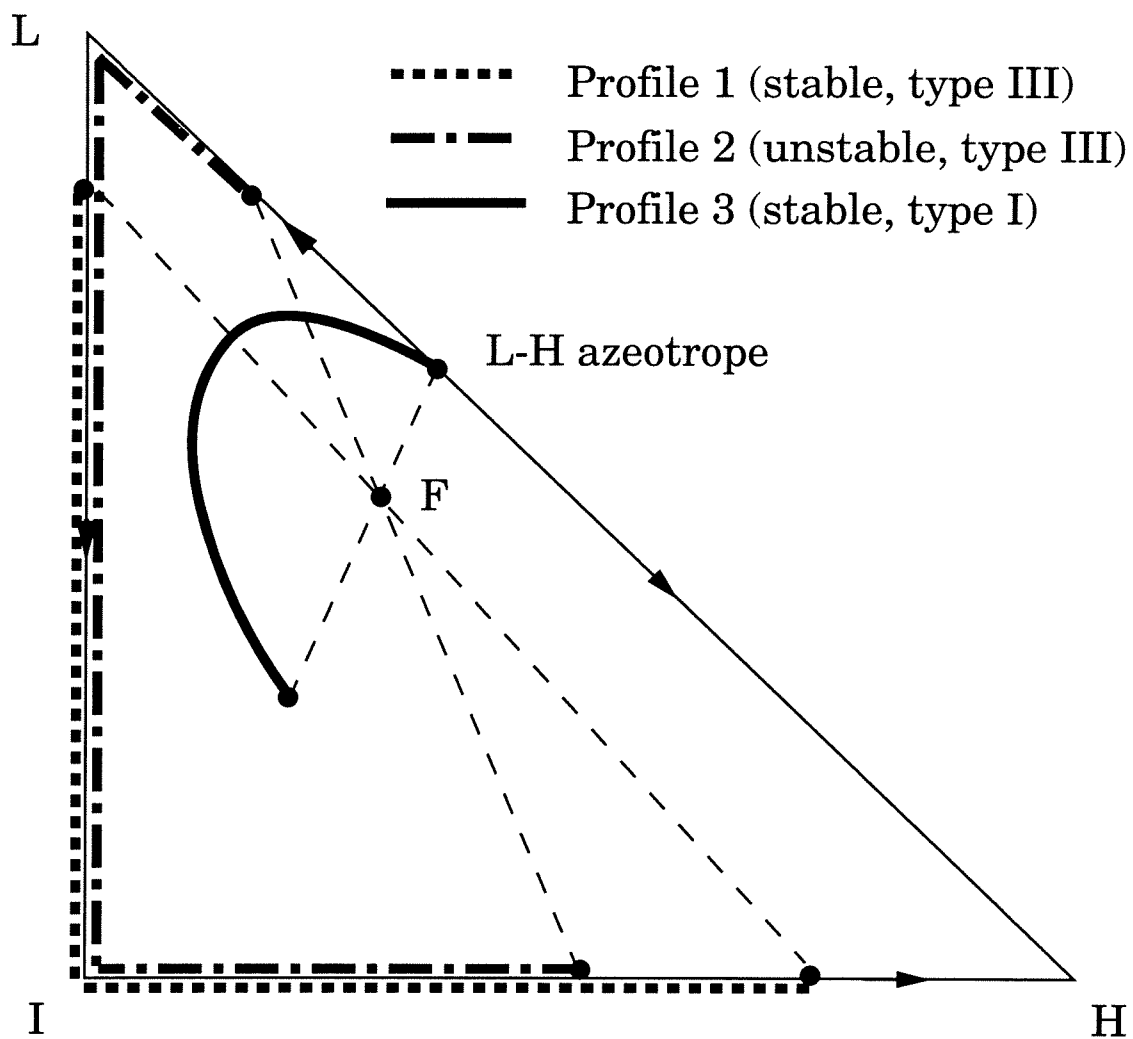


Figure 4.20: The three steady state profiles for the 001 class mixture acetone (L) - heptane (H) - benzene (I-E) and some given feed F.

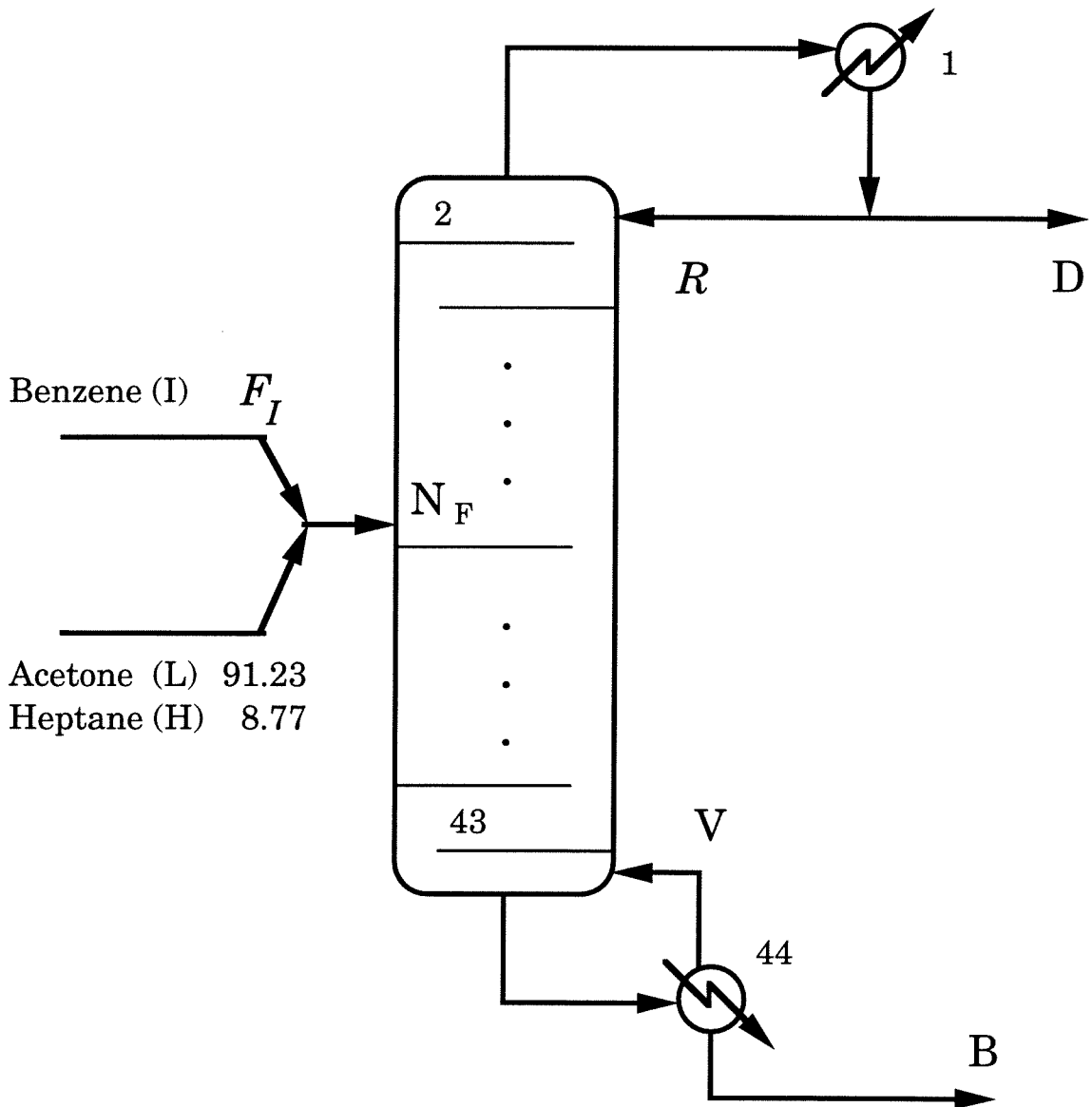


Figure 4.21: The characteristics of the column simulated by Aspen Plus.

the azeotropes and the distillation line boundary computed using the above physical properties set.

We have shown above that the introduction of the distillation line boundary does not qualitatively affect the existence of multiplicities. Note, however, that the region of feed compositions that lead to multiplicities is now restricted to the shaded region illustrated in Figure 4.15b and that differences (with the 001 class predictions) in the column profiles are expected because of the XY boundary (Figure 4.15b). For example, in the ∞/∞ case for feeds in the region to the right of the boundary, the type III column profiles are restricted by the XY boundary and consequently the highest purity of acetone that can be recovered in the distillate is restricted by the XY boundary, too. In addition, for the diagram shown in Figure 4.16 and the column characteristics depicted in Figure 4.21, multiplicities exist in the ∞/∞ case for distillate flows between 94.0 and 100.0 kmols/hr. If the XY boundary did not exist, the corresponding distillate flow range would be between 91.23 and 100.0 kmols/hr.

For any ternary mixture, column design, feed composition and (distillate or bottoms) product to feed ratio, we can locate the column composition profiles of the ∞/∞ multiplicities in the composition space. Although, this ∞/∞ prediction can be very detailed, we are not going to do that. Instead, a very rough estimate of the ∞/∞ profiles is to be used as initial profiles for the simulations. More specifically, we are not going to use the thermodynamic model for any calculation, e.g., to obtain some distillation line ($\underline{x} - \underline{y}(\underline{x})$ calculation sequence which corresponds to some ∞/∞ tray column profile) or any temperature profile estimate. Only some very basic information about the profile characteristics is used for the construction of the initial profiles.

First, because of the proximity of the XY boundary to the triangle edges we are going to ignore the boundary and construct the initial profile estimates based on Figure 4.20 (001 class). Second, based on the main characteristics of the multiple steady state profiles shown in Figure 4.20 and the overall feed composition, we roughly estimate the location of the distillate and bottoms product in the composition space so that the material balances are approximately satisfied for some distillate flow in

the distillate multiplicity range. Third, based on the ∞/∞ profiles, we identify the singular points its profile contains. By recognizing the fact that many trays are required to approach a singular point, we separate the column in sections of trays located at singular points and sections below, above or between singular points. We arbitrarily assign an equal number of trays for each section. The whole estimated profile is generated by linear interpolation between the two end compositions of each section.

Although the above, abstract description of how to construct a rough initial profile for simulations may seem very complicated, in practice, it is very simple. Note that Aspen Plus performs the linear interpolation automatically, so we typically have to specify the composition of only three to six trays.

Figure 4.22 shows two such initial profiles in the composition triangle. The one marked as IP3-BF100, is an initial profile based on the characteristics of profile 3 of Figure 4.20 for a column with a benzene feed of 100 kmol/hr. This profile consists of two sections: the composition on trays 1 to 22 is that of the acetone - heptane azeotrope (singular point) while the compositions of trays 23 to 44 are linearly distributed between the acetone - heptane azeotrope and the estimated location of the bottoms (tray 44) composition. The latter was computed by an approximate material balance for the overall feed composition and for a distillate flow in the multiplicity range.

Similarly, the initial profile IP1-BF10 (Figure 4.22) is based on the characteristics of profile 1 of Figure 4.20 for a column with a benzene feed of 10 kmol/hr. This profile consists of three sections: fourteen tray compositions are distributed along the acetone - benzene edge, sixteen tray compositions are located at the benzene corner (singular point) and fourteen trays are distributed along the benzene - heptane edge. Again, the locations of the distillate and the bottoms were selected so that the material balances are (approximately) satisfied. Appendix A contains the necessary additions to the Aspen input file if the IP3-BF100 or the IP1-BF10 profile is to be used as initial estimate for the simulation.

Table 4.1 summarizes the simulation results for eight sets of column specifications (input). The benzene feed flowrate, F_I , the feeds tray, N_F , the reflux flowrate, R ,

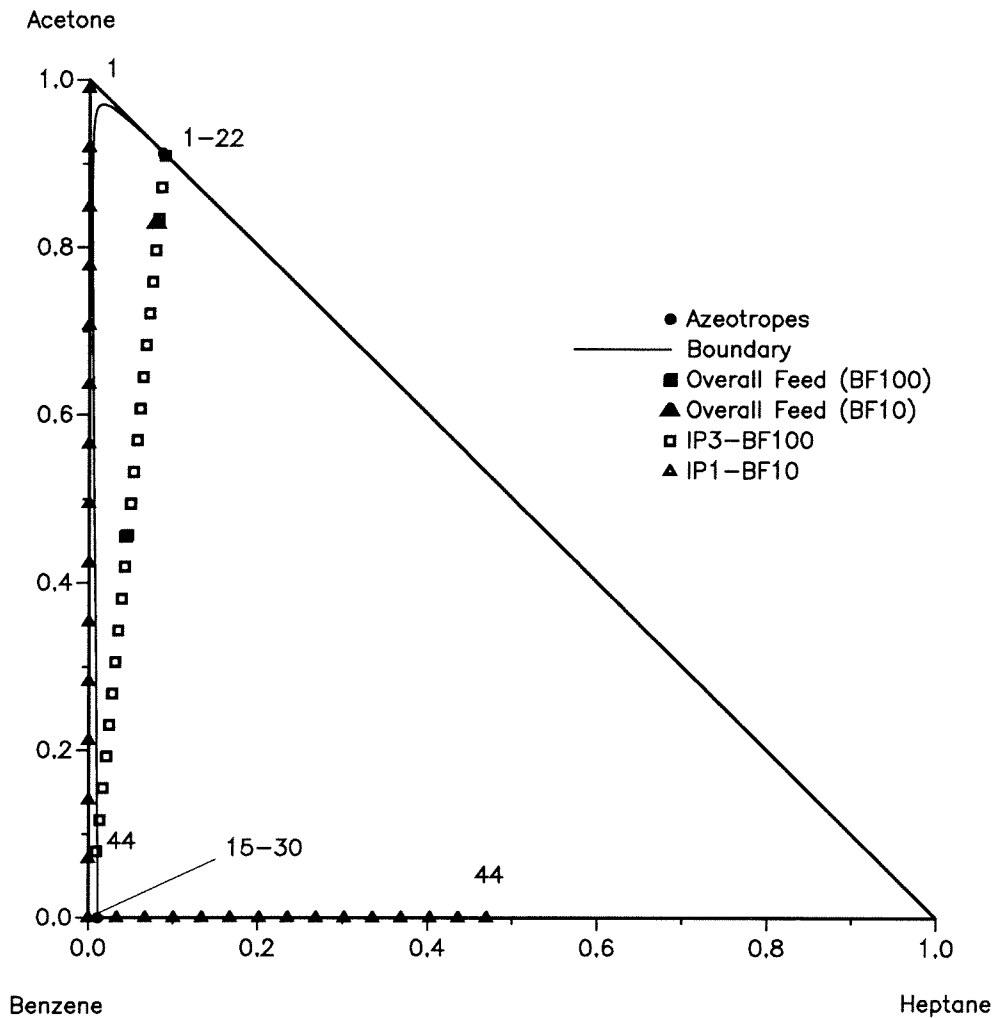


Figure 4.22: Two profiles, IP3-BF100 and IP1-BF10, used as initial estimates in simulations. Some indicative tray numbers are shown. BF: Benzene feed.

Table 4.1: Simulation results using Aspen Plus and different sets of benzene feed flowrate, F_I , feeds tray, N_F , reflux flowrate, R , distillate flow, D and with or without a user-supplied initial column profile. F_I , R and D in kmols/hr; CF: Convergence failure.

INPUT					OUTPUT		
F_I	N_F	R	D	User-supplied Initial Profile	x_{DL}	x_{DH}	x_{DI}
100	22	10000	95	None	.96	.01	.03
				IP3-BF100	.91	.09	.00
			94	None	CF		
				IP3-BF100	.91	.09	.00
		1000	95	None	.96	.01	.03
				IP3-BF100	.95	.05	.00
			94	None	.97	.01	.02
				IP3-BF100	.95	.05	.00
			93	None	CF		
				IP3-BF100	.95	.05	.00
10	22	500	94	None	.91	.09	.00
				IP1-BF10	.97	.01	.02
		1000	94	None	.91	.09	.00
				IP1-BF10	.97	.02	.01
	32	1000	93	None	.91	.09	.00
				IP1-BF10	.98	.01	.01

and the distillate flow, D , are different in these eight sets while all the other column parameters are fixed to the values reported in Figure 4.21. Two benzene feed flowrates (100 and 10 kmols/hr) are used resulting in two different overall feed compositions. The mole fractions of acetone, heptane and benzene in the distillate (x_{DL} , x_{DH} and x_{DI} resp.) of the solution Aspen Plus converged to, are reported in Table 4.1 as the simulation output. For each set of input specifications, there are two outputs. The first one corresponds to the solution computed without using any user-supplied initial profile, the second one using some user-supplied initial profile.

If $F_I=100$ and no user-supplied initial profile is used, Aspen Plus fails to locate a solution in two out of the five input sets. For the other three input sets, Aspen Plus calculates a solution in which the main impurity in the distillate is benzene. Figure 4.23 shows the profile computed by Aspen Plus without using a user-supplied

initial profile for the first set of input specifications. It seems that when $F_T=100$, Aspen Plus converges to a solution corresponding to profile 1 of Figure 4.20.

Using IP3-BF100 as the initial profile for the computation, Aspen Plus converges for all five sets of input specifications ($F_T=100$) to a solution resembling the profile 3 of Figure 4.20. For the first and second specification sets, this is quite obvious since the distillate is located at the acetone - heptane azeotrope. For the third, fourth and fifth specification sets, however, the distillate composition is 95% acetone and 5% heptane. It is therefore not that clear, by this information alone, whether they correspond to profile 3 or profile 2 of Figure 4.20. The fact that their bottoms compositions do not lie on the benzene - heptane binary edge and the fact that the distillate composition (95% acetone and 5% heptane) does not change as the distillate flow varies, however, indicate that they also correspond to profile 3 of Figure 4.20. The fact that the distillate is not located at the acetone - heptane azeotrope is due to the expected discrepancy of finite columns from the ∞/∞ predictions. Figure 4.23 shows the solution computed using IP3-BF100 as the initial profile for the first set of input specifications. The initial estimate IP3-BF100 is also shown.

In the two cases the computation failed to converge, we used as initial estimate another profile resembling profile 1 of Figure 4.20. Another solution was not calculated, however. Note that the initial estimate used was a rough estimate and therefore, it could be substantially improved by using more ∞/∞ case information. Using a better estimate may lead to the desired solution. Note, however, that in these two cases, the distillate flow is very close to the limits (second specification set in Table 4.1) or outside (fifth specification set in Table 4.1) the distillate flow multiplicity range predicted in the ∞/∞ case. Hence, it is possible that multiplicity, and consequently a profile corresponding to profile 1 of Figure 4.20, does not exist for these two specification sets. Nevertheless, using the ∞/∞ predicted profile as an initial estimate for simulations, we have been able to (1) compute a solution in the two cases where convergence has failed and (2) compute a second solution in the other three cases. Note that we were unsuccessful in calculating the third solution, corresponding to profile 2 of Figure 4.20, probably because of its instability.

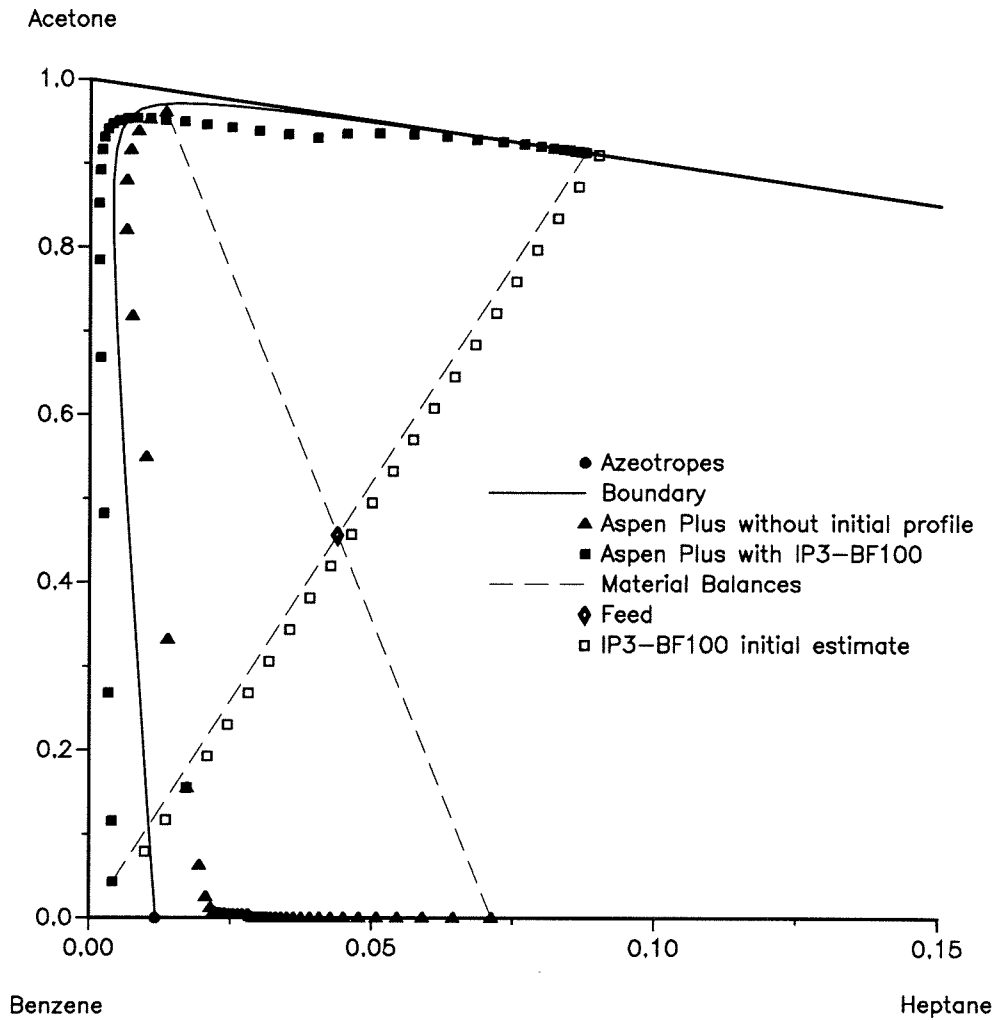


Figure 4.23: Solutions computed by Aspen Plus for $F_I=100$, $N_F=22$, $R=10000$ and $D=95$.

If $F_I=10$ and no user-supplied initial profile is used, Aspen Plus calculates a solution in which the distillate is located at the acetone - heptane azeotrope (profile 3 of Figure 4.20) for all three specification sets shown in Table 4.1. Using IP1-BF10 as the initial profile for the computation, Aspen Plus converges for all three sets of input specifications to another solution corresponding to profile 1 of Figure 4.20. Figure 4.24 shows both solutions computed by Aspen Plus in the composition triangle for the last set of input specifications. Note that the solution computed using IP1-BF10 as the initial profile crosses the distillation line boundary and achieves a 98% acetone purity at the distillate. The boundary crossing in finite columns also means that the distillate flow multiplicity range extends beyond its ∞/∞ limits. The last specification set shows multiplicities for $D=93$ kmols/hr while the ∞/∞ predicted range was between 94 and 100.

This last set of examples ($F_I=10$) shows that, when the existence of multiplicities is ignored, the “blind” use of a commercial simulator may result in misleading conclusions and decisions regarding the separation under consideration. Based on the simulation results without a user-supplied initial profile, one would conclude that the column could not break the acetone - heptane azeotrope. Using the ∞/∞ column profile predictions, we were able to show that there exists another eligible solution that breaks the azeotrope.

4.5 Conclusions

In this chapter, we briefly review the ∞/∞ analysis (chapters 2 and 3) by presenting the three basic steps of the analysis: the characteristics of the column profiles, the location of the feasible product regions and the construction of the bifurcation diagram. We then present all the information that can be directly obtained from the analysis of the ∞/∞ case, i.e., the ∞/∞ predictions. More specifically, we can predict the existence of multiplicities, the feed composition region that leads to multiplicities, the feasible product regions, the bifurcation diagram, the location of turning (limit) points, the product flowrate multiplicity range and the column composition profiles.

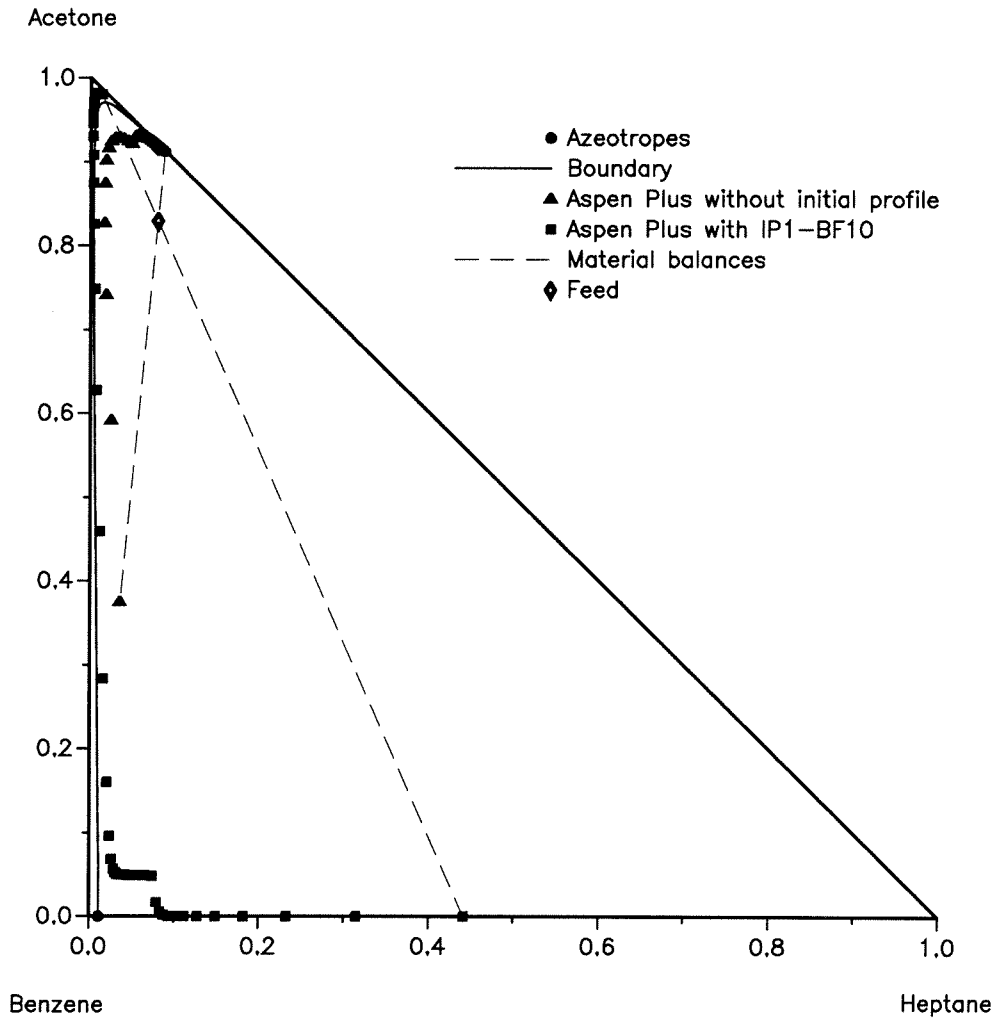


Figure 4.24: Solutions computed by Aspen Plus for $F_I=10$, $N_F=32$, $R=1000$ and $D=93$.

Next we present the implications of the existence of multiple steady states for distillation design, synthesis and simulation. We discuss the problems multiplicities may cause, how multiplicities may affect design decisions and in what ways the ∞/∞ predictions may be helpful. We first discuss the problems for column operation and control (erratic behavior, instabilities, start-up problems) but then we focus on the implications of multiple steady states for distillation design, synthesis and simulation.

We show how multiplicities may affect the entrainer selection. Using the ∞/∞ predictions, we demonstrate the identification of classes of mixtures with unique steady state for any feed or with inherent and robust multiple steady states. We further show how multiplicities may be avoided by the appropriate column design and separation scheme selection. Using the ∞/∞ analysis, we identify the key features of VL(L)E responsible for the existence of multiple steady states. This is a valuable information in the case there are doubts about the accuracy of the VL(L)E data used, because one can predict if this ambiguity of the VL(L)E data may lead to erroneous conclusions about multiplicity and because it gives indications on how to design the appropriate experiments to resolve whether multiplicities exist or not.

Next we show how the existence of multiple steady states restricts the feasible product sets for stable steady state operation and how the ∞/∞ analysis can provide information on the distance from instability. On the other hand, we demonstrate that it is possible that we may not want to stay away from the unstable steady state because operation at the unstable steady state may have some advantages, e.g., the specifications may be achievable with a smaller number of trays and/or lower reflux (compared to the operation at the stable steady state).

Finally, we discuss the problems multiple solutions may cause in simulations and consequently for design. We show that if the existence of multiple solutions is ignored, the “blind” use of a commercial simulator may result in misleading conclusions and decisions regarding the separation under consideration caused by the negligence of some eligible, and possibly, attractive solutions. We show that using the ∞/∞ predicted profiles as initial estimates for simulations, there is a better chance, but no guarantee, to find all the solutions and to compute a solution in cases convergence

has failed.

Acknowledgements: We acknowledge gratefully the financial support of the Donors of the Petroleum Research Fund administered by the American Chemical Society and of the I. S. Latsis Foundation.

4.6 Literature Cited

Aspen Plus, Release 8, Aspen Technology Inc., Cambridge, MA, 1988.

Doherty, M. F., and J. D. Perkins, "On the Dynamics of Distillation Processes. I. The Simple Distillation of Multicomponent Non-reacting, Homogeneous Liquid Mixtures," *Chem. Eng. Science*, 1978, **33**, pp. 569-578.

Horsley, L. H., "Azeotropic Data - III," Advances in Chemistry Series 116, American Chemical Society, Washington, D.C., 1973.

Kienle, A., E. D. Gilles, and W. Marquardt, "Computing Multiple Steady States for Homogeneous Azeotropic Distillation Processes," presented at ESCAPE-3, Graz, Austria, 1993.

Kovach III, J. W., and W. D. Seider, "Heterogeneous Azeotropic: Experimental and Simulation Results," *Comput. Chem. Eng.*, 1987, **11**(6), pp. 593-605.

Laroche, L., N. Bekiaris, H. W. Andersen, and M. Morari, "Homogeneous Azeotropic Distillation: Separability and Flowsheet Synthesis," *Ind. Eng. Chem. Res.*, 1992, **31**(9), pp. 2190-2209.

Matsuyama, H., and H. Nishimura, "Topological and Thermodynamic Classification of Ternary Vapor-Liquid Equilibria," *J. Chem. Eng. Jpn.*, 1977, **10**(3), pp. 181-187.

Pham, H. N., and M. F. Doherty. "Design and Synthesis of Heterogeneous Azeotropic Distillations - II. Residue Curve Maps," *Chem. Engng. Sci.*, 1990a, **45**(7), pp. 1837-1843.

Pham, H. N., and M. F. Doherty. "Design and Synthesis of Heterogeneous Azeotropic Distillations - III. Column Sequences," *Chem. Engng. Sci.*, 1990b, **45**(7), pp. 1845-1854.

Stichlmair, J. G., J. R. Fair, and J. L. Bravo, "Separation of Azeotropic Mixtures

via Enhanced Distillation,” *Chem. Eng. Prog.*, 1989, (1), pp. 63-69.

Zharov, V. T., and L. A. Serafimov, “Physicochemical Fundamentals of Simple Distillation and Rectification” (in Russian), pp. 160-168, Khimia, Leningrad, 1975.

4.7 Appendix

Aspen Plus (1988) is used for the simulation of an acetone (L) - heptane (H) - benzene (I-E) column. The Aspen Plus physical properties option set SYSOP7, i.e., the UNIFAC liquid activity coefficient model and the Redlich-Kwong equation of state for vapor phase properties, is used. The outside loop convergence tolerance and feed flash tolerance has been decreased to 10^{-7} (default 10^{-4}). Because of the mixture’s liquid phase nonidealities the nonideal algorithm is used and the maximum number of outside loops is set to 100 (default 25).

The column has 44 stages (including the reboiler and the total condenser), operates under atmospheric pressure and there is no pressure drop in the column. The azeotropic feed composition is 91.23% acetone and 8.77% heptane and the azeotropic feed flow is 100 kmols/hr. The Aspen Plus input file is listed below:

```

IN-UNITS    MET
OUT-UNITS   MET
COMPONENTS A C3H6O-1/ H C7H16-1/ B C6H6
PROPERTIES SYSOP7
FLWSHEET
  BLOCK MSSCOLUMN IN=FAZEO FBENZ OUT=TOP BOT
STREAM FAZEO V-FRAC=0. PRES=1
  MOLE-FLOW A 91.23/H 8.77/B 0.00
STREAM FBENZ V-FRAC=0. PRES=1
  MOLE-FLOW A 0.00/H 0.00/B #BFF#
BLOCK MSSCOLUMN RADFRC
  PARAM NSTAGE=44 ALGORITHM=NONIDEAL MAXOL=100 &
    TOLOL=0.0000001 FLASH-TOL=0.0000001
  FEEDS FBENZ #NF# / FAZEO #NF#
  PRODUCTS BOT 44 0/TOP 1 0
  P-SPEC 1 1. / 44 1.
  TRAY-REPORT TRAY-OPTION=ALL-TRAYS
  COL-SPECS RDV=0. D=#DF# L1=#RF#

```

Note that, the above input file cannot be run as is because the numerical values

of the benzene feed flowrate, the feeds tray, the reflux flowrate, and the distillate flow have been replaced with the character sets with the number sign at their beginning and end (#BFF#, #NF#, #RF#, #DF# resp.). In order to obtain the simulation results of Table 4.1, these character sets should be substituted with the corresponding numerical values listed in Table 4.1.

In addition, in order to obtain the simulation results of Table 4.1 using one of the two user-supplied initial profiles (IP3-BF100 or IP1-BF10), the following lines should be added at the end of the input file:

```
; IP3-BF100 initial profile
X-EST 1  A 0.91 / H 0.09 / B 0.00 /
        22 A 0.91 / H 0.09 / B 0.00 /
        44 A 0.08 / H 0.01 / B 0.91
Y-EST 1  A 0.91 / H 0.09 / B 0.00 /
        22 A 0.91 / H 0.09 / B 0.00 /
        44 A 0.08 / H 0.01 / B 0.91
```

or

```
; IP1-BF10 initial profile
X-EST 1  A 0.99 / H 0.00 / B 0.01 /
        15 A 0.00 / H 0.00 / B 1.00 /
        30 A 0.00 / H 0.00 / B 1.00 /
        44 A 0.00 / H 0.47 / B 0.53
Y-EST 1  A 0.99 / H 0.00 / B 0.01 /
        15 A 0.00 / H 0.00 / B 1.00 /
        30 A 0.00 / H 0.00 / B 1.00 /
        44 A 0.00 / H 0.47 / B 0.53
```

Note that Aspen Plus requires that both liquid and vapor estimates (X-EST, Y-EST resp.) should be provided. The vapor initial profiles for both IP3-BF100 and IP1-BF10 are identical to the corresponding liquid initial profiles. No temperature profile estimate is included.

Chapter 5 Conclusion

In chapter 2 we study multiple steady states in ternary homogeneous azeotropic distillation. First we examine in detail the infinite reflux and infinite number of trays (∞/∞) case. We present a systematic procedure which determines whether multiplicities exist for any given residue curve diagram and feed composition. Through this procedure we answered the following questions:

Given a ternary homogeneous mixture and its residue curve diagram, we can, for the ∞/∞ case

- (1) find whether multiple steady states exist for some feed composition and
- (2) locate the region of feed compositions that lead to these multiple steady states.

We derive (1) the necessary and sufficient geometrical condition for the existence of multiple steady states and (2) the condition the feed compositions must satisfy to lead to multiple steady states. A few other important results are the following:

In the case of straight boundaries we found that two neighboring saddles is a necessary condition for the existence of multiplicities.

If multiple steady states exist under the straight boundaries assumption, then, assuming that the azeotropic compositions do not change, these multiplicities still exist even if the boundaries are curved, although the appropriate feed region is changed.

Highly curved boundaries (pseudosaddles) can induce multiple steady states.

For columns operating at finite reflux the geometrical condition is only a sufficient condition for the existence of multiple steady states. We use an example to show that the prediction for the existence of multiple steady states in the ∞/∞ case carries over to columns operating at finite reflux and with a finite number of trays. We further

show that, although the predictions were made in the ∞/∞ case, it does not mean that multiple steady states do not exist for realistic operating conditions (low reflux and entrainer feed flows and small number of trays). However, apart from the fact that the ∞/∞ case predictions carry over, the observations presented here should not be generalized because they are specific to the particular example. We also present an example which illustrates that highly curved boundaries can induce multiplicities.

We offered some comments on the effect of the thermodynamic model on the existence of multiplicities and we show that some of the results presented here do not depend on the specific thermodynamic model used. Finally, we briefly discuss the effect of multiplicities on the column design and operation. The consideration here is whether it is necessary to operate in the single steady state region (i.e. avoid the multiplicity region). A more thorough investigation of this topic is needed.

In chapter 3 we examine in detail the existence of multiple steady states in the ∞/∞ case of a ternary mixture. More specifically, we answer the following questions: Given a ternary (homogeneous or heterogeneous) mixture and its VL(L)E diagram (residue curve diagram for packed columns, distillation line diagram for tray columns),

- (1) find whether multiple steady states exist for some feed composition and
- (2) locate the feed composition region that leads to these multiple steady states.

The existence of multiplicities (question 1) can be checked by the procedure depicted in Figure 5.1 which is summarized in the following:

Locate the singular points (pure components and azeotropes) in the VL(L)E diagram. Locate the m distillation regions. In every distillation region containing k singular points, there is one unstable node, one stable node and $k-2$ saddles. For each region there exist two routes which go from the unstable node to the stable node along the region boundaries (a total of $2m$ routes).

For each route, mark the n singular points along the route as follows: point 1, the unstable node; points 2 to $n-1$, the saddles; point n , the stable node. The only eligible column profile lower end compositions along this route lie on the part between points 2 and n . This is the profile lower end route. Accordingly, the eligible column

profile upper end (overhead vapor) lies on the part of the route between points 1 and $n-1$. This is the profile upper end route. These two routes define the locations of the upper and lower end column profile compositions for which the geometrical condition should be checked (type III column profiles).

Note, however, that the geometrical condition directly involves the distillate and bottom product routes which may be different from the profile upper and lower end routes depending on the type of the equipment used at the column ends (condenser, reboiler, decanter). In chapter 3, we show how the distillate and bottoms routes (associated with a given pair of upper and lower profile end routes) can be located for any equipment combination. Tables 5.1a and 5.1b show how the distillate and bottom product routes are related to the profile upper and lower end routes for some equipment types and for tray and packed columns respectively.

Finally, we define the continuation path (and its direction) as the path generating all possible column profiles starting from the profile with $D=0$ and ending at the profile with $D=F$. Multiple steady states occur when D decreases along this path. This can be checked by the following condition:

Geometrical, necessary and sufficient multiplicity condition: Pick a distillate D and a bottom product B , both located on some pair of distillate and bottoms product routes and such that (1) the line segment $D'B'$ crosses the line segment DB (to ensure that there exists a feed composition associated with both profiles) and (2) the column profile that runs from D to B along the distillation region boundaries contains at least one saddle singular point (type III column profile). Now pick D' and B' sufficiently close to D and B respectively and such that the column profile from D' to B' is a “later” profile along the continuation path. For the existence of multiple steady states it is required that: As we move along the continuation path from D to D' and accordingly from B to B' , the line that passes from D and is parallel to BB' crosses the $D'B'$ line segment.

Finally, for columns with decanter and a given distillate policy, we show that discontinuity is possible at the transition from heterogeneous to homogeneous profiles along the continuation path. In this case, in addition to the aforementioned geomet-

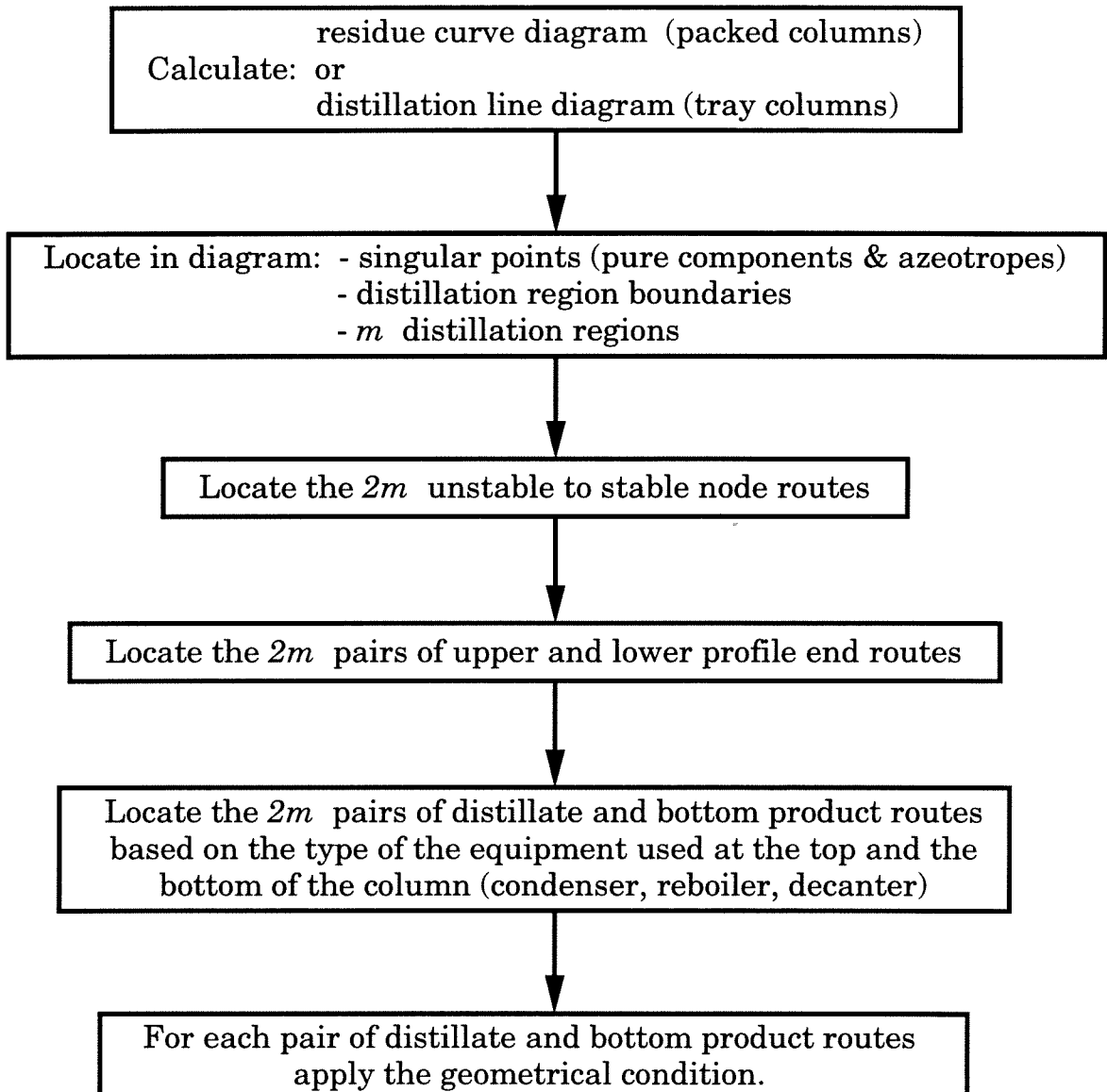


Figure 5.1: The general procedure for checking the existence of multiple steady states in the ∞/∞ case of any ternary mixture.

rical condition, one has to check the distillate flowrate ranges of the heterogeneous and homogeneous branches of the continuation path for possible distillate flowrate overlap and consequently multiplicity.

The condition for the appropriate feed region (question 2) is summarized in the following:

Appropriate feed region condition: Pick a distillate D . Find the set of all bottom products such that the geometrical condition is satisfied for the picked D . Name this set $S_B(D)$. Note that $S_B(D)$ is always part of a distillation region boundary and that in some rare cases, $S_B(D)$ may contain an inflexion point and/or it may consist of more than one non-connected boundary segments. Draw the straight line segments connecting D with the end points of each boundary segment that belongs to $S_B(D)$. For the chosen D , the appropriate feed composition is the union of the areas enclosed by each boundary segment that belongs to $S_B(D)$ and the corresponding straight line segments connecting D with the end points of the boundary segment of $S_B(D)$. Pick another distillate D and repeat. In general, for each distillate D there exists a different set of bottoms compositions, $S_B(D)$, that satisfies the geometrical condition. Therefore, for any given mixture, the feed compositions that lead to multiplicities lie in the union of all the areas enclosed by each boundary segment that belongs to *some* $S_B(D)$ and the corresponding straight line segments connecting the distillate D associated to $S_B(D)$ with the end points of the boundary segment of $S_B(D)$.

The procedures and conditions described above constitute the fully detailed, accurate and totally general answers to the questions about the existence of multiplicities and the feed compositions that lead to these multiplicities in the ∞/∞ case. Given a mixture and its VL(L)E diagram, we show via an illustrative example how the specific VL(L)E diagram structural information can be used to simplify these conditions (unavoidably by reducing the degree of generality) to some very simple tests. We also discuss the differences between packed and tray columns, between residue curve and distillation line diagrams, the effect of tray efficiency as well as the role of the vapor line for heterogeneous mixtures. Since residue curve boundaries are easier to calculate than distillation line boundaries, we derive guidelines on when it is justified

Table 5.1: The distillate and bottoms routes for various types of equipment (condenser/reboiler/decanter). a. tray columns b. packed columns.

a. Tray columns (tray efficiency=1)

Total Reboiler	B route = lower end route
Partial Reboiler B = liquid	
Total Condenser	D route = upper end route
Partial Condenser D = vapor	
Total (or Subcooled) Condenser & Decanter with policy $D_2=0$	D route composed of: - the homogeneous part of the upper end route & - the part of the 1st phase of the heterogeneous liquid boiling envelope (or binodal curve) that can be obtained from the phase split of the heterogeneous part of the upper end route

b. Packed columns (\approx tray columns w/ tray efficiency $\rightarrow 0$)

Total Reboiler	B route = lower end route
Partial Reboiler B = liquid	B route = line of liquid compositions in equilibrium with vapor compositions on the lower end route
Total Condenser	D route = upper end route
Partial Condenser D = vapor	D route = line of vapor compositions in equilibrium with liquid compositions on the upper end route
Total (or Subcooled) Condenser & Decanter with policy $D_2=0$	D route composed of: - the homogeneous part of the upper end route & - the part of the 1st phase of the heterogeneous liquid boiling envelope (or binodal curve) that can be obtained from the phase split of the heterogeneous part of the upper end route

to use residue curve boundaries for the study of multiplicities of tray columns (at the expense of less quantitative accuracy).

As an illustrative example throughout chapter 3 we use the mixture ethanol - water - benzene. For this mixture and the specific VL(L)E model and parameters used, we derive the following conclusions regarding multiplicities in the ∞/∞ case solely based on (1) the residue curve boundaries, the heterogeneous region envelope, the distillation line boundaries and the line of vapor compositions in equilibrium with liquid compositions on the residue curve boundaries, if accurate quantitative results are needed, or (2) the residue curve boundaries, the heterogeneous region envelope and the vapor line, if somewhat less accurate quantitative results are sufficient.

Columns without decanter: In this case, we identify that the existence of multiplicities critically depends on the location of the distillate path away from the binary edges and more specifically in the heterogeneous region. We show that the location of the vapor line is very crucial in this case. We further show that the reboiler type has absolutely no effect on the existence of multiplicities for this particular mixture class.

For tray columns with tray efficiency 1, we conclude that multiplicities exist regardless of the condenser type. For packed columns, multiplicities exist if a partial condenser is used and the distillate product consists of the vapor phase only. A unique steady state exists, however, for packed columns with a total condenser. Finally, for tray columns with a total condenser, we conclude that there exists a tray efficiency value η^* such that multiple steady states exist only if $\eta > \eta^*$.

Columns with decanter: We show that the existence of multiplicities depends on the distillate policy. The most common distillate policy for this mixture, i.e. recovering as distillate a portion of the entrainer-poor phase only ($D_2=0$) and refluxing a mixture of the two liquid phases, is studied in detail. We conclude that under this distillate policy: (1) the existence of multiple steady states is generic for this heterogeneous mixture class and therefore the presence of multiplicities does not critically depend on some specific VL(L)E characteristic as long as the basic qualitative structural properties of the VL(L)E diagram are preserved, (2) consequently,

using different reboiler, condenser and column types does not qualitatively affect the existence of multiplicities although some quantitative differences are expected.

Finally, using numerically constructed bifurcation diagrams, we show that the ∞/∞ case predictions carry over to columns operating at finite reflux and with a finite number of trays. We also discuss a different, degenerate type of multiplicity (infinite number of profiles with the same product compositions for a specific distillate flowrate) whose practical implications are unclear and therefore, a more thorough investigation of this topic is needed.

In chapter 4, we briefly review the ∞/∞ analysis (chapters 2 and 3) by presenting the three basic steps of the analysis: the characteristics of the column profiles, the location of the feasible product regions and the construction of the bifurcation diagram. We then present all the information that can be directly obtained from the analysis of the ∞/∞ case, i.e., the ∞/∞ predictions. More specifically, we can predict the existence of multiplicities, the feed composition region that leads to multiplicities, the feasible product regions, the bifurcation diagram, the location of turning (limit) points, the product flowrate multiplicity range and the column composition profiles.

Next we present the implications of the existence of multiple steady states for distillation design, synthesis and simulation. We discuss the problems multiplicities may cause, how multiplicities may affect design decisions and in what ways the ∞/∞ predictions may be helpful. We first discuss the problems for column operation and control (erratic behavior, instabilities, start-up problems) but then we focus on the implications of multiple steady states for distillation design, synthesis and simulation.

We show how multiplicities may affect the entrainer selection. Using the ∞/∞ predictions, we demonstrate the identification of classes of mixtures with unique steady state for any feed or with inherent and robust multiple steady states. We further show how multiplicities may be avoided by the appropriate column design and separation scheme selection. Using the ∞/∞ analysis, we identify the key features of VL(L)E responsible for the existence of multiple steady states. This is a valuable information in the case there are doubts about the accuracy of the VL(L)E data used, because one can predict if this ambiguity of the VL(L)E data may lead to

erroneous conclusions about multiplicity and because it gives indications on how to design the appropriate experiments to resolve whether multiplicities exist or not.

Next we show how the existence of multiple steady states restricts the feasible product sets for stable steady state operation and how the ∞/∞ analysis can provide information on the distance from instability. On the other hand, we demonstrate that it is possible that we may not want to stay away from the unstable steady state because operation at the unstable steady state may have some advantages, e.g., the specifications may be achievable with a smaller number of trays and/or lower reflux (compared to the operation at the stable steady state).

Finally, we discuss the problems multiple solutions may cause in simulations and consequently for design. We show that if the existence of multiple solutions is ignored, the “blind” use of a commercial simulator may result in misleading conclusions and decisions regarding the separation under consideration caused by the negligence of some eligible, and possibly, attractive solutions. We show that using the ∞/∞ predicted profiles as initial estimates for simulations, there is a better chance, but no guarantee, to find all the solutions and to compute a solution in cases convergence has failed.

Chapter 6 Future Work

In this work, we provided a simple physical explanation and we developed simple graphical predictive rules for the occurrence of multiplicities in both homogeneous and heterogeneous ternary mixtures by investigating the limiting case of infinite reflux and infinite number of trays. Although not included in this manuscript, we have been able to extend these ideas and results to quaternary mixtures. The composition space is now the unit pyramid and although some problems arise due to the increased dimensionality, the extension of the graphical rules is relatively straightforward. The extension to mixtures of more than four components, however, is not trivial. Note, however, that other azeotropic distillation problems, such as, the entrainer selection and the flowsheet synthesis and design, in the case of multicomponent mixtures are also far from a general solution.

Recently, the application of diagrams similar to the residue curve diagrams for the design and synthesis of reactive distillation columns has been studied (Venimadhavan et al., 1994; Buzad and Doherty, 1995). Although these methods are not yet fully developed, we believe that multiplicity prediction techniques for reactive distillation can be developed using these reactive distillation diagrams. The extension, for example, to mixtures with equimolar, fast reactions (equilibrium-controlled process) seems quite straightforward.

We have shown that the predictions of the existence of multiplicities in the ∞/∞ case carry over to the case of finite reflux and finite number of trays; we cannot predict, however, in what extent. Moreover, multiple steady states may exist in the finite case caused by a mechanism different from the one in the ∞/∞ case (maybe in some of the multiplicity examples reported by Kienle et al., 1993). Furthermore, state multiplicities have been reported in some simulation studies (e.g., Rovaglio and Doherty, 1990); it is not clearly understood whether these multiplicities are real or just numerical artifacts. Finally, the multiplicities studied here occur for columns

without controllers (open-loop). What happens to multiplicities for columns with controllers? Are there control strategies for which the open-loop multiplicities vanish in columns with controllers? All the above issues, related to the existence of multiple steady states, need to be addressed in future studies.

Multiplicities may cause problems in column operation and control. When two or more steady states exist for the same inputs it is possible that while operating at the desirable steady state some disturbances or changes of the operating conditions push the column profile to another undesirable steady state or result in erratic column behavior. Moreover, preliminary studies have shown that, in some cases, stable steady states exhibit exotic behavior never before encountered in distillation, namely, open-loop oscillations which means that the steady state is a stable focus in the state space. The study of the control characteristics of the stable steady states is thus essential for the proper operation of such columns. Finally, there might be separation sequences where it is desirable to operate at an unstable steady state. Therefore, the stabilization of the unstable steady state is essential in these cases.

The existence of multiple steady states raises new questions and problems for distillation control and operation. For example: When is the control of a column operating in the presence of other steady states difficult?; What are the areas of attraction of the stable steady states?; What is the appropriate start-up strategy that would drive the column to the desired steady state?; How difficult is it to stabilize the unstable steady state? etc. These topics, related to the effect of multiplicities on column operation and control, are not investigated in this work but they are questions future studies have to answer. These answers could lead to the development of column design and synthesis guidelines on when, i.e., for what column designs, it is important to avoid the existence of multiplicities, with what design modifications this can be achieved, for what column designs the existence of multiplicities does not pose an operational problem, etc.

References

Buzad, G., and M. F. Doherty, "New Tools for the Design of Kinetically Controlled

Reactive Distillation Columns for Ternary Mixtures,” *Comput. Chem. Eng.*, 1995, **19**(4), pp. 395-408.

Kienle, A., E. D. Gilles, and W. Marquardt, “Computing Multiple Steady States for Homogeneous Azeotropic Distillation Processes,” presented at ESCAPE-3, Graz, Austria, 1993.

Rovaglio, M., and M. F. Doherty, “Dynamics of Heterogeneous Azeotropic Distillation Columns,” *AIChE J.*, 1990, **36**(1), pp. 39-52.

Venimadhavan, G., G. Buzad, M. F. Doherty, and M. F. Malone, “Effect of Kinetics on Residue Curve Maps for Reactive Distillation,” *AIChE J.*, 1994, **40**(11), pp. 1814-1824.